Bulletin of the
Mineral Research and Exploration

http://bulletin.mta.gov.tr

POSSIBLE INCISION TIME OF THE LARGE VALLEYS IN SOUTHERN MARMARA REGION, NW TURKEY

Nizamettin KAZANCI[a], Ömer EMRE[b], Korhan ERTURAÇ[c], Suzanne A. G. LEROY[d], Salim ÖNCEL[a], Özden İLERİ[f] and Özlem TOPRAK[e]

[a] *Ankara Üniversitesi Mühendislik Fakültesi, Jeoloji Müh. Bölümü, 06100 Tandoğan/Ankara*
[b] *Fugro Sial Yerbilimleri Müşavirlik ve Mühendislik LTD, Farabi Sokak, No:40/4, 06680 Çankaya - Ankara*
[c] *Sakarya Üniversitesi, Fen Edebiyat Fakültesi, Coğrafya Bölümü, Esentepe Sakarya.*
[d] *Institute for the Environment, Brunel University, Uxbridge, Middlesex UB8 3PH, (London), UK.*
[e] *Gebze Yüksek Teknoloji Enstitüsü, 41400 Gebze, Kocaeli*
[f] *Maden Tetkik ve Arama Genel Müdürlüğü, Ankara*

Keywords:
Marmara, morphology, large valleys, erosion rate, incision time

ABSTRACT

Surface water and sediments derived from the southern Marmara region (= Susurluk Drainage basin- SDB) transport to lakes Manyas and Ulubat first and then go to the Sea of Marmara via the Kocasu River only. The present drainage system of the SDB provides a good opportunity to study erosion rate and subsequently occurrence times of large-scale valleys in the region. To achieve it, depositional characteristics and ion contents of the ancient lacustrine sediment have been investigated and re-interpreted using cores taken from Lake Ulubat. The boron content of these sediments increased upward suddenly at 4 m depth, most probably due to starting of erosion at Emet borate beds in the drainage basin. Taking into consideration equilibrium between natural erosion and sedimentation, the incision rate in the Emet valley was found to be 1.4 cm.yr-1. From here one can calculate a time span of 75 kyr for the formation of the whole valley itself. However, it is known that working of the geological processes was not monotonous in the past; hence, this date is not absolute. Newertheless, formation of the large valleys of the southern Marmara region should not be older than 300 kyr. An important reason rapid erosion was likely lowered base-level as the Marmara Sea was a closed lake during the last Glacial Period. High altitudinal difference between source and depositional areas caused acceleration of for erosion.

1. Introduction

Eastern and southern parts of the Marmara region are characterized with rivers in deep valleys and step like drainage systems (Figure 1). Geology, rock types and active faults in the region are the reason for the morphology (Figure 2, 3). In general the valley slopes are with low and high angles, mountain tops are relatively long and with sharp edged ridges (Figure 4, 6). This is the reason why the region's morphology has drawn attention and has been studied relatively well (Ardel 1943; Erinç 1955; Darkot and Tuncel 1981). In previous work morphologies of the Marmara region were described but nothing notable had been said how and with what processes these morphologies had developed. In the works the origin of the rough land forms were claimed to be related to the young tectonics and that these structures had torn the Oligo-Miocene peneplaines (Pamir 1938; Erinç 1973; Erol 1981; Emre et al., 1998; Yılmaz et al., 2010). The information from these studies enables us to indirectly learn the development time of the landform in the region and it could be stated that present-day morphologies have developed since Late

* *Corresponding author : Nizamettin.Kazanci@ankara.edu.tr*

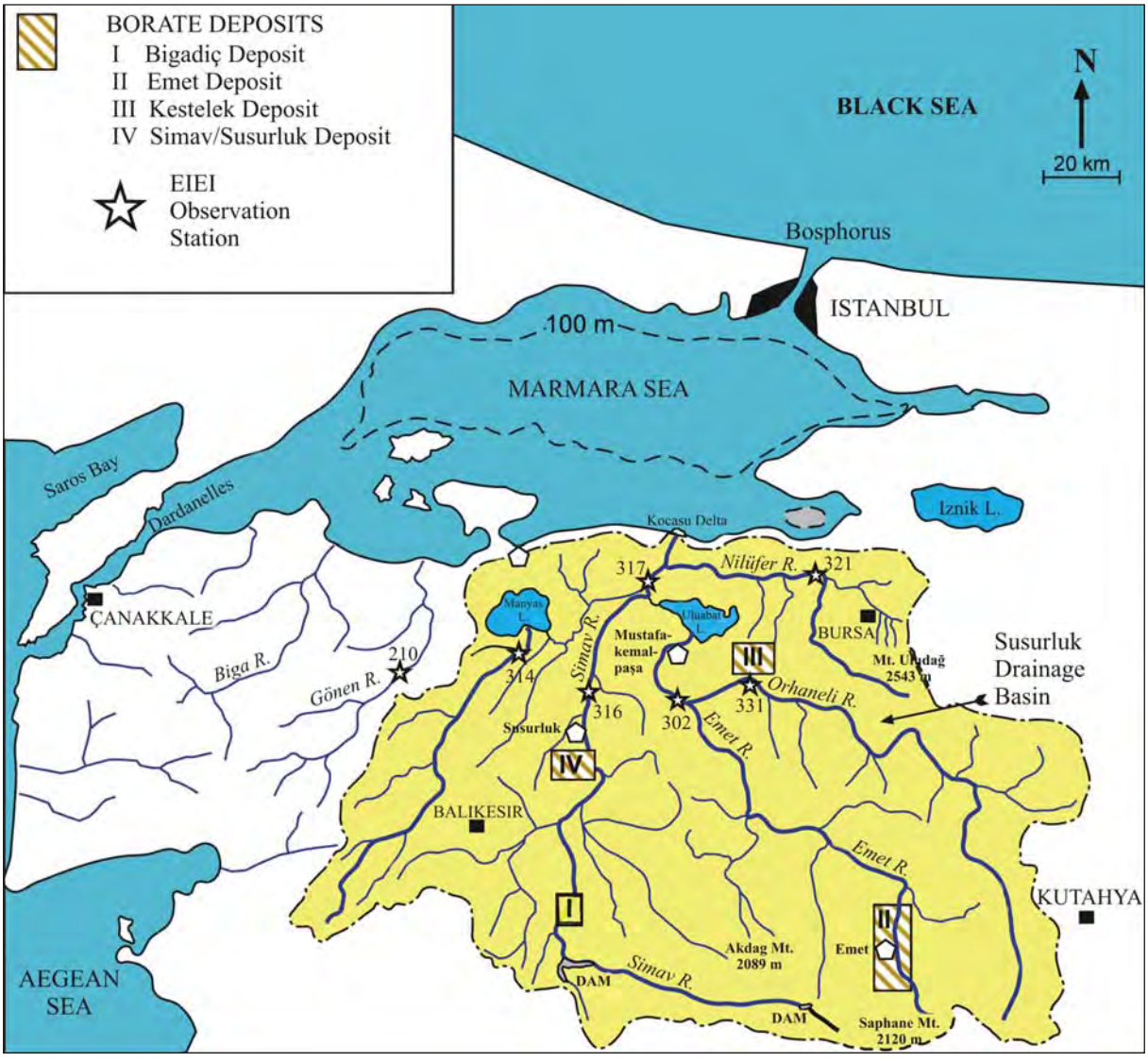

Figure 1- Boundaries of the Susurluk drainage basin in the Southern Marmara region

Miocene. On the other hand detailed geology of the region is well known (Bingöl et al., 1973; Ergül et al., 1980; Gözler et al., 1985; Ercan et al., 1990).

In these studies, apart from describing location, morphologies have not been dealt with. Emre et al., (1998) carried out detailed studies on the notectonic period morphological evaluations of the Southern and more particularly the Eastern Marmara regions, they related the developments and landforms in the Neogen and Quaternary to the regional stratigraphy but they did not give an age in figures. Yılmaz et al, (2010) generalized all of this evolution approach to the whole of the Marmara Sea region. Generation of land forms is slow and includes various complicated processes because of this in many of the geomorphological studies workers try to avoid giving an age for the development time of the medium to large scale landforms. On the other hand not knowing the development ages of the land forms makes them not to be considered as geological data but as a geological problem. The same problem exists in the Susurluk drainage basin (SDB) (SDB is a hydrologic definition and it should be understood as 'water collection area'). There are numerous canyons and/or large valleys in the area. The ages of these features are also not known.

In this study from the deposition rate in the Ulubat Lake an attempt was made to estimate the development ages of the big valleys in the region. Lake sediments have been used as data. General characteristics of the lake deposits, factors controlling deposition and deposition rate have been studied in previous works (Kazancı et al., 2006; 2010). Here the

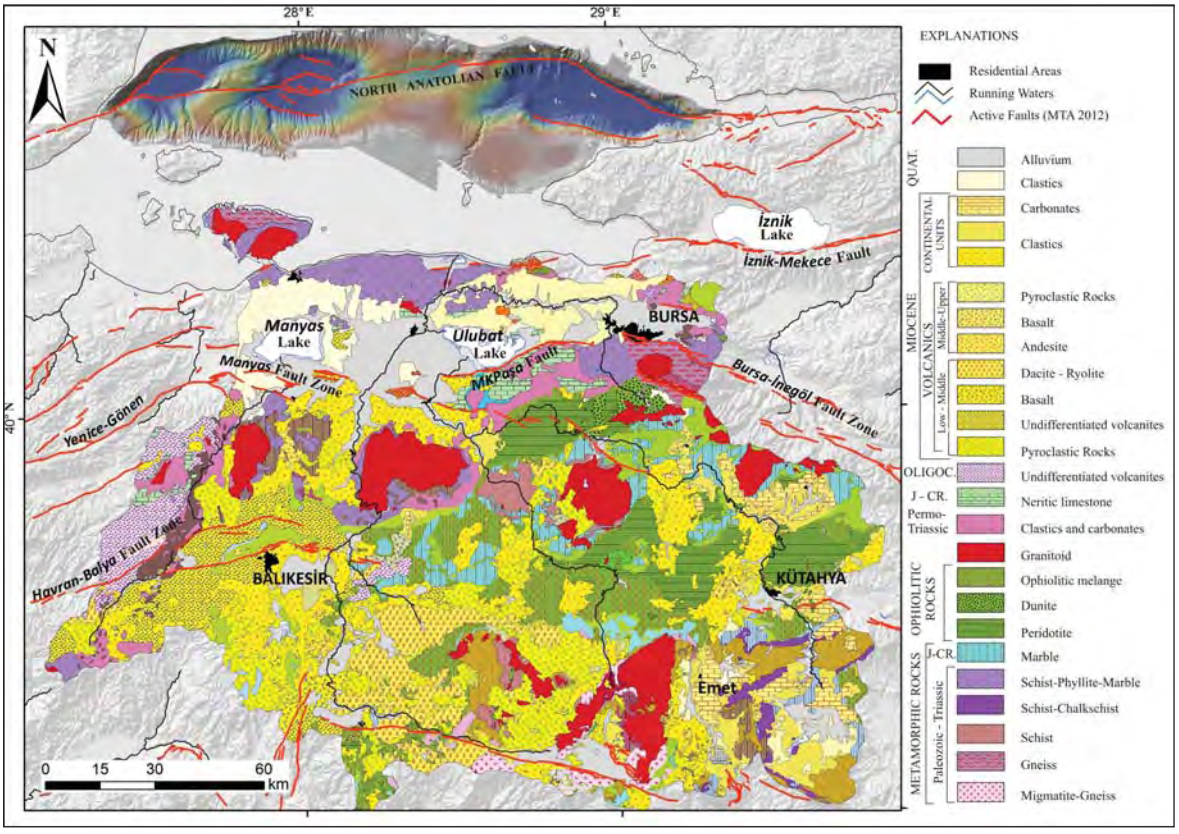

Figure 2- Simplified geological map of the Southern Marmara Region (MTA, 2002 has been used for the distribution of the units; Emre et al., (2012) has been used for the tectonic lineaments. This reference is given as "MTA, 2012" in the reference list).

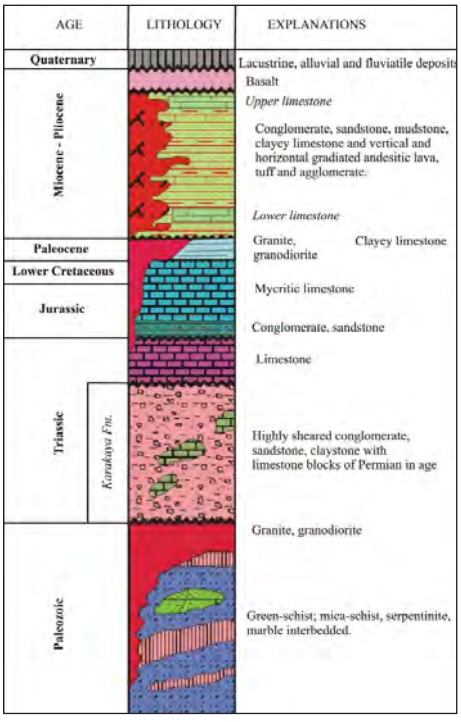

Figure 3- Generalized stratigraphic column of the study area (compiled from previous work. For details look at the text, not to scale).

established balance on the erosion, transport, and deposition for the Ulubat Lake is used to give the age of the landforms in the region. In a particular area if the landforms are not crosscutting one another then they are in general of the same age (Chorley et al., 1984). For example in a karstic region with large and small caves, valleys with differing orientations or volcanic or intrusion features in a volcanic terrain will have developed within the same period of time. Within this period of time, the development time of various size features may be short or may be long. The important thing is, not to know the development age of one single form but the development period of similar forms. Although it may not be absolute but still with knowing the deposition rate or erosion rate development ages may be estimated (Einsele, 1992; Einsele and Hinderer 1998).

In this study age estimations have been attempted for the erosion related medium and large scale land forms in the Southern part of the Marmara Sea, particularly in the Susurluk drainage basin (SDB) (Figures 1, 2) Most distinct valleys in the region have been carved by Simav Stream, Emet Stream and Orhaneli Stream (Figures 1, 4). Rock units subjected

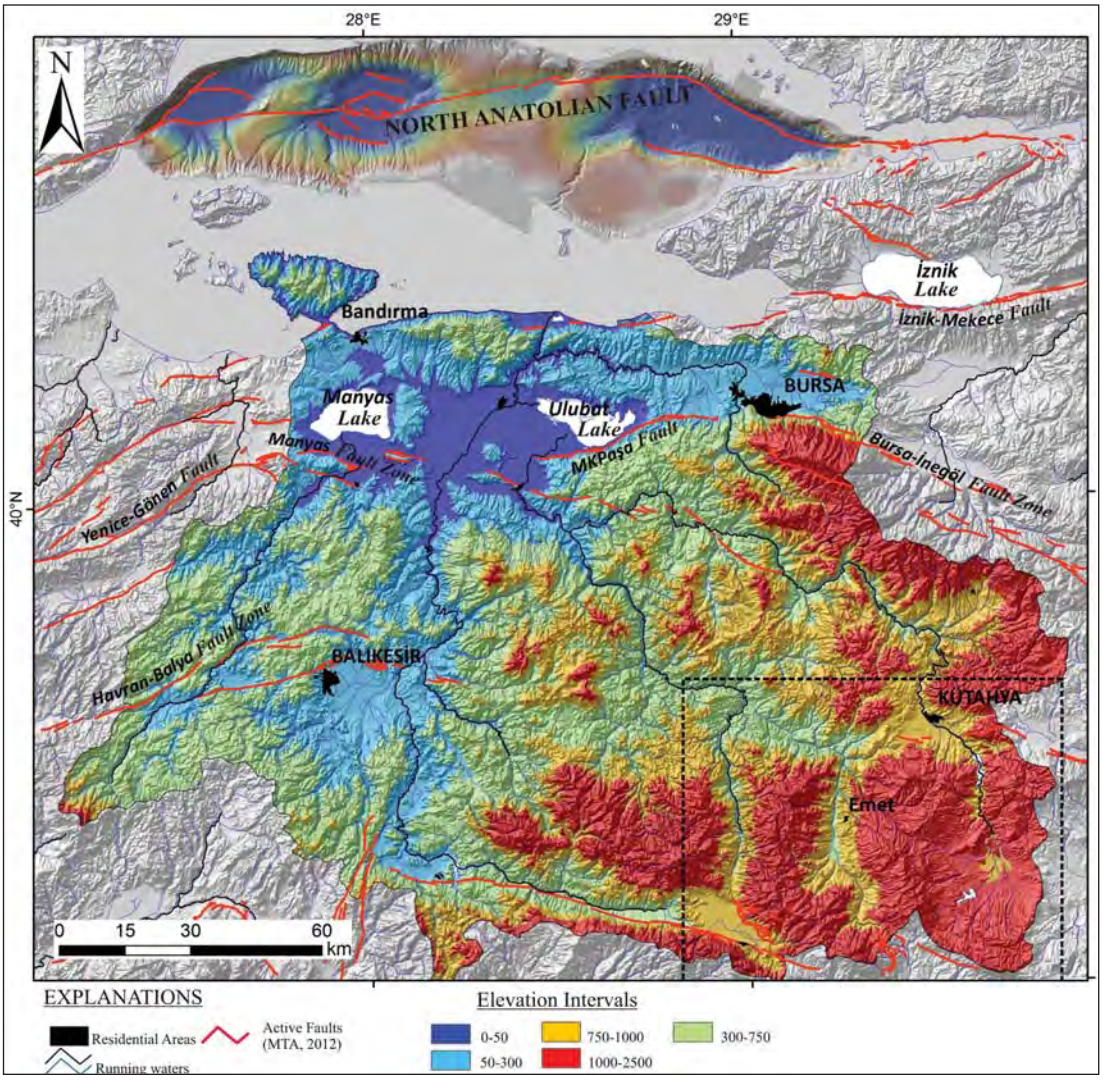

Figure 4- General topographic characters and physographic elements of the Southern Marmara region. Active faults have been taken from Emre et al., 2012. Dotted rectangle is the figure 5 area. Colours in the sea area are not to scale.

to erosion in the region, host particulary boron and many other industrial raw material and mineral deposits (Ergül et al., 1980; Helvacı, 1984, 1986; Ercan et al., 1990).

At present all of the eroded materials with their minerals and trace elements are first transported into Manyas and Ulubat Lakes, the remaining parts are transported into the Marmara Sea through Karacabey pass and deposited there forming the Kocasu delta (Figures 1, 2). When the sea level is low, these materials are carried on farther and were deposited on the Southern Marmara shelf and in the İmralı trench (Emre et al., 1998; Sorlien et al., 2012).

In summary, depositions in the Southern half of the Marmara Sea and in the Ulubat lake on one hand and incision and fragmentation of the SDB on the other form two sides of an erosion-deposition balance. In this study trace elements present in the deposits have been used to estimate caving rate of the Emet Stream valley.

2. Geography

Southern Marmara region mentioned in this study is roughly described as the region surrounded by Çanakkale-Edremit-Balıkesir-Kütahya-İznik Lake-Marmara Sea, in North Western Turkey (Figure 1). As mentioned in the introduction, the Susurluk drainage basin covers about 2/3 of this part (28.000

km^2, Figure 1). Leaving the area between Çanakkale-Edremit-Manyas Lake outside, in the remaining parts of the study area, topography increases from north towards south, reaching an elevation of 2089 m at the drainage dividing line at Akdağ and 2120 m elevation at Şaphanedağ. With 2543 m elevation, Uludağ in Bursa is the highest peak in Western Turkey and is located in the eastern border of the drainage basin (Figures 1, 4).

Manyas Lake and Ulubat Lake are two distinct geographical elements in the study area. These two lakes are situated in the Southern Marmara basin and are 150 km^2 and 138 km^2 areas respectively. The name of the Lake is actually 'Uluabat' but in short it is used as 'Ulubat'. In this study 'Ulubat' name is used. The main streams discharging their waters into the Manyas Lake are Kocaçay (162 km), Simav/Susurluk Stream (321 km), Emet Stream (278 km), Orhaneli Çayı (276 km) and Nilüfer Stream (172 km). Emet and Orhaneli (Stream) streams join together and form the Mustafakemalpaşa Stream and discharges its water content into the Ulubat Lake. The streams leaving the Manyas and Ulubat lakes and the Simav Stream and Nilüfer Stream before reaching to the sea they join together and become the Kocasu River. This Kocasu River has a rather large delta developed in the Marmara Sea (Kazancı et al., 1999). Biga Stream and the Gönen Stream are the other important running waters in the region but outside the SDB basin. They also flow through the big valleys. Kazdağı and neighbouring peaks are important topographical heights in the drainage basins. In this part the general slope is westwards (Figure 4). The region receives in general more rain than Turkey's average (Erdoğan, 1988).

3. General Geology

The Southern Marmara region has rock units from Paleozoc to Quaternary (MTA 2002) (Figures 2, 3). Uludağ and Menderes metamorphic massifs are within the region. They attained their topographic heights in Neotectonic period (Ergül et al., 1980; Yılaz et al., 1990; Okay, 2008). Basement rocks are overlain by Neogene sediments with low topography and Quaternary sediments (deposits) in the low plains (Figures 2, 4).

The stratigraphy of the area has previously been well studied (Bingöl et al., 1973; Gözler et al., 1985; Yılmas et al., 1990; Okay et al., 1991). Late Tertiary volcanics, detritic sedimentary rock, clayey limestones and evaporites are the main units present in the study area (Figures 2, 3), Metamorphic rocks and carbonates are present in lesser amount and form the higher grounds in the southern parts (Yalçınkaya and Avşar, 1980). Miocene units in general have at the bottom stream-lake sediments, towards the upper parts lava flows, tuff and clayey limestones and marls alternate with tuffites. These Miocene lake deposits cover relatively extensive areas around Simav and Emet (Baş, 1987; Ercan et al., 1990). These units host mainly borate and various other mineral deposits (Helvacı and Firman, 1977; Yalçınkaya and Avşar 1980) (Figure 2). Borate bearing Neogene sediments (Borate deposits) sit on the lake limestones (in the local stratigraphy they are called 'Alt Kireçtaşı-meaning Lower limestone which has clayey marl lithology (Figure 3). On top of the borate deposits there are limestones with silicified parts which are resistant and have protected the borate deposit from erosions (Helvacı, 1986). At the very top of the succession the units are lava flows, volcanic breccias and agglomerates. In places where these hard resistant units were broken, fragmented, large deep valleys developed (Figures 4, 6).

Topographicaly lower parts of the Southern Marmara region are mainly covered with thin Quaternary, mostly alluvial and fluvial sedimentation (Emre et al., 1997*a*, *b*, 1998; Kazancı et al., 1997, 1998). Karacabey-Manyas plains which are a typical example of the young cover, has extensive coverage within the SDH. The plain's base is Late Pleistocene –Holocene and has discordant contact relation with the units below and consists of loosely cemented sediments. To the south of the town Mustafakemalpaşa in the thickest part, drillings intercepted 40 m thick young sediments. The upper part (Middle –Late Holocene) is the same age as Manyas and Ulubat Lakes (Emre et al., 1997*b*).

In summary; in the stratigraphy of the Southern Marmara, it is noticeable that Middle-Late Neogene sediments cover large areas and drainage systems with deep valleys primarily developed in these units (Figures 2, 3).

3.1. Morphotectonic Characters

Three main group of landforms with different development processes and ages control the morphology of the Northwestern Anatolia. They are from north towards south Kocaeli-Trakya (Thrace) peneplaine, Marmara Sea and Southern Marmata plateous (Pamir, 1938; Şaroğlu et al., 1987; Emre et al., 1998; Yılmaz et al., 2010). Distinct topographic

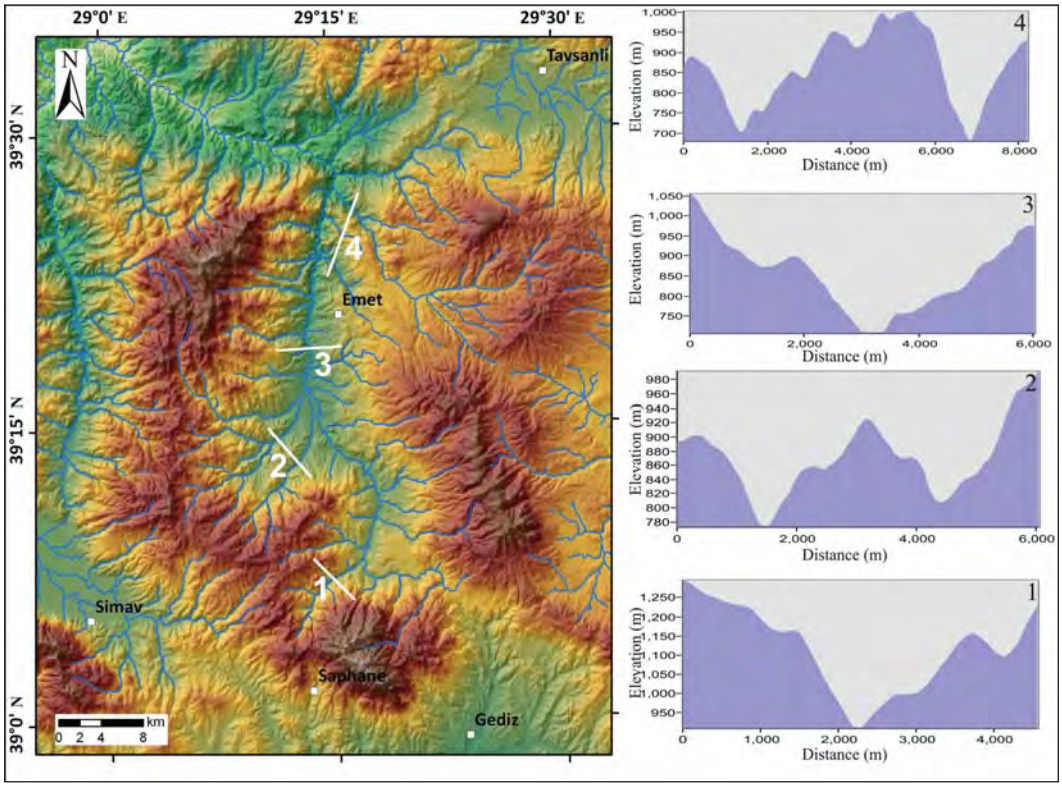

Figure 5- Secondary cleavages in the Emet valley and topographical sections.

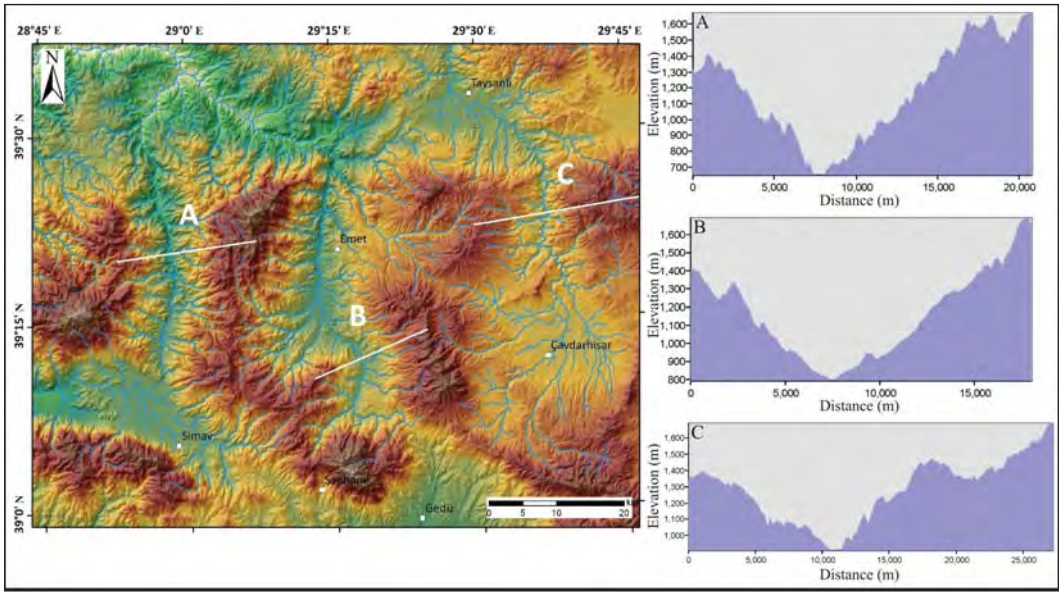

Figure 6- Large valleys in the Susurluk drainage basin and their topographic sections. A Alapur valley, B Emet valley, C Orhaneli valley. Note that valley depths change between 700 and 1200 meters.

disharmonies provide transitions among these reliefs. Oligocene-Miocene Kocaeli-Trakya peneplaine is a residual topography representing Paleotectonic morphology in the region. It helps to understand the Neotectonic period morphological changes and is kind of key area for that matter (Emre et al., 1998). The Marmara Sea basin between the Kocaeli-Trakya peneplaine and the Southern Marmara plateous actually consists of numbers of tectonic depressions developed in the Northern Anatolian Fault Zone

(NAF) (Figure 4). These tectonic depressions were flooded through İstanbul and Çanakkale straights and acquired marine form. Thickness of the filled in material in this marine basin located along the NAF system is about 6 km, indicating a high rate of tectonic subsidence.

The Southern Marmara plains of the study area are the most distinct landform in the region. Gently sloping plains/slopes with 200 - 800 m elevations are common morphological features (Figure 4). The heights made of crytalline units form irregular mountainous parts (Figure 2). As some of these heights consist of erosion resistant rock units, so they represent residual Pre-Paleotectonic period topography. On the other hand some of these heights like Uludağ and Kazdağ are surrounded by active faults and they are the landforms which gained their heights in the Neotectonic period. Erosional and tectonic depressions/basins filled with Quaternary sediments are the morphologic landforms buried in the low height belt in the gently sloping plains/slopes in the Southern Marmara regions. Manyas and Ulubat Lakes are located in the Karacabey-Manyas depression. Karacabey–Manyas depression, Balıkesir plain, Simav plain, Tavşanlı plain are some of the important examples of these features (Figures 2, 4).

Physiographic extensions in the region within the above explained general form developed in the Neotectonic period and are in accord with the present day active fault zones (Şaroğlu et al., 1987). MTA recently published an updated 'The Active Fault Map Series'. These maps provide the opportunity to make correlations between morphological features with the active faults in the region (Emre et al., 2005, 2011 *a*, *b*, c; Emre and Doğan, 2010). NAF is in the form of a plate boundary. Northwestern Anatolia is situated in the transition zone between the NAF and Aegean graben systems which has developed within the Western Turkey tectonic tension regime. The NAF zone is the main tectonic structure separating the Kocaeli-Trakya peneplaine and the Southern Marmara plains (Emre and Doğan, 2010). The faults controlling the present-day morphologies in the Southern Marmara are in two groups. The fault in the north extending between Geyve and Bandırma is the southern branch of the NAF. This fault is separating the Marmara Sea basin and the Southern Marmara plains (Emre et al., 2005). Geomorphologic evolution and running water cleavages (stream valleys) are the results of climatical processes and tectonics.

4. Material and Method

In this part first of all hypothetic approaches will be explained as they formed the basis of the interpretations. Field and laboratory data will be dealt with later

In the geographic use land forms are explained on the base of average elevation of the location and according to this average value land forms are described as plains, hills, mountains, ridges and valleys. Ridges and valleys are the main elements showing land reliefs in a region. Running water valleys have developed by means of lateral and deep scouring and are the channels in the drainage basin transporting and depositing materials altered and eroded in the denudation process. So knowing the occurring and developing ages of running water valleys is important. That is the same as knowing the starting age and evolution processes of the landforms in that particular area. In other words with this, ages of landforms are made known.

In this sudy to give ages to the valleys Emet borate deposits cut through by Emet Çayı (Emet stream) is a suitable guide (reference) (Figure 1). In this area the first borate operation started in 1956 and since 1970 the number of pits has increased. In different locations Espey 1, Espey 2, Killik, Hamamköy, Hisarcık mines started operating and have been operating with differing production rates. Mineralogical and chemical data on these deposits are given in Helvacı (1984, 1986) and Helvacı and Alonso (2000). According to these studies there is more than one kind of mineral in these deposits colemanite being the most important mineral. The generation of borate mineralization is related to the introduction of the volcanics into the lake environment.

At present the entrances of operating borate mines (Espey 1, 2, Hisarcık, Killik, and Hamamköy) are in the Emet Çayı valley and they are about 15 m above the present base of the valley. In other words, naturally or artificially the valley base has been scoured 15 m down through the borate deposits. As this is the discharge area for the river, the waters started cutting through the borate deposits and the boron element flowed into the Ulubat Lake. The rate of accumulation would be more than when it first started. With this approach, recent excessive boron accumulation in the lake has resulted during the time span for this 15 m deep down abrasions. Erosion depth obtained from this correlation would be

generalized to the total valley depth. With this correlation the valley development time span and abrasion rate would probably be estimated.

In the SDB there are borate deposits (Kestelek deposit). At present the mine is operating by open pit methods, the drainage of it is by means of the Orhaneli Çayı (Figure 1). Here the mine is below the thalweg elevation. To reach the mine, excavation is necessary. (The borate deposit has not been subjected to the natural erosion yet). So in this study the source of boron ion in the Ulubat lake is considered to be the Emet deposits.

The data used in this study have been obtained from the work carried out in the Southern Marmara region during 1995-2005. Findings of these studies have previpusly been reported in Kazancı and Görür, 1997; Kazancı et al., 1998; 2003 and also in the papers on; Limnology, Paleo-limnology, Environment and Environmental Pollutions, Lakes Geology, Active Tectonics, Geological Evolution of the coasts of the Marmara (Emre et al., 1998; Leroy et al., 2002; Kazancı et al., 2004, 2006, 2010). In this study some data on the Ulubat Lake have been interpreted on the development of land forms.

The first limnology studies on the Ulubat Lake was carried out during 1997-1998, the drillings in the lake were conducted in 2002 and 2004 (Figure 7). Field methods and results achieved have been given in detail in Toprak (2004) and Kazancı et al., (2004). Some of the processes and prominent findings are; in the lake 1-10 m long 12 separate core samples from 5 different locations were taken by using '52 mm diameter Livingstone corer' sampler (AK02LV1-12, AK04LV1-3). In the lake near to the shore, in the shallow parts 1.2 – 1.8 m long 5 core samples were taken in 2 m long plastic tubes (AK02PVC1-5). Every recovered core samples, at 2 cm intervals; grain size, magnetic susceptibility, organic material contents, carbonate contents, pH, heavy metal contents, arsenic (As) and boron (B) contents were analysed (Figure 8). Additionaly the upper parts of the core samples near to the lake surface were analysed for Pb^{210}, Pb^{214} and Cs^{137} isotopes in the Physics Department at Dublin University. The lower parts of the cores were analysed for ^{14}C (Poznan, Poland). And each given their age separately. Ages given in the first two methods showed variations with short intervals. Ages given in the last method showed variations with long time intervals. Both methods are considered to be reliable (Leroy et al., 2002; Kazancı et al., 2004). As the analyses on the cores were conducted with 2 cm intervals, this showed that all these analyses results have changes all along the core lengths, meaning how the environmental conditions in the lake have changed in time from the past to the present. In this study critical data were the boron content of the cores (Figure 7).

Boron contents in the lake sediments with the other pollutants were analysed in the laboratories in the Gebze High Technological Institute. In general in whole of the cores (B) contents show sudden increase at the 400 cm and 50 cm depths (Kazancı et al., 2004; Toprak, 2004). This sudden increase shows that there were sudden boron introduction to the lake, indicating larger amount introducted to the lake from the source area. These changes have also been reported in other studies (Turgut, 2005), (Figure 8).

5. Findings

5.1. Susurluk Drainage Basin and Emet Stream

In the Susurluk drainage basin in the Southern Marmara region, there are numerous and differing types of valleys, namely short, long, deep and shallow valleys (Figure 4). This drainage web discharging into the Marmara Sea is set up on the Southern Marmara Plateau with elevations between 200 and 800 m. Large rivers flow into deep and narrow valleys buried into the plateau surface (Figure 4). Some joining troughs developed along their lengths through tectonic and erosional processes joining the basins and superimposed and buried meanders in the Pre Neogene basement rocks are the common character of the large rivers in the SDB basin. Orhaneli Stream, Emet Stream and Simav Stream basins are the water collecting channels (Figures 1, 4). Because of this, the data collected along the Emet River can be generalized for all running water in the basins.

The Emet Stream valley is one of the deepest cleft in the area. It traverses the middle and Southeastern parts of the SDB which represents at least 2/3 of the whole of the area (Figures 1, 4, 6). Second character of this part is; all of the waters and the sediments collected from the eroded parts are first transported into the Ulubat Lake and afterwards to the Marmara Sea through one channel (The Kocasu River) (Figure 1), That is to say Ulubat Lake and the Kocasu delta are the lithological representative of the whole of the SDB (Kazancı et al., 1999). EİEİ and DSİ have quality control observation stations at the locations where streams reach and leave the lakes. In addition

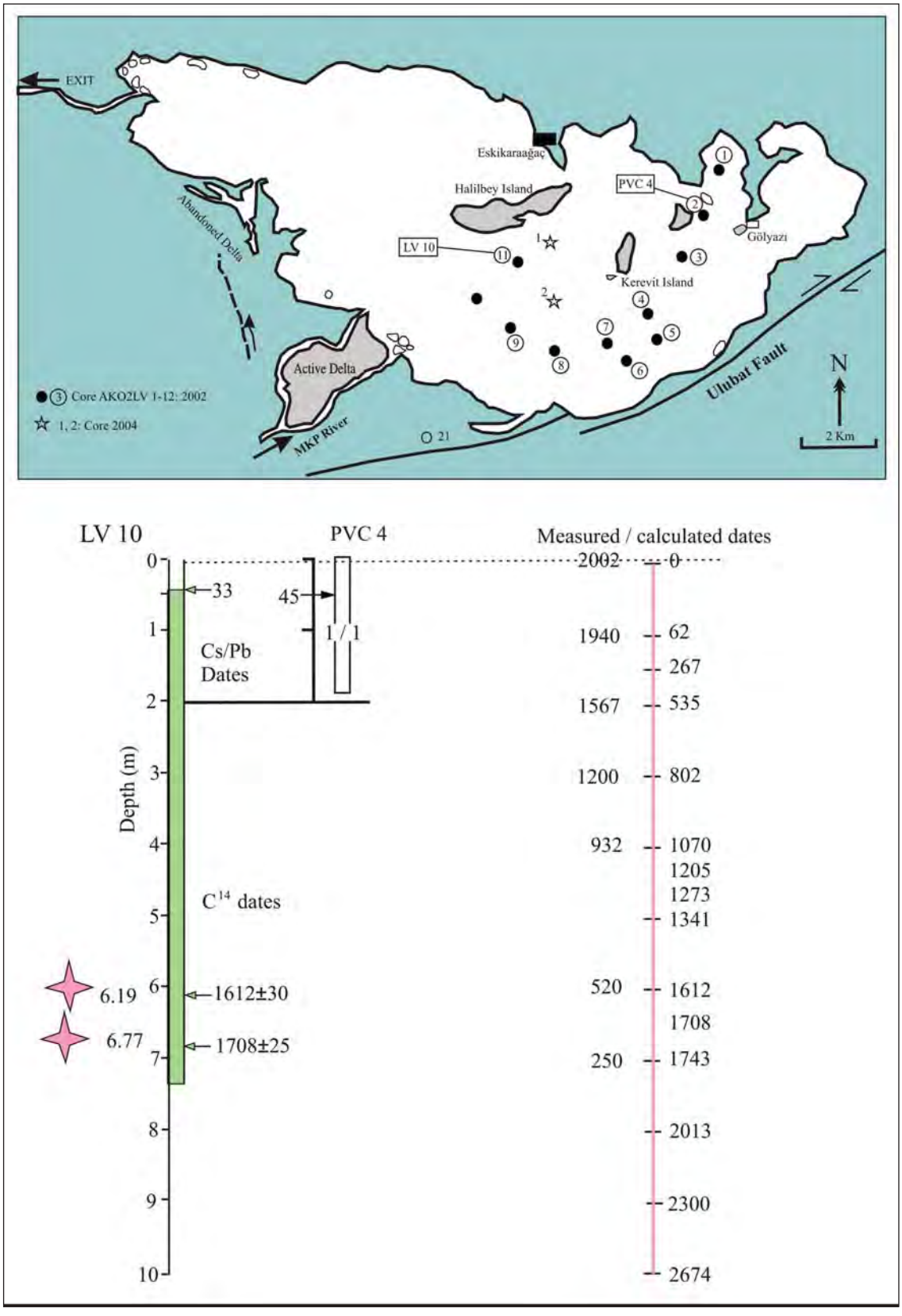

Figure 7- Drilling locations in the Ulubat lake and depth-age relations obtained from the recovered cores.

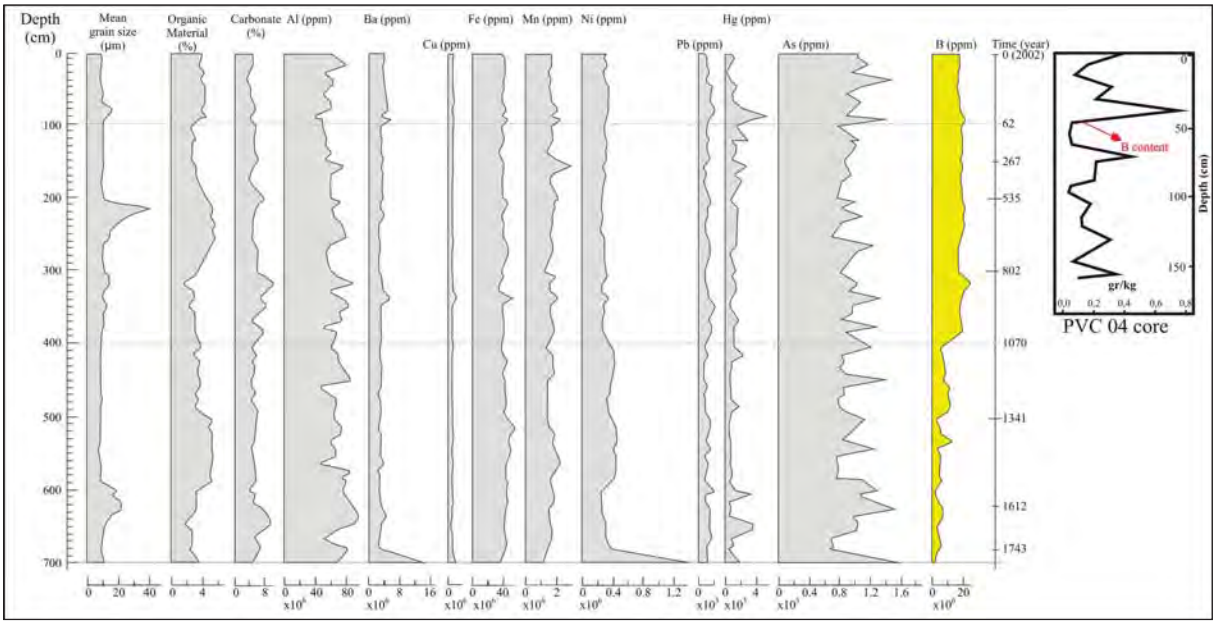

Figure 8- Grain characters of the Ulubat lake sediments and vertical distributions of some of the elements

to all other data, analyses of EİEİ and DSİ have also been taken into considerations (Figure 1) (EİEİ 1993; 1996; 2000). In short all available data have been collected to evaluate the hydrologic, sedimantologic and climatologic characters of the SDB. In recent years numbers of large and small dams have been constructed so the amount of sediments transported into the lakes has decreased. The total amount of material the Kocasu River transports is estimated to be 464,950 ton/year, and the eroded amount is 115 ton/year/km^2. Same estimations for Mustafakemalpaşa Stream (MKP) are; 1,258,143 ton/year and 167 ton/year/km^2 (EİE 1993; Kazancı et al., 2004).

SDB could be divided into four morphological areas. First one is the alluvium plains acting as pre sedimentation basin before rivers reach the final discharge point, the Marmara Sea. Manyas-Karacabey plains are situated in the area morphologicaly known as Southern Marmara Depression. It extends E-W direction, is tectonic in origin, and has been shaped and achieved their plain character by the channel floodings of the Kocaçay and MKP Stream (Emre et al., 1997 b). This depression gently slopes eastwards, the Manyas lake is situated at the west end (average elevation of the water level is 14 m) and the Ulubat Lake (average elevation of the water level is 2 m) (Figure 1). They both are shallow fresh water lakes. They used to be considered very old and tectonically developed but it has since been shown that they developed in Holocene as a result of blockage of their course (Emre et al., 1997 a).

The second morphological area is the hill side which is of eroded origin zone (slope zone) extending to the present day valley base and the plains. This zone also reflects the subject of study 'sinking (burial) of running waters. Valley slopes have high angles. In some parts they are escarpments and have tectonic origin and in some parts they have rugged topography of ridges and hills, which are the remains of high plains. About 20-25% of the SDB is made of these kinds of areas.

Third morphological unit are the 'erosion plains'. Erosion plains have 200-800 m elevations and their heights in general increase from north to south. Erosions developed on the basement rocks and Miocene-Early Pliocene successions. The SDB erosion plains were shaped after Early Pliocene and it could be said that regional scale 'sinkings of running water' have developed after this period. These plains form about 55-60% of the study area.

The fouth morphological area is the 'high ridges-mountains', heights on the erosion plains (Figures 1, 4, 6). This area is mostly forest covered and they form about 12-15% of the study area. Akdağ (2089 m), Şaphanedağ (2120 m), and Uludağ (2543 m) are the prominent peaks and they form the water dividing lines (Figures 1, 2).

Medium and large size valleys are situated in the hill side zone in the study area. Development age of these features will be a subject of this work. The

Simav valley, Emet valley, Orhaneli valleys are the most noticeable in the SDB and are quite alike with their slope morphologies (Figures 4, 6). Their lengths vary. For example although they have the same name the Simav Stream is longer but Simav valley is shorter (about 45 km) than others. Digital topographical data analyses show that Orhaneli Streamvalley is 220 km long; Emet Stream valley is 225 km long. The end of the two valleys is the place where the waters meet and there onwards it becomes the Mustafakemalpaşa Stream (Figures 1, 4). At the source area the elevation of the valley base of the Emet valley is 1250 m but about 30 km down the valley towards Emet town it drops down to 750 m elevation. Still, despite of this fast fallin the elevation, the average slope angle of the Emet valley is 004%.. Elevations of the valley hill sides are 1650-1250 m. Despite of the deep valleys there are no g troughs because the land is made of loose Neogene units (Figure 2).

The Bursa meteorology station reports that the 52 years average rainfall in the area is 710 mm. Based on the EİEİ's data, it has been calculated that Mustafakemalpaşa Stream carry 1.3 x 10^6 tons of suspended materials a year and erosion rate is quite high (Kazancı et al., 2004). Among these transported materials boron and some other heavy elements have been scoured from the borate deposits within the Emet valley.

5.2. Ulubat Lake sediments and their age

As it was mentioned in the previous part the subject of this study is the lake bottom sediments of the shallow Ulubat Lake (maximum depth 2.5 m). Ulubat Lake is a fresh water lake and occupies 138 km^2 areas. The Limnological characters of the lake have been studied previously (Kazancı et al., 1998; 2006; Çelenli, 2000; Toprak, 2004). Water level of the lake shows climatical variation and because of the pesticides the lake is getting increasingly polluted. There is no lake protection management. So this is speeding up eutrofication Çelenli, 2000; Dalkıran et al., 2006; Reed et al., 2008; Kazancı et al., 2010).

Sedimentation is transported to the lake by means of the Mustafakemalpaşa Stream and this river has built up a delta at the south shore (Figure 7). With the incoming material this delta is enlarging and is in the impact area of the Ulubat fault (Emre et al., 1997*b*). The amount of material transported into the lake is about 1.3 x 10^6 tons of suspended materials. Within thelast 30 years sediment accumulation in the lake floor has reached 1.6 cm/year (Kazancı et al., 2004). Materials on the lake floor are; silt bearing mud. It is bluish gray coloured and in places has abundant organic material. The drillings carried out in 2002 near to the south shore, recovered most 7.8 m long core. In 2004 10 m long cores were recovered in drillings carried out in the central part of the lake, as the drills started intercepting hard rocks so they could not advance any longer. Around the lake area Pleistocene rocks of a type unlike the lake type are present. Based on the non lake type detritial sediments encountered in the drill cores is considered to be the basement rocks of the lake floor on which the lake developed. This suggests that the maximum thickness of the deep sediments of the Ulubat Lake is about10 m.

In the above section detail information have been given on the characters of the drillings, core names, and core samples for analyses were taken at 2 cm and 10 cm. Total organic material and total carbonate contents show variations in cycles but mineralogical contents are sporadic (Figure 8). In the lake sediments evaporites and some other chemical sediments indicating closed environments have not been detected, indicating that the lake in the past was in the same condition as it is now. Pollen analyses indicate that before the lake was formed the area was marsh land for a short period. The area then acquired fresh water and the marsh developed into the lake (Kazancı et al., 2004).

The most interesting point on the subject is the sudden increase in Boron content found in the cores between 400 cm and 50 cm depths (Figure 8). The boron content is from lower parts up are on average 0.6 g/kg. At the 400 cm level it shoots up to 1.8 g/kg. The boron content decreases between 100-50 cm levels and between 50 cm-0.00 levels again show increase (Figure 8) This must be directly related to the borate deposits in the source areas.

To be able to understand the changes, depth-age model of the lake sediments has been set up (Figure 7). The age of the sediments from the upper part to 45 cm down have been determined by Pb^{210} method and have been found to be 33 years and 40 years by the Cs^{137} method, deposition rates were 1.6 cm/year and 1.48 cm/ year. At the 619 cm level, plant seeds with the ^{14}C method have given 1612± 30 years (calibrated) age and at 677 cm level, plant remains gave 1708± 25 years (calibrated) age. These values represent 0.37 cm/year (400 cm/1070 year; 1000 cm/2674 year) deposition rate. In general the oldest

sediments in the lake were 2670 years old. In the same way according to the deposition rates, the dates of the 400 cm and 50 cm levels where boron contents showed sudden increase were, according to the Gregorian calendar, AD 932 and AD 1971 (Figure 7).

6. Discussion and Conclusions

Erosion and deposition rate in SDB. It has been known for over 2 centuries that climate and erosion in connection with it play important role in land forming processes, to be able to make it understandable various models have been proposed (Chorley et al., 1984, p. 19-42 and documents in it). In a particular area if sediments developed by erosions are swept away and are deposited in a particular place, then for that particular place the denudation rate could be calculated (Einsele, 1992). Major and trace element contents act as a guide to erosion-accumulation balance, so if these elements are present then reliable calculations can be made (Einsele and Hinderer, 1998).

The material eroded from the Emet valley transported and accumulated into the Ulubat Lake has high boron contents. High boron content helps to understand the role of the climatological-lithological changes in the development processes of the valley. As stated previously the age of the sediments in the Ulubat Lake, down to 45 cm from the top has been found to be 33 years (or according to the sampling date 2004-33 = 1971) and age of the sediments at 400 cm level has been found to be 1070 years (as a date (2004-1070 =934). The year 1971 (33 years old) coincides with the intensive open pit borate mining activities in the source areas. This time connection explains the relation of high boron contents in the Emet Stream with the open pit borate mining, causing sudden increase in the boron content in the deposited materials in the lake. This topical approach could be extended to the sudden boron increases 400 cm of depth cores. At present borate deposits are about 15 m above the valley base. This approach indicates that during last 1070 years borate deposits have been abraided 15 m down from the upper most elevation (Figure 9). From this, abrasion rate of the rivers within the borate deposits has been calculated to be (1500 cm/1070 year) 1.4 cm/year.

This abrasion rate calculated for the most recent part of the Emet Stream valley may be found quite high for the wide intervalled geological events, but there are examples of relatively short periods in the literature (Clayton, 1998; Einsele and Hinderer, 1998; Wilson et al., 2003).

Taking the calculated abrasion rate and the lithological succesion into consideration it has been calculated that it has taken 75,000 years of abrasion for the valley to become 650 m deep as it is to day. In

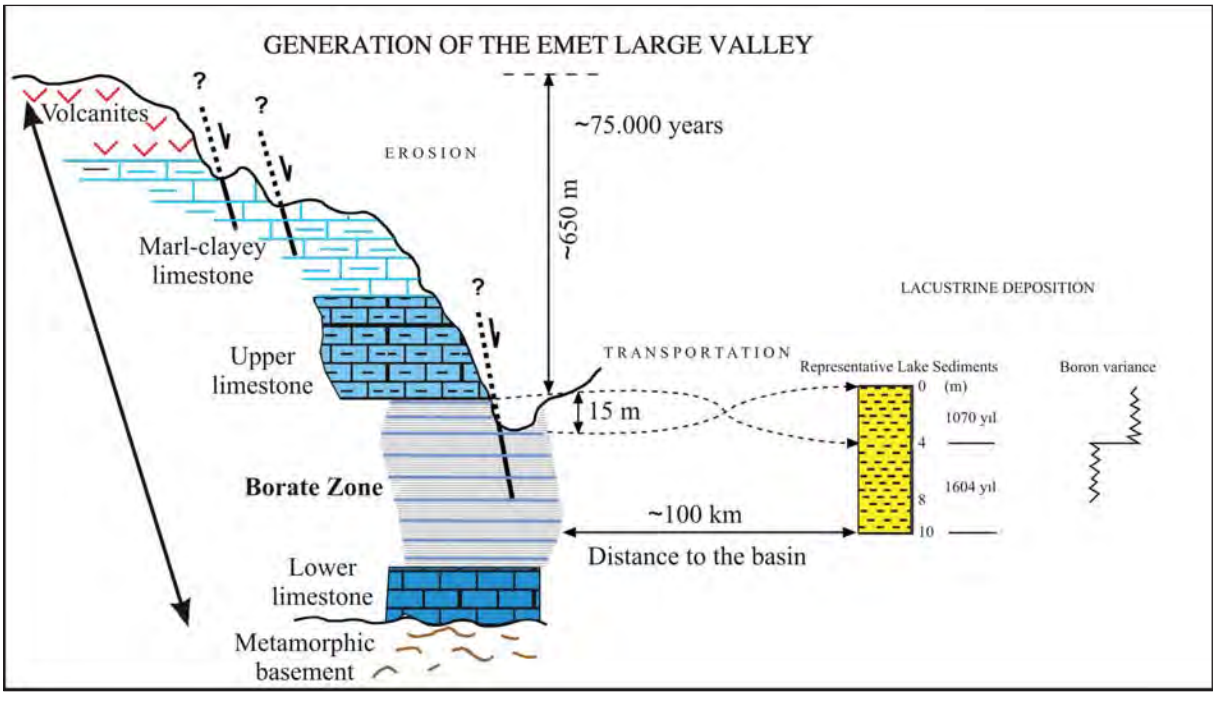

Figure 9- Generation processes of the Emet valley and the age.

the Emet area the borate-bearing Neogene succession in the upper parts have relatively eosion-resistant limestones with silica intercalations (Figure 9). The Schmidt hammer tests conducted on these limestone samples showed that these limestones were at least twice more erosion-resistant than the borate-bearing units. This indicates that the erosion rate of the silicified limestones was half rate of the others (0.7 cm/year), in other words they were eroded twice as late. Geological studies show that with foldings and repetitions the thickness of the limestones is estimated to be at most 400 m (Helvacı and Firman, 1977; Helvacı, 1986). When necessary calculations are made (400 m/0.7 cm/year), the abrading age of the resistant successions has been found to be 57,000 years. The remaining borate-bearing succession with volcanics (about 250 m thick) with the normal abrading rate would be about 16,500 years. With all these calculations the valley has processed its development within 73,000 - 75,000 years (Figure 9). In these calculations it is assumed that erosion continued uninterrupted right through. This point is discussed in the next section.

Incision age of the Emet River valley. The Resistance of rocks to mechanical loads can easily be measured by various methods in the laboratories (2 and 3 axis stress tests) and in the field (Schmidt hammer). The data obtained from these tests are taken into consideration when studying the engineering structures. In general hard rocks have higher mechanical resistance. But resistance being high or low does not necessarily mean that it is more or less resistant or resistant to the natural erosion (abrasion). Natural erosion resistance depends on various parameters, among those 'slope angle'; 'climate'; 'rain type' are most important (Ghorley et al., 1984; Selby, 1994). In a particular area natural erosion can be expressed indirectly with 'erosion or transported sediment load'. On this subject 'transportation of a unit amount of sediment load from a unit area' can be very meaningful (Selby, 1994). Emet Stream in its course downstream joins the MKP Stream. The erosion caused by the Emet Stream and MKP Stream(=swept sediment load from a unit area) with 167 ton/year/km^2 which is relatively quite a high value. Even half of this value is considered to be quite high erosion rate for narrow strech of lands (Selby, 1994).

Radiometric dating carried out on the core samples recovered from the lake showed that the emplacement age of the Ulubat Lake is 2670 years and average deposition rate of deposits has been found to be 0.37 cm/year. The variation of boron contents in the lake sediments has a direct connection with the erosion rate in the borate deposits in the resource area. From this connection abrasion rate in the Emet Valley (1.4 cm/year) which is about 4 times more than the deposition rate in the lake. It was supposed that, within the same drainage system, deposition would be equal to the erosion rate. But as the Ulubat Lake is an open lake, so it is now believed that large amount of material is re-transported to the Marmara Sea. This is how the differences can be explained.

The SDB is characterised with the presence of numerous valleys, because of this, topography in the district is rather rugged. It is in fact one of the most rugged land in the Northwestern Turkey (Figures 4, 6). V-type valleys and sharp ridges are the reason of the Neogene units covering large areas. The presence of numerous shallow and deep valleys in the region clearly shows that in the regional geomorphic system erosion was highly effective. This can be seen more clearly in studying the areal photographs and in field works. Most important of all is to know the erosion period and the reasons for trigering this much erosion. Conditions in the study area (drainage) was carried in one stream only. The presence of boron ion and variations on its abundancy, dating of the Ulubat Lake sediments, abrading of the borate successions on the Emet valley floor made it possible to calculate the rate of abrasion. In the previous part with retrospective calculation of the erosion rate, generation and development age of the 650 m deep Emet valley was found to be 75000 years. The handicap in this calculations is that it was assumed that erosions continued regularly at the same rate, like non stop sawing. Changing climatical conditions, movements on the interface and general floor levels, tectonics, anthropogenic effects would change abrasion rates. On the other hand however much there may be some missing points in the calculations generation age would not be taken any further than 300,000 years back from Middle Pleistocene. Otherwise it would not be possible to explain the accumulation rate in the lakes.

From the records of the EİEİ observation stations in the area, erosion-deposition rates in the area are quite well known. These informations could be generalized for the entire Southern Marmara region. For example, stratigraphy of the sediments in the Ulubat Lake is similar to those in the İznik Lake as it is in the Manyas Lake (Leroy et al., 2002; Ülgen et al., 2012). On the other hand within a wide period

interval it is not possible to know at what intervals and speeds erosions have developed. Excessively high and low temperatures, torrential rains, floods, hurricanes, etc may cause replacement of large amount of materials, but they are not long-lasting events and they do not represent the whole of the erosion time. Various age determinations showed that during the ice age in various parts of Anatolia rates of erosions and accumulations showed many variations (Landmann et al., 1996; Eastwood et al., 1999; Fortugne et al., 1999). So it is possible to say that large-scale valleys within relatively wide span of time interval (last 300,000 years) developed with varying erosions rates. What is certain is that, in Western Anatolia during the last 20,000 years, erosion rates have increased and changed considerably. It is noticeable that Prehistorical cultural remains for example tools made of stones are rarely found in Turkey, less than expected (leaving aside that excavations for these items are not as much as it should be) it is probable these items were subjected to high rate erosions and transportations. Many of the stone-made hand axes were probably carried away from their original sites and were buried under the lake and/or under sea sediments.

The SDB area basal elevations of the medium and large valleys are between 600 – 700 metres (Figures 5, 6). Depths of the valleys are at least that much. In most places they exceeds 1000 m and these deep valleys are quite close to the sea (Figures 1, 4 – 6). Considering the necessary erosion-transportation balance it is difficult to explain the develoment of valleys with a base close to the sea level with the present day morphology. It should be considered that during the last ice age and the period before that the Marmara Sea was a small closed lake (Smith et al., 1995; Aksu et al., 1999; Çağatay et al., 2000). That means the base level was much lower than what it is to day. When the previous landforms before the valley had developed are considered with reference to their base, they are 2500 – 3000 m lower now. Because of this height difference the Emet valley and their equals have been deeply abraided. At the present time sea level/base level elevation ratio is at maximum, so relative the abraiding rate is at minimum. Even then still abrasion rate is still 1.4 cm/year. It is understandable that erosion rate in the past was higher.

Are the valleys abraiding in the SDH related to the tectonic or to the climate? It is known that erosion-transport-deposition dynamics act according to a known base/ base level ratio, abrasion does not go below this level. Leaving some exceptional cases aside, reasons for deep abrasions (= base level dropping down) when either climate or tectonics being more effective (Chorley et al., 1984), increase in the sea level (= base level) cause drawning (flooding) of the running water valleys with alluvium (abrasions are reduced at the base but it can cause lateral abrasion). When this point is considered, the water level in the Marmara Sea is the base level for SDB, so it could be concluded that water level in the Marmara Sea is effective in the development of the valleys. In the Marmara depressions there are overlapping delta successions, these show that water level was very changeable, indicating that they went down to the basin's floor (Sorlien et al., 2012). Seismological records show that Kocasu Çayı followed a large submarine canyon at -85 m level and discharged its water into a lake in Çınarcık basin. This may show that during the last ice age deep abrasions must have caused the level of the SDB lakes to deepen. On the other hand seismological records also indicate extensive mass movements along the northern shore of the Marmara Sea. In this part, slope instabilities are related to seismic activities (Görür and Çağatay, 2010). An important point is if long lasting water level changes in the Marmara Sea are related to the tectonic or to the climate, this point should be explained.

There has been general agreement that terraces in the Marmara Sea were built by tectonic forces (Sakınç and Yaltırak, 1997; Kazancı et al., 2003). According to seismic data, the most extensive terrace area is at -85 m level and it is seen almost everywhere. Its development age is reported to be 11.000 years (Sorlien et al., 2012). Continuation of this to the deeper parts, in the south of the Çınarcık and Central Marmara pull-apart basins where the presence of a series of deltas has been discovered (Sorlien et al., 2012). These must have been built by the sediments transported from the SDB during the period while the shelf was outside and/or the water level was low. So it is clear that, waters sweeping the SDB have been discharged into the basins, developed during this deposition period along the NAF zone. As a result a 6 km thick basin fills has developed (Sorlien et al., 2012). This devopment of deltaic successions one on top of another reflects changes of water levels. At the same time this much of a thick accumulation of infill could also indicate sinking of the basin floor, in another words reflecs tectonic subsidence. Tectonics provided accumulation basins for the large amount of material transported from the SDB where deep valleys developed. Generations of the sediments have developed under the control of local and global climate changes and to the changes of the sea levels.

In summary; the high number of earthquakes having taken place shows that the study area is located in a tectonically active region (Soysal et al., 1981; Ambraseys and Finkel, 1991; Ambraseys, 2009). Abrupt height changes in the field, hanging valleys, land distortions indicate that tectonics were also effective in the past. But the effects of these tectonic activities on the evolution of the landforms have not been directly measurable. It is common that tectonics trigger mass movements and back space the hill sides. SDB is a place where almost all geomorphologic elements (lithology, climate, tectonics, erosion etc.) can be observed. In Early Neogene the İstanbul and Çanakkale straights had not developed yet, but the Southern Marmara region had large plains sloping gently towards the Black Sea. Following the development of the Marmara Sea, particularly during the last 300,000 years the Southern Marmara region, the study area, has been its subjected to great many changes and has acquired present day form. In these changes easily eroding lithologies and climate effects have been the main agents.

Acknowledgement

Large numbers of earthscientists and organizations gave support during 1995-2005 and we are very grateful to all who contributed. The data obtained have been used in this study. This was a part of a joint project with DPT (State Planning Organization) - TUBİTAK (Scientific, Technic Research Organization of Turkey) – University. Within the scope of a sea research project: geological mapping of the Neogene and Quaternary units in the Southern Marmara region, study of sea shore sediments, long and short term sea level changes in the Çayırova and Hersek plains, tsunami research and limnologic study of the Ulubat Lake have been carried out (TUBİTAK-YDABÇAĞ. 456/G, 598/G, 103Y102). MTA actively participated in the studies and gave valuable support. NATO gave support to the drillings in the Lake (EST.CLG.978645). GYTE gave support and numerous lake sediments were analysed by SEM, XRF, XRD, AAS methods without any charge. Some trace elements analyses were carried out at the Brunel University with financial support from NATO (NATO-CLG 978645).

Large numbers of researchers and university students took part in the above mentioned projects; while they were working on their research they gave support to this project by suggesting some ideas. Dr. Alper Gürbüz (N.Ü) helped drawing some of the figures and read the manuscript and gave some suggestions. Two referees and the Bulletin editor made some critical remarks and helped to improve the final text. Authors acknowledge gratefully all individual and organizational supports provided.

Received: 06.08.2013
Accepted: 30.10.2013
Published: June 2014

References

Aksu, A.E., Hiscott, R.N., Yaşar, D. 1999. Oscillating Quaternary water levels of the Marmara Sea and vigorous outflows into the Aegean Sea from the Marmara Sea-Black Sea drainage corridor. *Marine Geology* 153, 275–302.

Ambraseys, N. 2009. Earthquakes in the Mediterranean and Middle East; a Multidisciplinary Study of Seismicity up to 1900. *Cambridge University Press*, ISBN 978-0-521-87292-8.

Ambraseys, N., Finkel, C. 1991. Long-term seismicity of Istanbul and the Marmara Sea region. *Terra Nova* 3, 527-539.

Ardel, A. 1943. Marmara bölgesinin güneydoğu havzalarının morfolojik karakterleri. *Türk Coğrafya Dergisi* 2, 160-171.

Baş, H. 1987. Tavşanlı - Domaniç (Kütahya) volkanitlerinin özellikleri ve batı Anadolu Senozoyik volkanizmasındaki önemi. *Türkiye Jeoloji Bülteni* 30, 67-80.

Bingöl, E., Akyürek, B., Korkmazer, B. 1973. Biga Yarımadasının jeolojisi ve Karakaya Formasyonunun bazı özellikleri. *Cumhuriyetin 50. Yılı Yerbilimleri Kongresi Tebliğleri Kitabı*, s. 70-76, Ankara.

Chorley, R.J., Schumm, S.A., Sugden, D.E. 1984. Geomorphology. Methuen, London, 605 s.

Clayton, K. M. 1998. The rate of denudation of some British lowland landscapes. *Earth Surface Processes and Landforms* 22, 721-731.

Çağatay, M.N., Görür, N., Algan, O., Eastoe, C., Tchapalyga, A., Ongan, D., Kuhn, T., Kuscu, I. 2000. Last glacial-Holocene palaeoceanography of the Sea of Marmara: timing of last connections with the Mediterranean and the Black Seas. *Marine Geology* 167, 191-206.

Çelenli, A. 2000. Uluabat Gölü Çevre Jeokimyası. *İstanbul Teknik Üniversitesi Fen Bilimleri Enstitüsü, İstanbul, Doktora Tezi* (unpublished).

Dalkıran, N., Karacaoğlu, D., Dere, S., Şentürk, E., Torunoğlu, T. 2006. Factors affecting the current status of a eutrophic shallow lake (Lake Uluabat, Turkey): Relationships between water physical and chemical variables. *Chemical Ecology* 22, 279-298.

Darkot, B., Tuncel, M. 1981. Marmara Bölgesi coğrafyası. *İstanbul Üniversitesi Coğrafya Enstitüsü Yayını*, No 118, İstanbul.

Eastwood, W. J., Roberts, C. N., Lamb, H. F., Tibby, J.C. 1999. Holocene environmental change in southwest Turkey; a palaeoecological record of lake and catchment-related changes. *Quaternary Science Reviews* 18, 671-695.

EIE, 1993. Türkiye Akarsularında Sediment Gözlemleri ve Sediment Taşınım Miktarları. *EIEI Genel Müdürlüğü*, Yayın no 87-44, Ankara.

EIE, 1996. Türkiye Akarsularında Su Kalitesi Gözlemleri. *EIEI Genel Müdürlüğü*, Yayın no 96-4, Ankara.

EIE, 2000. Türkiye Akarsularinda Suspanse Sediment Gözlemleri ve Sediment Taşınım Miktarları. *EIEI Genel Müdürlüğü*, Yayın no 20-17, Ankara.

Einsele, G. 1992. Sedimentary Basins: Evolution, Facies and Sediment Budget. *Springer*, Berlin, 628 pp.

Einsele, G. Hinderer, M. 1998. Quantifying denudation and sediment accumulation systems (open and closed lakes): basic concepts and first results. *Palaegeography, Palaeoclimatology, Palaeoecology* 140, 7-21.

Emre, Ö., Erkal, T., Kazancı, N., Görmüş, S., Görür, N., Kuşçu, I. 1997*a*. Güney Marmara'nın Neojen ve Kuvaterner'deki morfotektoniği. İç: Güney Marmara Bölgesinin Neojen ve Kuvaterner Evrimi (Ed. N.Kazancı ve N. Görür), Araştırma Projesi sonuç raporu. TUBITAK, YDABCAG-426/G, Ankara, s. 36-68.

Emre, Ö., Kazancı, N., Erkal, T., Karabıyıkoğlu, M., Kuşçu, İ. 1997*b*. Ulubat ve Manyas Göllerinin oluşumu ve yerleşim tarihcesi. Iç: Güney Marmara Bolgesinin Neojen ve Kuvaterner Evrimi (Ed. N.Kazancı ve N.Görür), *Araştırma Projesi Sonuç Raporu*. *TÜBITAK*, YDABCAG-426/G, Ankara, s. 116-134.

Emre, Ö., Erkal, T., Tchapalyga, A., Kazancı, N., Keçer, M., Ünay, E. 1998. Doğu Marmara Bölgesi'nin Neojen ve Kuvaterner'deki evrimi. *Maden Tetkik ve Arama Dergisi* 120, 119-145.

Emre, Ö., Özalp, S., Doğan, A., Özaksoy, V., Yıldırım, C., Göktaş, F. 2005. İzmir yakın çevresinin diri fayları ve deprem potansiyelleri. *MTA Raporu*, No 10754, Ankara (unpublished).

Emre, Ö., Doğan, A. 2010. 1/250.000 Ölçekli Türkiye Diri Fay Haritası, Ayvalık (NJ 35-2) paftası, *Maden Tetkik ve Arama, Türkiye Diri Fay Haritası Serisi*, no 2, 32 s. Ankara.

Emre, Ö., Doğan, A., Özalp, S. ve Yıldırım, C. 2011*a*. 1/250.000 Ölçekli Türkiye Diri Fay Haritası, Bandirma (NK 35-11B) paftası. *Maden Tetkik ve Arama, Türkiye Diri Fay Haritası Serisi*, no 3, 55 s. Ankara.

Emre, Ö., Doğan, A., Özalp, S. 2011*b*. 1.250.000 Ölçekli Türkiye Diri Fay Haritası, Balıkesir (Nj 35-3) paftası. *Maden Tetkik ve Arama, Türkiye Diri Fay Haritası Serisi*, no 4, 35 s. Ankara.

Emre, Ö., Duman, T.Y., Özalp, S. 2011*c*. 1/250.000 Ölçekli Türkiye Diri Fay Haritası, Kütahya (Nj 35-4) paftası. *Maden Tetkik ve Arama, Türkiye Diri Fay Haritası Serisi*, No 4, Ankara.

Emre, Ö., Duman, T.Y., Özalp, S. 2012. Türkiye 1/250.000 ölçekli diri fay haritası. *Maden Tetkik ve Arama Genel Müdürlüğü*, Ankara.

Ercan, T., Ergül, E., Akçaören, E., Çetin, A., Granit, S., Asutay, J. 1990. Balıkesir Bandırma arasının jeolojisi, Tersiyer volkanizmasının petrolojisi ve bölgesel yayılımı. *Maden Tetkik ve Arama Dergisi* 110, 113-130.

Erdoğan, T. 1988. Balıkesir İklim Etüdü. Devlet Meteoroloji İşleri Genel Müdürlügü, Ankara.

Ergül, E., Öztürk, Z., Akçaören, F., Gözler, M.Z. 1980. Balıkesir ili – Marmara Denizi arasının jeolojisi. *Maden Tetkik ve Arama Genel Müdürlüğü Raporu*, no 6760, Ankara (unpublished)

Erinç, S. 1955. Orta Ege Bölgesi'nin jeomorfolojisi. *Maden Tetkik ve Arama Genel Müdürlüğü Raporu* No: 2217 (unpublished).

Erinç, S. 1973. Türkiye'nin şekillenmesinde neotektoniğin rolü ve jeomorfoloji-jeodinamik ilişkileri. *Jeomorfoloji Dergisi* 5, 11-26.

Erol, O. 1981. Neotectonic and geomorphological evolution of Turkey. Z. Geomorph. N.F. Suppl. Bd, 40, 193-211.

Fontugne, M., Kuzucuoğlu, C., Karabıyıkoğlu, M., Hatté, C., Pastre, J. F. 1999. From Pleniglacial to Holocene: a 14C chronostratigraphy of environmental changes in the Konya Plain, Turkey. *Quaternary Science Reviews* 18, 573-591.

Görür, N., Çağatay, N. 2010. Geohazards rooted from the northern margin of the Sea of Marmara since the late Pleistocene: a review of recent results. *Natural Hazards* 54, 583-603.

Gözler, M.Z., Ergül, E., Akçaören, F., Genç, Ş., Akat, U., Acar, Ş. 1985. Çanakkale Boğazı doğusu – Marmara Denizi güneyi – Bandırma – Balıkesir – Edremit ve Ege Denizi arasındaki alanın jeolojisi ve kompilasyonu. *MTA Raporu*, no 7430, Ankara (unpublished).

Helvacı, C. 1984. Occurrence of rare borate minerals: veatchite-A, tunnellite, terrugite and cahnite in the Emet borate deposits, Turkey: *Mineral Deposita* 19, 217-226.

Helvacı, C. 1986. Geochemistry and origin of the Emet borate deposits, western Turkey. Bulletin of the Faculty of Engineering, Cumhuriyet University, Serie A- *Earth sciences* 3, 49-73.

Helvacı, C., Firman, R.J. 1977. Emet borat yataklarının jeolojik konumu ve mineralojisi. *Jeoloji Mühendisliği Dergisi* 2, 17-28.

Helvacı, C., Alonso, R.N. 2000. Borate deposits of Turkey and Argentina; a summary and geological comparison. Turkish Journal of Earth Sciences 24, 1-27.

Kazancı, N., Bayhan, E., Suliman, N., Sahbaz, A., Ileri, Ö., Özdogan, M., Temel, A., Ekmekçi, M. 1997.

Manyas Gölü ve Güncel tortullari. Iç: Güney Marmara Bolgesinin Neojen ve Kuvaterner Evrimi (Ed. N.Kazancı ve N.Görür), Araştırma Projesi sonuç raporu. *TÜBITAK*, *YDABCAG-426/G*, Ankara, s. 192-238.

Kazancı, N., Görür, N. (Ed), 1997. Güney Marmara Bölgesi'nin Neojen ve Kuvaterner Evrimi. Deniz Araştırmaları Programı, Araştırma Projesi Sonuç Raporu. *TÜBITAK, YDABCAG-426/G*, Ankara, 240 s (unpublished).

Kazancı, N, Ileri, O., Suliman, N., Özdoğan, M., Bayhan, E., Şahbaz, A., Gencer, A, Ergin, M., Erkmen, C. 1998. Ulubat Gölü'nde guncel tortullasma. İç: Marmara Denizi Güneyi Kıyı ve Kıyı Ardı Istiflerinin Stratigrafisi, Sedimantolojisi ve Morfotektonigi. *TÜBITAK Raporu*, YDABCAG – 598/G, pp. 99 - 145.

Kazancı, N., Emre, Ö., Erkal, T., Ileri, Ö., Ergin, M., Görür, N. 1999. Kocasu ve Gönen Çayı deltalarının (Marmara Denizi güney kıyıları) güncel morfolojileri ve tortul fasiyesleri. *MTA Dergisi* 121: 1-18.

Kazancı, N., Kırman, E., Emre, Ö., Keçer, M., İleri, Ö., Doğan, A., İslamoğlu, Y., Alçiçek, M.C., Varol, B., Erkal, T., Ertutaç, K., Uysal, F., Özalp, S., Gül, A., Duman, T.Y. 2003. Doğu Marmara Kıyılarında Denizel Geç Kuvaterner Tortulları Ve Deniz Seviyesi Değişimleri. Deniz Araştırmaları Programı Araştırma Projesi Sonuç Raporu, Proje No: *TÜBITAK- YDABÇAG* 100 Y 077. Ankara, 117s (unpublished).

Kazancı N., Leroy S. A. G., Ileri O., Emre O., Kibar, M., Öncel, S. 2004. Late Holocene erosion in NW Anatolia from sediments of Lake Manyas, Lake Ulubat and the southern shelf of the Marmara Sea, Turkey. *Catena* 57, 277-308.

Kazancı N., Toprak, Ö., Leroy S. A. G., Öncel S., Ileri Ö., Emre Ö., Costa P., Erturaç, K. ve McGee E. 2006. Boron content of Lake Ulubat sediment: a key to interpret the morphological history of NW Anatolia, Turkey. *Applied Geochemistry* 21, 234 - 251.

Kazancı, N., Leroy, S. A. G., Öncel, S., İleri, Ö., Toprak, Ö, Costa, P., Sayılı, S., Turgut, C., Kibar, M. 2010. Wind control on deposition of heavy metals: the case study of Lake Ulubat in Anatolia, Turkey. *Journal of Paleolimnology* 43, 89–110.

Landmann, G., Reimer, A., Lemcke, G., Kempe, S. 1996. Dating Late Glacial abrupt climate changes in the 14,570 yr long continuous varve record of Lake Van, Turkey. *Palaeogeography, Palaeoclimatology, Palaeoecology* 122, 107-118.

Leroy, S.A.G., Kazancı, N., Ileri, Ö., Kibar, M., Emre, Ö., McGee, E., Griffiths H.I. 2002. Abrupt environmental changes within a late Holocene lacustrine sequence south of the Marmara Sea (Lake Manyas, N-W Turkey). *Marine Geology* 190, 531-552.

MTA, 2002. 1/500 000 Ölçekli Türkiye Jeoloji Haritaları, İstanbul ve İzmir paftaları. *Maden Tetkik ve Arama Genel Müdürlüğü*, Ankara.

Okay, A.İ. 2008. Geology of Turkey: A synopsis. *Anschnitt* 21, 19-42.

Okay, A.I., Siyako, M., Burkan, K.A. 1991. Biga Yarımadasının jeolojisi ve tektonik evrimi. *Türkiye Petrol Jeologları Derneği Bülteni* 2, 83-121.

Pamir, H. N. 1938, İstanbul Boğazı'nın teşekkülü meselesi. *Maden Tetkik ve Arama Dergisi* 3-4, 61-68.

Reed, J. M., Leng , M. J., Ryana, S., Black, S., Altınsaçlı¸ S., Griffiths, H.I. 2008. Recent habitat degradation in karstic Lake Uluabat, western Turkey: A coupled limnological – palaeolimnological approach. *Biological Conservation* 141, 2765-2783.

Sakınç, M., Yaltırak, C. 1997. Güney Trakya sahillerinin denizel Pleyistosen çökelleri ve Paleocoğrafyası. *MTA Dergisi* 119, 43-62.

Selby, M.J. 1994. Hillslope sediment transport and deposition. İç: Pye K. (Ed) Sediment Transport adn depositiona Processes. *Blackwell Pub*., *London*, s. 61-88.

Smith, A.D., Taymaz, T., Oktay, F., Yüce, H., Alpar, B., Başaran, H., Jackson, J.A., Kara, S., Şimşek M. 1995. High-resolution seismic profiling in the Sea of Marmara (northwest Turkey): Late Quaternary sedimentation and sea-level changes. *Geological Society of America Bulletin* 107/8, 923-936.

Sorlien, C.C, Akhun, S.D., Seeber, L., Steckler, M.S., Shillington, D.J., Kurt, H., Çifçi, G., Poyraz, D.T., Gürçay, S., Dondurur, D., İmren, C., Perinçek, E., Okay, S., Küçük, H.M., Diebold, J.D. 2012. Uniform basin growth over the last 500 ka, North Anatolian Fault, Marmara Sea, Turkey. *Tectonophysics* 518–521, 1–16.

Soysal, H., Sipahioğlu, S., Kolçak, D., Altınok, Y. 1981. Earthquake Catalogue of Turkey and its Surrounding, BC2100-AD1900. Tech. Sci. Res. Council of Turkey (*TUBITAK*), Project Rep. No 341, Ankara (in Turkish).

Şaroğlu, F. Emre, Ö., Boray, A. 1987. Türkiye'nin diri fayları ve depremselliği. *Maden Tetkik ve Arama Genel Müdürlüğü Raporu* No: 8174 (unpublished).

Toprak, Ö. 2004. Ulubat Gölü tortullarının organik madde ve ağır metal içeriği. Yüsek Lisans Tezi, *Gebze Yüksek Teknoloji Enstitüsü*, Gebze, Kocaeli, 117 s (unpublished).

Turgut, C. 2005. Ulubat Gölü çökellerinde ve göl suyunda metal konsantrasyonlarının incelenmesi. Yüksek Lisans tezi, *Gebze Yüksek Teknoloji Enstitüsü*, Gebze, Kocaeli, 92 s (unpublished).

Ülgen, U.B., Franz, S.O., Biltekin, D., Çağatay, M.N., Roeser, P.A., Doner, L., Thein, J. 2012. Climatic and environmental evolution of Lake İznik (NW Turkey) over the last ~ 4700 years. *Quaternary International* 274, 88-101.

Wilson, C.G., Matisoff, G., Whiting, P.J. 2003. Short-term erosion rates from an inventory balance. *Earth Surf. Proc. Landforms* 9, 967-977.

Yalçınkaya, S., Avşar, Ö.P. 1980. Mustafakemalpaşa (Bursa) dolayının jeolojisi. *Maden Tetkik ve Arama Raporu* Derleme no: 6717, Ankara (unpublished).

Yılmaz, Y., Gökaşan, E., Erbay, A.Y. 2010. Morphotectonic development of the Marmara Region. *Tectonophysics* 488, 51-70.

Yılmaz, Y., Gürpınar, O., Genç, S.C., Bozcu, M., Yılmaz, K., Şeker, H., Yiğitbaş, E., Keskin, M. 1990. Armutlu Yarımadası ve civarının jeolojisi. *TPAO Raporu*, no 2796, 210 s, Ankara (unpublished).

Bulletin of MTA (2014) 148: 19-42

Bulletin of the
Mineral Research and Exploration

http://bulletin.mta.gov.tr

TECTONO - SEDIMENTARY EVOLUTION OF BUCAKKIŞLA REGION (SW KARAMAN) IN CENTRAL TAURIDES

Tolga ESİRTGEN[a]

[a] *General Directorate of Mineral Research and Exploration, Dept. of Geological Researches, 06800, Ankara, Turkey*

Keywords:
Bozkır unit, mélange, Inner Tauride Ocean, rift volcanism, orogenic collapse.

ABSTRACT

The study area located in Bucakkışla region in Central Taurides consists of rock units of the melange which form Bozkır unit of the Tauride units and the overlying cover rocks. There are volcanic, ophiolitic and sedimentary rocks which generated in different environmental conditions. These rock groups comprise units which formed in Middle-Upper Triassic-Paleocene periods in Inner Tauride Ocean that had been opened between Tauride – Anatolide continents. Within the scope of this study, lithostratigraphic characteristics of Huğlu, Boyalı hill, Korualan nappes and cover rocks which form Bozkır Unit and tectono sedimentary evolution of the study area was built up by paleontological and structural features. Due to rifting, which started in Middle Upper Triassicin the region, the products of the rift volcanism in rifting center and the carbonate deposition on margins of basin have occurred. The continuation of extension which initiated rifting caused collapse in the basin in Middle Upper Triasic – Lower Senonian. Deep marine deposition has occurred at the center of basin, however pelagic and neritic limestones were deposited in basin margins during this time. The region has become compressed by the effect of a new tectonical regime which had been effective starting from Santonian. This compression caused new melanges to take place due to reverse faults and thrust. The formation of these melanges has continued until the end of Paleocene period. However, there has not been observed any formation depending on the compression in post Paleocene. The nappes have moved southward by the effect of compression until Eocene. But then, these nappes could not advance forward anymore so, northward back thrusts took place as basin was closured andreached the collisional stage. Sequences which had become imbricated structures by back thrusts were subjected to collapsing by the stop of compression and the gravitational effect. All sequences in the imbricated structure were cut by dip slip normal faults and lacustrine basins were formed on fallen blocks. The formation of Early Oligocene terrestrial deposits in these lakes indicates that the collapse occurred in Oligocene or immediately before this time, and this allows the dating of new tectonical period. Early Oligocene deposits to become tilted by dip slip faults show that new tectonic period in the region has also continued after Oligocene.

1. Introduction

Triassic-Cretaceous aged tectono stratigraphic units cropping out in Bucakkışla region, in Central Taurides (SW Karaman) consist of rock lithologies representing different deformation stages (Figure 1a, b). These rocks located within Bozkır Unit (Özgül, 1997) extend along the Tauride belt. The unit has a widespread mélange appearance covering blocks and slices in different sizes with lithologies such as; basic submarine volcanite, tuff, diabase, ultrabasite, serpentinite, pelagic and neritic limestone, and

* *Corresponding author : tolgaesirtgen@yahoo.com*

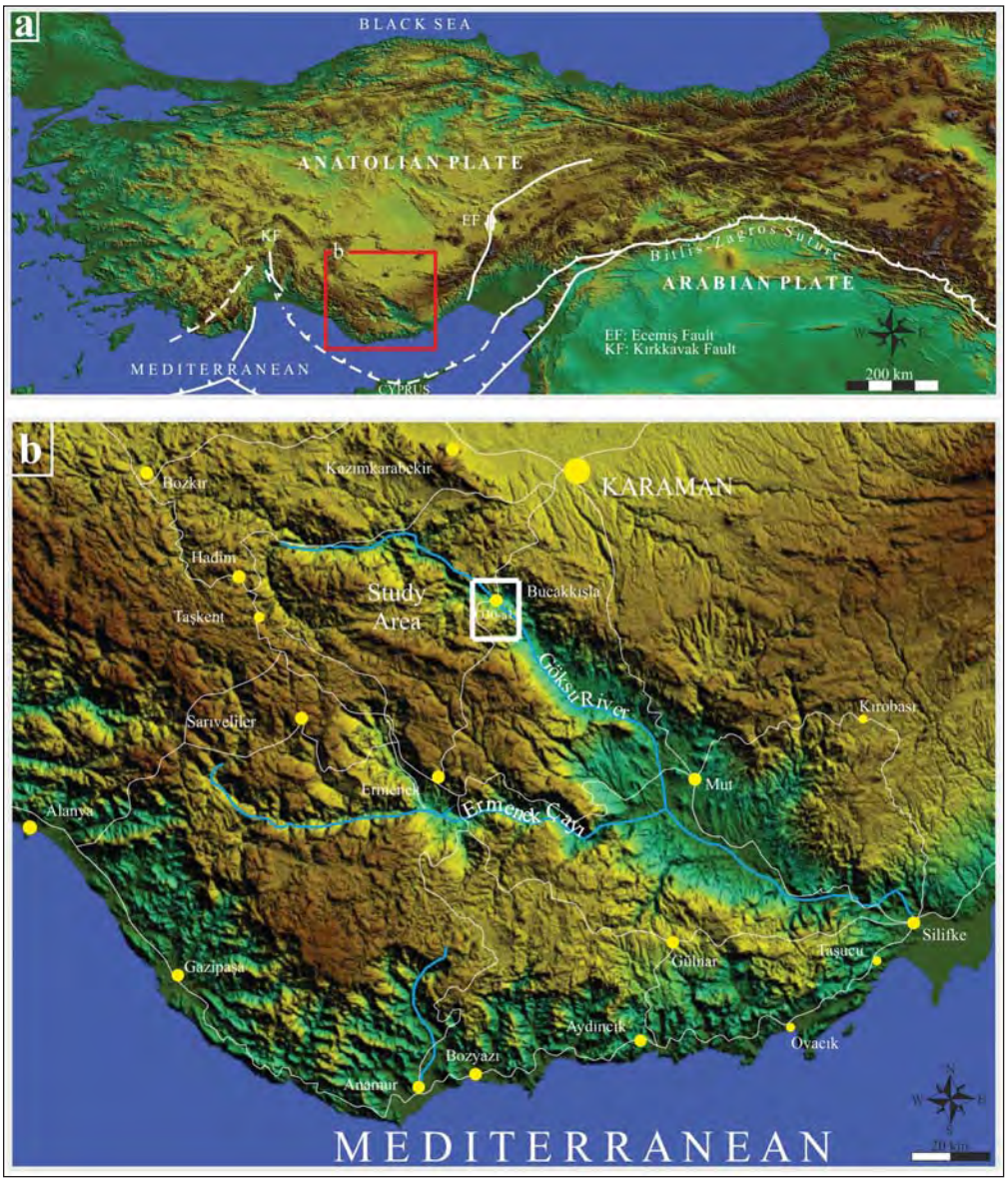

Figure 1- Location of the study area and topographic view showing main tectonic lines of Turkey; a) 90 m resolution SRTM data, Jarvis et al., (2008), b) location map of the study area.

radiolarite. These rock groups form the products of Inner Tauride Ocean defined in the region (Görür et al., 1984; Görür et al., 1998). The Inner Tauride Ocean which was formed due to Triassic rifting restricts the northern boundary of the Tauride–Anatolide platform (Robertson et al., 2012). Cover rocks which have developed since Oligocene take place over Bozkır unit. The structural and textural features of all these rocks, their components and contact relationships among them present strong evidences on the geological evolution. It ranges from rifting to obduction-subduction, from the closure of the ocean to collision and post collisional orogenic collapse which developed in the region during Triassic-Quaternary period. There are many studies which have been made both on İzmir-Ankara-Erzincan Ocean and on the southern branch of the Neotethys in literature (Robertson and Woodcock, 1981; Şengör and Yılmaz, 1981; Göncüoğlu et al., 1997; Robertson, 1998; Dilek et al., 1999; Robertson, 2000; Kelling et al., 2001; Stampfli et al., 2001; Kelling et al., 2004; Robertson et al., 2004). However, studies that have been made on the rock assemblages of the oceanic branch called "Inner Tauride Ocean" and its evolution within this period is either limited (Görür et al., 1984; Görür et al., 1998; Dilek et al., 1999; Okay and Tüysüz, 1999; Andrew and Robertson, 2002; Robertson et al., 2009;

Pourteau et al., 2010; Robertson et al., 2012) or the presence of the Inner Tauride Ocean is neglected (Göncüoğlu, 1986; 1992). The study area is located among typical regions in which the geological development of the Inner Tauride Ocean was observed. The purpose of this study is to reveal data related to different tectonical regimes of Triassic-Miocene period in the region which covers structural and stratigraphical data of all these tectonical movements in Central Taurides and to build up the geological evolution of the region.

2. Stratigraphy

The stratigraphical succession of the study area in Central Taurides consists of Huğlu, Boyalı tepe, and Korualan nappes described within Bozkır unit by Özgül (1997) and Oligo-Miocene rocks situated as cover rocks that overlie on them. Since Huğlu, Boyalı tepe and Korualan groups presents a structural relationship among them, these were defined as nappe slices and named as Huğlu nappe, Boyalı tepe nappe and Korualan nappe in the study (Figure 2). Oligo-Miocene cover rocks, formed by Fakırca and Mut formations, occurred after nappe movements and were not affected from these movements (Figure 3a, b). The ages and apparent thicknesses of basement and cover rocks were shown in stratigraphical section (Figure 4).

2.1. Huğlu Nappe

This unit was first named by Monod (1977) and crops out in southwest of the study area (NW of

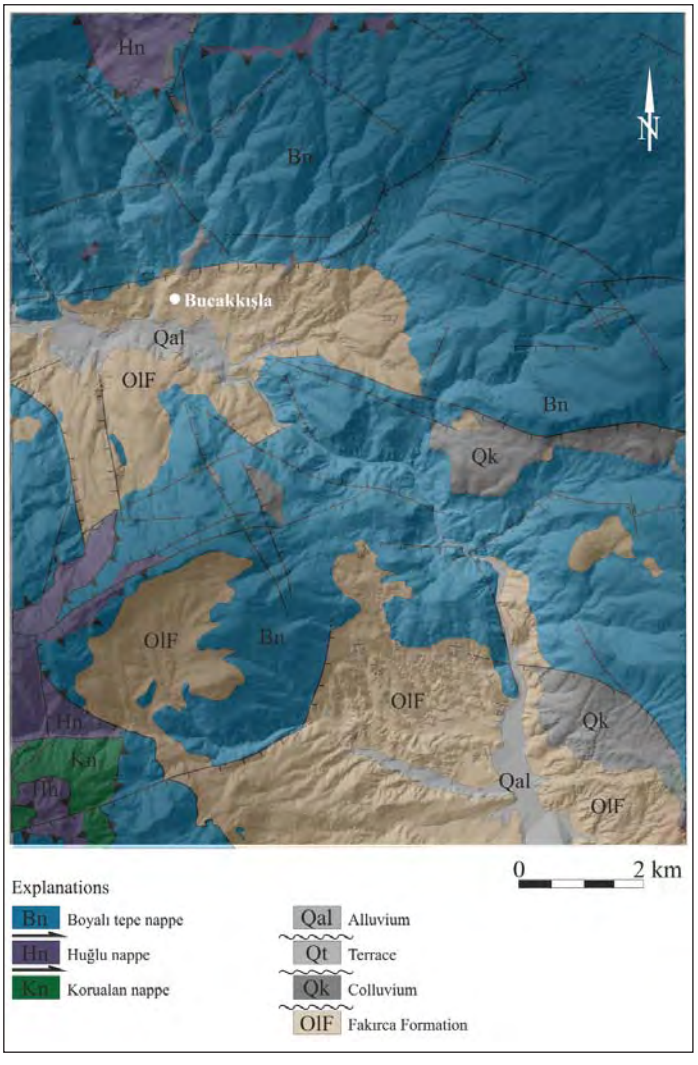

Figure 2- Map showing positionsof nappes, their relations with each other and cover units in the study area.

Yukarı Akın and Akın villages). Although Huğlu nappe consists of the oldest unit cropping out in the study area, it is tectono stratigraphically located in the middle of succession. Huğlu nappe is formed by three formations as; Dedemli formation, Mahmut hill limestone and Kovanlık mélange. It overlies Kovanlık nappe and is underlain by Boyalı hill nappe.

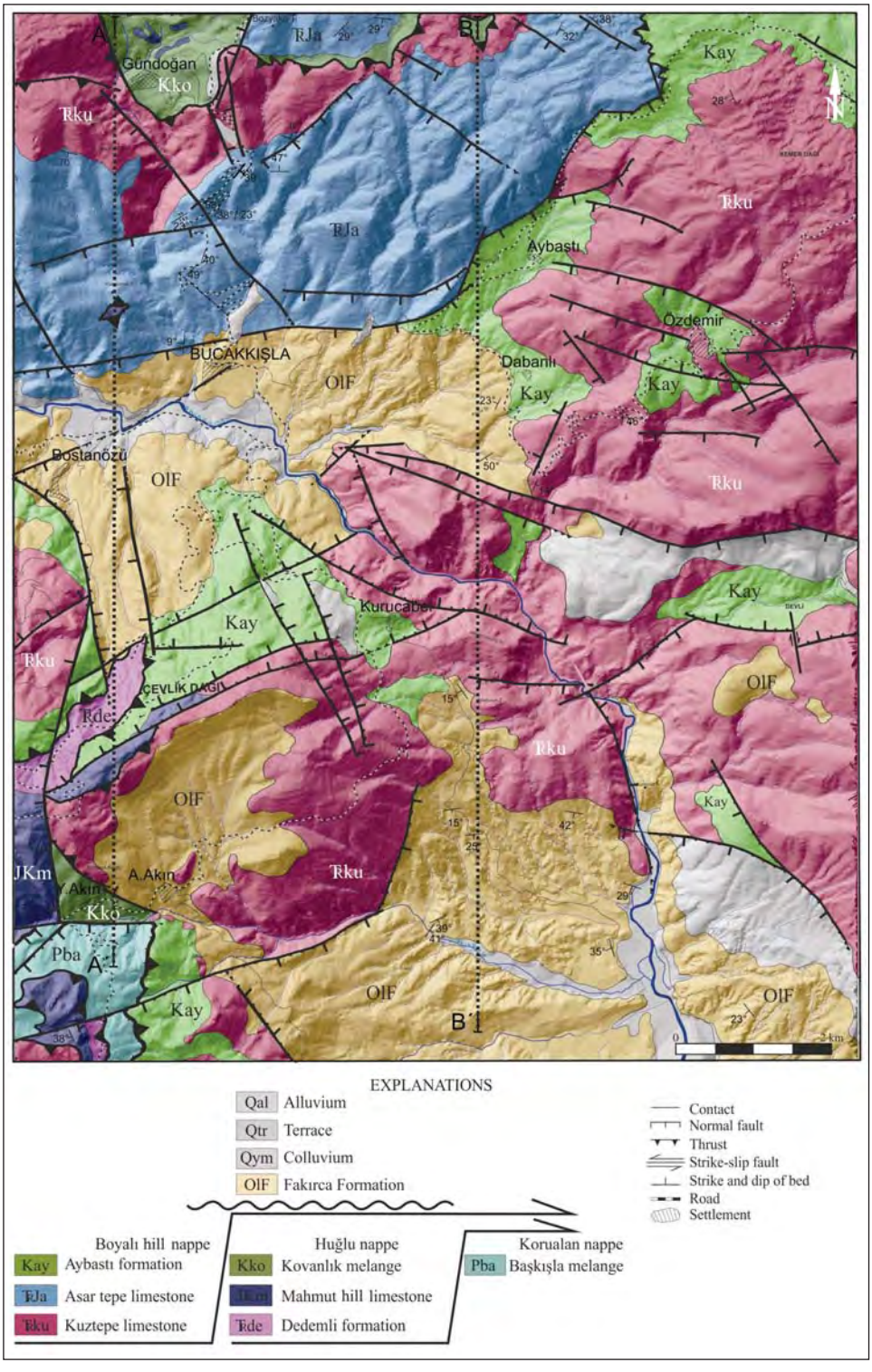

Figure 3a- Relief topography map of the study area (sheet O30-a1).

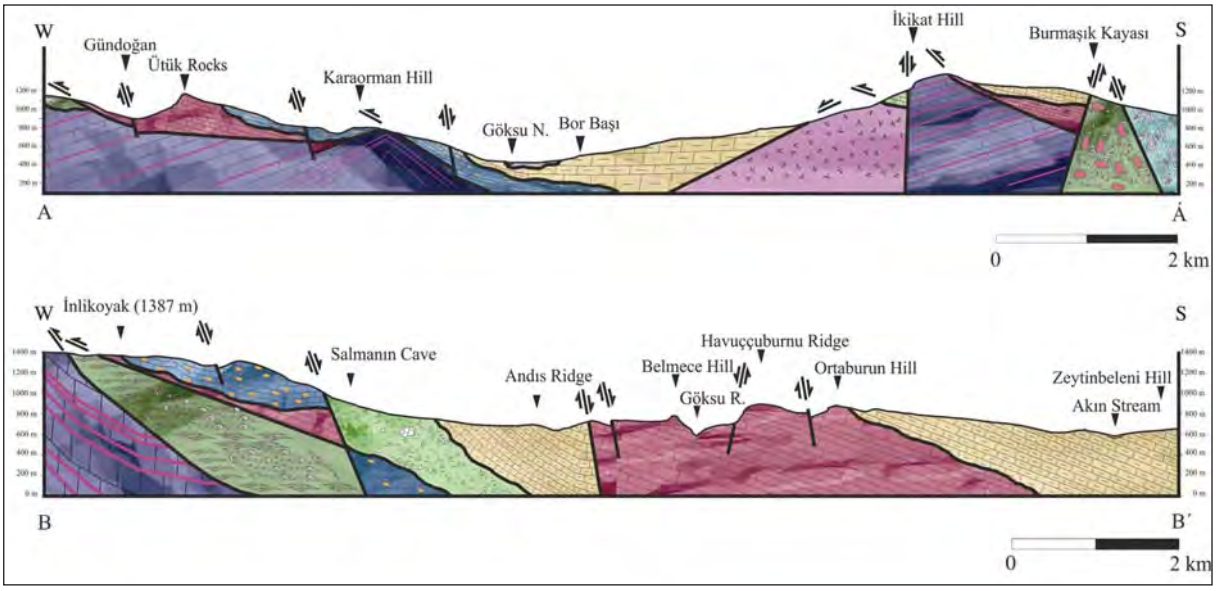

Figure 3b- N-S trending geological cross sections between A-A' and B-B'.

2.1.1. Dedemli Formation

Huğlu nappe which is located at the lowermost part of the Huğlu nappe was named by Özgül (1976) and is composed of green and brown colored, vitrified tuff, volcanites and occasionally clastic rocks (Figure 5a, b).

Tuffs are bedded, folded in varying scales and fractured. Rock compositions in thin sections are composed of glass shards, quartz, plagioclase, biotite crystals and rock clasts. Crystals located in the rock are fine grained. Quartz and biotite minerals are anhedral, however plagioclases are euhedral. Sieve texture is dominant in some of the plagioclases. Rock pieces are glassy and in porphyritic texture. These components were bonded by a binder which is formed by argillized and chloritized, altered glass shards. Intensive alteration is observed throughout the rock (chloritization and silicification). Clastic rocks are composed of quartz, plagioclase, calcite minerals and rock fragments. These rock fragments are represented by volcanic rock fragments that display microlitic, porphyritic, trachytic and glassy texture; by fine grained mica-quartz schist fragment, fine grained biotite schist fragment and by fossilliferous limestone fragments in few amounts. Clastic rocks are generally grain supported. Spatially, calcite binders are observed. Grains are angular to subangular, subrounded and medium sorted. In thin section views of these rocks, widespread vein developments are seen which are filled by secondary carbonate minerals. The rockis defined as lithic arenite.

The formation crops out on northern slopes of the Çevlik Mountain in the study area (501000E/4085500N) and has an apparent thickness of about 150 meters. Dedemli formation tectonically overlies Başkışla mélange which is in southwest of the Yukarı Akın village. The unit is transitional with the overlying Mahmut tepesi limestone. The age of the unit which is composed of volcanic rocks and clastics in few amounts could not be determined. However, the age of the formation is interpreted as Anisian-Norinian because it is transitional with Mahmut tepesi limestone (Özgül, 1997). Monod, (1977) dated blocks of debris flow deposits as Anisian which constitute the unit. However, Mahmut tepesi limestones which are in transitional contact with Dedemli formation were dated as middle Carnian (Tekin, 1999; Tekin and Bedi, 2007). Therefore, the age of the formation was accepted as Anisian–middle Carnian.

Although it is claimed that, Dedemli formation has geochemically calc alkaline character by Gökdeniz (1981), it is stated that the unit is made up of tuff and basic volcanites and have blown out submarine alkaline basalts during rifting in Middle-Upper Triassic period (Whitechurch et al., 1984; Tekin, 1999). Robertson and Dixon (1984) claim that, micro continental block of Turkey was rifted from Gondwana in Triassic period. Depending on these data, it is seen that Dedemli formation is a unit which is made up of rift environment product composed of alkali volcanic rocks.

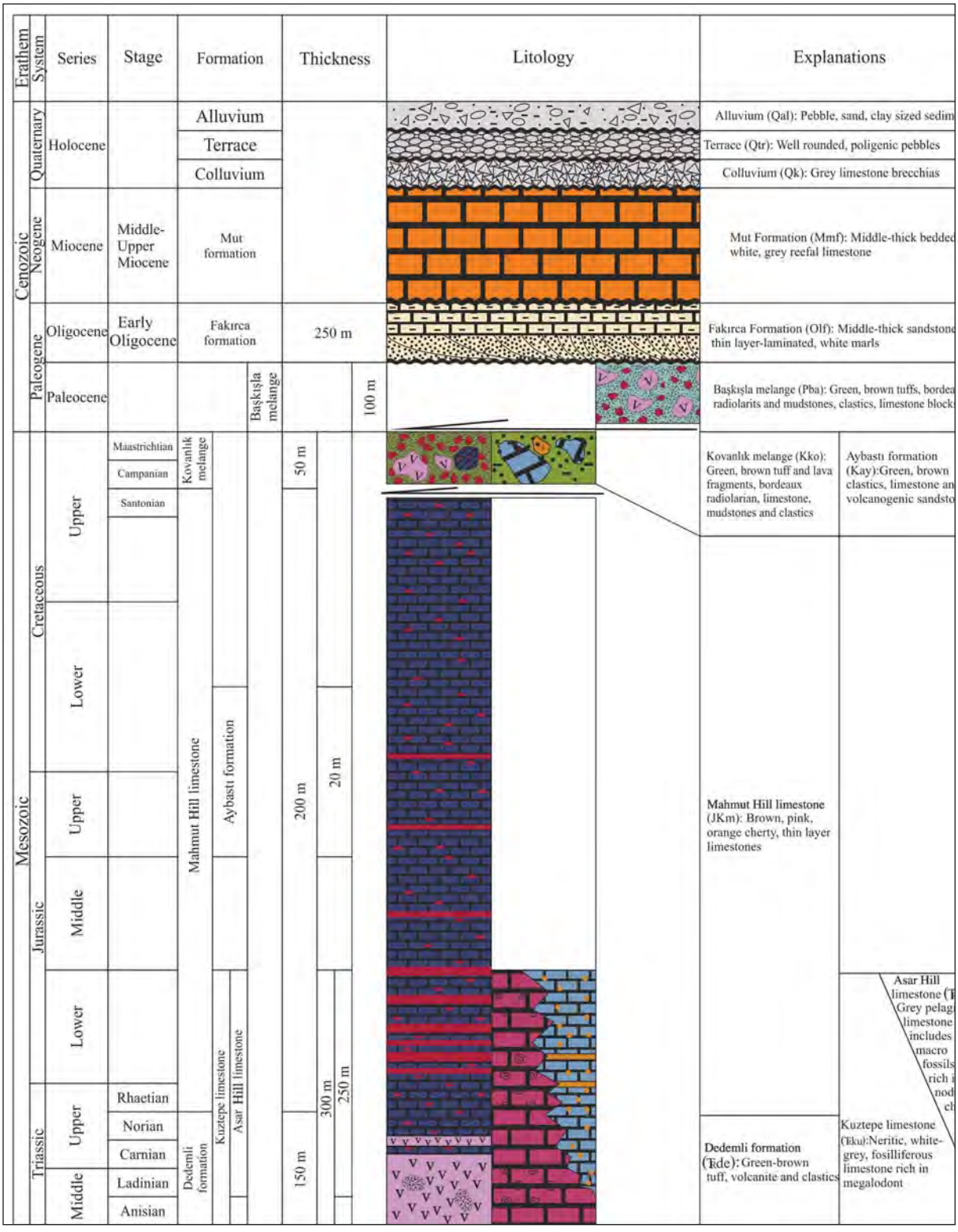

Figure 4- Unmeasured column section showing the general stratigraphy of the units in the study area.

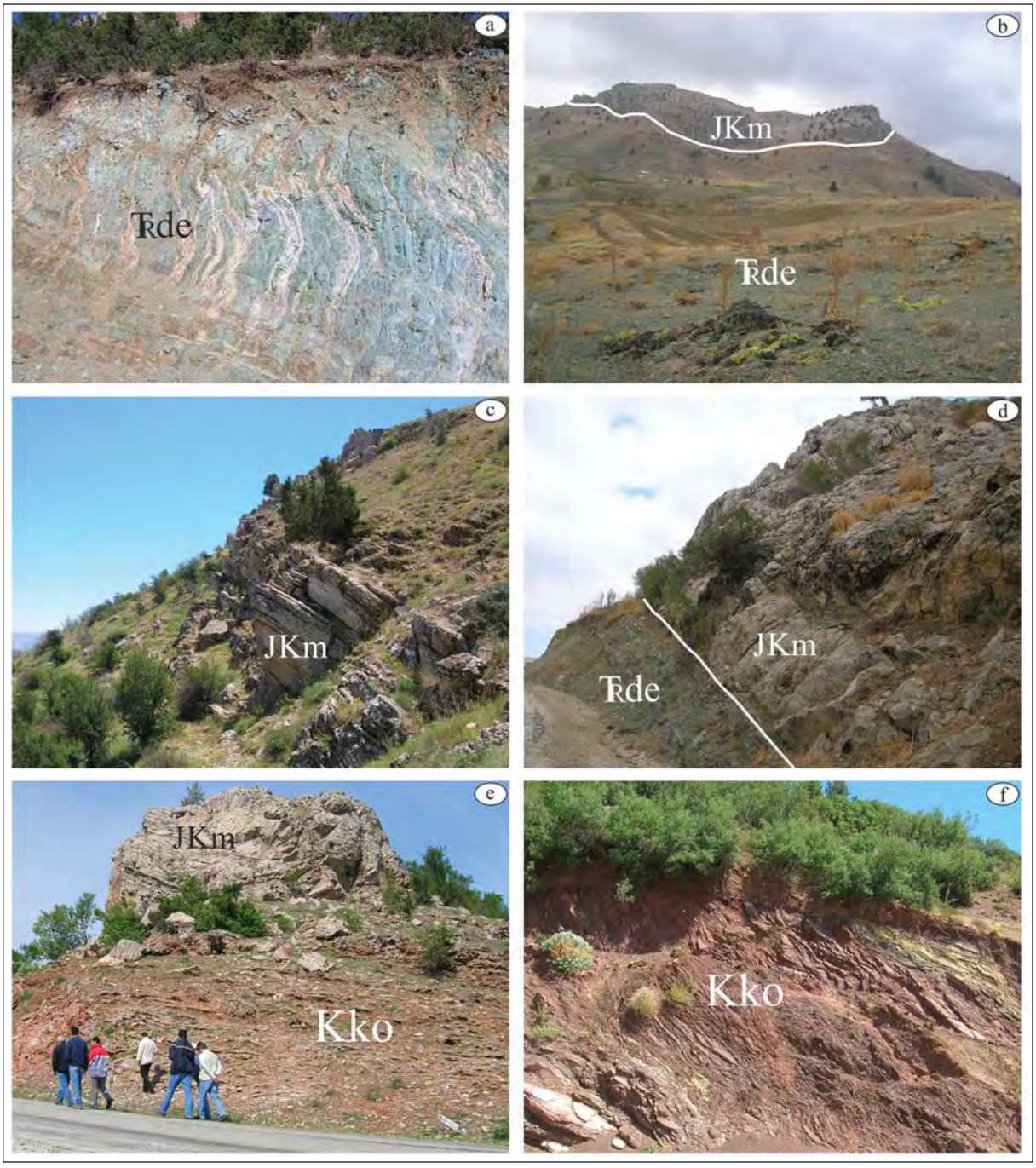

Figure 5- a) Folded tuffs of the Dedemli formation, b) Dedemli formation and transitional Mahmut Hill limestone, c) Thinly bedded, folded limestones of the Mahmut Hill limestone, d) Transitional contact relationship of Mahmut hill limestone with Dedemli Formation, e) Kovanlık melange and the Mahmut hill limestone block within, f) Folded, thin radiolarite-mudstone alternation of the Kovanlık melange.

2.1.2. Mahmut Hill Limestone

The nomenclature of Mahmut hill limestone was given by Özgül (1997). The unit is composed of brown, orange, pink colored, cherty, fine bedded and folded pelagic limestones (Figure 5c,d). It crops out on northwestern slopes of the Çevlik Mountain, north of Yukarı Akın village (500500E/4083000N) in the study area. The deposition of the unit begins with volcanites of Dedemli formation transitionally and is most probably unconformably overlain by Kovanlık mélange. Mahmut hill limestones are represented by

different ages in different parts of the Central Taurides and have been deposited in a broad time period ranging from Middle–Late Triassic to early Senonian (Özgül, 1977). In latter studies, Middle Carnian age was obtained from radiolarians in cherty limestones constituting the unit (Tekin, 1999; Tekin et al., 2001; Tekin and Bedi 2007). The age of the unit was accepted as middle Norian-Santonian. It has an apparent thickness of about 200 meters and presents a continuous succession which does not display any definite facial change during deposition. This formation which forms a dense succession is considered that it has a limited material transport from land and as deposited on a pelagic environment that has a very low depositional rate.

2.1.3. Kovanlık Mélange

Kovanlık mélange was first named by Özgül (1997) and is a unit in which rock fragments with different sizes, types and ages are located within red-bordeaux matrix altogether. Pink-bordeaux colored, radiolarite-mudstone alternation is composed of green-brown colored tuff and lava fragments, limestone blocks and other clastic rocks. Mafic rock fragments are also observed in the unit though less (Figure 5e, f). The apparent thickness of the unit which crops out in the vicinity of Yukarı Akın and Gündoğan villages (502000E/4094400N) is around 50 meters in the study area. Kovanlık mélange begins with alternation of radiolarite-mudstone over Mahmut tepesi limestone and continues with conglomerate consisting of Pebble-size tuff, lava, limestone and radiolarite fragments. There is not observed any definite bedding which dips or grades in the unit. These characteristics indicate deposits of massive debris flow product. Petrographical studies of the rocks which form the unit according to Streckeisen (1976) show that, limestones are composed of biomicrite, and mafic rocks are composed of gabbro and serpentinite (Figure 6a, b, c, d, e, f ,g, h ,i, j).

Biomicrites which constitute the mélange consist of much radiolarian microfossils filled with silica within crypto-microcrystalline carbonate crystals. Fractures which are observed in various thicknesses and large amounts were filled up by micro-meso crystalline carbonate minerals. These fractures were generally stained by ironoxides and hydroxides. Grains that constitute gabbro minerals are subhedral and granular in texture. The rock which is coarse grained is mainly composed of plagioclase, clinopyroxene, orthopyroxene and olivine minerals. Plagioclase minerals are subhedral, anhedral with poiklitic twinning and are intensively altered. In most plagioclases; sericitization and argillization (in occasion) and zeolitization are observed. Most mafic minerals constituting the rock are composed of clinopyroxene minerals and orthopyroxene in minor amounts. Pyroxenes which are mainly subhedral and anhedral were not altered unlike plagioclases. Some clinopyroxene minerals consist of orthopyroxene in the form of exsolution lamellae. Olivine minerals are totally transformed into serpentine minerals. Serpentine minerals which form serpentinite display sieve texture. It is made up of crysotile minerals that display vertical arrangement on edges and antigorite minerals among them. Magnetite was detected as the widespread opaque mineral type in thin section studies of opaque minerals. Less chromium and millerite minerals in trace amounts are also observed as opaque mineral. Talcose characteristic is present occasionally.

The age of Kovanlık mélange was given as early Senonian (Özgül, 1997) as it overlies Mahmut hill limestone and consists of fragments belonging to these limestones. Tekin (1999) emphasized that the age of Mahmut hill limestone which he named as Huğlu limestone was limited by Santonian. The age of Kovanlık mélange should be Santonian to post Santonian as it consists of Mahmut hill limestones.

Kovanlık mélange which has different origin rock types is an ophiolitic mélange. Ophiolitic rocks defined within this mélange are described as SSZ type ophiolites “supra-subduction zone type”. These rocks are based on geochemical contents like Lycian, Beyşehir, Divriği and Mersin ophiolites which are located in the same belt (Şengör and Yılmaz, 1981; Şengör, 1984; Robertson and Dixon, 1984; Dercourt et al., 1986; Parlak et al., 1996a, 1996b; Okay and Tüysüz, 1999; Barrier and Vrielynck, 2009; Robertson et al., 2012). This unit is tectonically overlain by Boyalı Hill nappe.

2.2. Boyalı Hill Nappe

Middle Triassic-Lower Jurassic limestones with megalodonts in western Taurides were first decribed by Gutnic and Monod (1970) called the “Boyalı hill”. The same unit which crops out as well in Central Taurides was studied by Özgül (1997) in the name of Boyalı tepe group. The same rock groups cropping out in the study area were investigated under the name “Boyalı hill nappe”, too. Boyalı hill nappe consists of three formation as Kuztepe limestone, Asar hill limestone and Aybastı formation in the study area (Figure 7a, b, c, d, e, f).

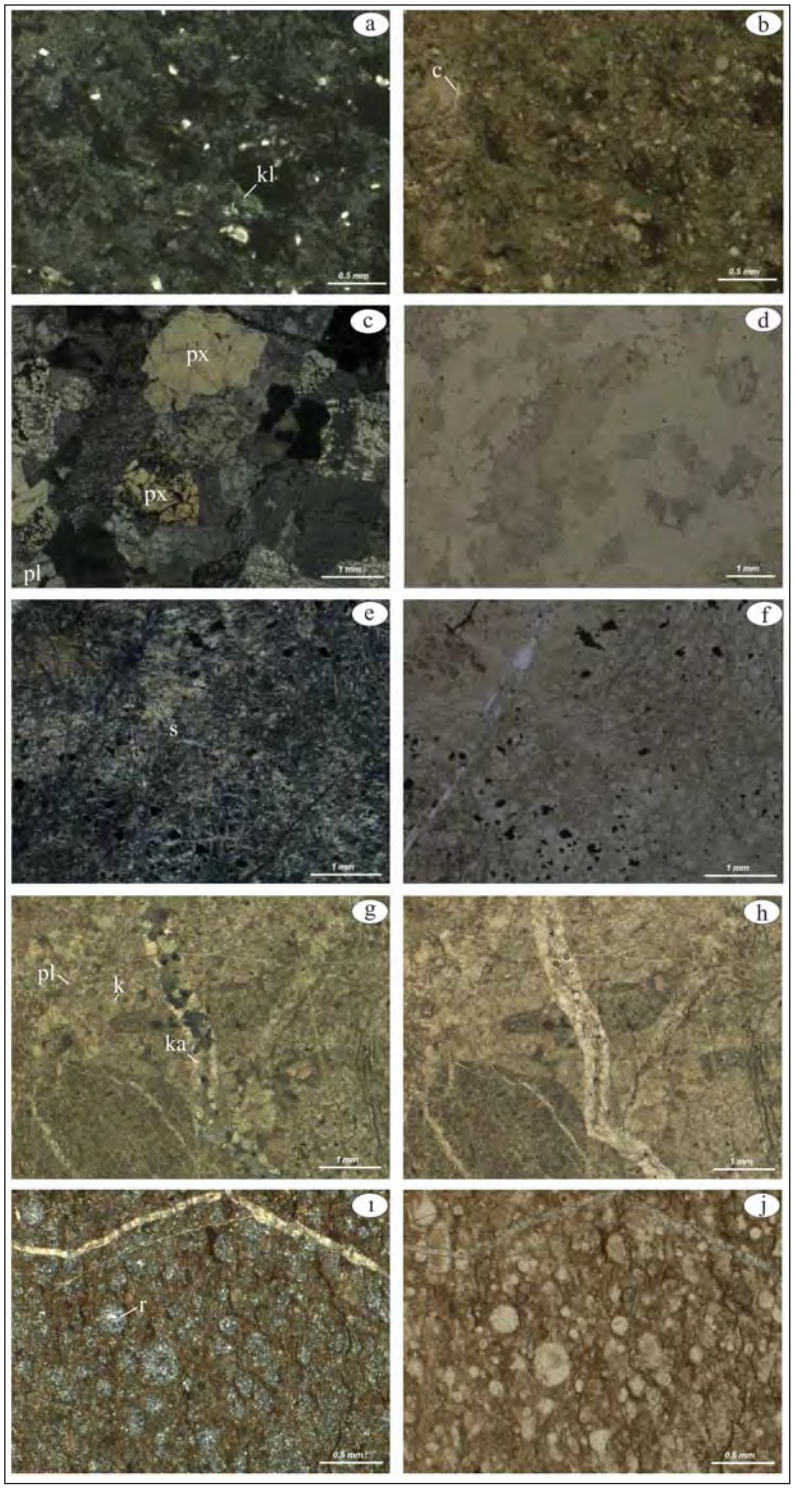

Figure 6- Petrographical views belonging to different lithologies which form the Kovanlık Melange; a) lithic arenite, b) silicified, chlorite glassy tuff, c) biomicrite, d) gabbro, e) and f) serpentinite.

2.2.1. Kuz Hill Limestone

This unit is composed of white, occasionally gray, much megalodont fossilliferous limestone and was described and named as Kuz hill limestone by Özgül (1997) on Kızıltepe ridges located in southeast Aslantaş of Bozkır. It has an apparent thickness of about 300 meters in the study area and is exposed at southeast of Bucakkışla village (505500E/ 4088300N), at north of Yukarı and Aşağı Akın villages and in vicinities of Kurucabel and Bostanözü villages. The primary basal contact of the unit is not observed. Kuz hill limestone tectonically overlies all units that form Huğlu and Korualan nappes and gradually passes into Asar hill limestones in the upper boundary of the succession. According to

Figure 7- a) Megalodont fossils of Upper Triassic Kuz hill limestone, b) thick bedded neritic limestones of the Kuz hill limestone, c), d) articulated, dark brown pelagic limestones with chertnoddles of the Asar hill limestone, e) clastics of radiolarite and limestone collected from different units in Aybastı formation, f) spherical deformation in volcanic material sandstones in Aybastı formation.

petrographical studies, Kuz hill limestones have the characteristics of biomicrite and micritic limestone (Figure 8a, b). Giant crystal growths (Figure 8c) and dolomitizations (Figure 8d) are observed in the form of fracture fills within limestones. Brecciation, fracture growth, veins with carbonate fillings and iron stains in occasion are probable. Late Noran-Rhaetian (Late Triassic) ages were taken from *Aulotortus* gr. s*inuosus* Weynschenk, *Aulotortus communis* (Kristan), *Aulotortus* cf. *tenius* (Kristan), *Aulotortus* spp., *Auloconus* sp., *Thaumatoporella parvovesiculifera* (Raineri) fauna in Kuztepe limestones. *Aulotortus* sp., *Turriglomina* sp., *Ammobaculites* sp., *Frondicularia* sp., *Ophthalmidium* sp., *Cetates* sp., Lamellibranch shell sections andsponge spicules fauna gave the age of Ladinian-Carnian (Middle-Late Triassic). According to *Ophthalmidium*sp., pelagic pelecypoda sections, *Ophthalmidium* sp. fauna Late Triassic-Liassic? ages were determined. Based on all these findings, the age of the Kuztepe limestone was determined as Ladinian-Liassic? (Figure 9a, b, c, d).

It is considered that Kuztepe limestones that had been formed widely by the benthic foraminiferas and in micritic limestone facies were deposited in a relatively low energy neritic environment. Gradual deepening is observed in the depositional environment towards upper parts of the succession which forms Kuztepe limestones. This deepening in the basin becomes distinctive in Asar tepe limestones. Deepening begins towards the end of Rhaetian and reaches the maximum in Liassic and grasps slope-basin conditions (Ekmekçi et al., 2007).

2.2.2. Asar Hill Limestones

This unit, which is composed of much cherty, macro fossilliferous, gray pelagic limestone was first defined by Özgül (1976) in Asar Hill (south of Bozkır county) and named as Asar Hill limestone. Layer thicknesses are planar generally ranging in between 10 to 60 cm in limestones. Cherts are observed within limestones in the form of independent, yellow-brown colored, nodular cherts with various frequencies with

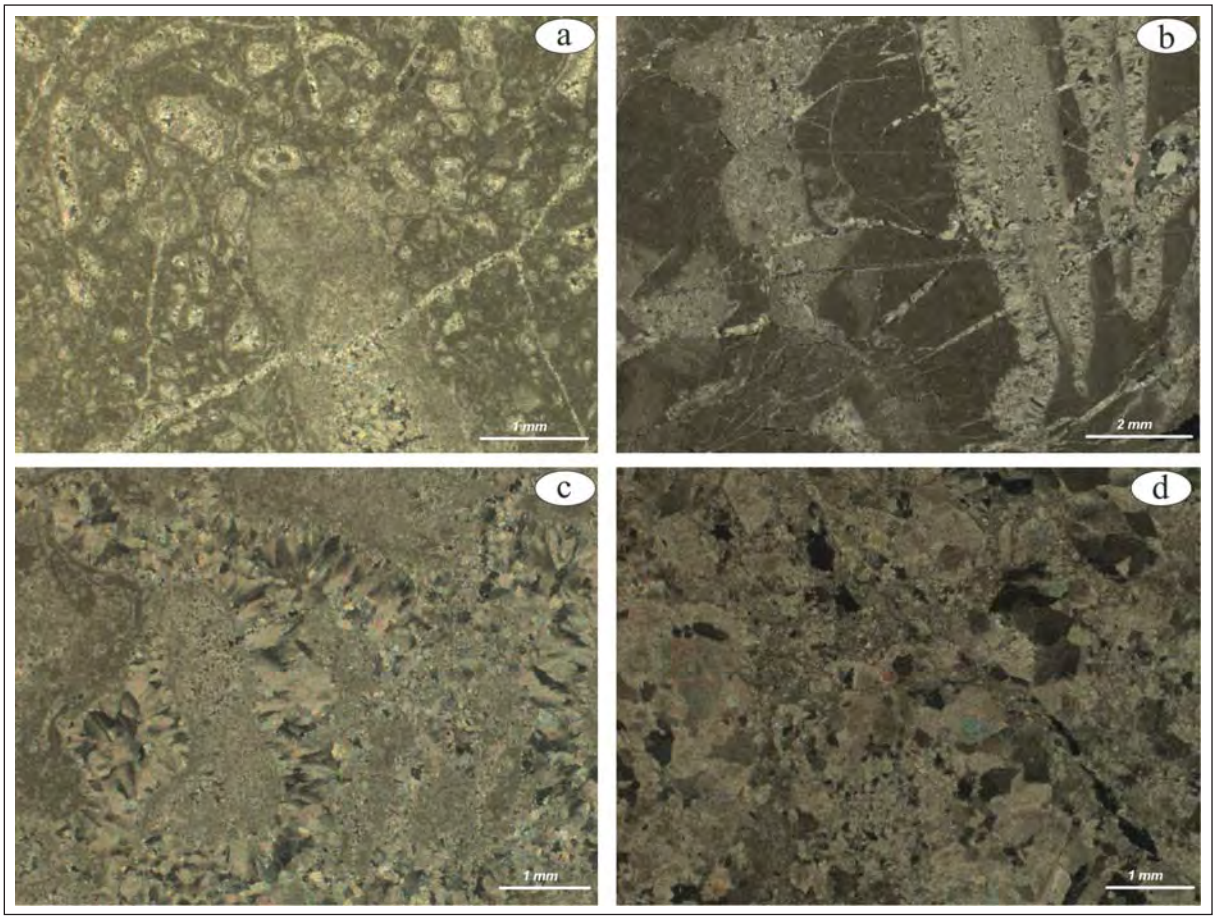

Figure 8- Tectonical effects in thin sections of petrographical samples belonging to different lithologiescollected in Kuz hill formation, a) biomicrite, b) micritic limestone, c) limestone, d) dolomite.

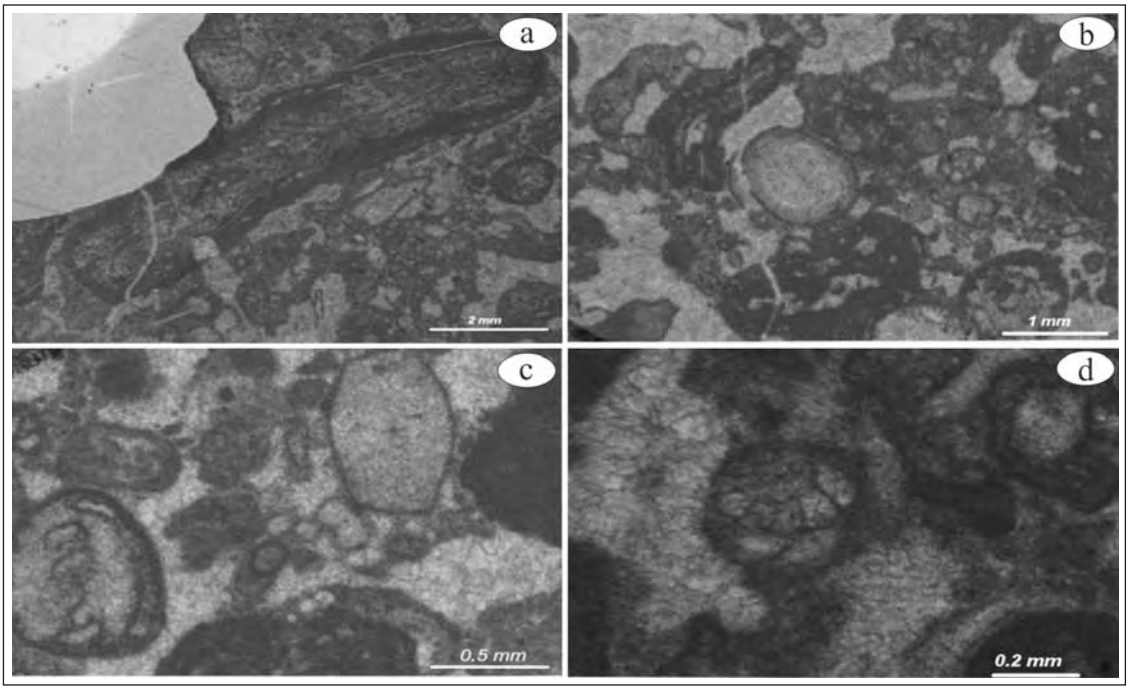

Figure 9- Fossil content of the Kuztepe limestone; a) *Griphoporellacurvata,* b) *Aulotortus* sp., c) *Aulotortussinuosus,* d) *Trochammina* sp.

a diameter size of 5-10 cm. The unit extensively crops out in NW of the study area (502500E/4091700N) and has an apparent thickness of about 80-100 meters. Asar hill limestones which makes a gradual transition into Kuz hill limestones at the bottom are unconformably overlain by the clastics of Aybastı formation in Aybastı village in north of the study area. Silicified dolomitic limestone (Figure 10a) and biomicrite (Figure 10b) determinations were made in petrographical studies of limestones.

According to paleontological studies performed in Asar Hill limestones *Aulotortus* sp., *Turriglomina* sp., *Ammobaculites* sp., *Frondicularia* sp., *Ophthalmidium* sp., *Cetates* sp., lamellibranch shell sections and sponge spicule fauna Ladinian-Carnian (Middle-Late Triassic) ages were obtained; *Aulotortus* sp., *Endothyra* sp. fauna gave Late Triassic age, and from shell sections of radiolaria and pelagic pelecypoda Carnian-Liassic age was detected (Figure 11a, b, c). The age of the formation was given as Ladinian to Early Jurassic based on fossil determination.

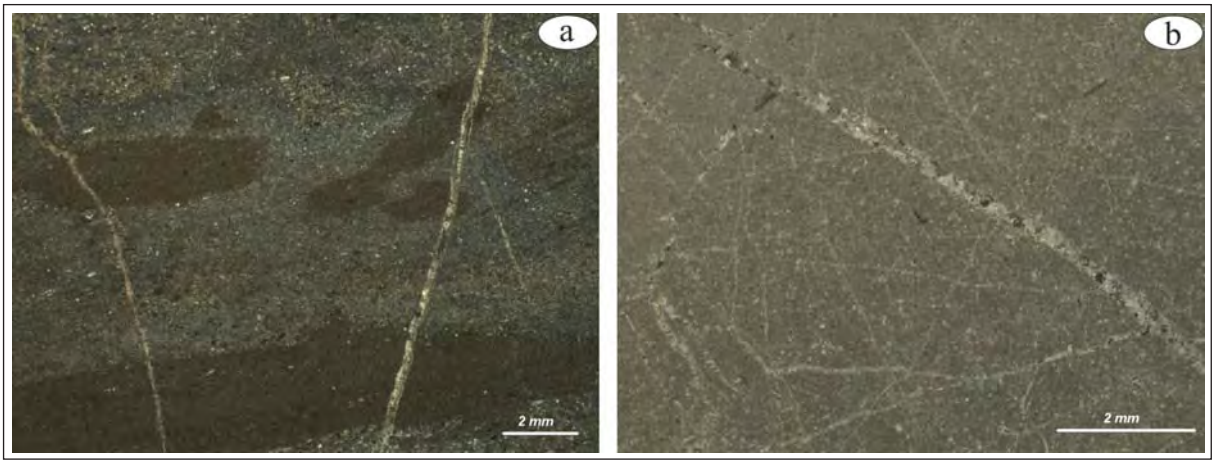

Figure 10- Lithologies defined on petrographical studies of Asar hill limestone, a) silicified dolomitic limestone, b) biomicrite.

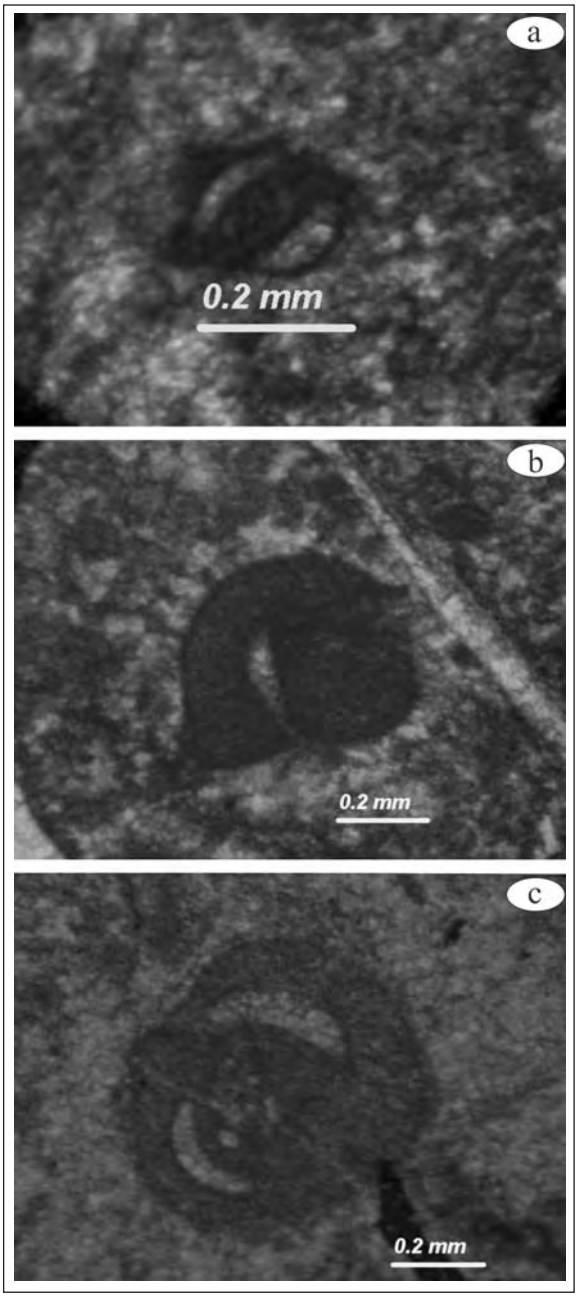

Figure 11- Fossil content of the Asar hill limestone, a) *Ophthalmidium* sp., b) *Galeanellapanticae,* c) *Galeanellapanticae*.

2.2.3. Aybastı Formation

Aybastı formation was first defined by Esirtgen (2009) in the vicinity of Bucakkışla and it takes its name from Aybastı village in NE of Bucakkışla. The formation is a unit in which rock fragments have various sizes, types, and ages are located within brown colored matrix together. This formation is composed of yellow to brown colored chert, bordeaux mudstone, green to brown colored tuff and lava fragments, limestone blocks, and brown colored volcanic sandstone and conglomerates. It is considered that angular limestone blocks of which their sizes reach few meters occasionally belong to Kuztepe limestones. Conglomerates are generally observed in the form of chaotic mixture of volcanic blocks. Spherical deformations in volcanoclastic sandstones are widespread.

Type locality of the formation is the section between the east of Bucakkışla village and the south of Aybastı village in the study area (506000E/4091000N). Aybastı formation has an apparent thickness of about 20 meters and unconformably overlies Kuz hill and Asar hill limestones, and unconformably underlies Fakırca formation. The thickness of the formation thins out towards north of Aybastı village. Aybastı formation can be correlated with Kemaliye formation defined by Özgül et al. (1978) in Munzur mountainous territory of Eastern Taurides.

For paleontological determinations of samples collected from the formation Malm?-Neocomian? age was determined according to *Quinqueloculina* sp., *Ophthalmidiidae, Miliolidae, Nodosariidae,* Brachiopoda fauna (Figure 12a, b). However, the age of the unit was accepted as late Campanian-early Maastrichtian (Özgül et al., 1978) due to insufficient paleontological data.

2.3. Korualan Nappe

It crops out in southwest corner of the study area, around Yukarı Akın, Aşağı Akın villages and was first defined by Özgül (1997) as Korualan group. These rock assemblages display a nappe structure with Huğlu nappe and Boyalı tepe nappe, and are named as "Korualan nappe". Only the Başkışla mélange among rock assemblages which form Korualan nappe crops out in the study area.

2.3.1. Başkışla Mélange

Başkışla mélange was first defined by Özgül (1997) in Central Taurides. It is formed by the chaotic mixture with clastics of limestone, radiolarite, debris flow, volcanites and green tuffs (Figure 13a, b).

The type locality of the mélange is Başkışla village in southwest of the study area and forms the youngest unit defined in nappe slices. The only locality wherethe mélange can be seen is the south of Yukarı Akın village (501300E/4082500N). Başkışla

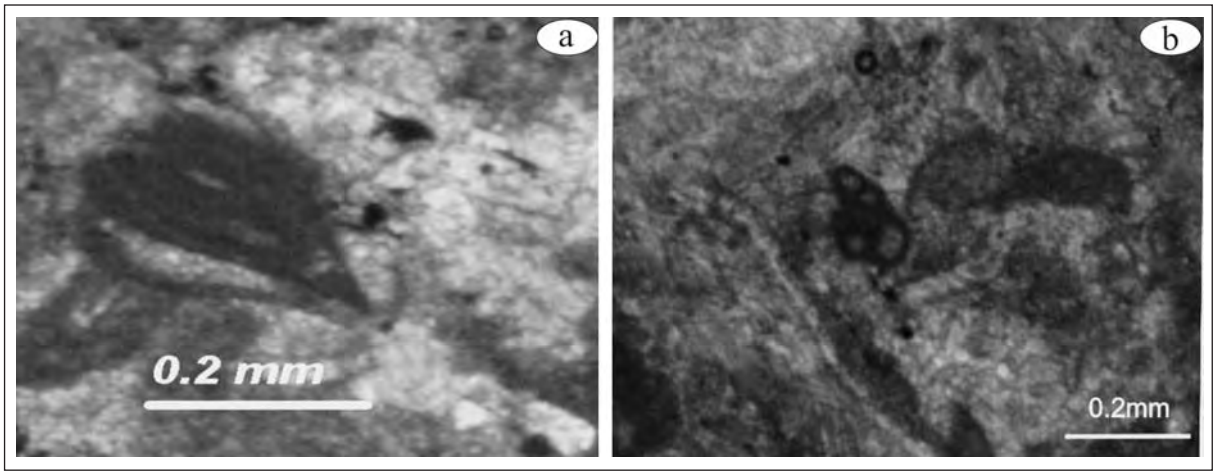

Figure 12- Fossil content of the Aybastı formation, a) *Ophtalmidiiade*, b) *Miliolidae*

mélange possesses an apparent thickness of about 100 meters in the study area and rock units in the mélange show similarities with other units forming other nappe slices. Green tuff and volcanites resemble to Dedemli formation, however thin bedded limestones with radiolarite resemble to Mahmut hill limestone and Kuz hill limestone. Özgül (1997) emphasizes that the age of formation of the mélange should be late and post Senonian considering the age intervals of blocks which the mélange consists of. However, the minimum age should be Paleocene as the unit consists of materials belonging to Kovanlık mélange. Both lower and upper boundaries are tectonically in contact with other nappe slices. Mélange was influenced from compressional regime which has begun in Late Cretaceous and continued until Late Eocene. Kuz hill limestone is located as thrusted extending from south to north over Mahmut hill limestone in south of Yukarı Akın village. This tectonic slice which is formed by Kuztepe and Mahmut hill limestones thrusts over Başkışla mélange. These three units again tectonically overlie Mahmut hill limestones in the northernmost part of the area. Başkışla mélange is made up of debris flow products of different rock lithologies and displays a chaotic view. It also is considered as a product of basin which was opened in front of nappes. Rock groups were most probably subjected to the same deformation due to the compression that continues in the region.

2.4. Fakırca Formation

Lacustrine deposits located over Mesozoic basement rocks in Mut basin was first named by Atabey et al. (2000) as Fakırca formation dedicated to Fakırca village in northwest of Mut. The formation which begins with the deposition of conglomerate, sandstone and mudstones is generally composed of thin bedded, cream white colored, limestone-marl

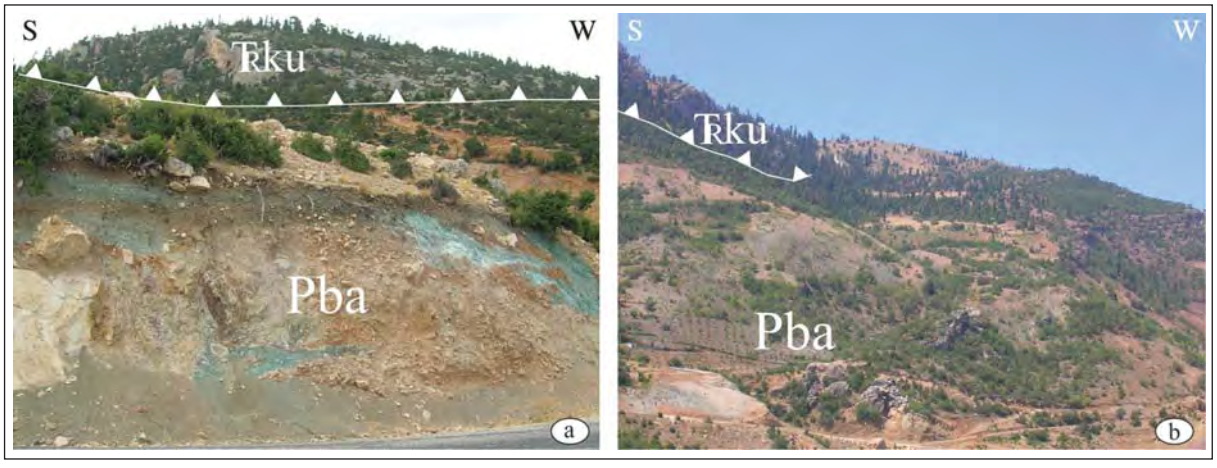

Figure 13- a), b) Tectonical relationship between Başkışla melange and Kuz hill limestone of the Boyalı hill nappe which overlies the melange in N-S directions.

alternation (Figure 14a, b). The apparent thickness of Fakırca formation is about 250 meters and its type locality is in the vicinity of Topalhacı farm in Göksu valley (508000E/4081800N).

The formation has definite angular unconformity with Mesozoic units at the bottom. It again displays an angular unconformity with the overlying Mut formation. The Fakırca formation was dated as; Burdigalian by Gedik et al., (1979); Oligocene-Lower Miocene by Bilgin et al., (1994); Upper Oligocene-Akitanian by Tanar and Gökçen (1990); Akitanian-Burdigalian by Özdoğan (1999); Akitanian–Lower Burdigalian by Atabey et al., (2000), and as Early Oligocene by Kayseri et al., (2006). Conglomerate, sandstone and mudstone succession deposited at the bottom of Fakırca formation indicate alluvial fan deposits. And the overlying, planorbis type gastropoda fossil bearing, marl-limestone alternation shows a fresh water lacustrine environment (Ilgar et al., 2010).

2.5. Mut Formation

Miocene limestones of the Mut formation are located with an angular unconformity over Fakırca formation in near eastern part of the study area (Figure 15a, b).

All Miocene limestones cropping out in Mut basin and its vicinity were named as Mut formation by Gedik et al., (1979). The formation is composed of medium to thick bedded, white, gray reefal limestones. Mut formation represents reef accumulations that formed in transgressive stage of the marine (Atabey et al., 2000). Mut basin was submerged due to marine transgression that developed in Late Burdigalian time in the basin.

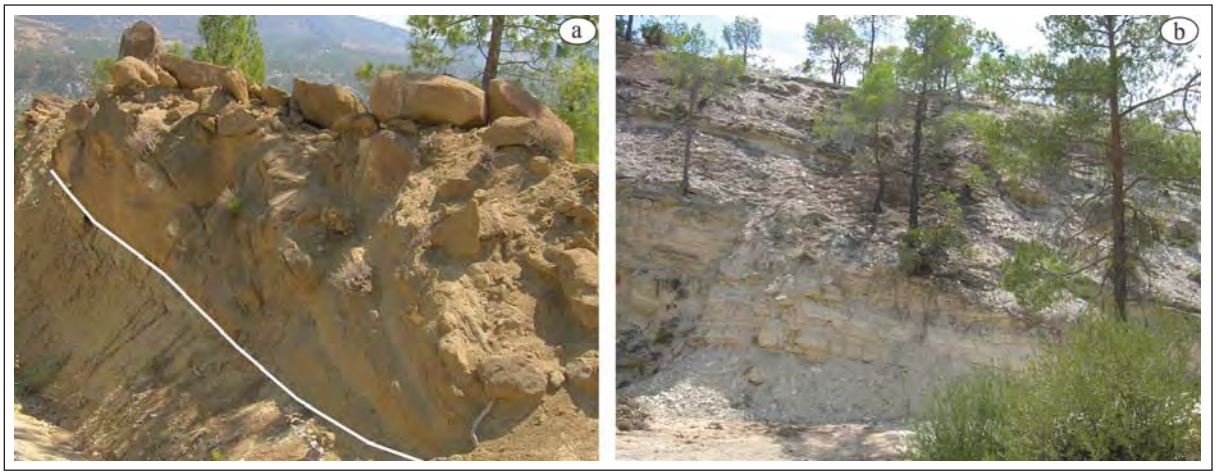

Figure 14- a) Tangential sandstone-mudstone alternation at the bottom of Fakırca formation, b) Laminated marl-limestone alternation of the Fakırca formation.

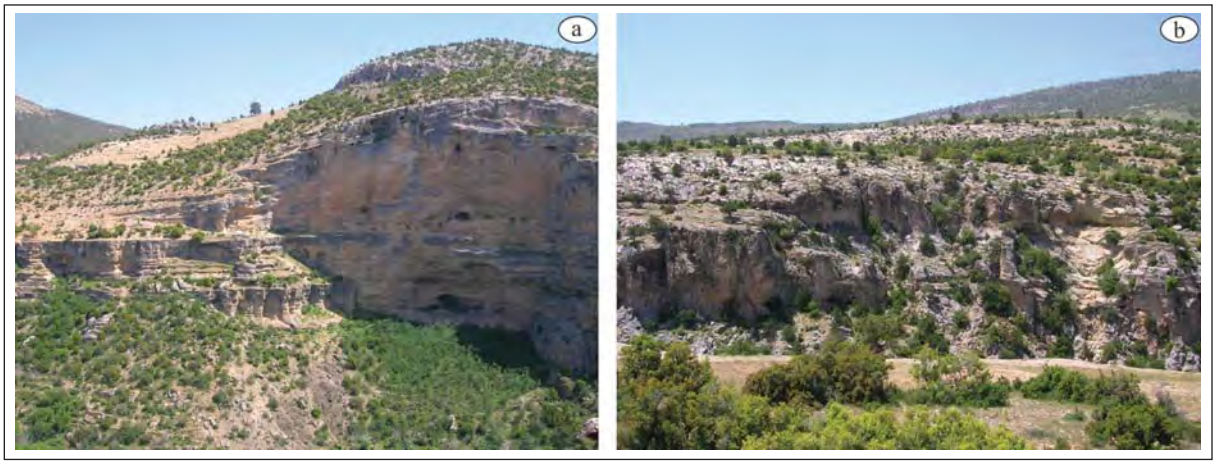

Figure 15- a) Reef flank which forms the Mut formation, b) limestones showing the geometry of the reef core.

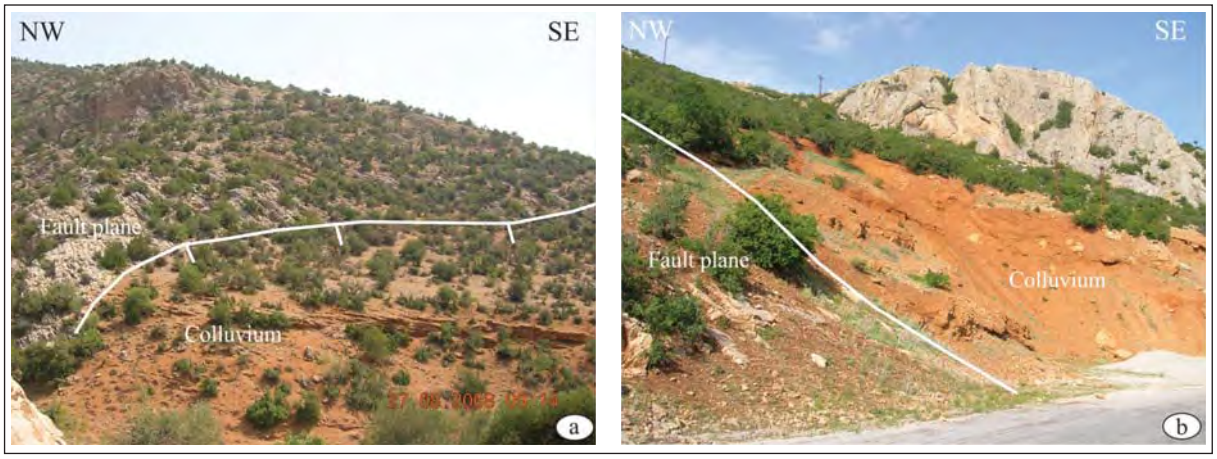

Figure 16- a) Colluvials in front of the normal fault cutting Asar hill limestone, b) colluvials in front of the normal fault cutting Mahmut hill limestone.

Hence, carbonate platform, patch and bornier reefs and lagoonal deposits of he Mut formation have started to deposit on bedrock and Fakırca formation in the basin starting from this time (Ilgar et al., 2010). The age of the Mut formation was determined as Upper Burdigalian-Tortonian (Atabey et al., 2000).

2.6. Plio-Quaternary Deposits

Colluivals, terraces and alluvials form Plio-Quaternary deposits cropping out in the study area. Colluvials are formed by deposits which consist of brick colored, pebble-sand size angular grains in valley margins and fault scarps which show bedding due to granular arrangement (Figure 16a, b).

These deposits have often spaces among grains. Terraces are observed in the form discontinuous outcrops at 4-5 meter above the valley bottom in Göksu valley and consist of very well rounded, well sorted polygenic pebbles (Figure 17).

Figure 17- Field view of terraces along the edges of Göksu River.

These are located on both sides of the Göksu valley at the same levels. There is not observed any effect of active tectonism in terraces which are above the bottom due to stream cutting. Alluvials are generally located inside and on margins of the Göksu valley (502500E/4089650N).

Alluvials which are composed of polygenic material with much pebbly limestone and pebbly chert in occasions have few meters thicknesses and are the youngest unit.

3. Tectonic Evolution and Discussion

Taurides are formed by 6 tectonic units with characteristic features which can be traced almost along the belt (Özgül, 1976). The Geyikdağı unit, which is paraautochthonously located below other units, covers rock units deposited between Cambrian-Tertiary periods of time. This unit is tectonically overlain by Bozkır, Bolkardağı and Aladağ units in north and by Alanya and Antalya units in south. Bozkır unit which is the subject in this study extends from Milas to Munzur Mountains along the Tauride belt. This unit is known as western Lycian nappes around Fethiye-Köyceğiz (Graciansky, 1967; Brunn et al., 1971), as eastern Lycian nappes around Korkuteli (Brunn et al., 1971) in western Taurides; as Beyşehir-Hoyran nappe around Beyşehir-Seydişehir in Central Taurides (Gutnic et al., 1968), as ophiolitic series around Hadim-Bozkır (Özgül, 1971) and as schist-radiolarite formation in Karaman region (Blumenthal, 1956). The unit is formed by different rock groups defined as Huğlu, Boyalı hill and Korualan nappes. Basic submarine volcanite, tuff, diabase, ultrabazite, serpentinite, pelagic and neritic limestone and radiolarites constitute rock groups which represent Triassic-Cretaceous times. It has a mélange characteristic because of its internal structure. Triassic-Quaternary geological evolution of this mélange and the rock units covering the mélange are successively mentioned below.

3.1. Rifting Stage

Due to rifting in Triassic in north of Gondwana, numerous oceanic basins have been opened, and these basins located among continental blocks have continued their presences during Mesozoic-early Senozoic periods (Robertson et al., 2012). Data related to this rifting and opening are widely observed in southern Mediterranean Sea. Depending on rifting of Tauride-Anatolide continent in Triassic, oceanic basin called "Inner Tauride Ocean" was opened in the region (Görür et al., 1984, Görür et al., 1998). Dedemli formation which is known as the lowermost unit of Huğlu nappe is considered to have formed as the product of rift volcanism that had occurred during rifting of Inner Tauride Ocean in Anisian-middle Carnian periods. These units, which form the Bozkır nappe, can be correlated with Alihoca and Mersin mélanges which consist of siliceous deposits such as Triassic aged alkaline lava and radiolarian located within the same belt (Dilek and Whitney, 1997; Parlak and Robertson, 2004; Robertson et al., 2012).

While on one hand, tuff, tuffite, volcanic glass, alkali basic volcanic rocks and lavas originating from the mid-oceanic volcanism have been deposited, on the other hand clastic rocks that generated due to sediment transportation from platform margin have accompanied to this volcanism (Figure 18a).

3.2. Subsidance Stage

Kuz hill limestone which was formed by thick bedded limestones and deposited in a neritic environment is vertically and laterally transitional with Asar hill limestone which is composed of pelagic deposits (Figure 18b). Asar hill limestone among rocks which was deposited during Ladinian-Early Jurassic periods transforms into limestones with chert nodules in middle–upper sections of the succession and grades into bedding layers consisting cherts. This change, which is observed towards middle-upper sections of the succession, is interpreted as the deepening of depositional environment in time and as the condition in deposition of environment has descended below calcite compensation depth (CCD). Deepening and transgression in the basin can be related to eustatic sea level rise and/or to collapse in the basin. In middle Carnian-Santonian period pelagic, cherty limestones were deposited which form Mahmut hill limestones over Dedemli formation in deep marine environmental. The basin margin of this ocean, which is located on the northern part of the Tauride carbonate platform and composed of passive margins, had subsided during Jurassic-Early Cretaceous (Reed, 1982; Andrew and Robertson, 2002; Robertson et al., 2012). Mahmut hill limestones have a transitional contact relationship with Dedemli formation. The presence of Mahmut hill limestones which were deposited on Dedemli formation consists of rift volcanism products and indicates that the volcanic activity and rifting in the basin starting from middle Carnian has ended.

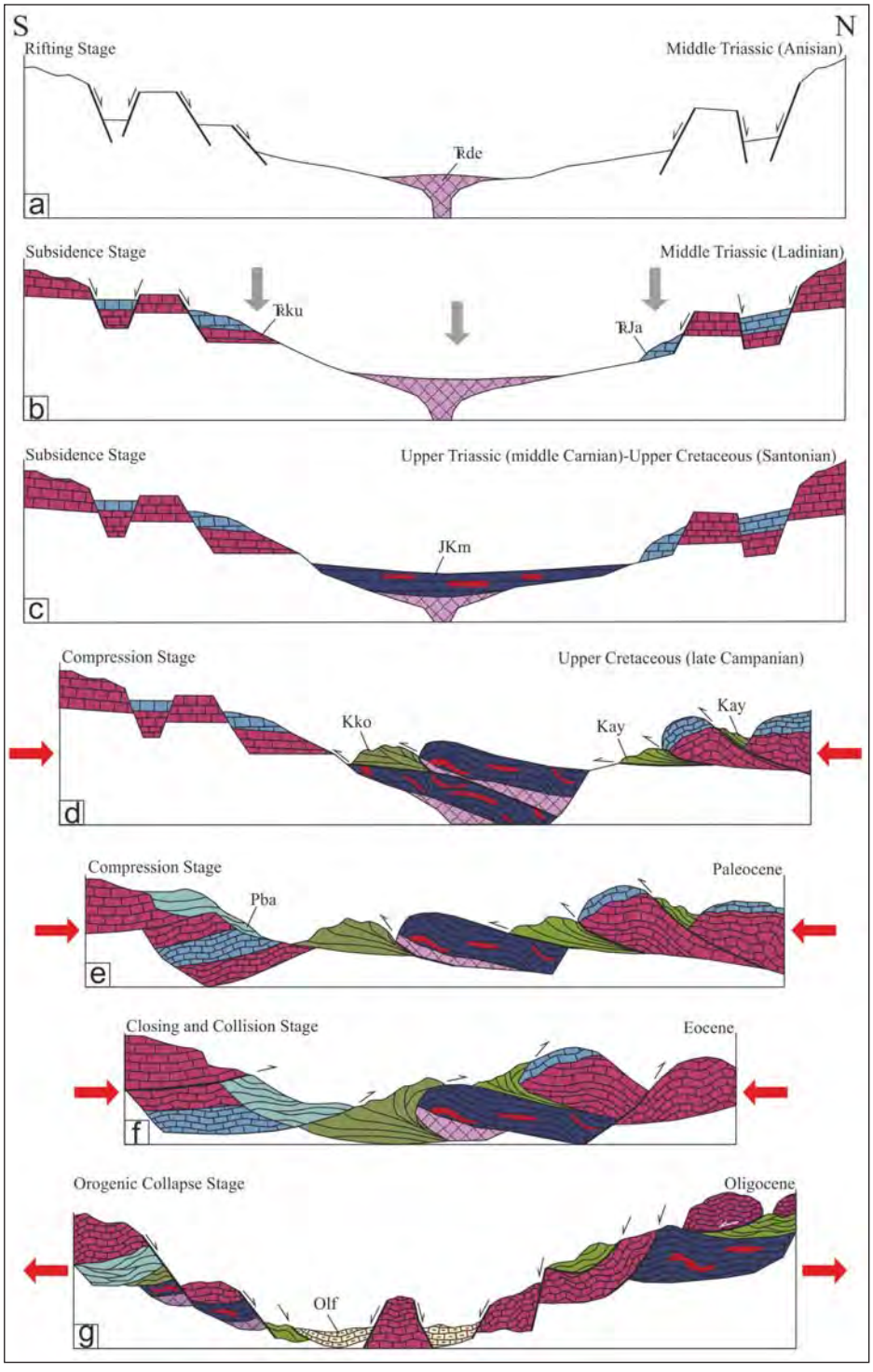

Figure 18- Middle Triassic-Oligocene period geological evolution of the study area: a) the rift volcanism in Anisian, b) the deposition of pelagic limestones in deep and the deposition of neritic limestones in shallow sections of the basin in Ladinian, c) the closure of rift volcanism and the deposition of pelagic, cherty limestones in Middle Carnian-Santonian, d) the beginning of compressional stage in late Campanian, the formation of Kovanlık mélange and Aybastı formation, e) the continuation of the compressional stage and the formation of Başkışla Melange in Paleocene, f) the formation of collision and back thrusts in Eocene, g) the formation of post collisional orogenic collapse in Oligocene the formation of lagoonal basins and the lagoonal deposition of Fakırca formation in Oligocene.

As Mahmut hill limestones were deposited in deep sections of the basin (Figure 18c), Kuz hill and Asar hill limestones continued to deposit on platform margins of the same basin.

3.3. Compressional Stage

The location of Kovanlık mélange to be over Dedemli and Mahmut tepesi formations in rift center, its formation by picking up fragments from those units and this mélange to consist of SSZ type ophiolites were geochemically interpreted as the beginning of compression and of the subduction-obduction process in the region (Figure 18d). When Santonian age of Mahmut Hill limestone is taken into consideration which was determined by Tekin (1999), the age of Karanlık melange could be Post Santonian.

The beginning of compression and subduction-obduction stages with Kovanlık mélange means at the same time that the tectonic regime prevailing in the region has changed, so this period was dated as post Santonian. The formation of SSZ type ophiolites and the ophiolitic mélange during this period of time developed due to northward subduction of Inner Tauride Ocean in Late Cretaceous (Robertson et al., 2012). The units belonging to Kovanlık mélange due to this subduction-obduction began to occur and move northward in time.

As Kovanlık mélange was formed in inner parts, the Aybastı formation was formed in late Campanian-early Maastrichtian period on Kuztepe and Asar tepe limestones of the marginal basin by taking materials from these units (Figure 18d). The unconformable location of Aybastı formation on Kuztepe and Asar tepe limestones reflects non-depositional period that developed between middle Jurassic–early Campanian age intervals. It indicates that the upper sections of the succession formed by limestones were removed from environment by tectonical and/or erosive processes.

Başkışla mélange, according to Özgül (1997), gives the view of chaotic mélange of blocks which their sizes reach hundreds of meters and have similarities with rock units belonging to other slices of the Bozkır unit (probably derived from them). Green tuff and tuffites in the unit resemble to volcanites of Dedemli formation, the radiolarite and cherts resemble to Mahmut tepesi formation and Kovanlık mélange and limestones resemble to Kuztepe limestones of the Boyalı tepe group. Başkışla mélange probably began to occur in Paleocene by taking material from all units that had generated earlier (Figure 18e). The youngest unit which is older than this formation is Kovanlık mélange. Başkışla mélange is formed by units belonging to Kovanlık mélange and blocks of Kuztepe limestone. This situation was interpreted that the subduction-obduction processes that generate Kovanlık mélange continued, and formed Başkışla mélange in latter stages also including Kuztepe limestones into its body. Hence, Bozkır nappe overlain the northern margin of the Anatolide-Tauride platform starting from Campanian-Maastrichtian period (Bergougnan, 1975; Dürr, 1975; Ricou et al., 1975; Özgül, 1976; Özgül et al., 1978; Şengör and Yılmaz, 1981). Rocks belonging to Bozkır unit not to display any metamorphism or significant deformation support the opinion that this unit was emplaced into the region by the closure of Inner Tauride Ocean.

3.4. Closing and Collisional Stage

The Southern branch of Neotethys partly remained open during Paleocene-Early Eocene period. Forever the inner Tauride Ocean was largely closed and entered into uplifting Subarial period (Koçyiğit, 1983; Robertson, 2000; Robertson et al., 2012). Marine Lutetian sedimentation in Central Taurides is represented only by clastics in olistolith and olistostromal flysch facies in successions belonging to Geyikdağı unit. Olistoliths located within this flysch belong to Bolkardağı and Aladağ units and were transported into Lutetian basin and were included into deposition (Özgül, 1997; Andrew and Robertson, 2002). Bolkardağı and Aladağ units overlie Geyikdağı unit in the next stage. Bozkır mélange, which forms Kovanlık and Başkışla mélanges too, continued to emplace towards south, like Bolkardağı and Aladağ units (Alan et al., 2007, Robertson et al., 2009).

The structural relationships of Huğlu, Boyalı tepe and Korualan nappes which constitute Bozkır unit in the study area, are seen in the form of thrusts onto each other towards north (Figure 18f). Huğlu nappe is the lowermost nappe and successively Korualan, Huğlu and Boyalı tepe nappes are located on it. Başkışla mélange remains between the two Huğlu nappes in south of the study area. However, Başkışla mélange is younger than the units of Huğlu nappe. Besides, Huğlu nappe overlying Başkışla nappe is tectonically overlain by Boyalı hill nappe. Boyalı hill nappe consists of Kuztepe limestone which is older than its units.

This structural relationship shows that nappe slices which emplaced towards south during the closure of Inner Tauride Ocean had moved in the opposite direction during collisional stage and completed its formation advancing northward in the form of back thrusts. The units has taken their recent positions with these back thrust movements.

3.5. Orogenic Collapse Stage

The characteristic of the tectonic movement investigated in Central Taurides in post Eocene is still in debate and it is claimed that post collisional compressive movements continued, and erosion and terrestrial deposition occurred in Oligocene too (Kuşçu et al., 2010). Kaymakçı et al. (2010) pointed out that the second deformational phase occurred as a result of the convergence of Africa-Eurasia in southwestern Anatolia during Late Eocene-Oligocene. However, Oligocene time both in Bucakkışla region and in Ermenek, Mut, Silifke and Çamlıyayla regions is represented by lacustrine clastic and carbonate deposits (Bilgin et al., 1994; Ilgar, 2004; Ilgar and Nemec, 2005; Ilgar et al, 2010). All depositional environments in which these lacustrine depositions had occurred were restricted by dip slip normal faults and fault controlled sedimentation developed in these areas.

All pre Oligocene units which have developed in the region depending on NS trending compressional movement in Central Taurides have been compressed until Late Eocene and become imbricated and completed their orogenic evolutions. The units, which had reached its maximum height,was then collapsed due to a pause or end in compression after orogeny, or due to extension and gravity effect that had developed in the region (Figure 18g). Based on this orogenic collapse event, units that form nappes were cut by dip slip normal faults, so small lacustrine basins were formed in front of faults on falling blocks. The first unit that deposited on these lagoons is the Fakırca formation.

The lower age of the unit to be Early Oligocene indicates that, orogenic collapse event had occurred just in and/or before Oligocene. Early Oligocene deposits are as well inclined southeast in Bucakkışla region. The inclination of the Fakırca formation shows that tectonic lines that caused orogenic collapse and the formation of negative areas have not lost its activity during and after Early Oligocene period.

These depositional areas which formed based on dip slip normal faults were interpreted as the end of compressive movements which began in early Senonian in regional scale and a new tectonical regime started which caused Oligocene deposition in central Taurides.

4. Results

Bozkır unit which crops out in Bucakkışla region consists of basic submarine volcanite, tuff, diabase, ultrabzite, serpentinite, pelagic-neritic limestone and radiolarites and has a giant mélange appearance that covers blocks and slices in various sizes. These rock units has been formed in Inner Tauride Ocean that restricts the north of Tauride-Anatolide platform. In the region, rifting, collapse, compression, closure and collisional events and tectonostratigraphical sequences have occurred during Triassic-Eocene time periods. The study area has been subjected to orogenic collapse and lagoonal deposition has developed in this collapse region. These evolutionary stages were summarized below;

Rifting in north of Gondwana which occurred in Middle-Upper Triassic and the Dedemli formation consisting of tuff and alkali volcanic rocks as rift volcanism product was formed during this time period.

Kuz hill and Asar hill limestones were deposited on basin margins in Ladinian-Early Jurassic period.

Mahmut hill limestones which developed on rift volcanics indicate that the volcanic activity and rifting in the basin ended starting from middle Carnian.

Pelagic Asar tepe limestone to turn into chert nodular limestone towards the upper parts of the succession during Ladinian-Early Jurassic time periods was interpreted as the deepening of depositional environment in time and as the decrease of conditions in depositional environments to a level lower than calcite compensation depth (CCD).

The beginning of compression and subduction-obduction stages with Kovanlık mélange also mean that tectonic regime effective in the region changed and this period was dated as post Santonian.

The lithology of Paleocene aged Başkışla mélange and its stratigraphical position show that compression in the region continued.

During Paleocene-early Eocene period, Inner Tauride Ocean has been largely closed and Bozkır unit has continued to emplace southward. However, recent locations of Korualan, Huğlu and Boyalı tepe nappes which constitutes Bozkır unit in the study area indicate that nappe slices moved during collisional stage in reverse direction and completed its formation advancing northward in the form of back thrusts.

Lacustrine Oligocene deposits which developed over nappe slices and restricted by dip slip normal faults show that compressional regime in the region has ended. Early Oligocene units to incline depending on dip slip faults indicate that the tectonic process which caused Oligocene basin to open have also continued after Oligocene.

Acknowledgement

This study comprises one part of the MSc Thesis conducted within the project of "Orta Torosların Jeodinamik Evrimi" (The Geodynamical Evolution of Central Taurides) carried out in Taurides by MTA. Paleontological determinations were carried out by Sibel Şener and Burcu Coskun Tunaboylu, and petrographical studies were made by Talia Yaşar and Nezihe Şatvan Gökçe. Dr. Ayhan Ilgar and Veysel Işık have contributed a lot to this study by precise reviewing this paper. I would present my special thanks to everyone and especially to my beloved wife Esra Esirtgen, who supported me in this study.

Received: 11.04.2013
Accepted: 15.01.2014
Pubhished: June 2014

References

Alan, İ., Şahin, Ş., Keskin, H., Altun, İ., Bakırhan, B., Balcı, V., Böke, N., Saçlı, L., Pehlivan, Ş., Kop, A., Hanilçi, N., Çelik, Ö.F. 2007. Orta Toroslar'ın Jeodinamik Evrimi Ereğli (Konya)- Ulukışla (Niğde)- Karsantı (Adana)- Namrun (İçel) Yöresi, *Maden Tetkik ve Arama Genel Müdürlüğü Raporu*, No: 11006, 261 S. (unpublished)

Andrew, T., Robertson, A.H.F. 2002. The Beyşehir–Hoyran–Hadim Nappes: Genesis and emplacement of Mesozoic marginal and oceanic units of the northern Neotethys in southern Turkey. *Journal of the Geological Society*, London 159, 529-543.

Atabey, E., Atabey, N., Hakyemez, A., İslamoğlu, Y., Sözeri, Ş., Özçelik, N., Saraç, G., Ünay, E., Babayiğit, S. 2000. Mut-Karaman Arası Miyosen Havzasının Litostratigrafisi ve Sedimantolojisi (Orta Toroslar). *Maden Tetkik ve Arama Dergisi* 122, 53-72.

Barrier, E., Vrielynck, B. (eds) 2009. Palaeotectonic Maps of the Middle East, Middle East Basins Evolution Programme.*Université Pierre et Marie Curie*, Paris.

Bergougnan, H. 1975. Relations entre les edifices pontique et taurique dans le Nord-Est de I'Anatolie. *Bull. Sot.GBol.Fr., Ser*. 7.17: 1045-1057.

Bilgin, A.Z., Uğuz, M.F., Elibol, E., Güner, E., Gedik, İ. 1994. Mut-Silifke-Gülnar yöresinin (İçel İli) jeolojisi. *Maden Tetkik ve Arama Genel Müdürlüğü Rapor* No: 9715, Ankara (unpublished).

Blumenthall, M. M. 1956. Karaman ve Konya Havzası Güneybatısında Toros Kenar Silsileleri ve Şist Radyolarit Formasyonu stratigrafi meselesi. *Maden Tetkik ve Arama Dergisi*, No: 48, Ankara.

Brunn, J.H., Dumont, J.H., Graciansky, P.C., Gutnic, M., Juteau, T., Marcoux, J., Monod, O., Poisson, A. 1971. Outline of the geology of the Western Taurids. Campbell, A.S. (Ed.). Geology and history of Turkey: *Pet. Expl. Soc. Libya Tripoli*, 225-255.

Dercourt, J., Zonenshain, L. P. Ricou, L.-E., Kozmin, V.G., Le Pichan, X., Knipper, A.L., Grandjacquet, C., Sbortshikov, I.M., Geyssant, J., Lepvrier, C., Pechersky, D. H., Boylin, J., Sibuet, J. C., Savostin, L.A., Sorokhtin, O., Westphal, M., Bazherov, M.L., Lauer, J. P., Biju-Dural, B., 1986 1986. Geological evolution of the Tethys belt from the Atlantic to the Pamirs since the Lias. *Tectonophysics*, 123, 241–315.

Dilek, Y. Whitney, D.L. 1997. Counterclockwise P-T-t trajectory from the metamorphic sole of a Neo-Tethyan ophiolite (Turkey).*Tectonophysics*, 280, 295-310.

Dilek,Y., Thy, P., Hacker, B., Grundvig, S. 1999. Structure and petrology of Tauride ophiolites and mafic intrusions (Turkey): implications for the Neotethyan Ocean. *Geological Society of America Bulletin* 111 (8), 1192-1216.

Dürr, S. 1975. Uber Alter und geotektonische Stellung des Menderes-Kristallins/SW-Anatolien und seine Aequivalente in der mittleren Aegaeis. *Habilitations-Schrift, Marburg*/ Lahn, 107 s.

Ekmekçi, E., Özkan Altıner, S., Altıner, D., Yılmaz, İ.Ö., Erdoğan, K., Coşkun, B., Şener, S., Şenel, M., Işıntek, M. 2007. Domuzdağ Napında Üst Triyas-Liyas Foraminifer Biyostratigrafisi: Noriyen-Resiyen Karbonat Platformunun Pelajikleşmesi İle İlgili Veriler.*61. Türkiye Jeoloji Kurultayı Bildiri Özleri Kitabı*, S. 315-316.

Esirtgen, T. 2009. Bucakkışla Bölgesinin (Karaman Güneybatısı-Orta Toroslar) Tektonik Evrimi.*MSc Thesis*, 107 S.

Gedik, A., Birgili, Ş., Yılmaz, H., Yoldaş, R. 1979. Mut-Ermenek-Silifke Yöresinin Jeolojisi ve Petrol olanakları.*Türkiye Jeoloji Kurumu Bülteni* 22, 7-26.

Gökdeniz, S. 1981. Recherches Geologiques Dans Les Taurides Occidentoles Entre Karaman Et Ermenek, Turquie.Le titre de doctour 3 eme cycle, *Universite de Paris-Sud Centre D'orsay*, 202 s.

Göncüoğlu, M.C. 1986. Geochronological data from the southern part (Niğde area) of the Central Anatolian massif. *Mineral Research and Exploration Institute of Turkey (MTA) Bulletin*, 105/106, 111-124.

Göncüoğlu, M.C., Erler, A., Toprak, V., Yalınaz, K., Olgun, E., Rojay, B. 1992. Orta Anadolu Masifin Batı Kesiminin Jeolojisi. Vol. 2. Orta Kesim. *Turkish Petroleum Corporation (TPAO) Reports*, 3155.

Göncüoğlu, C.M., Dirik, K., Kozlu, H. 1997. Pre-Alpine and Alpine terranes in Turkey: explanatory notes to the terrane map of Turkey. In: Papanikolaou, D., Sassi, F.P. (Eds.), IGCP Project no: 276; Paleozoic domains and their alpidic evolution in the Tethys. *Annales Géologiques des Pays Helléniques*, pp. 515-536.

Görür, N., Oktay, F.Y., Seymen, I. ve Şengör, A.M.C. 1984. Paleotectonic evolution of Tuz Gölü Basin complex, central Turkey.*In*: Dixon, J.E. ve Robertson, A.H.F. (eds) The Geological Evolution of the Eastern Mediterranean. *Geological Society, London, Special Publications*, 17, 81–96.

Görür, N., Tüysüz, O. ve Şengör, A.M.C. 1998. Tectonic evolution of the central Anatolian basins. *International Geology Review*, 40, 831-850.

Graciansky, P.C. de., 1967. Existance d'une nappe ophiolitique a lettremite accidentale de la chaine Sud – Anatolienne. *C.R. Acad. Sci., Paris* 264, 2876-2879.

Gutnic, M., Keller, D., Monod, O. 1968. Decouverte de nappes de charriage dans le nord du Taurus occidental (Turquie mSridionale). *C.R. Acad. Sci., Paris* 226, 988-901.

Gutnic, M., Monod, O. 1970. Un serie Mesozoigue condansee dans les nappes du Taurus Occidental, la serie du Boyalı Tepe: *C.R.,* somm*, soc. Geol. France, fasc*., 5, 166-167.

Ilgar, A. 2004. Zorunlu Regresyon, Transgresyon ve Sediman Getiriminin, Havza Kenarı Çökelme Sistemlerinin Sedimantolojik ve İstif Stratigrafik Gelişimi Üzerindeki Kontrolü, Ermenek Havzası (Orta Toroslar). *Maden Tetkik ve Arama Dergisi* 128, 49-78.

Ilgar, A., Nemec, W. 2005. Early Miocene lacustrine deposits and sequence stratigraphy of the Ermenek Basin, Central Taurides, Turkey. Gilbert Kelling, Alastair Robertson ve Frans van Buchem (ed). Cenozoic Sedimentary Basins of South Turkey de.*Sedimentary Geology, Special Publication*, 173, 233-275.

Ilgar, A., Yurtsever, Ş., Nemec, W., Lovlie, R., Messina, C. 2010. Toroslarda Oligo-Miyosen Havzalarının Tektono-Sedimanter Evrimi ve Gölsel Ermenek Havzasının Erken Miyosen Manyetostratigrafisi ve Astronomik Denetimli İklimsel Değişimlerin Belirlenmesi. *Maden Tetkik ve Arama Genel Müdürlüğü Raporu*, No: 11125, 95 S. (unpublished)

Jarvis, A., Reuter, H., I, Nelson, A., and Guevara, E. 2008. Hole-Filled Seamless SRTM Data (online) V4.*International Centre for Tropical Agriculture* (CIAT) available from http://srtm.csi.cgiar.org.

Kaymakçı, N., İnceöz, M., Ertepınar, P., Koç, A. 2010. Late Cretaceous to Recent kinematics of SE Anatolia (Turkey).*Geological Society of London, Special Publication* 340, 409-435.

Kayseri, M.S., Akgün, F., Ilgar, A., Yurtsever, Ş., Derman, S. 2006. Palynostratigraphy and Palaeoclimatology of the Ermenek and Mut Regions (Southern Turkey) in the Earliest Oligocene Period. *Abstract 7th European Palaeobotany-Palynology Conference, Prague*, s. 63.

Kelling, G., Egan, S.E., Gürbüz, K., Şafak, Ü., Ünlügenç, Ü. C. 2001. Oligo-Miocene basins of south-central Turkey: synthesis and appraisal. *Programme withAbstracts, Fourth International Turkish Geology Symposium*, 24-28 Sept., 2001. Çukurova University, Adana, Turkey, p. 17.

Kelling, G., Robertson, A.H.F., van Buchem, F.S.P. 2004. Cenozoic sedimentary basins of southern Turkey: an introduction. *Sedimentary Geology* 173,-3.

Koçyiğit A. 1983. Hoyran Gölü (Isparta Büklümü) Dolayının Tektoniği.*Türkiye Jeoloji Kurumu Bülteni* 26-1, 1-10.

Kuşçu, İ., Gençalioğlu-Kuşçu, G., Tosdal, R.M., Ulrich, T.D., Friedman, R. 2010. Magmatism in the southeastern Anatolian orogenic belt: Transition from arc to post-collisional setting in an evolving orogen. In: Sosson, M., Kaymakçı, N., Stephanson, R., Bergarat, F., Storatchenoko, V. (eds) Sedimentary Basin Tectonics from the Black Sea and Caucasus to the Arabian Platform. *Geological Society, London, Special Publications*, 340, 437-460.

Monod, O. 1977. Recherches ge'ologiques dans Ie Taurus Occidental au sud de Beyşehir (Turquie). These, l'universite de Paris sud "Centre d "Orsay", *Docteur es Sciences*, 442 s. (unpublished).

Okay, A.I., Tüysüz, O. 1999. Tethyan sutures of northern Turkey. Durand, B., Jolivet, L., Horvath, F., Seranne, M. (Ed.), Mediterranean Basins: Tertiary extension within the Alpine Orogen.*Geological Society of London, Special Publication* 156, 475-515.

Özdoğan, M. 1999. Mut (NW) havzasındaki Miyosen yaşlı çökellerin depolanma özellikleri ve sedimantolojik evrimi.*H.Ü. PhD. Thesis*, 135 s. (unpublished).

Özgül, N. 1971. Toroslar'ın kuzey kesiminin yapısal gelişiminde blok hareketlerinin önemi. *Türkiye Jeoloji Kurumu Bülteni* 14-1, 85-101.

Özgül, N. 1976. Toroslar'ın Bazı Temel Jeoloji Özellikleri. *Türkiye Jeoloji Kurumu Bülteni* 19, 5-78.

Özgül, N. 1997. Bozkır-Hadim-Taşkent (Orta Toroslar'ın Kuzey Kesimi) Dolayında Yer Alan Tektono-Stratigrafik Birliklerin Stratigrafisi.*MTA Dergisi* 119, 113-174.

Özgül, N., Turşucu, A., Özyardımcı, N., Bingöl, I., Şenol, M., Uysal, S. 1978. Munzurlar'ın, temel jeoloji özellikleri. *Türkiye Jeoloji Kurumu 32. Bilimsel ve Teknik Kurul., Bildiri Özetleri*, s. 10-11.

Parlak, O. Bozkurt, E., Delaloye, M. 1996*a*. The Obduction Direction of the Mersin Ophiolite: Structural

Evidence from Subophiolitic Metamorphics in Central Tauride Belt, Southern Turkey. *International Geology Review*, Vol. 38, p. 778-786.

Parlak, O. Delaloye, M., Bingöl, E. 1996*b*. Mineral chemistry of ultramafic and mafic cumulates as an indicator of the arc related origin of the Mersin ophiolite (southern Turkey). *Geological Rundsch* Vol. 85, p. 647-661.

Parlak, O., Robertson, A. H. F. 2004. Tectonic setting and evolution of the ophiolite-related Mersin Mélange, southern Turkey: its role in the tectonic–sedimentary setting of the Tethys in the eastern Mediterranean region. *Geological Magazine*, 141, 257-286.

Pourteau, A., Candan, O., Oberhanslı, R. 2010. High-pressure metasediments in central Turkey: constraints on the Neotethyan closure history. *Tectonics*, 29.

Read, J.F. 1982. Carbonate platforms of passive (extensional) continental margin, types characteristics and evolution. *Tectonophysics* 81, 192-212.

Ricou, L.-E., Argyriadis, I., Marcoux, J. 1975. L'Axe calcaire du Taurus, un alignement de fendtres araboafricains sous des nappes radiolaritiques, ophiolitiques et metamorphiques. *Bulletin de la Société Géologique de France* 7, 17, 1024-1044.

Robertson, A.H.F. 1998. Mesozoic–Tertiary tectonic evolution of the easternmost Mediterranean area: integration of marine and land evidence. In: Roberstson, A.H.F., Emeis, K. C., Richter, C., Camerlenghi, A. (Eds.).*Proceedings of the Ocean Drilling Program, Scientific Results*.

Robertson, A.H.F. 2000. Mesozoic-Tertiary tectonic-sedimentary evolution of a south Tethyan oceanic basin and its margins in southern Turkey.Bozkurt, E., Winchester, J.A., Piper, J.D.A. (Ed.), Tectonics and Magmatism in Turkey and the Surrounding Area.*Geological Society of London, Special Publication* 173, 97-38.

Robertson, A. H. F. 2002. Overview of the genesis and emplacement of Mesozoic ophiolites in the Eastern Mediterranean Tethyan region. *Lithos*, 65, 1-67.

Robertson, A.H.F., Woodcock, N.H. 1981. Gödene Zone, Antalya Complex, SW Turkey: volcanism and sedimentation on Mesozoic marginal ocean crust. *Geologische Rundschau* 70, 1177-1214.

Robertson, A.H.F., Dixon, J.D. 1984. Introduction: Aspects of the Geological Evolution of the Eastern Mediterranean. *In*: Dixon, J.E. & Robertson, A.H.F. (eds) The Geological Evolution of the Eastern Mediterranean. *Geological Society, London, Special Publications*, 17, 1–74.

Robertson, A.H.F., Ünlügenç, Ü. C., İnan, N., Taşlı, K. 2004. The Misis–Andırın complex: a mid-Tertiary melange related to latestage subduction of the neo-tethys in S. Turkey. *J. Asian Earth Sci*. 22, 413-453.

Robertson, A.H.F., Parlak, O., Ustaömer, T. 2009. Melange genesis and ophiolite emplacement related to subduction of the northern margin of the Tauride-Anatolide continent, central and western Turkey. *Geological Society of London, Special Publications* 311, 9-66.

Robertson, A.H.F., Parlak, O., Ustaömer, T. 2012. Overview of the Palaeozoic-Neogene evolution of Neotethys in the Eastern Mediterranean region (southern Turkey, Cyprus, Syria). *Petroleum Geoscience*,Vol. 18, pp. 381-404.

Stampfli, G.M., Mosar, J., Favre, P., Pillevuit, A., Vannay, J. C. 2001. Permo- Mesozoic evolution of the western Tethyan realm: the Neotethys/East- Mediterranean connection. In: Ziegler, P.A., Cavazza, W., Robertson, A.H.F., Crasquin-Soleau, S. (Eds.), Peri Tethys memoir 6: Peritethyan rift/wrench basins and passive margins. *IGCP 369 Mémoires du Museum National d'Histoire Naturelle, Paris*, pp. 51-108.

Streckeisen, A. 1976. To each plutonic rock its proper name. *Earth Sci. Rev*. 12: 1-33.

Şengör, A.M.C. 1984. The Cimmeride orogenic system and the tectonics of Eurasia.*Geological Society of America, Special Paper*.

Şengör, A.M.C., Yılmaz, Y. 1981. Tethyan evolution of Turkey: A plate tectonic approach. *Tectonophysics* 75, 181-241.

Tanar, Ü., Gökçen, N. 1990. Mut-Ermenek Tersiyer İstifinin Stratigrafisi ve Mikropaleontolojisi.*MTA Dergisi*,110, 175-181.

Tekin, U., K. 1999. Biostratigraphy and systematics of Late Middle to Late Triassic radiolarians from the Taurus Mountains and Ankara region, Turkey. *Geol. Paläont. Mitt. Innsbruck, Sonderband* 5, 1-296.

Tekin, U., K., Ekmekçi, E., Kozur, H.W. 2001. Dating of the Huğlu tuffite based on the radiolarian fauna, Huğlu unit (Beyşehir-Hoyran nappes), Central Taurides, Turkey. *4th International Turkish Geology Symposium, Abstracts*, p. 264.

Tekin, U., K., Bedi, Y. 2007. Middle Carnian (Late Triassic) Nassellaria (Radiolaria) of Köseyahya nappe from eastern Taurides, eastern Turkey. *Rivista Italiana di Paleontologia e Stratigrafia*, Vol. 113, pp. 167-190.

Whitechurch, H., Juteau, T., Montigny, R. 1984. Role of the Eastern Mediterranean ophiolites (Turkey, Syria, Cyprus) in the history of the Neo-Tethys.*Geological Society of London, Special Publications*, v. 17; p. 301-317.

Bulletin of the
Mineral Research and Exploration

http://bulletin.mta.gov.tr

NEOGENE STRATIGRAPHY OF THE NORTHERN PART OF KARABURUN PENINSULA

Fikret GÖKTAŞ[a]

[a] *The General Directorate of Mineral Research and Exploration, Regional Directorate of Aegean, İzmir, TURKEY*

Keywords:
Karaburun peninsula, Neogene stratigraphy, Early Miocene volcanism, paleogeography, K/Ar geochronology

ABSTRACT

The terrigenous Neogene lithology in north of Karaburun peninsula is represented by Lower-Middle Miocene rock units which are cut and bounded by NW-SE trending synthetic faults. Dominant lacustrine sedimentation (Haseki and Hisarcık formations) of Early-Middle Miocene period which was separated by upper and lower regional unconformities, and the Early Miocene mafic volcanism (Karaburun volcanites) were studied within the scope of Karaburun group. Haseki formation which reflects Early Miocene sedimentation begins with fills of alluvial fan of the Salman member and is basically formed by algal-biostromal Yeniliman limestone and lacustrine deposits of Aktepe member. With synsedimentary emplacement of the 1st phase Karaburun volcanites over Yeniliman limestone platform, the dominant sequence which is micritic limestone intercalating with diatomite of the Aktepe member was deposited in environmental conditions deepening towards shore-face. The effectiveness of NW trending boundary faults which gave rise to 2nd phase of the Karaburun volcanism, shaping the western edge of Foça depression towards the end of Early Miocene has not changed the dominant depositional environment, and lacustrine sedimentation has continued with Hisarcık formation. Green and fine clastic shore-face sediments (Karabağları member) of the Hisarcık formation which deposited the latest between Early Miocene-Middle Miocene overlie Aktepe sequence with submarine parallel unconformity. Karaburun volcanism which is represented by high potassium andesitic products with calc alkaline character (pyroclastics and olivine- phyric lavas) is synchronous with sedimentation of Haseki formation and has two phases. Pyroclastic rocks which are in facies of base-surge, air-fall and ash-fall in lesser amount were emplaced before lava eruptions. K/Ar aged, 1st phase products, which are 18.2±1.0 my according to K/Ar dating, are in the position of stratigraphical reference level which separates Yeniliman limestone from Aktepe member. Second phase products are emplaced in Aktepe sequence.

1. Introduction

This study aims at reflecting the stratigraphical evolution of Early-Middle Miocene terrigeouns deposits cropping out in north of Karaburun peninsula and thesynsedimentary mafic volcanites (Figure 1). As listed in Çakmakoğlu and Bilgin (2006), detailed geological investigations which began with Kalafatçıoğlu (1961) all around the peninsula are mainly related to pre Neogene rock units. The main topic of the Neogene studies are the ones related with magmatism (Innocenti and Mazzuoli, 1972; Borsi et al., 1972; Türkecan et al., 1998; Helvacı et al., 2009).

The first detailed tectono-stratigraphic study related to Neogene rock units in coastal Aegean region was made by Kaya (1979). Türkecan et al., (1998) studied petrographical and mineralogical characteristics of "Yaylaköy" and "Karaburun"

* *Corresponding author : fikretgoktas50@gmail.com*

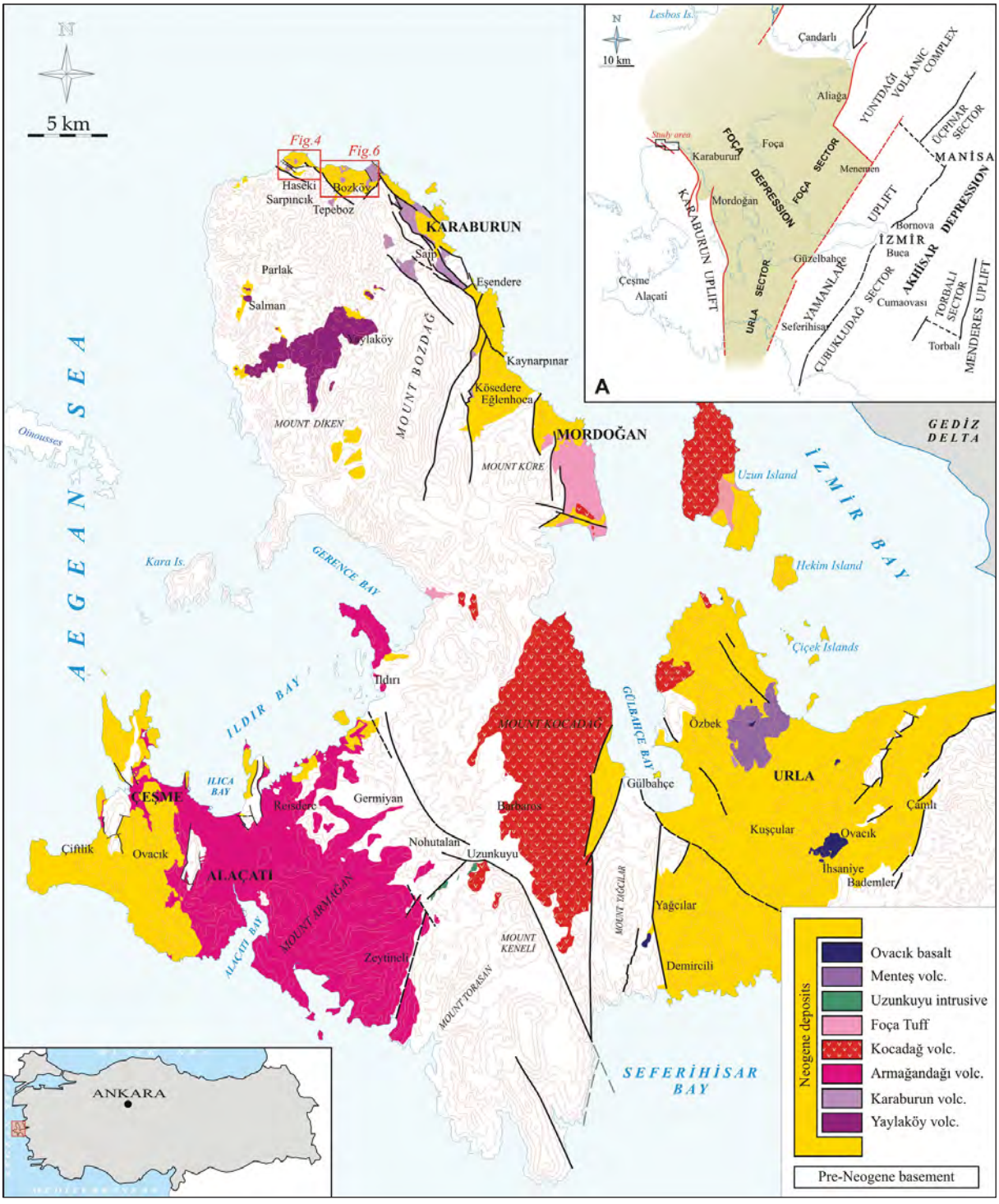

Figure 1- Location of the study area and its position within Foça Depression reflected by modifying Kaya (1979) (A).

volcanites where they were distinguished in northern part of the peninsula, and took 18.5±3.1 my and 16.0±07 my K/Ar ages from Karaburun volcanites. Helvacı et al., (2009) stated that Karaburun volcanites were formed from olivine bearing basaltic andesite and shoshonite, and took 17.0±0.4 my $^{40}Ar/^{39}Ar$ age from Yaylaköy volcanites which high potassium calc-alkaline andesite rocks symbolized. In both studies, which do not contain any stratigraphical detail, it was accepted that the generalized Neogene sedimentation and volcanism showed laterally related development thoroughly.

Major element analyses of lava samples taken from Karaburun volcanites were carried out in the Dept. of Mineral Analysis and Technology of MTA, however K/Ar analysis was performed in Tubingen University (Germany).

All stratigraphic units were named, described and mapped in 1/25 000 scale in this study the first timeby dividing them into groups, formations and members in the area.

2. Stratigraphy

Pre Neogene basement rocks which propagate in north of Karaburun peninsula (Figure 2) is formed by "Küçükbahçe" (Ordovician-Cambrian?) and "Dikendağı" (Carboniferous-Silurian) formations, Camiboğazı formation (Ladinian), İzmir flysch (Late Cretaceous-Early Tertiary) which the neritic carbonates symbolize and by Yeniliman serpentine rocks (Çakmakoğlu and Bilgin, 2006) . The region remained as nondepositional area starting from the emplacement of İzmir-Ankara zone to the beginning of Early Miocene sedimentation.

Neogene rock units in the study area are represented by dominant lacustrine Lower-Middle Miocene deposits which are described within Karaburun group and by Lower Miocene mafic volcanites. Haseki formation and Karabağları member forming the lower part of Hisarcık formation and Karaburun volcanites were distinguished within Karaburun group (Figure 3). Karaburun group is time stratigraphic equivalent of "Çeşme group" suggested by Göktaş (2010) in Çeşme peninsula.

2.1. Haseki Formation

Haseki formation which reflects Early Miocene sedimentation is dominantly formed by lake deposits. The unit which has taken its name from the Haseki village was studied as being separated into gravel dominant Salman member, algal biostromal Yeniliman limestone and Aktepe member represented by micritic limestone (Figure 3). Two phased Karaburun volcanites are located within lake section of the formation (Kv.I and Kv.II; Figure 3).

One of the data which could date Haseki formation is 18.2±1.0 my K/Ar age taken from 1st phase Karaburun volcanite between Yeniliman limestone and Aktepe memberin this study. And the other data is the upper age limit in which "Yeniliman small mammal fauna" was described by Saraç (2003)

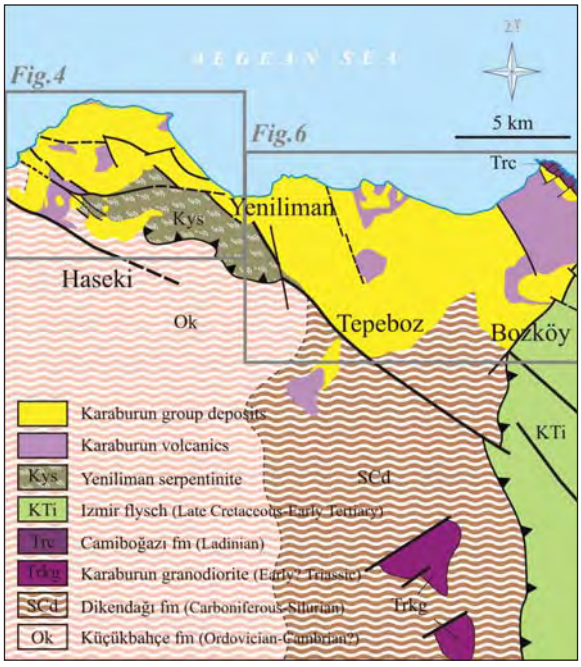

Figure 2- Geological map of Pre Neogene rock units which spreads in the study area (modified from Çakmakoğlu and Bilgin, 2006).

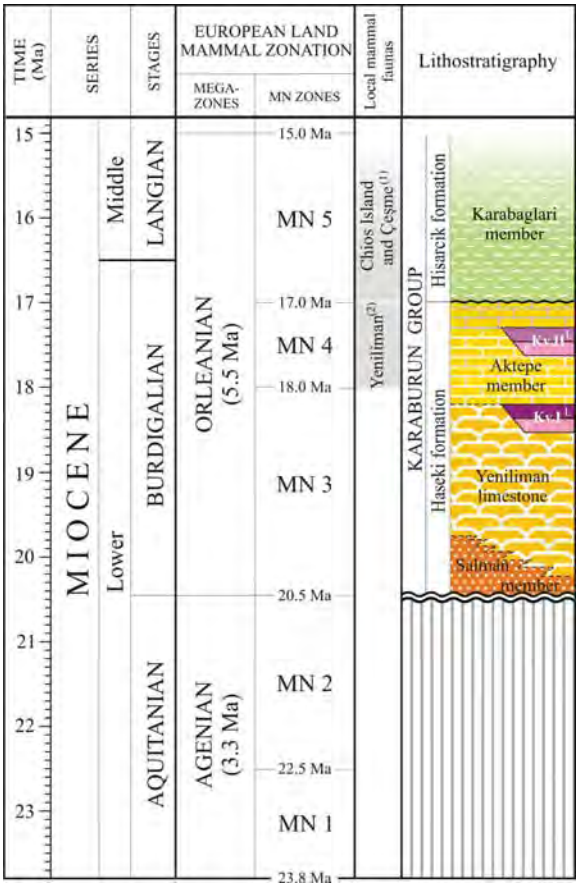

Figure 3- Generalized stratigraphic section of the study area. Time table is according to Steininger (1999). (1) Besenecker (1973), (2) Saraç (2003). Kv: Karaburun volcanites. L: Lava, P: Pyroclastic.

corresponds to 17 my in the biostratigraphy of Steininger (2000) (Figure 3). According to 21.3 K/Ar age, which Borsi et al., (1972) dated from 1st phase Yaylaköy volcanites overlying the Salman formation (Aras et al., 1999; Çakmakoğlu et al., 2013), the sedimentation might have started in Early Miocene. Though, geochronology and biochronology data in broad sense indicate Early Miocene, the sedimentation is mainly considered to have begun in late early Miocene.

"Şifne formation" (Göktaş, 2010), which evolved from alluvial to lacustrine environment in Çeşme peninsula, and Lower Miocene deposits composed of alluvial "Yeniköy conglomerate" and lacustrine "Zeytindağ formation" (Kaya, 1979) described in Foça peninsula are regional equivalents of the unit. Lacustrine deposit which is formed by Yeniliman limestone and Aktepe memberis time stratigraphic equivalent of Zeytindağ formation. The absence of deposits which can be correlated with Haseki formation in Urla basin was explained with non-deposition (Göktaş, 2011).

2.1.1. Salman Member

The sub unit describes conglomerate dominant sequence forming the basement of Haseki formation. It is known that alluvial fan and alluvial fan deposits around Salman village and Yaylaköy (Figure 1) are represented in the name of "Salman formation" (Aras et al., 2000; Çakmakoğlu, 2008; Çakmakoğlu et al., 1999, Çakmakoğlu, 2013). The nomenclature of the unit which was reduced to member level was changed in this study.

Type location of the sub unit which shows lateral discontinuity spread between Haseki village and Bosköyis around Düdükçü Hill (Figure 4). The apparent thickness of the sequence is maximum 50 meters.

The sedimentary sequence consists of poorly bedded conglomerate, sandstone and mudstone in fewer amounts and shows a fining upward from bottom to top. Disorganized coarse gravels are located in lower part of reddish brown-paleo oxide

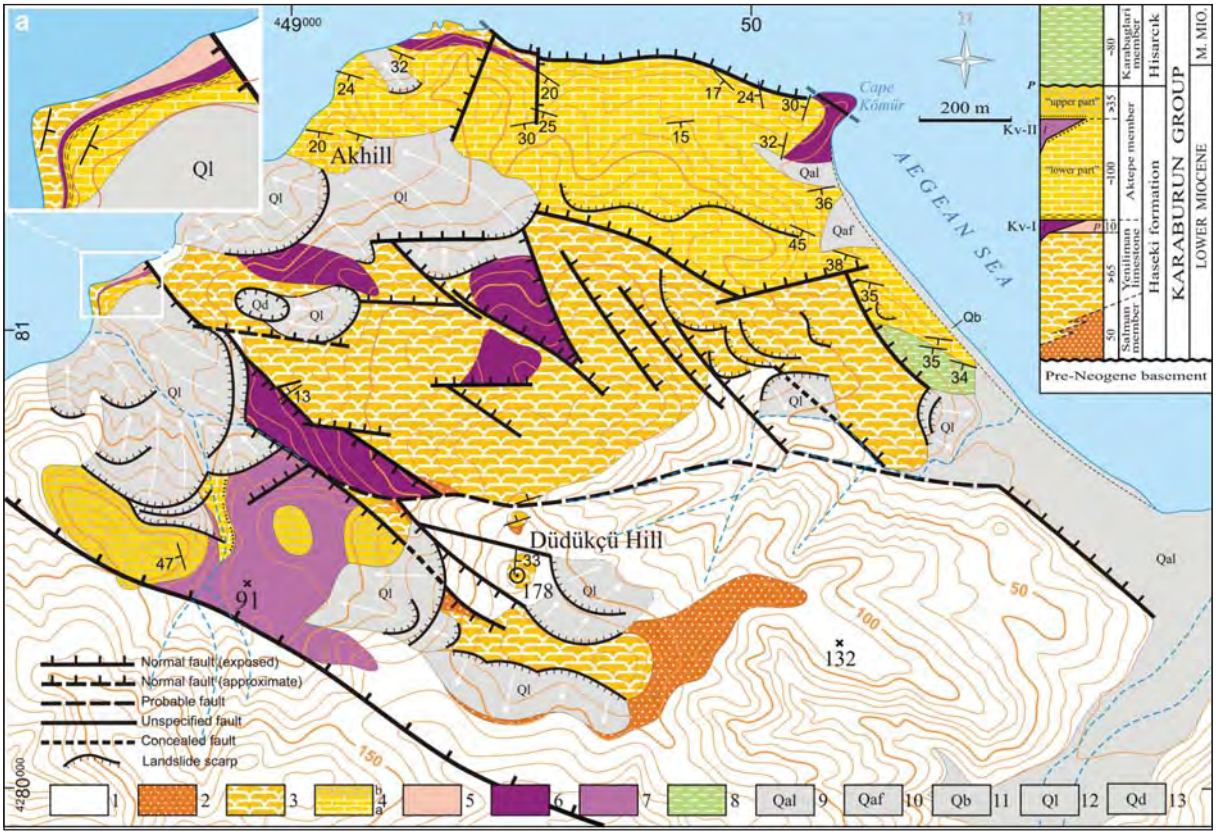

Figure 4- Geological map of north of Haseki. 1) Basement rocks, 2) Salman member, 3) Yeniliman limestone, 4) Aktepe member; a: lower, b: upper, 5) 1st stage Karaburun volcanites (pyroclastic), 6) 1st stage Karaburun volcanites (lava), 7) 2nd stage Karaburun volcanites (lava), 8) Karabağları member, 9) Alluvial, 10) Alluvial fan deposits, 11) Sand deposits, 12) Landslide debris, 13) Doline. PU: Parallel unconformity, L: lava, P: pyroclastic.

colored sequence cropping out in north of Haseki village (Figure 5).

Conglomerate is in degree of low textural maturity, intercalated with badly sorted, pebbly-coarse sand, blocky in varying amounts and is unbedded. The ratio of coarse components, as dense as it could be grain supported, with respect to matrix is generally very high (Figure 5a). Less distinctive, cross layered, conglomerate-pebbly sandstone layers gradually increase towards the upper layers of deposit. Conglomerate is formed by single or multilayered lateral discontinuities. It is generally made up of small gravels and grains or intra material supported (Figure 5b). Pebbles, which are angular to sub spherical, have elongated and sheet like shapes. Sandstone is generally coarse to very coarse sand sized, consists of small cobble and pebble, grain supported, and is medium to badly sorted. All rock type components forming the sedimentary sequence were derived from Küçükbahçe and Dikendağı formations (Figure 2) and formed by shale, greywacke and vein quartz in the order abundance. Lateral intertongue of LLH-SH (Laterally Linked Hemispheroid-Stacked Hemispheroid) morphotype stromatolith which is the lateral continuity of Yeniliman limestone and red colored small conglomerate-sandstone-sandy mudstone levels are observed around Bozköy (Figure 5c and d).

The sub unit which overlies Küçükbahçe and Dikendağ formations and Yeniliman serpentine with angular unconformity forms Early Miocene basin bottom. It also reflects the beginning of continental Neogene sedimentation. The relationship is lateral intertonguing from bottom to top in the generalized stratigraphical section.

The burial of boundary faults which separates Haseki formation from basement rocks with post sedimentary vertical activities and the Salman member, which gives a limited observation because of Yeniliman limestone cover, reflects time transgressive alluvial fan deposit which developed Early Miocene basin margins. Disorganized coarse gravels which form the lower section of the deposit

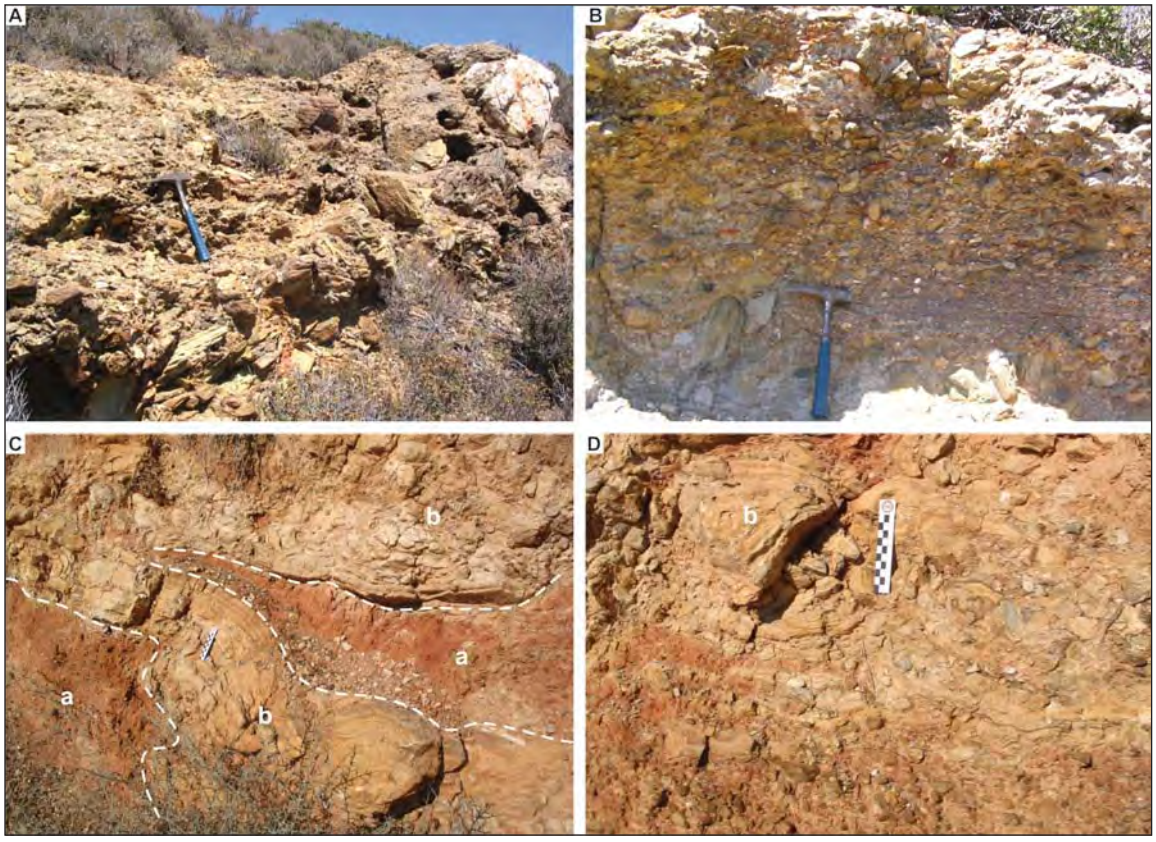

Figure 5- Sediment facies of the Salman member. A) Debris flow facies, B) Braided stream channel fill facies, C) Lateral intertongue between LLH type stromatolith horizons of alluvial deposits of the Salman member (a) and the overlying Yeniliman limestone, D) some stromatoliths (b) are observed as autochthonously grown around deposited pebbles. Hammer size 33 cm, scale 10 cm.

are in debris flow facies and describe the proximal fan deposition. Cross bedded conglomerate and pebbly sandstone layers which increasetowards upper parts are channel and bar deposits of the braided rivers developed on fans.

Salman member can be correlated with Yeniköy conglomerate in Foça peninsula because of their positions at the beginning and of similar environmental characteristics. The sub unit is the equivalent of non-systematically described Bozköy formation by Helvacı et al., (2009). The presences of its conjugates which are not exposed in Çeşme peninsula were confirmed by drilling data (Göktaş, 2010).

2.1.2. Yeniliman Limestone

The sequence consists of algal biostromal-biohermal limestone from bottom to top and was first distinguished in this study in the name of "Yeniliman member". The type locality is the Yeniliman district of the Salman village. The apparent thickness of the sequence which mainly crops out between Yeniliman and Bozköy is higher than 120 meters (Figures 4 and 6).

The sequence dominant in algal limestone which was formed by organisedimentary structures that stromatolites symbolize seldom consists of green, massive sandstone interlayers and lenses of diagenetic chert. The biostromal limestones which were formed by in-situ growing stratiform stromatoliths are dominant in the sequence. According to textural classification of Dunham (1962), the limestone in "algal boundstone" facies is medium to coarse crystalline and is generally very hard. The decomposition surface is in dark gray or yellowish gray and fresh rock is in beige color. It is generally thick (100-30 cm), occasionally medium (30-10 cm) or very thick (>100 cm), tabular parallel layered and is algal laminated (Figures 7a and b). Within biogenic limestone sequence; "undulated and parallel laminated" stromatolites are abundant (Figures 7c andd) however, the ones that are "tabular and parallel laminated" are in minority. Fenestral cavities parallel to algal laminae become widespread in some places (Figure 7e). According to geometrical classification of Logan et al., (1964), LLH morpho type stromatolites are widespread, but LLH-SH morpho types are seldom observed (Figure 7f). Thin branched species which areseldom observed have been post mortem reworked and formed biosparitic levels among algal laminated sections.

A stromatolite bioherm different than widespread algalswas observed in the uppermost part Yeniliman limestone sequence which is 6 m thick (Figure 4a) cropping out600 meters away from SW of Aktepe. Algal mass, which its decomposion surface is

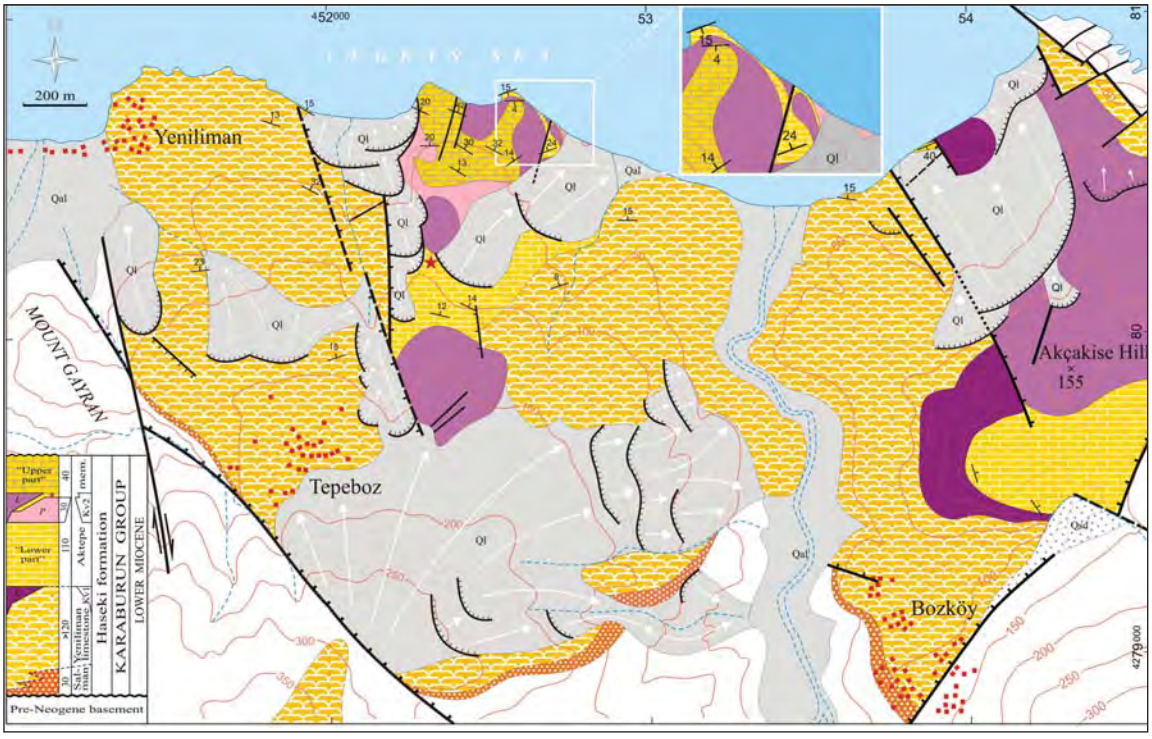

Figure 6- Geological map of Tepeboz-Bozköy surround. Red star denotes for finding locality of MN+ mammal fauna.

Figure 7- Specific rock type facies of the Yeniliman limestone. A) very thick undefined bedding, (Jacob stick 140 cm.); B) Planar, parallel, medium-thick bedding; C, D) stromatolith bioherm made up of undulated parallel alg laminae (hammer size 33 cm); E) fenestral spaces developed parallel to algal laminae; F) stromatolith bioherm with LLH morphotype; G, H) bioherm which columnar stromatoliths formed (scale 10 cm).

yellowish brown and fresh surface is dark brown, is formed by the columnar stromatolites with diameters exceeding 10 cm. Textural features such as; grain supported packaging without inter material and cementation with spar calcite indicatesrudstonefacies of Dunham (1962) (Figures 7g and h).

Yeniliman limestone rests on basement rocks by means of transgressive basement clastics in places where it laterally overcomes Salman alluvial deposits. NW trending faults that activated post sedimentation or re-activated around Bozköy and Tepeboz, have formed a contact between Yeniliman limestones and basement rocks burying Salman alluvial deposits. The first phase products of Karaburun volcanism (in spread areas) distinguish Yeniliman limestone from Aktepe member. Algal limestones within close vicinity of volcanic centers have been braided by pyroclastic rocks in base-surge and air-fall facies which emplaced before lava eruptions or by lava flows. In places, where the first phase volcanism is not available, the continuity of lake sedimentation is clearly observed between Yeniliman limestone and Aktepe member.

Algal limestone deposits have been formed by autochthonous stromatolites which developed on coastal part of the Lower Miocene perennial lake. Not to encounter oncoids (spheroidal stromatolites) which are mobile algal solvation products within the deposit reflects low energy conditions in which transportation or wave solvation has not sufficiently developed.

2.1.3. Aktepe Member

The sequence which is formed by tabular, parallel, fine to medium layered micritic limestone consists of algal limestone and diatomite interlayers (Figure 8a). The member took its name from Aktepe (N of Haseki village) (Figure 4).

Type locality is Aktepe vicinity and the thickness of the sedimentary sequence is more than 100 meters. The Aktepe sequence which forms the vertical continuation of Yeniliman limestone is distinguished by diatomite intralayers which occurred after the first phase Karaburun volcanites had intervened. The proportional relation between micritic limestone and diatomitic layers is variable within deposit.In addition to limestone dominant sections which bears diatomitic intralayer in decimeter thicknesses, there are limestone-diatomite alternations or diatomitic layers that have thin limestone layers-laminae (Figure 8b).

The sequence, which rests on first phase lava flow with transgressive overcome in SW Aktepe, begins with gray colored sandstone layer which is massive and carbonate cemented. Medium-coarse grained sandstone layer consists of white and thin mollusk gastropods, specifically in millimeter size. The overlying, pale yellow, disintegration colored massive mudstone sequence consists of tabular parallel, fine to medium layered, micritic limestone interlayers (Figure 4a). There is a 3 meter thick, red-yellow-green zoning, poorly consolidated, massive and laterally discontinuous mudstone layer at the bottom of sequence which overlies the first phase lava flow in NE Aktepe (Figure 4). The bottom section of the 7 meter thick sedimentary sequence cropping out Kömür Burnu surround is made up of siltstone-micritic limestone alternation (Figure 4). Limestone and diatomite intercalations made up of laminated stromatolites are observed in lower parts of fine to medium layeredsequence which is dominant inmicritic limestone which developed following fine clastic layers in mentioned localities. Algal limestone layers which become rare towards the upper parts are reddish brown and are distinctively medium to thick layered. Horizontal bands made up of branched algal fragments in millimeter and centimeter sizes, completely silicified layers and chert bands in thicknesses varying in between 5-15 cm are observed within horizontal layers. Diatomite facies is mostly laminated, with chert lenses as arranged parallel to lamination in centimeter size, and is white colored, poorly consolidated clayey in variable ratios (Figure 8b). White colored chert lenses in millimeter thicknesses are widespread in fine to medium layered micritic limestone facies which become dominant towards upper sections of the deposit.

Aktepe sequence which is observed in west of Düdükçü Tepe is relatively divided into lower and upper layers by the lava flow belonging to second phase of the Karaburun volcanism (Figure 4). Fluvial pebbles made up of small pebbles take place at the contact of lower limestone deposit with overlying lava flow. However, the bottom of upper limestone deposit ends with medium to fine layered limestones with whitish, pale gray, disintegration surface. At the bottom of this sequence, there is a massive, intensely bioturbated, yellowish pale brown, high carbonate cemented, fine to medium grained, transgressive sandstone layer with a thickness of more than 1 meter.

In north of Tepeboz village (Figure 6), with the emplacement of pyroclastics which the second phase Karaburun volcanism had produced, the depositional

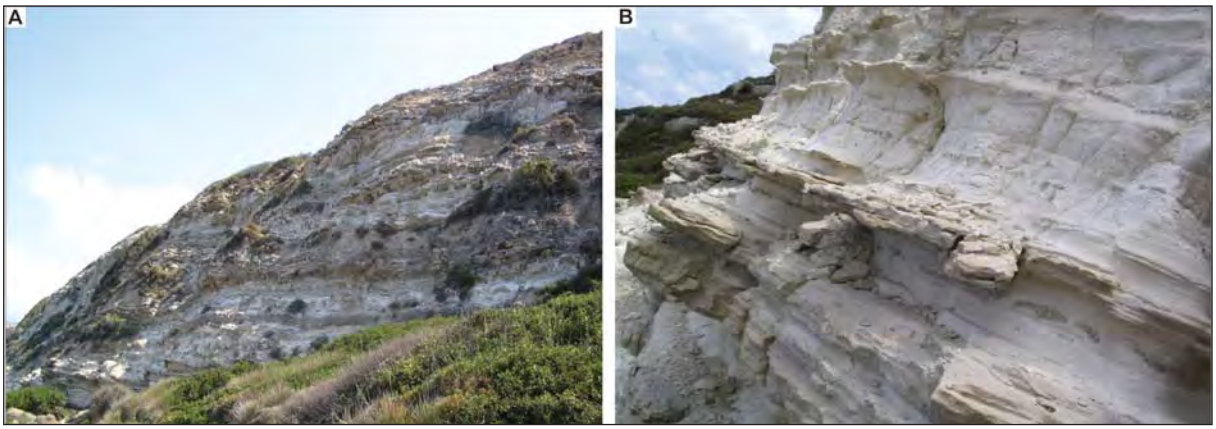

Figure 8- Aktepe member. A) General view, B) micritic limestone intercalations and clayey diatomite horizons covering chert lenses.

environment of the Aktepe limestone has become shallow and fine clastics between pyroclastics and the overlying lava flows have been deposited. The sequence of which its 3 meters can be observed consists of small mammal remnants belonging to MN4 biozone (*Cricetodon* sp., *Democricetodon* cf. gracilis, Megacricetodon cf. bavaricus) described by Saraç (2003). This biozone is also composed of coarse sandstone-pebblestone intercalations, traces of bioturbation, nodular-laminar caliche formations, and claystone and siltstone layers bearing organic material in varying proportions (Figure 9). The pyroclastics of small volume lava eruptions which remain outside the spread area are overlain by

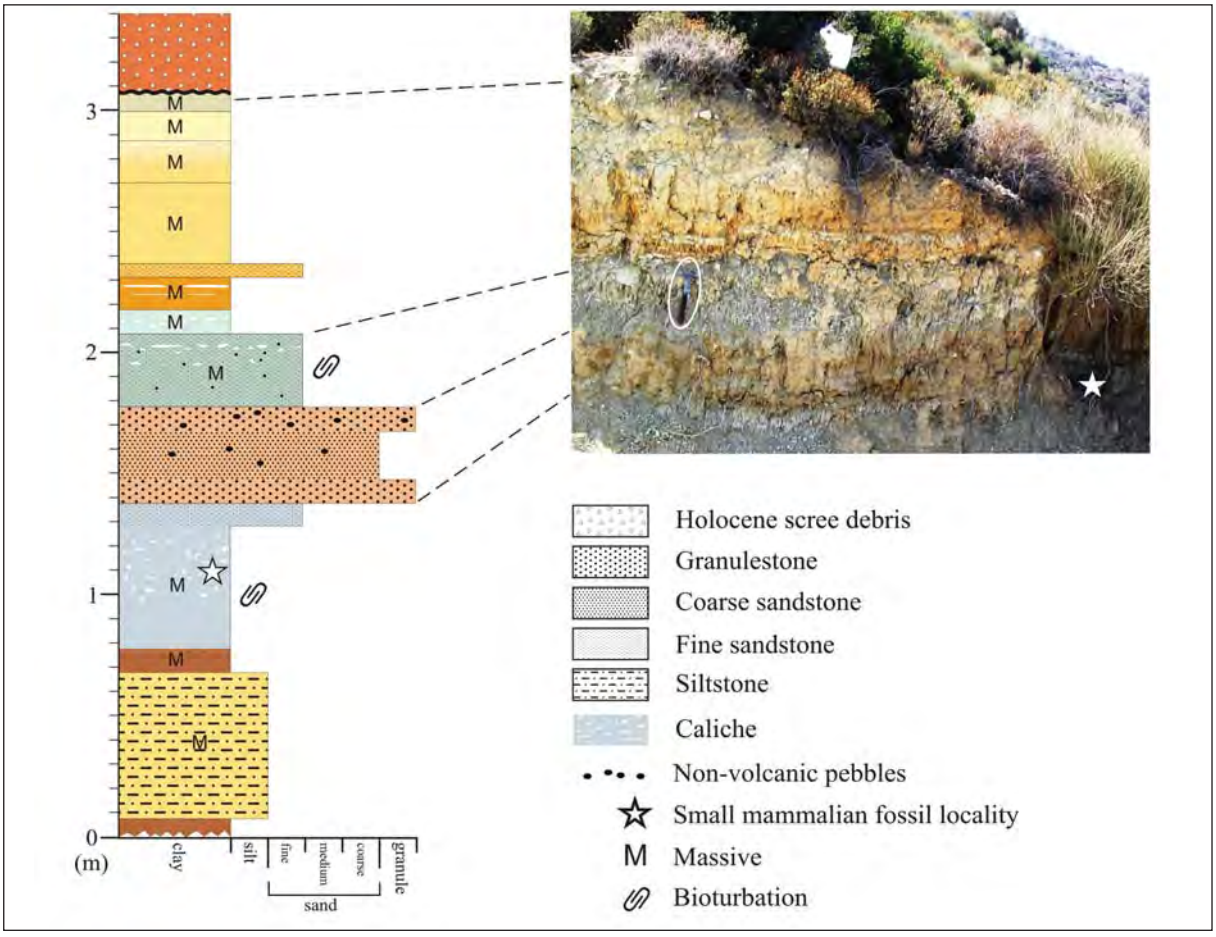

Figure 9- Measured section of the succession containing small mammal remnants belonging to MN4 biozone within Aktepe Member.

lacustrine deposits of the upper section of the Aktepe member. The upper part begins with silicified limestones which deformed by the fine to medium layered and algal laminated diagenetic silica emplacement following the diatomite layers with green claystone intercalations (Figures 10b and c).

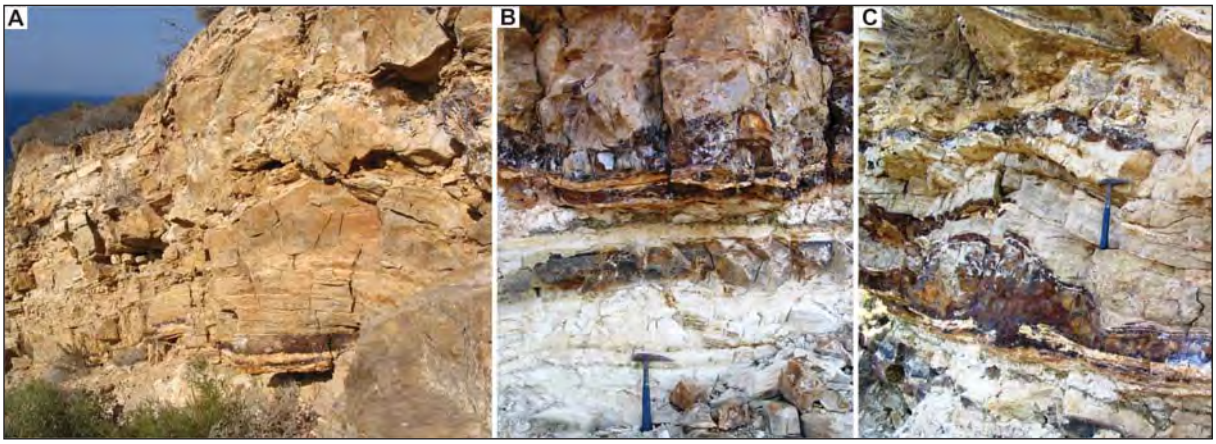

Figure 10- A) Upper section of the Aktepe member; B, C) at the bottom section of the upper part, chert bands in decimeter scale which caused diagenetic deformation in laminar stromatolithic limestones over cherty diatomite horizons take place.

During extensional phase which caused the occurrence of first phase Karaburun volcanism the basin was relatively deepened and Aktepe sequence was deposited in slowly changing environmental conditions from shallow areas where Yeniliman limestone had been deposited towards shoreface. The silica increase in medium which was approved by diatomite formation is related with volcanic exsolutions.

The sedimentary sequence can be correlated with Ovacık formation in Çeşme peninsula, defined by Göktaş (2010) in terms of general rock type composite consisting rock stratigraphic location and diatomite.

2.2. Hisarcık Formation

The unit is composed of claystone–siltstone dominant sequence intercalating with sandstone in bottom and limestones on top. Typical exposures of the sedimentary sequence reflecting Middle Eocene lacustrine deposition extends along the shoreline between NE Bozköy and Eşendere port which is outside the study area (Figure 1). The name of the formation was taken from Hisarcık district which is approximately 2 km's to the northwest of Karaburun county center (Göktaş, 2014). The lower part of the sedimentary sequence of which its upper section had been eroded was studied within Karabağları member in the study area (Figure 4). The unit is the equivalent of "Çiftlik formation" which was described by Göktaş (2010) in Çeşme peninsula.

2.2.1. Karabağları Member

The sedimentary sequence is generally composed of green claystone-siltstone-sandstone-conglomerate. The name of the sub unit was taken from Karabağları location which is 1 km away from NE of Karaburun county center (Göktaş, 2014). The measured thickness of the sequence which is represented by a small outcrop is approximately 80 meters in the study area (Figure 4).

Karabağları member consists of claystone-siltstone-sandstone of which their relative proportions vary irregularly and conglomerate lithofacies in few amounts in the study area. Claystone and siltstone which forms the dominant rock type assemblage is generally green colored, carbonated, massive or tabular parallel, fine to medium layered and laminated. Sandstone interlayers are seldom encountered in decimeter thickness. Sandstone is mostly coarse grained, grain supported, well sorted and medium to fine consolidated. Trough like cross bedded, pebble stone and sandstone layers crop out in front of NW trending normal fault which is in contact with Yeniliman limestone (Figure 4). Main components are well rounded small pebbles and coarse grained sands.

Mammal faunas defined in Azmakdere member, which is the equivalent of the sub unit in Çeşme peninsula (Göktaş, 2010) and in equal horizons in Chios (Keramaria unit: Besenecker, 1973) belong to

MN5 biozone and are dated to 15 my (Besenecker, 1973; Bonis et al., 1998; Koufos, 2006). According to biochronological data based on lithostratigraphical correlation, it was accepted that sedimentation of Karabağları member had begun in Early Miocene the latest and mainly developed in Middle Miocene (Figure 3).

The contact between Aktepe member and the overlying Karabağları member is sharp and conformable. There was not observed any gap in deposition between the two consecutive shore-face sequences. It is clear that depositional conditions have suddenly changed and continental derived sediment transportation increased with the activation of boundary faults. Therefore, it was considered that the relation between the two units could be explained with paraconformity that had developed in submarine. The sedimentary sequence has decreased by erosion that had continued until today.

Green claystone-siltstone dominant sequence of the Karabağları member was deposited in lacustrine shore-face environment. Sandstone layers which take place among suspension layers and reflect deposition in high energy conditions indicate transportation by wave and currents, and reworking. Trough like, cross bedded sandstone-conglomerate assemblage that have paleoreduction colors were interpreted as the products of river transportation in submarine sections of delta fans flowing into lake.

2.3. Karaburun Volcanites

Pyroclastics of calc alkaline volcanism which were identified as evolved lithostratigraphically in two phases during Late Early Miocene and small scale lava flows were distinguished and studied under "Karaburun volcanites" title (Figure 11). The name "Karaburun volcanites", which was first given by Türkecan et al., (1988), was also embraced in this study as it had been in used in the study of Helvacı et al., (2009).

Karaburun volcanism which developed in Early Miocene basin formed synchronous products with lacustrine sedimentation within Haseki formation (Figure 12). Each phase shows a binary facies association mainly as pyroclastics at bottom and as lavas on top. The hydrovolcanic origin of the base-surge facies which symbolizes pyroclastics and this facies to contain limestone pieces which subjected to plastic deformation tells that the volcanism has started in submarine. The lavas can be correlated with mafic lava layers (Sarıyer member) distinguished by Kaya (1979) in lacustrine Zeytindağ formation which is located in Foça peninsula. The timestratigraphic equivalent of first phase volcanites in Çeşme peninsula which is defined as early period product of the Armandağı volcanism (Türkecan et al., 1988) is the rhyolitic "Alaçatı tuff" (Göktaş, 2010).

Major element data related to 8 samples collected from Karaburun volcanites (Table 1) were plotted on TAS diagram of Le Bas et al., (1986). Hence, it was observed that 6 of them were in andesite region and 2 samples were in basaltic-andesite area (Figure 13a). All sub alkaline samples are calc alkaline in character. Samples which were studied in K_2O vs SiO_2 diagram of Le Maitre et al., (2002) cumulate in high potassium, basaltic andesite area (Figure 13b).

Textural and petrographical characteristics of lavas investigated are similar. The main phenocryst is olivine in samples that have hypocrystalline porphyritic texture (Figure 14a). Most of olivine phenocrysts and microphenocrysts were calcified (entirely in some places) starting from fractures and edges (Figure 14b). Plagioclase minerals are generally prismatic and show polysynthetic twinning. Pyroxene group minerals which are generally observed as microlites in the groundmass are brownish, of some are twinned and glomeroporphyritic in texture. The groundmass, which generally shows pilotaxitic and interstitial textures, is composed of plagioclase (Figures 14c and d), pyroxene and olivine microlites that are irregularly distributed or have less defined flow direction, and seldom volcanic glass components. Quartz crystals which are magmatically corroded, observed in most samples were surrounded by microlite and microcrystals of pyroxene (Figures 14e,f, g and h).

2.3.1. First Phase Volcanites

The first phase volcanites which are in the position of lateral discontinuity reference layer separating Yeniliman limestone and Aktepe member from each other in the generalized stratigraphy indicates the beginning of Neogene volcanism in Karaburun peninsula (Figures 4 and 12). A few meters thick pyroclastics which emplaced before lava eruptions are mainly in base surge and air fall facies. As a result of K/Ar radiometric dating analysis, 18.2±1.0 my total rock age was determined in lavas (Table 2).

Yellowish gray, pale brownish-yellow colored pyroclastic sequence, which is observed over Yeniliman limestone in NW Aktepe, is about 5

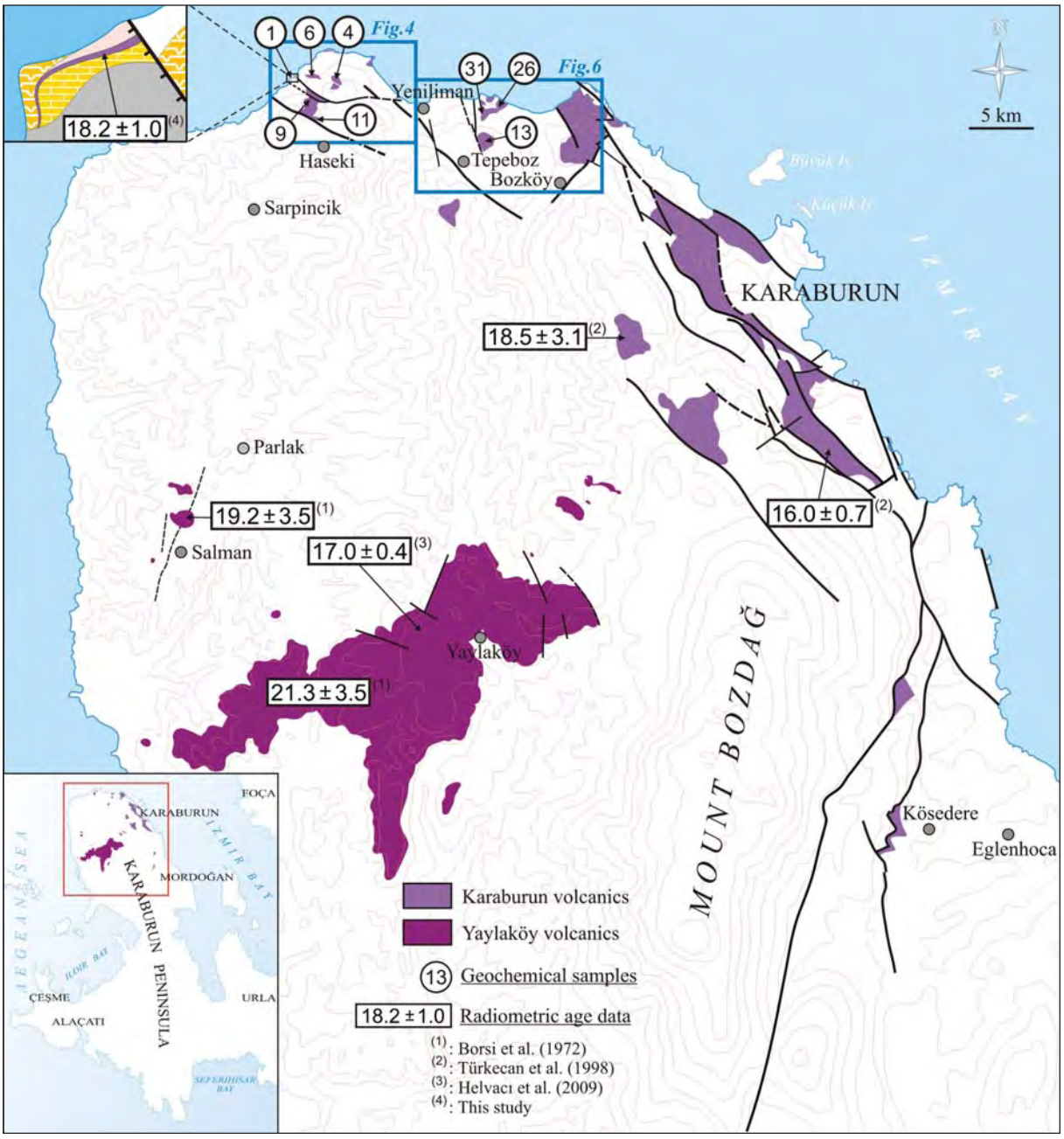

Figure 11- The distribution of mafic volcanites in northern section of the Karaburun peninsula.

Table 1- Results of major element analyses related to lava samples taken from Karaburun volcanites.

Sample	Coordinate	SiO_2	$Al2O_3$	Fe_2O_3	MgO	CaO	Na_2O	K_2O	TiO_2	P_2O_5	MnO	SrO	BaO	L.O.I
1K	0448690E/4281115N	53.6	14.4	6.8	3.4	9.4	3.0	2.1	0.7	0.2	0.2	0.08	0.08	5.85
4K	0449415E/4281065N	56.4	16.4	7.1	5.2	6.5	3.4	2.1	0.7	0.3	0.2	0.08	0.08	1.45
6K	0449072E/4280155N	54.9	15.8	7.6	6.0	7.2	3.3	1.8	0.7	0.3	0.1	0.07	0.08	1.60
9K	0449088E/4280757N	53.5	14.9	6.9	2.8	9.3	3.0	2.2	0.7	0.3	0.1	0.08	0.08	5.80
11K	0449140E/4280285N	53.4	14.7	6.9	3.3	9.3	2.9	2.2	0.7	0.2	0.1	0.08	0.08	5.80
13K	0452355E/4279932N	55.4	16.4	7.2	4.2	8.1	3.2	2.1	0.6	0.2	0.1	0.07	0.07	2.05
26K	0452715E/4280655N	54.8	16.4	7.5	5.3	7.6	3.2	2.0	0.7	0.2	0.2	0.07	<0.01	1.85
31K	0452320E/4280265N	56.4	16.2	6.9	3.2	7.2	3.6	2.3	0.6	0.3	0.1	0.09	0.11	2.60

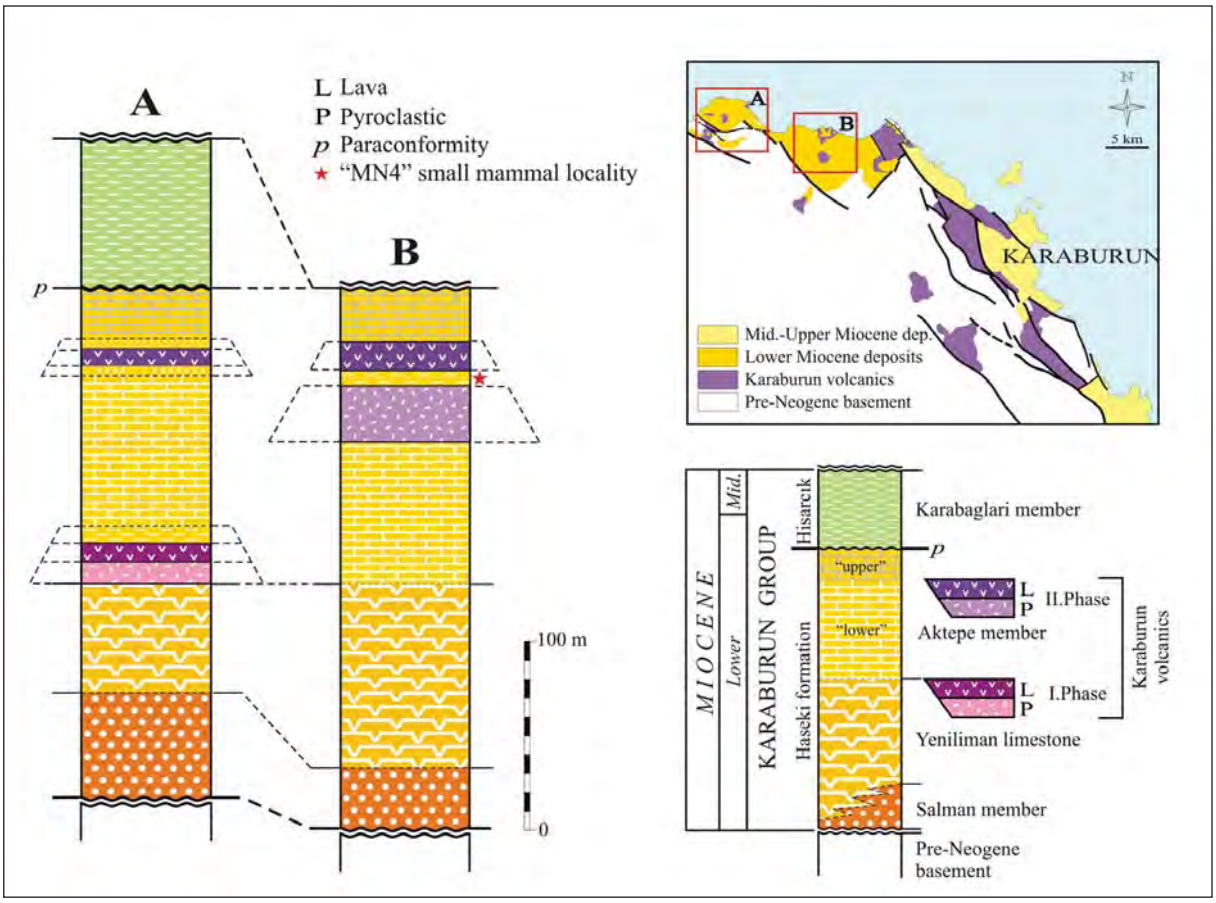

Figure 12- The location of Karaburun volcanites within Haseki formation.

Table 2- Result of K/Ar analysis of the lava sample which represents the 1st stage.

Sample	Material	K (%)	$^{40}Ar^{rad}$ (ccSTP/gr)	$^{40}Ar^{rad}$ (%)	Age (My)
1K	Whole-rock	2.235	1.591×10^{-6}	28.9	18.2±1.0

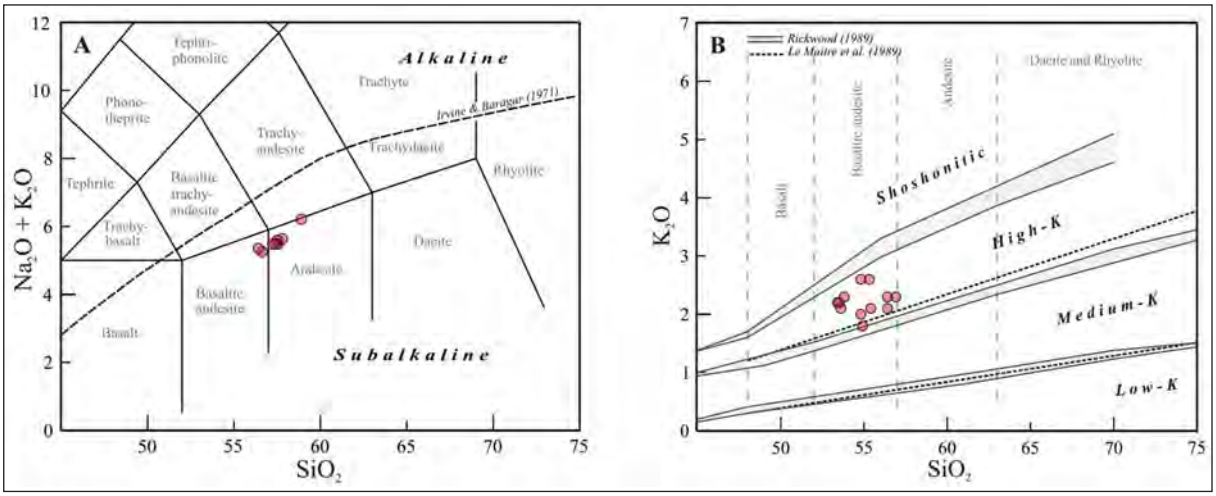

Figure 13- The assessment of Karaburun volcanites in diagrams of (A) total alkaline silica according to Le Bas et al. (1986) and (B) K_2O vs. SiO_2 (Le Maitre et al., 2002).

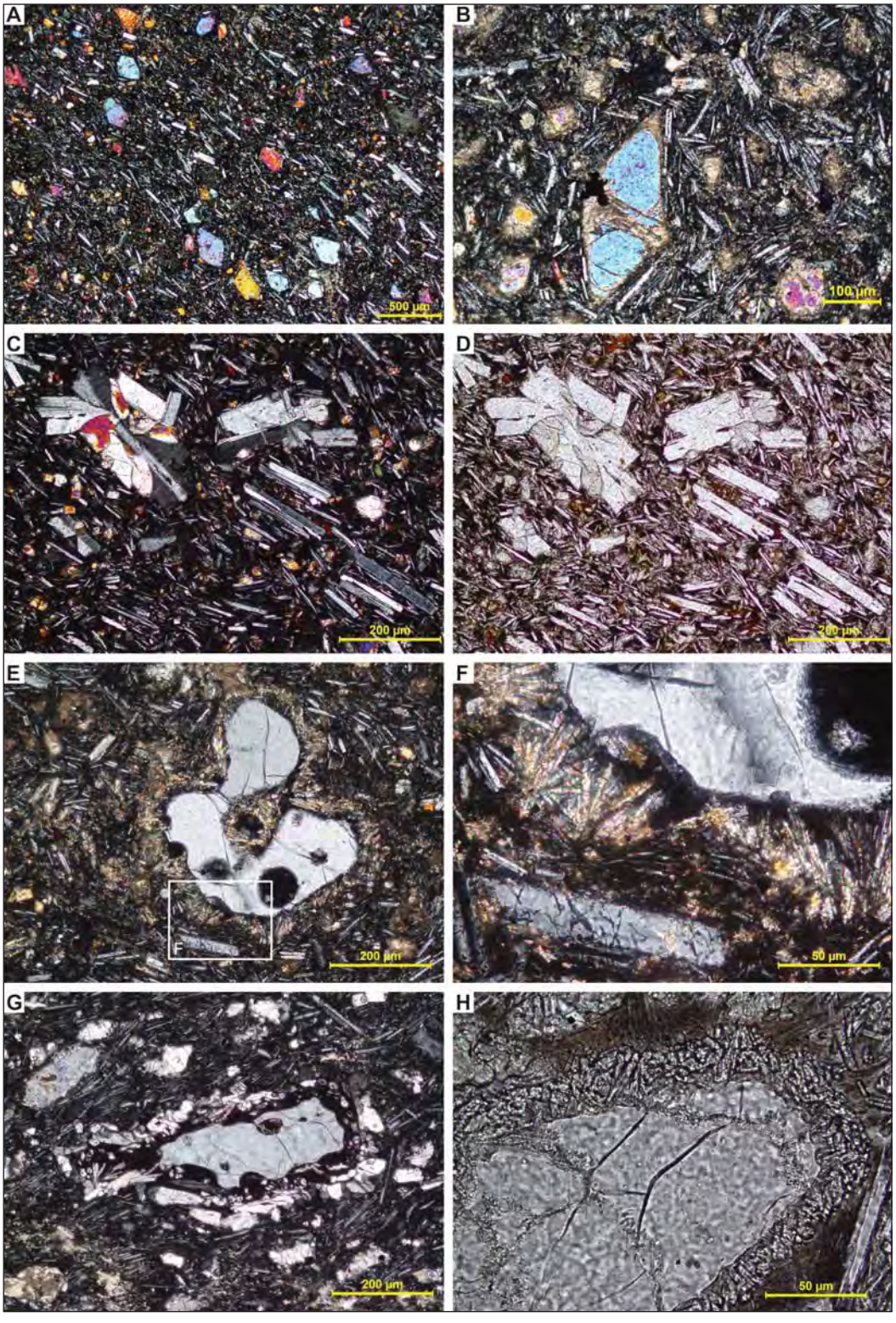

Figure 14- Microphotos reflecting mineralogical and petrographical characteristics of Karaburun volcanites. A) Hypo crystalline porphyric texture in which olivine phenocrysts and oriented plagioclase microliths are observed; B) Calcification in euhedral olivine phenocryst; C, D) orientation and glomero porphyritic texture in plagioclase microliths and micro phenocrysts (C: cross nicol; D: planenicol); E, F, G, H) Quartz crystals which subjected to magmatic corrosion were occasionally surrounded by radiate acicular or anhedral pyroxene microliths.

meters thick and composed of base surge at bottom (3 m) and air fall deposits (2 m) on top (Figure 15). The base surge layer is made up of tuff layers by which pyrogene material in centimeter to decimeter thicknesses with a size of coarse ash-lapilli was formed and seldom consists of blastic lava clasts (Figure 16a). Lapilli size components forming air fall layer that has indefinite bedding are angular and grain supported. Lava flow with a thickness of 7 meters located on the sequence has widespread gaseous voids. Calcite and chalcedony infillings are observed in some voids which display flow oriented lensoidal sections.

The volcanic sequence in NE of Aktepe begins with about 3 meters thick pyroclastics. The uppermost section of the pyroclastic sequence is composed of air fall layers in decimeter thicknesses. Along the 1 meter thick bottom section of the overlying lava flow, typical red colored, agglutinated spatter lava layer is located because of thermal oxidation. Lava fragments in decimeter size have dense gas voids. However, the overlying blackish lava flow has a flow foliation (Figure 16b).

2.3.2. Second Phase Volcanites

The second phase volcanites which were emplaced as synchronous with the sedimentation into Aktepe member is composed of pyroclastic at bottom and lava layers on top (Figures 4 and 12).

The pyroclastic sequence which is formed by base surge, air fall and ash fall facies is thicker compared to previous phase. Type locality is about 1 km away from NE of Tepeboz village (Figure 6). Fine clastic sequence which is 3 meters thick located in between pyroclastics and the overlying lava flow reflects volcanic inactivity between the pyroclastic emplacement and lava eruption (Figure 12b). Yellowish, pale gray colored pyroclastic sequence is formed by the tabular, parallel, and fine to medium layered, coarse ash tuff-lapilli tuffassemblage (Figure 17A). The thickness of thin ash-tuff layers in ash fall facies reducing down to 1 cm. pyroclastic flow structures in base surge deposits are seldom observed (Figure 17b). Lapilli tuff layers, consisting of angular to sub angular, centimeter sized porous/non-porous mafic pyroclastics were interpreted as air fall deposit. Air fall deposits varyin between 10 to 60 cm, completely massive and are specifically grain supported (Figure 17c). However, ballistic lava fragments are seldom (Figure 17d and e). Beside homogenous lava clastics, fragments transferred from previously emplaced pyroclastics and hydrated limestones are observed. The plastic deformation observed in the fragments of silicified limestone which was subjected to thermal oxidation (Figure 17f) supports that pyroclastic emplacement is synchronous with sedimentation. Both physical and petrographical characteristics of second phase lavas resemble to previous phases.

3. Stratigraphical and Paleogeographical Evolution

In studies related to mammal biostratigraphy carried out in Lower Miocene basin fills within scope of Aegean collapse, the faunal assessment below MN3 biozone was not made (according to Steininger, 1999; between 18-20,5 my) (Manisa-Beydere fauna: Dönmez et al., 1993; Menemen-Bozalan fauna: Saraç, 2003; Bornova-Sabuncubeli fauna: Bruijn et al., 2006). Borsi et al., (1972) took K/Ar ages (21.3-19.2 my) from mafic lavas which cut as syn sedimentary and overlie deposits of Salman formation around Yaylaköy. These data not only make a specific approach to the beginning of

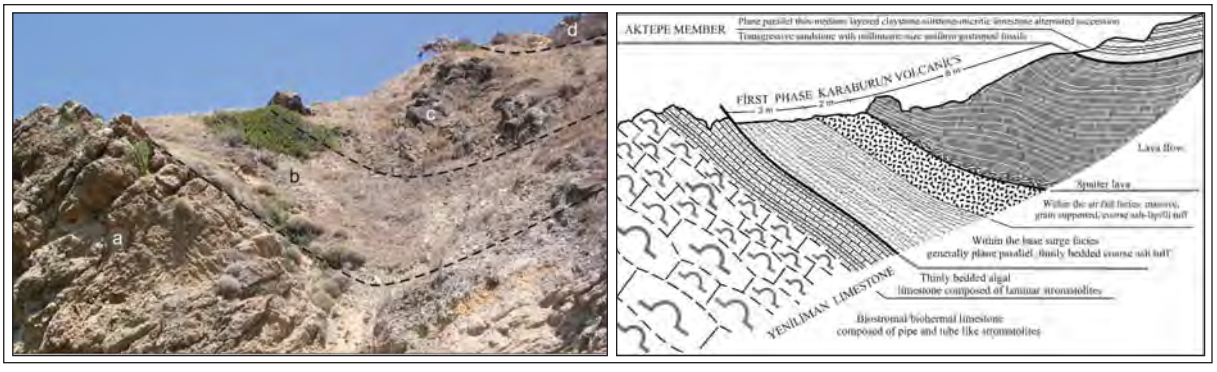

Figure 15- First stage Karaburun microliths located between Yeniliman limestone and Aktepe member. a) Yeniliman limestone, b) pyroclastic deposit, c) lava, d) Aktepe member.

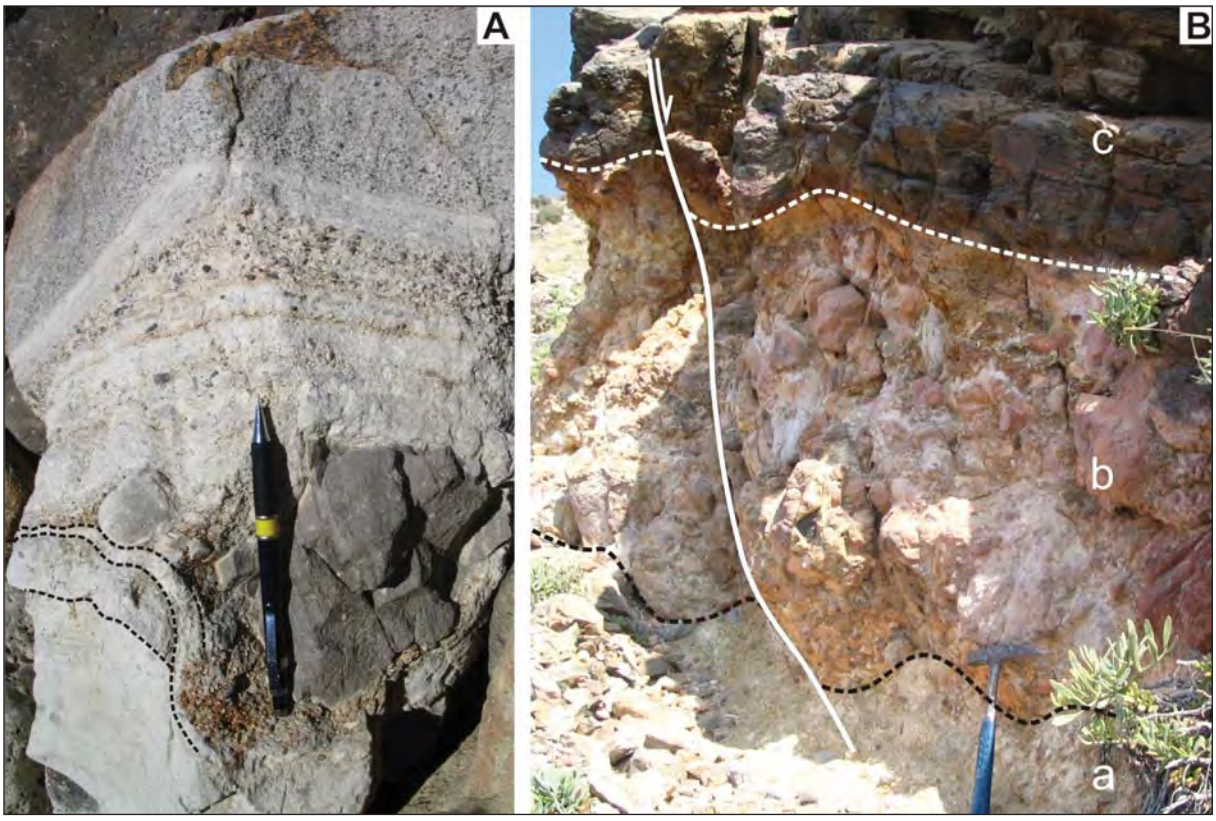

Figure 16- First stage Karaburun volcanites exposing in NE Aktepe, A) ballistic lava clasts observed in base surge deposits; B) vertical order of volcanic facies' developed from explosion stage to lava flow stage: a) back fall deposits. B) spatter lava horizon which lava fountain generated, c) Flow layered lava horizon.

sedimentation but also is not sufficiently reliable as it consists of high error margin (± 3.5 my). K/Ar dating obtained (17.0 my) by Helvacı et al., (2009) from the same lavas in the area probably reflects the second phase of Yaylaköy volcanism (which is known as 2 phased from previous studies). First phase Karaburun volcanites in which K/Ar age was taken as 18.2±1.0 my in this study shows the beginning of calc alkaline Neogene volcanism in NE Karaburun volcanites (Figure 11).

In the study area, Early Miocene deposition begins with alluvial fan deposits of the Salman member which was emplaced with an angular unconformity over basement rocks. This depositis defined by the algal biostromal Yeniliman limestone. Organosedimentary limestone sequence deposited in the vicinity of a "stable" and "open" lacustrine was formed by spreads of stromatolitic algals. Lateral and vertical continuities of autochthonous stromatolites reflect shallow and low energy depositional environments of the shore-line with routine bathymetry. The shore-face and off-shore of the lake or open lacustrine deposits are partly observed in Foça peninsula but are mainly submerged in the Aegean Sea.

During the extensional phase, the development of syn-sedimentary emplacement of the first phase Karaburun volcanites over algal limestone platformhas occurred. During this phase, the depositional environment (from off-shore to shore-face) has become relatively deeper and Aktepe member has conformably and transitionally been deposited over Yeniliman limestone during continuous lacustrine deposition. Diatomitic interlayers were deposited depending on the increase in volcanogenic silica as algal limestone interlayers in the dominant fine layered/laminated, micritic limestone of the Aktepe member becomes less in upward direction.

Early Miocene basin spreaded over much larger areas than Foça depression in which Haseki formation and regional equivalences had been deposited (Kaya, 1979). Over structural blocks which limit the depressional area (Karaburun height on west and Yamanlar height on east), relatively Lower

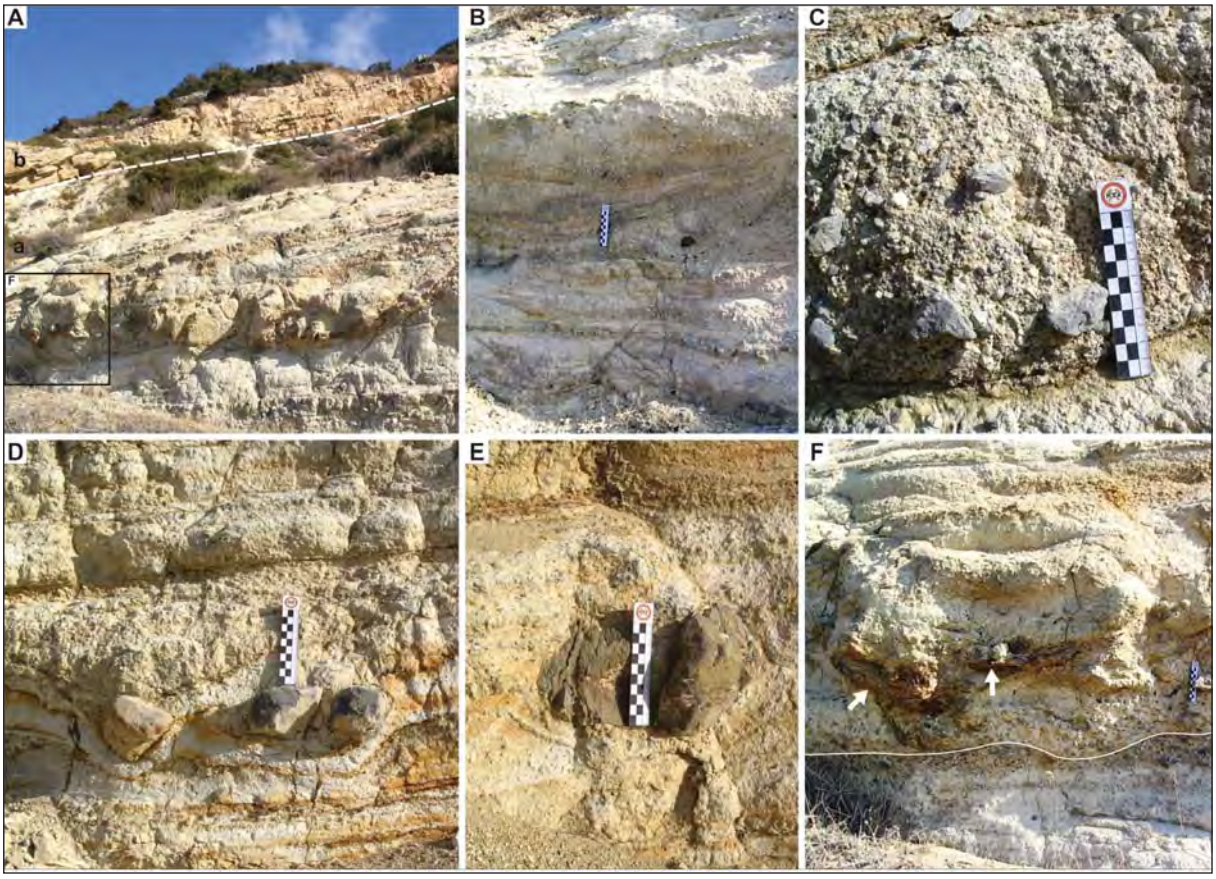

Figure 17- Second stage pyroclastics, A) General view; a) pyroclastic deposit, b) Aktepe member "upper section", B) sections which display pyroclastic flow structure of base surge deposits; C) back fall deposit; D, E) Ballistic lava clasts; F) Limestone pieces which subjected to plastic deformation.

Miocene erosion residual deposits are located (Aras et al., 1999; Çakmakoğlu et al., 2013; Dönmez et al., 1993). As it is understood from the distribution of alluvial and lacustrine deposits in Karaburun peninsula, the Bozdağ which rises in Great Early Miocene Lake in coastal Aegean region (Figure 1) was as in similar position as today. Probably; towards the end of Early Miocene, the Foça depression that occurred in Early Miocene basin by remodeling of Karaburun and Yamanlar heights has then transformed into a basin in which Middle Miocene lacustrine deposition had developed. In other words, Early Miocene lacustrine deposition has continued during Middle Miocene following the unconformity related with the formation of Foça depression.

4. Results

Continental Lower-Middle Miocene deposits and Lower Miocene volcanites in the north of Karaburun peninsula, which had not been previously investigated, were distinguished the first time. Lithofacial characteristics were described within generalized stratigraphic order classifying sequences as group, formation and member, and their environmental characteristics were studied. In doing so, the regional correlation of these rock units was tested.

It was determined that, the Early-Middle Miocene sedimentation which was divided into 2 formations within the scope of Karaburun group, began to deposit with alluvial fan deposits and developed dominantly in lacustrine environment. It was also detected that; small size, first products of the Karaburun volcanism were emplaced between algal biostromal Yeniliman limestone deposited on the shore of Early Miocene lake and on the micritic limestone dominating shore-face sequence of Aktepe member. It was interpreted that, the silica which formed diatomite and cherts in Aktepe member was originated from this volcanism. It was suggested that the lacustrine sedimentation against disconformity between the shore-faces of Aktepe member and the

overlying Karabağları member were not interrupted and continued at least during Middle Miocene.

Karaburun volcanism which developed during the deposition of Haseki formation was activated in two phases and each phase was formed by pyroclastic facies at bottom and by lava facies at top. The first phase reflecting the beginning of Neogene volcanism in Karaburun peninsula was dated as 18.2±1.0 my by K/Ar method. Hydrovolcanic pyroclastic rocks in base-surge facies which quotes lava eruptions and reflects that the volcanism has begun in submarine was first described and distinguished as a member on map scale. Petrographical and geochemical analyses of lavas which are outside the area in previous studies were carried out. Olivine-phyritic textured lavas were named as andesite based on total alkaline-silica contents and it was shown that they took place within high potassium calc alkaline series.

Acknowledgement

The geology of the study area was mainly completed during the preparation of 1/500.000 scale İzmir sheet conducted by the coordination of Dept. of Geological Researches of the General Directorate of Mineral Research and Exploration. So, this area was reviewed under the project name "Stratigraphy and Paleogeographic Evolution of Neogene and Quaternary Basins in Çeşme, Urla, Cumaovası, Kemalpaşa-Torbalı Depressions". I would also like to thank to Ass. Prof. İsmail Işıntek and Geol. Eng. (MS) Ferliz Mendikli for their contributions.

Received: 25.06.2013
Accepted: 05.11.2013
Published: June 2014

References

Aras, A., Göktaş, F., Demirhan, M., Demirhan, H., İçöz, S. 1999. Karaburun kilinin stratigrafisi, mineralojisivepişmeözellikleri. *1. Batı Anadolu Hammadde Kaynakları Sempozyumu (BAKSEM'99)*, 8-14 Mart 1999, İzmir, 238-247.

Bonis, L. De, Koufos, G.D., Şen, Ş. 1998. Ruminants (Bovidae and Tragulidae) from the Middle Miocene (MN5) of the Island of Chios, Aegean Sea (Greece). Neues Jahrbuch für Geologie und Paläontologie - Abhandlungen 210, 339-420.

Borsi, J., Ferrara, G., Innocenti, F., Mazzuoli, R. 1972. Geochronology and petrology of recent volcanics in the eastern Aegean Sea (West Anatolia and Lesbos Island). *Bulletin of Volcanology* 36, 473–496.

Bruıjn H. de, Mayda, S., Hoek Ostende L. van den, Kaya, T., Saraç, G. 2006. Small mammals from the Early Miocene of Sabuncubeli (Manisa, SW Anatolia Turkey). *Beiträge Paläontologie* 30, 57-87.

Çakmakoğlu, A., Bilgin, Z.R. 2006. Karaburun Yarımadası'nın Neojen öncesi stratigrafisi. *Maden Tetkik ve Arama Dergisi* 132, 33-62.

Çakmakoğlu, B. 2008. Karaburun Yarımadası'nın kuzey kesimindeki killerin stratigrafisi, sedimentolojisi ve ekonomik kullanım olanaklarının araştırılması. Yüksek Lisans Tezi, Dokuz Eylül Üniversitesi Fen Bilimleri Enstitüsü, Jeoloji Mühendisliği Bölümü, Ekonomik Jeoloji Anabilim Dalı, 49 s. İzmir.

Çakmakoğlu, B., Göktaş, F., Demirhan, M., Helvacı, C. 2013. Karaburun Yarımadası'nın kuzey kesimindeki killerin stratigrafisi, sedimantolojisi ve ekonomik kullanım olanaklarının araştırılması. *Türkiye Jeoloji Bülteni* 56/1, 39-58.

Dönmez, M., Türkecan, A., Akçay, A. E., Hakyemez, Y., Sevin, D. 1993. İzmir ve kuzeyinin jeolojisi, Tersiyer volkanizmasının petrografik ve kimyasal özellikleri. *Maden Tetkik ve Arama Genel Müdürlüğü Rapor No: 10181*, 123 s., Ankara (unpublished).

Dunham, R.J. 1962. Classification of carbonate rocks according to depositional texture. Ham W.E. (Ed.). Classification of Carbonate Rocks. *American Association Petroleum Geologist-Memoirs* 1, 108-121.

Helvacı, C., Ersoy, Y., Sözbilir, H., Erkül, F., Sümer, Ö.,Uzel, B. 2009. Geochemistry and $^{40}Ar/^{39}Ar$ geochronology of Miocene volcanic rocks from the Karaburun Peninsula: Implications for amphibole-bearing lithospheric mantle source, Western Anatolia. *Journal of Volcanology and Geothermal Research* 185, 181-202.

Göktaş, F. 2010. Çeşme Yarımadası'ndaki Neojen tortullaşması ve volkanizmasının jeolojik etüdü. *Maden Tetkik ve Arama Genel Müdürlüğü Rapor No: 11389*, 64 s. Ankara (unpublished).

Göktaş, F. 2011.Urla (İzmir) çöküntüsündeki Neojen tortullaşması ve volkanizmasının jeolojik etüdü. *Maden Tetkik ve Arama Genel Müdürlüğü Rapor No: 11568*, 112 s. Ankara (unpublished).

Göktaş, F.,2014.Karaburun (İzmir) çevresinin Neojen stratigrafisi ve paleocoğrafik evrimi. *Maden Tetkik ve Arama Dergisi* (in editor).

Irvine, N., Baragar, W.R.A. 1971. A guide to chemical classification of the common volcanic rocks. *Canadian Journal of Earth Sciences* 8, 523–548.

Innocenti, F., Mazzuoli, R. 1972. Petrology of İzmir-Karaburun volcanic area. *Bulletin of Volcanology* 36, 83-104.

Kalafatçıoğlu, A. 1961. Karaburun Yarımadası'nın jeolojisi. *Maden Tetkik ve Arama Dergisi* 56, 53-62.

Kaya, O. 1979. Orta Doğu Ege çöküntüsünün (Neojen) stratigrafisi ve tektoniği. *Türkiye Jeoloji Kurumu Bülteni* 22/1, 35-58.

Koufos, G.D. 2006. The Neogene mammal localities of Greece: Faunas, chronology and biostratigraphy. Hellenic Journal of Geosciences 41, 183-214.

Le Bas, M. J., Le Maitre, R. W., Streckeisen, A., Zanettin, B. 1986. A chemical classification of volcanic rocks based on total alkali-silica diagram. *Journal of Petrology* 27, 745-750.

Le Maitre, R.W. (ed) Streckeisen, A., Zanettin, B., Le Bas, M. J., Bonin, B., Bateman, P., Bellieni, G., Dudek, A., Efremova, S., Keller, J., Lameyre, J., Sabine, P. A., Schmid, R., Sørensen, H., Woolley, A.R. 2002. Igneous Rocks: A Classification and Glossary of Terms. Recommendations of the International Union of Geological Sciences Subcommission on the Systematics of Igneous Rocks. *Cambridge University Press*.236 p.

Logan. B. W., Rezak, R., Ginsburg, R. N. 1964. Classification and environmental significance of algal stromatolites. *Journal of Geology* 72, 68-83.

Rickwood, P.C. 1989. Boundary lines within petrologic diagrams which use oxides of major and minor elements. *Lithos* 22, 247-263.

Saraç, G. 2003. Türkiye omurgalı fosil yatakları. *Maden Tetkik ve Arama Genel Müdürlüğü Rapor No: 10609*, 218 s. Ankara (unpublished).

Steininger, F.F. 1999. Chronostratigraphy, Geochronology and Biochronology of the Miocene "European Land Mammal Mega-Zones (ELMMZ) and the Miocene "Mammal-Zones (MN-Zones)". Rössner, E.G. and Heissig, K. (Eds.). The Miocene Land Mammals of Europe. *Verlag Dr. Friedrich Pfeil*. München,9-24.

Türkecan, A., Ercan, T., Sevin, D. 1998. Karaburun Yarımadası'nın Neojen volkanizması. *Maden Tetkik ve Arama Genel Müdürlüğü Rapor No: 10185*, 35 s. Ankara (unpublished).

Bulletin of MTA (2014) 148: 63-68

Bulletin of the
Mineral Research and Exploration

http://bulletin.mta.gov.tr

THE IMPORTANCE OF BENTHIC FORAMINIFERAS IN DETECTING FEATURES OF ECOLOGICAL AND GEOLOGICAL STRUCTURES in EDREMIT BAY AND ON COASTAL AREAS OF DİKİLİ CHANNEL (NE AEGEAN SEA)

Engin MERİÇ[a], Niyazi AVŞAR[b], İpek, F. BARUT[c], Mustafa ERYILMAZ[d], Fulya YÜCESOY-ERYILMAZ[d], M. Baki YOKEŞ[e] and Feyza DİNÇER[f]

[a] *Moda Hüseyin Bey Sokak No: 15/4, 34710 Kadıköy, İstanbul*
[b] *Çukurova Üniversitesi, Mühendislik- Mimarlık Fakültesi, Jeoloji Mühendisliği Bölümü, 01330 Balcalı, Adana*
[c] *İstanbul Üniversitesi, Deniz Bilimleri ve İşletmeciliği Enstitüsü, Müşküle Sokak No: 1, 34116 Vefa, İstanbul*
[d] *Mersin Üniversitesi, Mühendislik Fakültesi, Jeoloji Mühendisliği Bölümü, Çiftlikköy Kampusu 33343 Mersin*
[e] *Haliç Üniversitesi, Fen-Edebiyat Fakültesi, Moleküler Biyoloji ve Genetik Bölümü, Sıracevizler Caddesi No: 29, 34381Bomonti, Şişli, İstanbul.*
[f] *Nevşehir Üniversitesi, Mühendislik ve Mimarlık Fakültesi, Jeoloji Mühendisliği Bölümü, 50300 Nevşehir*

Keywords:
Gulf of Edremit, Lesbos Island, Alibey and Maden Islands, Dikili Channel, Aegean Sea, Benthic Foraminifera.

ABSTRACT

Benthic foraminiferal assemblages from the Gulf of Edremit, Lesbos Island, Alibey and Maden islands and Dikili Bay have been investigated and various morphological abnormalities, as well as, colored tests and large sizes have been observed. Besides, abundance of alien species originating from tropical seas attracts attention. Interesting togethernesses were found between different genera and species. Significant differences were observed between the assemblages from the northwest and southeast coasts of the Gulf of Edremit. 57 genera and 97 species were identified in the samples from the northwest coast, where as only 32 genera and 48 species were found on the southeast coast. A diverse foraminifer assemblage were observed around the Ayvalık-Alibey and Maden islands, with large individual sizes, colored tests and morphological abnomalities. Abnormal togethernesses between different genera and species were also observed in this locality. Togethernesses between Peneroplis pertusus (Forskal)-Coscinaspira hemprichii Ehrenberg and Peneroplis planatus (Fichtel and Moll)- Coscinaspira hemprichii Ehrenberg are important findings in the benthic foraminiferal assemblages of Ayvalık Alibey and Maden islands. Orange and brown coloration observed on many Peneroplis pertusus (Forskal) and P. planatus (Fichtel and Moll) individuals is another important finding in this region. Besides, many individuals of Peneroplis pertusus (Forskal), P. planatus (Fichtel and Moll), Lobatula lobatula (Walker and Jacob), Cibicidella variabilis (d'Orbigny), Ammonia compacta Hofker, A. parkinsoniana (d'Orbigny), Challengerella bradyi Billman, Hottinger and Oesterle, Elphidium complanatum (d'Orbigny) and E. crispum (Linné) were found. The presence of Laevipeneroplis karreri (Wiesner), Peneroplis pertusus (Forskal) and P. planatus (Fichtel and Moll) and Sorites orbiculus Ehrenberg on the east coast of Lesbos Island indicates the presence of hotwater springs. An abnormally large Peneroplis planatus (Fichtel and Moll) individual were found. Besides, many Peneroplis pertusus (Forskal) and P. planatus (Fichtel and Moll) individuals with orange-yellow tests, like the ones in Ayvalık, were found, suggesting the presence of submarine springs with Fe content. An abnormal Peneroplis planatus (Fichtel and Moll) individual with three different apertures was found in Dikili samples. One of the apertures was typical of the species, whereas the other two have the aperture characteristics of Coscinospira hemprichii Ehrenberg. The aim of our study is to figure out the factors leading to abnormal test morphologies. It is suggested that the benthic foraminiferal assemblages found in the study area are affected by the physical environmental conditions such as, temperature and salinity, as well as the chemical factors, such as radioactivity.

* *Corresponding author: ienginmeric@hotmail.com, barutif@istanbul.edu.tr*

1. Introduction

Studies were carried out for benthic foraminiferas on the coasts of Edremit Bay, on the northwestern coasts of the Lesbos Island, in the vicinity of Alibey and Maden Islands of Ayvalık and onthe eastern coasts of Dikili Bay. During these studies the coarsening and coloring in tests, the remarkable morphological abnormality, the abundance of tropical sea types, the presence of individuals showing association between various genera and species and gypsum crystals which had been observed in sediments have revealed that different ecological environments took place in these localities (Figure 1) (Meriç et al., 2002, 2003*a* and *b*, 2008, 2009, 2012*a*).

2. Coastal areas of the Edremit Bay

When 18 young sediment samples which had been collected from the northwestern and southeastern parts of the Edremit Bay were studied, it was seen that there had been a great privilege between the benthic foraminiferal assemblages in which they contain. It was detected that 7 samples which were taken at depths of 15.00 – 334.50 meters in northwest had contained 57 genera and 97 species. However, total of 32 genera and 48 species were found in 11 samples collected on southeastern coasts. The privilege between the two regions makes us consider that there are different ecological conditions between these localities. Again, in 2 samples at northwest, *Peneroplispertusus* (Forskal), *P. planatus* (Fichtel and Moll) and *Cibicidellavariabilis* (d'Orbigny), which prefer tropical conditions, to be observed in 3 samples in this region clearly reveal that different environmental conditions developed in northwest with respect to the southeast. This area, in which the Edremit Bay is located, is the region where there are evident tectonic features the Aegean Sea possesses (Figure 1). There is observed an EW trending fault from the north of the bay (Boztepe-Güney et al., 2001). Apart from these, cold springs beneath the sea around Akçay and Ören and the presence of Küçükçetmi, Bostancı, Güre and Zeytinpınarı hot springs of which their water temperatures vary between 20- 59.5 °C is,on the contrary, one of the reasonshowing the significance of tectonism in the region. Another characteristic of the Biga Peninsula is that it has geothermal springs at south which vary between temperatures of 41-102 °C (Erişen et al., 1996; Şaroğlu et al., 2003). This feature can also be considered as there might be hot springs in the bay.

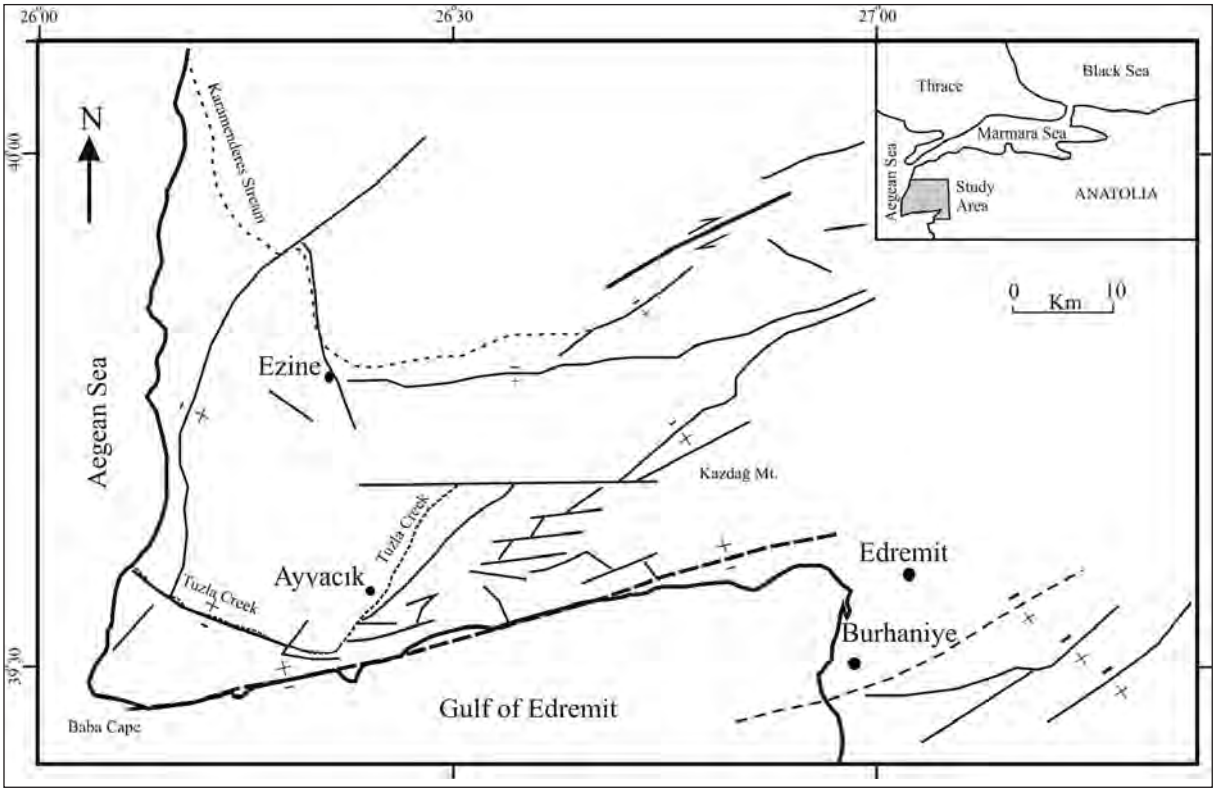

Figure 1- Fault map of the Biga Peninsula (modified from Boztepe-Güney et al., 2001).

In another investigation which was carried out in Edremit Bay, 11 samples were studied in terms of foraminiferas. The sediment sample number 2 which was taken from a depth of 82.00 meters was observed that it had contained 30 genera and 45 species. This situation reveals the presence of the most abundant genera and species of foraminifera in the region in one of 11 samples studied. However, *Eponidesconcameratus* (Williamson) and some other foraminiferal tests observed in the same sample at a size larger than 0.5 mm indicates the abundance $CaCO_3$ intake (58.1 %) in this locality in the study area (Meriç et al., 2012*a*). Also, when the foraminiferal assemblage of 4 samples collected from the eastern part of the Dikili channel (Figure 2) was studied, it was seen that number of species had varied between 32 and 41. Nevertheless, the presence of *Peneroplispertusus* (Forskal), *P. planatus* (Fichtel and Moll) which live in tropical conditions is another data supporting this idea. As a result, data obtained makes us think that there might be some thermal springs also beneath the sea like in coastal areas which developed due to the tectonismextending from north of Edremit Bay to the eastern coasts of the Dikili channels (Figure 1).

3. Alibey and Maden Islands

Total of 4 cores were drilled below the sea around Alibey and Maden Islands in northwest of Ayvalık with thicknesses varying 42 to 52 cm. In these sedimentary deposits, the abundance of *Peneroplispertusus* (Forskal) and *Peneroplisplanatus* (Fichtel and Moll) individuals were observed which are colored within an association of a rich benthic foraminiferal assemblage, several genera and species' such as *Peneroplispertusus* (Forskal), *P. planatus* (Fichtel and Moll), *Lobatulalobatula* (Walker and Jacob), *Cibicidellavariabilis* (d'Orbigny), *Ammonia compacta*Hofker, *A. parkinsoniana* (d'Orbigny), *Challengerellabradyi* Billman, Hottinger and Oesterle, *Elphidiumcomplanatum*(d'Orbigny), *E. crispum* (Linné) which show morphological abnormality and abnormal individuals presenting *Peneroplispertusus* (Forskal)-*Coscinospirahemprichii* Ehrenberg, *Peneroplisplanatus* (Fichtelve Moll)-*Coscinaspirahemprichii* Ehrenberg association. The abundance of individuals with coarse test belonging to genera and species' mentioned above indicates the abundance of $CaCO_3$ intake in this area. Again, there was observed abundant gypsum crystals in core section 3a between 28 – 45 meters starting from sea bottom. The presence of gypsum crystals which formedaround *Challengerellabradyi* Billman, Hottinger and Oesterle, *Elphidiumcrispum* (Linné) individuals and *Posidonia* fragments is an important feature for the region (Meriç et al., 2009). This situation shows that, there have been geothermal springs beneath the sea in recent (Figure 2) (Meriç and Suner, 1995; Meriç et al., 2003 and 2009).

4. Lesbos Island

Young sediment sample taken beneath the sea contains a rich benthic foraminiferal assemblage in east of PirgiThermis, the northeast of Mytilene settlement(southeast of Lesbos Island) (Figure 2). *Laevipeneropliskarreri* (Wiesner), *Peneroplispertusus* (Forskal) and *P. planatus* (Fichtel and Moll), *Soritesorbiculus* Ehrenberg among these assemblages reveal the presence of tropical conditions in this area. Besides; the occurrence of many *Peneroplispertusus* (Forskal) and *P. planatus* (Fichtel and Moll) tests in Ayvalık like orange – yellow color indicates the presence of iron bearing groundwaters in this area as well (Murray, 2006; Yalçın et al., 2008; Meriç et al., 2009, 2012 *b* and *c*). Especially, the assemblage in this region has shown its privilege with respect to the other 4 investigated points. There are many hot springs which have the characteristics of saline water with a temperature varying around 39.7, 43.5, 46.5, 46.9 and 69°C in southern and southeastern parts of the Island (Meriç et al., 2002). Therefore, the development of a different foraminiferal fauna similar to sebhkas in deserts around springs to develop because of thermal influxes is normal around young faults below the sea and in their close vicinities.

5. Dikili Bay

In 2 of 9 samples collected from the northern and southern coasts of the Dikili Bay, the presence of *Peneroplispertusus* (Forskal), *P. planatus* (Fichtel and Moll) and *Cibicidellavariabilis* (d'Orbiginy) which have various test shapes were identified. *Peneroplisplanatus* (Fichtel and Moll) individual among these presents a great abnormality in morphology. The aperture of the test developed in three different sections. One of them is single order aperture typical for it. However, the other two have the characteristics of *Coscinospirahemprichii* Ehrenberg. Apart from that, one *Rosalina* sp. and *Elphidiumcrispum* (Linné) individuals observed in the same region show abnormality in morphology. There are hot springs of which their temperatures

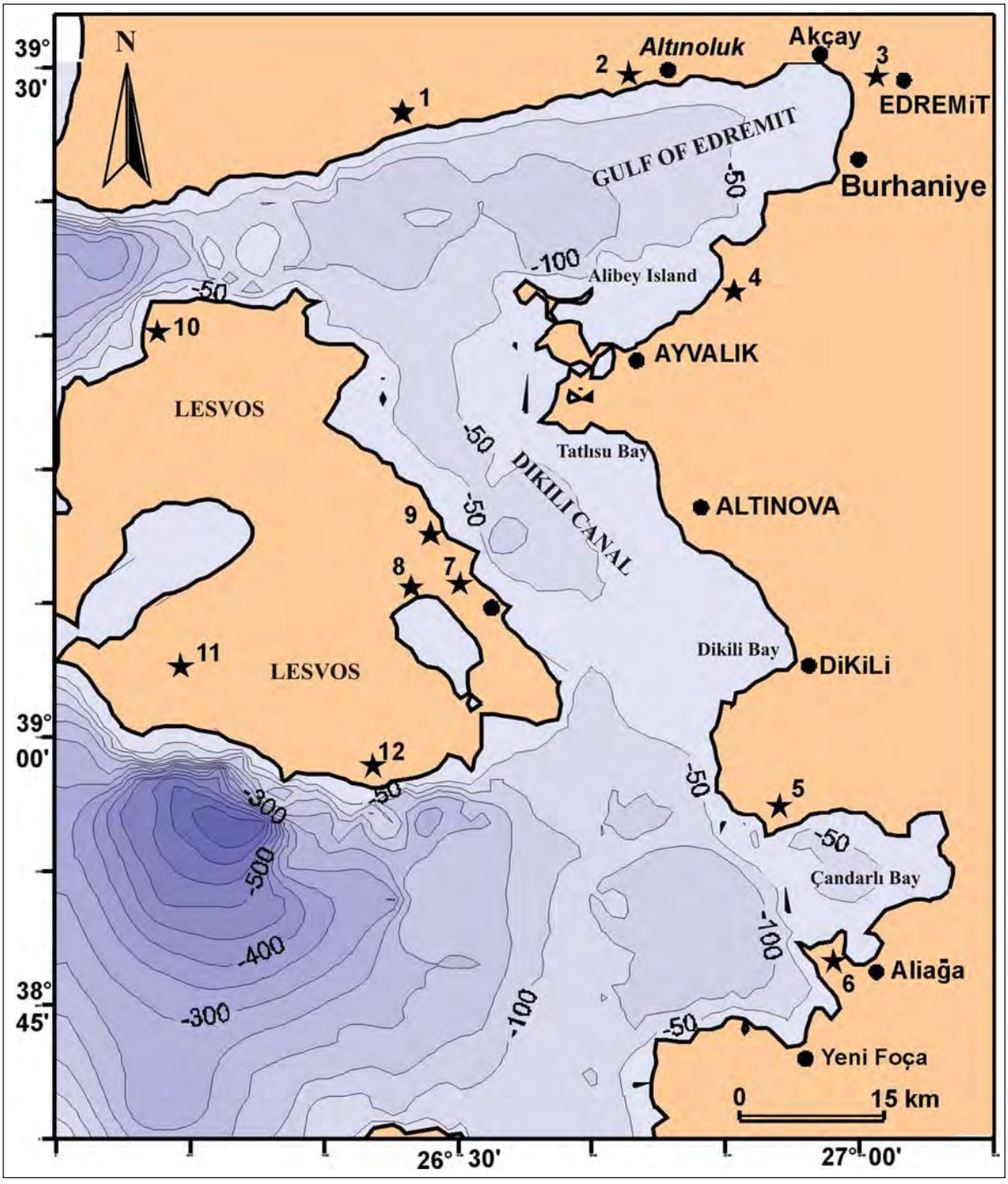

Figure 2- The bathymetry of Edremit Bay and Dikilie channel and hotsprings. (★ 1. Küçükçetmi, 2. Bostancı, 3. Güre, 4. Zeytinpınarı, 5. Bademli, 6. Ilıcaburun, 7. Pirgi Thermis, 8. Larisos, 9. Paralia Thermis, 10. Molivos, 11. Polichnitos and 12. Melinta hot springs)

vary between 40 – 60°C both on land and in the sea in Bademli and Aliağa Ilıcaburun along the road of Dikili – Çandarlı coast (Figure 2) (Meriç et al., 2003*b*). So, it is considered that there might be thermal springs which have heavy and trace elements having abnormal characteristics in or around the localities from where these samples were taken. That is why some benthic foraminiferal individuals have abnormally evolved.

6. Discussion and Resulsts

Due to the fault and/or faults located in the southern part of the Biga peninsula and in coastal areas of the Aegean Sea (Şaroğlu et al., 1992; Çiftçi et al., 2010), hot or cold springs have developed below the sea, similar to land areas. The abundance of $CaCO_3$ amount in compositions of these hot and cold springs, the springs of which their temperatures vary between 20-59°C along coastal areas, and the presence of geothermal springs which their temperatures reach 41-102°C indicate some geothermal springs under the sea. However, the presence of similar springs at eastern coasts of the Lesbos Island supports this idea (Meriç et al., 2003*a* and *b*).

The observation of a different life around the thermal spring at a depth of 10 meters, in south of Milos Island in Aegean Sea (Thierman et al., 1997) reveals thermal gains in areas where young faults are located in. Again, the presence of hydrothermal springs around many islands on Hellenic Island Arc supports this idea (Varnavas et al., 1999).

As for the study carried out in Haifa Bay, samples presenting a morphological abnormality at 30% among benthic foraminifers belonging to 217 species were encountered and the reason for this abnormality was shown as the presence of heavy metals in the composition of sea water (Yanko et al., 1998). The presence of heavy metals was again shown as a reason for the deformation of tests of foraminiferas (Yanko et al., 1999). In another study, the assumption that there was a relationship between tests of benthic foraminiferas showing abnormality in morphology and heavy metal in sea waters were assessed (Debenay et al., 2001).

There are not many streams or a stream network having the sediment charge capacity around Edremit Bay or the Dikili Channel. The interaction of groundwater with host rocks during its circulation, the intake of heavy and trace elements into its body and to transform it into mineralized spring in many locations in the sea could be considered as a reason for the increase in heavy metal values in marine environment mentioned. Clearly stating, the nature is not only affected by mankind.

In the regional investigation carried out among Edremit Bay, Alibey and Maden Islands, Dikili Bay and Lesbos Island, 143 samples were studied and 45 of them were chemically analyzed (Meriç et al., 2009, 2012*a*). Cu, Pb, Ni, Co, Mn, Cr, Fe and Al analyses were performed in samples taken from Edremit Bay (Meriç et al., 2012*a*). As a result, there was not observed any metal increase related to the expected depth in normal marine conditions as the environment is shallow marine and various marine and terrigenous environments are effective. However, the metal enrichment in Edremit Bay originates from metal ores located in NW Aegean region. As for the samples from Dikili Channel, the reason for metals to be in high content are especially the terrigenous gains flowing from Madra stream (Meriç et al., 2012*a*).

There were found heavy metals such as Cu, Co, Ni, Cr, Zn, Fe and Mn in 32 samples taken from cores 1b, 2a, 3b and 4a around Alibey and Maden islands (Meriç et al., 2009). It is clear that these were formed as a result of heavy metals which reached the sea by means of groundwaters through mine deposits along fault lines. However, according to foraminiferalassemblages in other cores, the biodiversity at this point is quite less. Apart from high Fe and Mn contents, the decrease in mollusk, ostracoda and *Posidonia* amounts observed in cores is another remarkable feature. Hence, it is understood that, groundwaters containing heavy metal and trace element have generated hydrothermal spring/springs and changed ecological conditions by reaching the sea by means of faults in or around this area (Meriç et al., 2009). Core number 4b shows a clear difference compared to other ones. All individuals are red brown, orange, yellow and partly gray colored in the community in which *Peneroplispertusus* (Forskal), *Peneroplisplanatus* (Fichtel and Moll), *Coscinaspirahemprichii* Ehrenberg are dominant. Also, the appearance of the sediment in red brown is a different character.

Hot or cold outflows beneath the sea, which were detected in mny location and are considered to have been still, are significant findings both to monitor fault lines in the sea and to determine its effect on temporal submarine life. Therefore, it is necessary to consider extraordinary characteristics such as; biodiversity in benthic foraminifers, test size/sizes in individuals, coloring on tests and morphological abnormality and common development among different genera and species'.

Received: 19.02.2013
Accepted: 05.07.2013
Published: June 2014

References

Boztepe-Güney, A., Yılmaz, Y., Demirbağ, E., Ecevitoğlu, B., Arzuman, S., Kuşçu, İ. 2001.Reflection seismic study across the continental shelf of Baba Burnu promontory of Biga Peninsula, Northwest Turkey.*Marine Geology*, 176, 75-85.

Çiftçi, B. N., Temel, Ö. R., İztan, H. Y. 2010. Hydrocarbon occurences in the western Anatolian (Aegean) grabens, Turkey: Is there a working petroleum system? *The American Association of Petroleum Geologists Bulletin*, 94 (12), 1827-1857.

Debenay, J.-P., Tsakiridis, E., Soulard, D., Grossel, H. 2001. Factors determining the distribution of foraminiferal assemblages in Port Joinville Harbor (Ile d'Yeu, France): The influence of pollution. *Marine Micropaleonotology*, 43, 75-118.

Erişen, B., Akkuş, İ., Uygur, N., Koçak, A. 1996. *Türkiye Jeotermal Envanteri, Maden Tetkik Arama Genel Müdürlüğü*, 480 s., Ankara.

Meriç, E., Suner, F.,1995. İzmit Körfezi (Hersek Burnu-Kaba Burun) Kuvaterner istifinde gözlenen termal veriler. (Ed. E.Meriç), İzmit Körfezi Kuvaterner İstifi 8l-90, İstanbul.

Meriç, E., Avşar, N., Bergin, F. 2002. Midilli Adası (Yunanistan-kuzeydoğu Ege Denizi) bentik foraminifer faunası ve toplulukta gözlenen yerel değişimler. *Çukurova Üniversitesi Yerbilimleri (Geosound)*, 40-41, 177-193, Adana.

Meriç, E., Avşar, N., Bergin, F., Barut, İ. F. 2003*a*. Edremit Körfezi (Kuzey Ege Denizi, Türkiye) güncelçökellerindekibentik foraminifer topluluğu ile ekolojik koşulların incelenmesi. *Çukurova Üniversitesi Yerbilimleri (Geosound)*, 43, 169-182, Adana.

Meriç, E., Avşar, N., Bergin, F., Barut, İ. F. 2003*b*. Dikili Körfezi'nde (Kuzeydoğu Ege Denizi) bulunan üç anormal bentik foraminifer örneği: *Peneroplis planatus* (Fichtel ve Moll), *Rosalina* sp. ve *Elphidium crispum* (Linné) hakkında. *Maden Tetkik Arama Dergisi*, 127, 67-81, Ankara.

Meriç, E., Kerey, İ. E., Avşar, N., Tuğrul, A. B., Suner, F., Sayar, A. 2003. Haliç (İstanbul) kıyı alanlarında (Unkapanı-Azapkapı) gözlenen Holosen çökelleri hakkında yeni bulgular. *Hacettepe Üniversitesi Yerbilimleri*, 28, 9-32, Ankara.

Meriç, E., Avşar, N., Yokeş, B., Dinçer, F. 2008. Alibey ve Madenadaları (Ayvalık-Balıkesir) yakın çevresi bentik foraminiferlerinin taksonomik dağılımı. *Maden Tetkik Arama Dergisi*, 137, 49-65, Ankara.

Meriç, E., Avşar, N., Mekik, F., Yokeş, B., Barut, İ. F., Dora, Ö., Suner, F., Yücesoy-Eryılmaz, F., Eryılmaz, M., Dinçer, F., Kam, E. 2009. Alibey ve Maden adaları (Ayvalık-Balıkesir) çevresi genç çökellerinde gözlenen bentik foraminifer kavkılarındaki anormal oluşumlar ve nedenleri. *Türkiye Jeoloji Bülteni*, 52 (1), 31-84, Ankara.

Meriç, E., Avşar, N., Nazik, A., Koçak, F., Yücesoy-Eryılmaz, F., Eryılmaz, M., Barut, İ. F., Yokeş, M. B., Dinçer, F. 2012*a*. Edremit Körfezi (Balıkesir) kıyı alanlarında oşinografik özeliklerin bentik foraminifer, ostrakod ve bryozoon toplulukları üzerindeki etkileri ile ilgili yeni veriler**.** *Türkiye Petrol Jeologları Derneği Bülteni,* Ankara. (inprint)

Meriç, E., Avşar, N., Nazik, A., Yokeş, B., Barut, İ. F., Eryılmaz, M., Kam, E., Taşkın, H., Başsarı, A., Dinçer, F., Bircan, C., Kaygun, A. 2012*b*. Ilıca Koyu (Çeşme-İzmir) bentik foraminifer-ostrakod toplulukları ile Pasifik Okyanusu ve Kızıldeniz kökenli göçmen foraminiferler ve anormal bireyler. *Maden Tetkik Arama Dergisi*, 145, 62-78.

Meriç, E., Avşar, N., Nazik, A., Yokeş, B., Dora, Ö., Barut, İ. F., Eryılmaz, M., Dinçer, F., Kam, E., Aksu, A., Taşkın, H., Başsarı, A., Bircan, C., Kaygun, A. 2012*c*, KaraburunYarımadası Kuzey Kıyılarının Oşinografik Özelliklerinin Bentik Foraminifer ve Ostrakod Toplulukları Üzerindeki Etkileri.*Maden Tetkik AramaDergisi*, 145, 22-47.

Murray, J.W. 2006. Ecology and Applications of Benthic Foraminifera. *Cambridge University Press*, Cambridge, New York, Melbourne, xi+446 p.

Şaroğlu, F., Emre, Ö., Kuşçu, A. 1992.1:100.000 ölçekli Türkiye'nin Diri Fay Haritası. *Maden Tetkik Arama Genel Müdürlüğü,* Ankara.

Şaroğlu, F., Ölmez, E., Kahraman, S. 2003. Çanakkale-Tuzla jeotermal alanının aktif tektoniği ve jeotermal sistem ile ilişkisi. 56. *Türkiye Jeoloji Kurultayı Bildiri Özleri Kitabı* (proceedings), 171-172, Ankara.

Thiermann, F., Akoumianaki, I., Hughes, J. A., Giere, O. 1997. Benthic fauna of a shallow-water gaseohydrothermal vent area in the Aegean Sea (Milos, Greece).*Marine Biology*, 128 (1), 149-159.

Varnavas, S. P., Halbach, P., Halbach, M., Panagiotaras, D., Rahders, E., Hubner, A. 1999.Chlaracterization of hydrothermal fields and hydrothermal evolution in the Hellenic Volcanic Arc. *International Conference Oceanography of the Eastern Mediterranean and Black Sea*.23 to 26 February 1999, Athens, Greece, Abstracts, 343.

Yanko, V., Ahmad, M., Kaminsky, M. 1998. Morphological deformities of benthic foraminiferal tests in response to pollution by heavy metals: Implications for pollution monitoring. *Journal of Foraminiferal Research*, 28 (3), 177-200.

Yanko, V., Arnold, A, Parker, W. 1999.The effect of marine pollution on benthic foraminifera: In Modern Foraminifera. Sen Gupta, B. (ed.).*Kluwer Academic Publishers*, 384 p.

Bulletin of the
Mineral Research and Exploration

http://bulletin.mta.gov.tr

GEOCHEMICAL CHARACTERISTICS OF LATERITES: THE AILIBALTALU DEPOSIT, IRAN

Ali ABEDINI[a], Ali Asghar CALAGARI[b], Khadijeh MIKAEILI[b]

[a] *Department of Geology, Faculty of Sciences, University of Urmia, 57153165, Urmia, Iran*
[b] *Department of Geology, Faculty of Natural Sciences, University of Tabriz, 5166616471, Tabriz, Iran*

Keywords:
Laterite, Protolith, Elemental distribution, Alibaltalu, Shahindezh, Iran

ABSTRACT

Alibaltalu laterite deposit is located ~20 km northeast of Shahindezh, south of West-Azarbaidjan province (NW of Iran). This deposit is developed as stratiform lenses along the boundary of Elika dolomites (Triassic) and Shemshak sandstones (Jurassic). The distribution fashion of minerals such as boehmite, diaspore, kaolinite, muscovite-illite, rutile, anatase, hematite and goethite in this deposit was accompanied by the development of four types of ore facies: (1) ferrite; (2) laterite; (3) bauxitic kaolinite; and (4) kaolinitic bauxite. Petrographically, the ores show conglomeratic, rounded-granular, veinlet, colloform, pelitomorphic, pseudo-porphyritic, nodular, and spongy textures. Comparison of distribution pattern of elements along a selective profile across the deposit reveals that ferrugenization-deferrugenization mechanism played a prominent role in distribution of Al, Si, Ti, HFSE, LREEs, HREEs, U, and Th during weathering processes. Distribution pattern of REEs normalized to chondrite indicates a poor differentiation of LREEs from HREEs and generation of poor negative Eu anomaly during the evolution of this deposit. These aspects along with ratios of Al_2O_3/TiO_2 and intense differentiation of Al from Fe in the course of weathering processes may indicate a mafic protolith for the deposit. Geochemical consideration of low-mobile elements demonstrates that this deposit is likely resulted from alteration and weathering of basaltic to andesitic rocks. By regarding to the distribution mode of elements such as Ni, Cr, Zr, and Ga within the ores, it can be deduced that this deposit was initially formed authigenically and then later was contaminated by other rock materials during erosion and transportation from its original place to the present site.

1. Introduction

Laterites are an important source of many metal ores, in particular iron, aluminium, nickel, gold, niobium, and phosphorus (Hill et al., 2000; Retallack, 2010). The controls necessary for the enrichment of these and other elements to achieve economic levels are a complex balance of geochemical, geographical, and biological parameters (Hill et al., 2000). Specific conditions leading to laterite formation have been documented previously (Bardossy and Aleva, 1990; Ma et al., 2007; Sanematsu et al., 2011). During past two decades lateritic deposits in different parts of the world were studied in detail for realization of factors related to mobilization and redistribution of major, minor, and trace elements (including REE) during weathering processes (Ma et al., 2007; Yang et al., 2008; Hao et al., 2010; Meshram and Randive, 2011; Sanematsu et al., 2011). These studies revealed that consideration of major and trace elements geochemistry is an indispensable tool to investigate various aspects of laterite formation such as parent rock composition, diagenetic and epigenetic processes related to lateritization, pH, Eh, drainage, climate, and minerlogical control.

Laterite deposits in Iran are apatially distributed in four regions, namely (1) the northwest of Iran, (2) the Zagros heights, (3) the Alborz mountain chain and (4) the central plateau of Iran (Calagari and Abedini, 2007; Abedini and Calagari, 2013*a*, *b*). They are restricted to Permian, Permo-Triassic, Triassic,

* *Corresponding author : abedini2020@yahoo.com and a.abedini@urmia.ac.ir*

Triassic-Jurassic, middle Cretaceous (Cenomanian-Turonian). In northwest of Iran, there are many lateritic deposits belonging mainly to Permian, Permo-Triassic, Triassic, and Triassic-Jurassic period. They chiefly were developed within carbonate rocks and often contain bauxite and kaolinite ores. No comprehensive studies has been done so far on factors influencing distribution of elements in Triassic-Jurassic ores of this type of deposits in northwest of Iran. In this study, Alibaltalu laterite deposit (located in 20 km northeast of Shahindezh, south of West-Azarbaidjan province, NW Iran) as a typical example of this type of deposits was chosen and textural and genetic characteristics, the mineralogical control on distribution of elements (especially trace and rare earth), and ultimately the protolith of this deposit were considered in detail.

2. Regional Geology

Based on depositional characteristics of residual deposits throughout the world (Bardossy, 1982) the lateritic deposit of Alibaltalu is reckoned to be a part of Irano-Himalayan karst bauxite belt. This deposit is part of the Sanandaj-Sirjan structural zone (Figure 1a). The palaeogeography of Iran in the Late Permian and Early Triassic indicates that the early Late Triassic compression phase (early Cimmerian event) was followed by extensional movements in north and central Iran (Esmaeily et al., 2010). The initiation of this extensional phase is locally indicated by continental alkali-rift basaltic lava flows and vesicular mafic rocks (Berberian and King, 1981; Vollmer, 1987). In Iran, the Late Triassic andesitic to basaltic volcanic rocks cover an eroded and often karstified surface of Middle Triassic carbonates (Early Cimmerian palaeorelief), at the base of the Shemshak Formation (lower Jurassic) (Annelles et al., 1975). The volcanic activity occasionally continued into the lower part of the Shemshak Formation. Some of these basic sources, however, due to laterization processes were partially converted into laterite.

3. Method of Investigation

Studies of lateritic ores in study area were carried out in two parts, (1) field and (2) laboratory. The field works include surveys for exploring the existing geological formations, determining the geometry of deposit, examining the lithology of bedrocks, cap rocks, and mesoscopic characteristics of the ores on outcrops, taking random and systematic samples from ores (preferentially perpendicular to the strike of layers and enclosing rocks), and finally preparing geological map of the area (Figure 1). By noting the lithologic variations in the area, ~40 samples from lateritic ores, bed rocks, and cap rocks were taken for close examination.

Laboratory works include identification of the existing ore textures and their mineralogical compositions. Laboratory studies began after preparation of 20 thin-polished sections and subsequently they were examined microscopically for the existing textures. The mineralogical composition of Six samples were determined by using X-ray diffraction (SIEMENS Diffractometer, Model D-5000, CuKα radiation, fixed graphite chromators, voltage 40kV, current 40 mA, Scanning speed per minute, scan range 2-70°, drive axis 2Θ) in Geological Survey of Iran. For geochemical interpretation 6 samples from lateritic ores were chemically analyzed by ICP-AES and ICP-MS methods at ALS Chemex laboratories in Canada. Loss on ignition (LOI) derives by weight difference after ignition at 1000°C. The results of chemical analyses along with detection limits are listed in table 1.

4. Results

4.1. Geology of Deposit

The most conspicuous rock units in the study area from the oldest to the youngest include formations such as Mila cherty dolomite and limestone (Cambro-Ordovician), Dorud sandstone and shale (lower Permian), Ruteh carbonate (upper Permian), Elika limestone and dolomite (Triassic), Shemshak sandstone, shale, and siltstone (lower Jurassic), sandy and marly limestone (upper Cretaceous), Fajan conglomerate (Eocene), and Karaj tuff and shale (Eocene) (Figure 1b). There are also a series of basaltic-andesitic rocks occurring as irregular patches within the upper part of Triassic carbonates. The prominent feature from economic geology point of view in the area is the presence of a horizon of stratiform and and lenticular lateritic ores along the boundary of Elika dolomite and Shemshak sandstone. This horizon extends about 400 meters and its average strike and dip are N15°W and 83°SW, respectively, with thicknesses ranging from 8 to 14 meters. A selective profile across this horizon exhibits six colored lithologic units including (1) violet-gray, (2) chocolate brown, (3) red, (4) multi-color, (5) yellow, and (6) brown (Figure 2). The boundaries between lateritic lenses and the enclosing

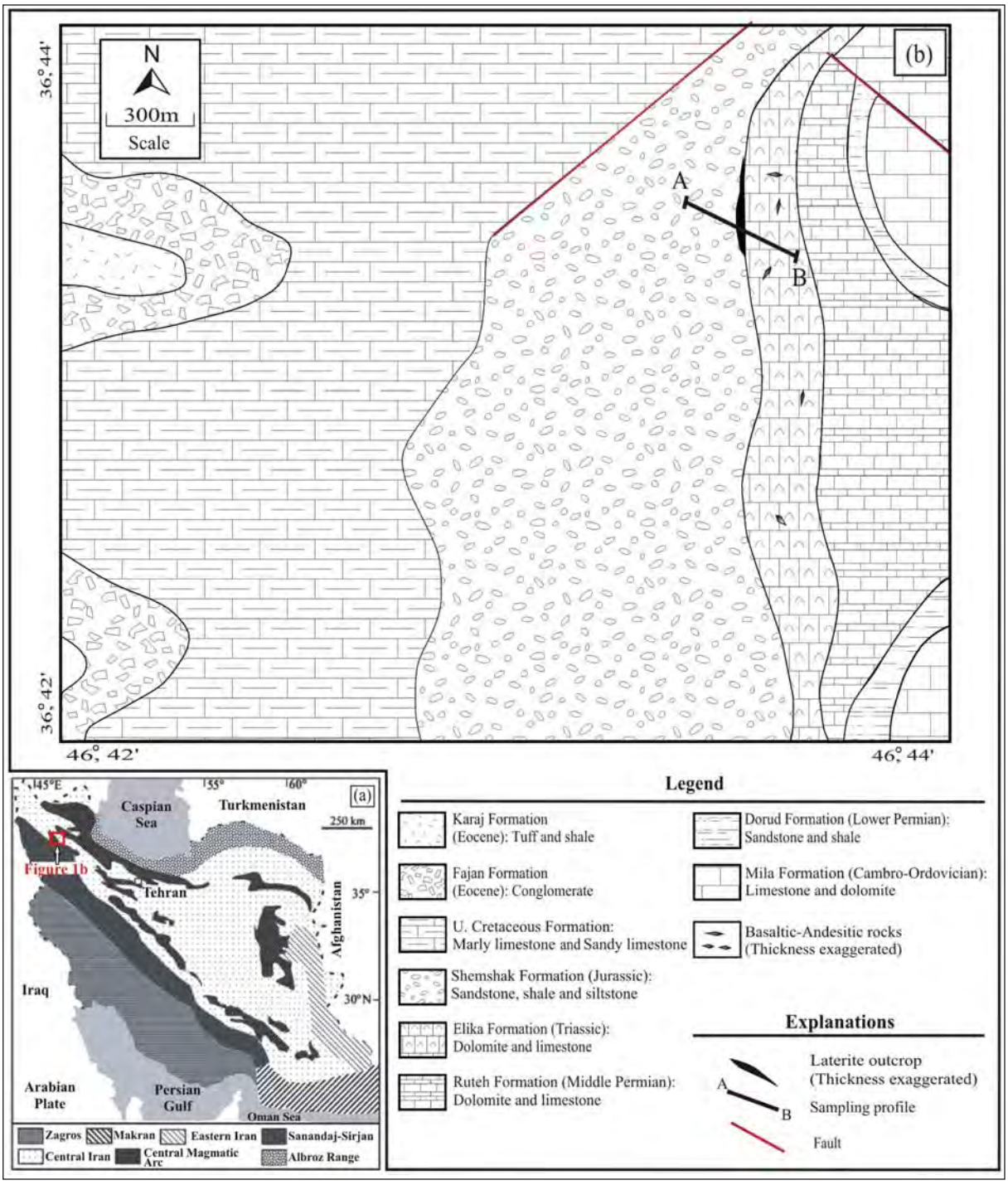

Figure 1- (a) Simplified regional geotectonic map of Iran showing some major geological-structural zones. Location of studied area is also marked (modified after Stöcklin, 1968). (b) Geologic map of the Alibaltalu area. Noticeable on this map is the position of lateritic lens.

bedrocks and cap rocks are quite sharp. There are cross-cutting fractures and joints within the enclosing rocks. Some volcanic rocks are present at contiguity of ore-bedrock boundary. The presence of organic matters in upper parts of the profile is also noticeable. The violet-gray ores have massive texture, fine alternate violet and gray layers, spheroidal bands consisting of limonite, goethite, and hematite (Figure 3a), delicate porous ring bands with limonitic nucleus (Figure 3b), rough feel, and rather high hardness. On the other hand, however, the chocolate brown ores are rather soft and have earthy aggregates. On the surface

Table 1- List of chemical analyses in ores of the studied profile done by ICP-AES and ICP-MS methods for major, minor, trace, and rare earth elements. Shown on this table are also are the detection limits of various elements. Values of oxides and L.O.I. are in wt% and of trace and rare earth elements are in ppm.

	Detection limit	R-1	R-2	R-3	R-4	R-5	R-6
SiO_2	0.01	28.2	5.1	31	4.7	39.5	32.1
Al_2O_3	0.01	17.1	2.8	27.6	2.2	33.2	33.6
Fe_2O_3	0.01	35.1	78.9	21.6	81.8	8.37	7.21
CaO	0.01	0.28	0.14	0.08	0.26	0.24	0.41
MgO	0.01	0.89	0.19	0.06	0.18	0.12	0.38
Na_2O	0.01	0.1	0.05	0.06	0.16	0.2	0.06
K_2O	0.01	2.82	0.45	0.05	0.27	0.08	0.9
TiO_2	0.01	1.78	0.22	4.5	0.11	4.89	4.33
MnO	0.01	0.43	1.53	0.02	1.36	0.01	0.06
P_2O_5	0.01	0.17	0.15	0.59	0.04	0.14	0.36
LOI	0.01	11.75	10.35	12.05	9.41	14.35	20.3
Total	–	98.62	99.88	97.61	100.49	101.1	99.71
U	0.05	6.81	1.53	13.35	1.78	15.2	18.65
V	5	85	5	281	5	358	367
Y	0.5	50.7	9.6	34.1	15.5	30.2	39.7
Zn	5	80	54	46	91	82	73
Zr	2	224	21	434	14	496	525
Ba	0.5	337	168.5	184	87.4	125.5	236
Co	0.5	27.4	21.9	3.3	19.8	6.6	18.8
Cr	10	50	10	80	20	120	180
Cs	0.01	13.9	1.29	0.28	0.84	0.37	1.97
Ga	0.1	25.6	4	31.7	3.8	40.4	46.6
Hf	0.2	5.9	0.5	10.7	0.3	12.3	13.1
Nb	0.2	32.6	1.6	75	0.6	101	116
Ni	5	15	5	31	5	34	79
Pb	5	66	17	38	7	49	32
Rb	0.2	112.5	16	2.7	11.3	3	24.7
Sr	0.1	280	171	3780	125.5	414	2280
Ta	0.1	1.9	0.1	4	0.1	5.6	7.1
Th	0.05	14	2.42	13.7	1.48	16.2	23
La	0.5	79.7	9.3	81.2	4.9	77.8	129
Ce	0.5	136	19.1	165.5	11	144.5	252
Pr	0.03	20.7	2.13	19.15	1.31	17.8	24.5
Nd	0.1	88.1	8.8	76.5	6.4	70.9	87.3
Sm	0.03	20.2	1.92	15.6	1.98	13	16.7
Eu	0.03	5.31	0.42	4.23	0.54	3.38	4.66
Gd	0.05	17.2	2	13.9	2.56	11.8	17.25
Tb	0.01	2.38	0.25	1.84	0.4	1.57	2.41
Dy	0.05	12.8	1.68	9.36	2.49	7.95	12.75
Ho	0.01	2.27	0.28	1.63	0.44	1.41	2.18
Er	0.03	6.69	0.85	4.39	1.33	3.82	5.92
Tm	0.01	0.81	0.02	0.47	0.05	0.45	0.83
Yb	0.03	6.19	0.79	3.92	1.16	3.03	5.73
Lu	0.01	0.83	0.07	0.47	0.12	0.4	0.8

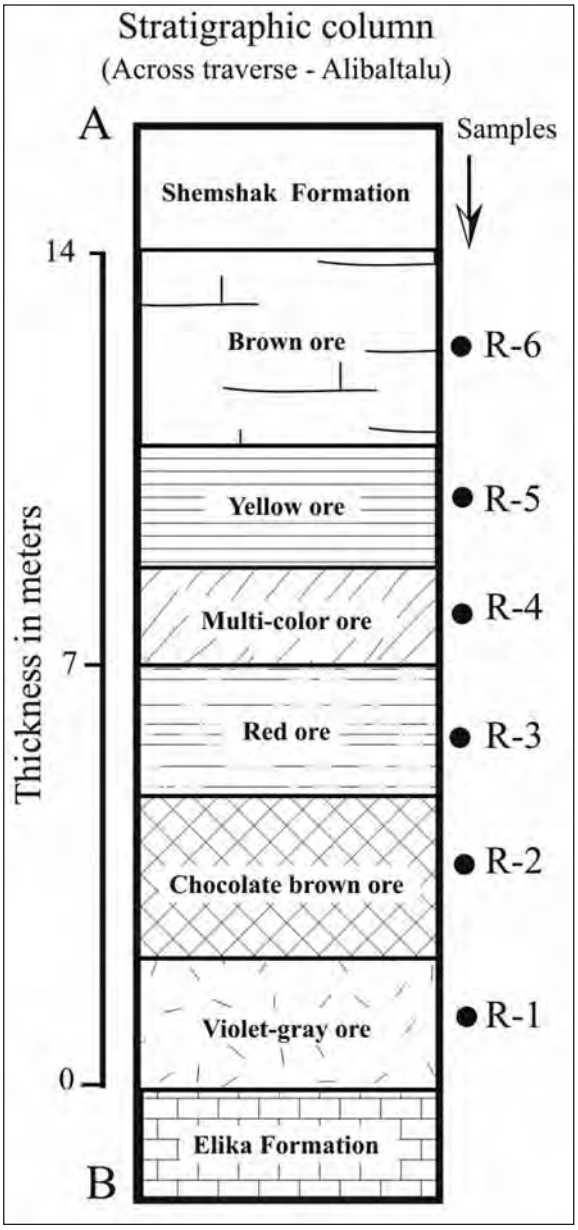

Figure 2- A stratigraphic column across the studied profile. Shown on this column is the location of samples taken for geochemical analyses (filled circles). Refer to figure 1 for the trend of sampling profile.

of the red ores, growth of goethite with a typical botryoidal texture and accompanying limonitization are conspicuous. In fact, these are the important geologic characteristics of the ores in this deposit.

4.2. Petrography and Mineralogy

Because of very fine-grained crystals in ores and their softness, their microscopic examinations are restricted chiefly to determination of mineral textures related to ore genesis. These studies exhibit that the marked texture-forming units of the ores include pelitomorphic matrix, detrital grains, nodules, concretions, and open-space fillers. These texture-forming units in the ores brought about nodular, pelitomorphic, conglomeratic (Figure 3c), colloform (Figure 3d), pseudo-porphyritic (Figure 3e), veinlet (Figure 3f), rounded-grain (Figure 3g), and spongy (Figure 3h) textures. XRD analyses demonstrate that the ores have rather simple mineralogy and include mineral assembages like boehmite, diaspore, kaolinite, muscovite-illite, rutile, anatase, hematite, and goethite which have individually abundances greater than 4%.

4.3. Geochemistry

Chemical analyses demonstrate that the major components of the studied ores are SiO_2 (4.70-39.50 wt%), Al_2O_3 (2.20-33.6 wt%), Fe_2O_3 (7.21-81.80 wt%), and TiO_2 (0.11-4.89 wt%) (Table 1). They mark a wide range of variations. Among these components, Fe_2O_3 exhibits a profound variation within the profile. Alkalis and earth alkalis along with P and Mn (in oxide form) are present in very low abundance and their total values range from 0.79 to 4.69 wt%.

Trace elements are present relatively in low quantity in the studied ores. They are, in order of abundance, mainly Sr (125.5-3780 ppm), Zr (21-525 ppm), Ba (87.4-337 ppm), V (5-358 ppm), and Ce (11-252 ppm). The rest exist relatively in lower amounts which, in decreasing abundance, are La, Cr, and Zn (in 10s ppm); Th, Rb, Pb, Ni, Nb, Hf, Ga, Cs, Co, Y, V, U, Dy, Gd, Sm, Nd, and Pr (in a few ppm to 10s ppm); and Ta, Eu, Tb, Ho, Er, Tm, Yb, and Lu (in a few ppm).

5. Discussion

5.1. Genetic Implications of The Deposit Using Textural and Mineralogical Evidence

5.1.1. Textural Evidence

Important textural characteristics of the studied ores are the existence of two groups of textures with contrasting origin. Pseudo-porphyritic, nodular, and plitomorphic textures are compatible with authigenic origin whereas conglomeratic and rounded-grain textures are indicative of allogenic origin (Bardossy,

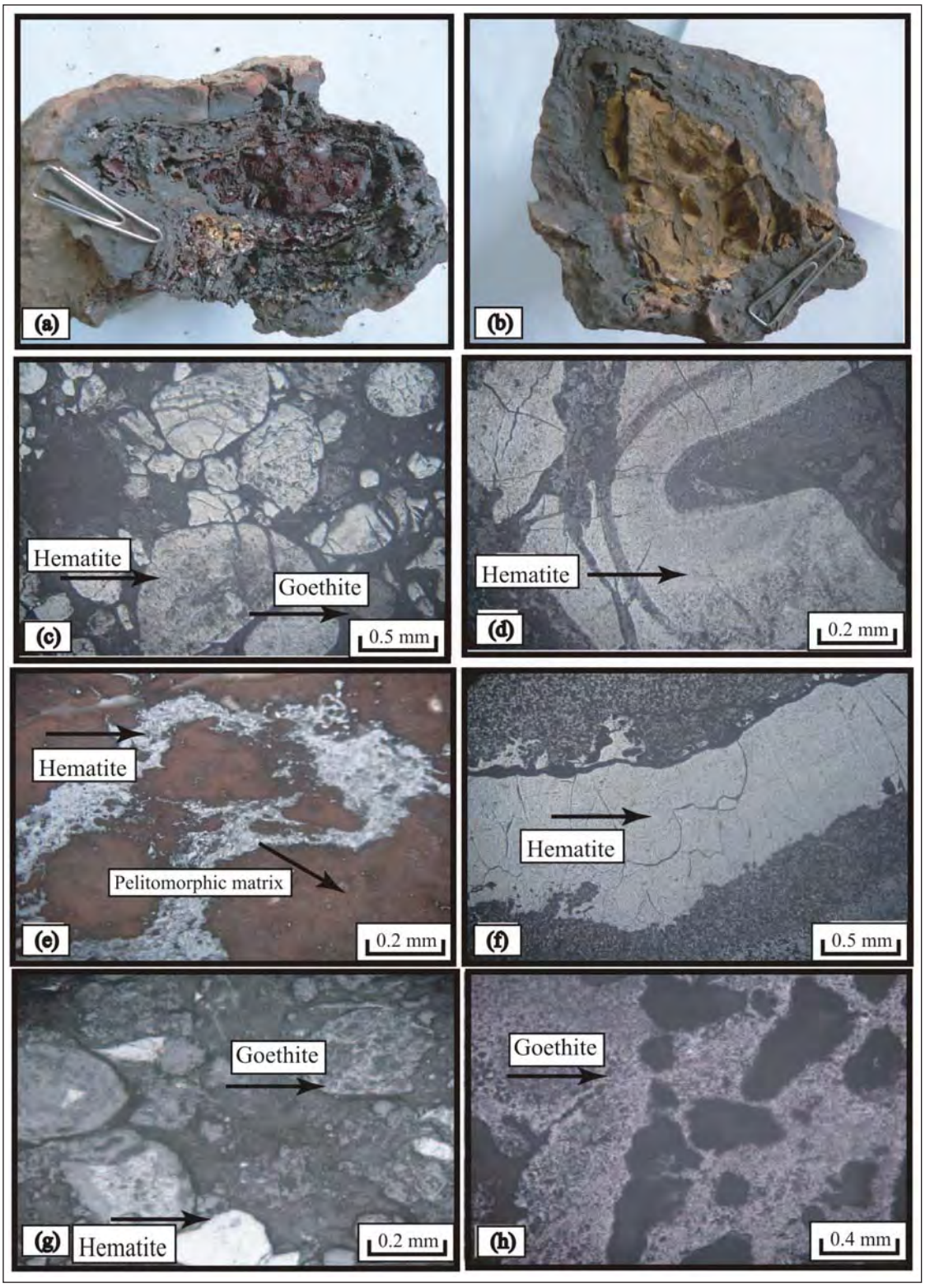

Figure 3- Macroscopic and microscopic (XPL) photographs of the studied ores. (a) Spheroidal weathering and delicate ring bands in porous violet-gray ores. (b) Limonitic core in violet-gray ores. (c) Conglomeritic texture. (d) Colloform texture. (e) Pseudo-porphyritic texture. (f) Veinlet rexture. (g) Rounded-grain texture. (h) Spongy texture.

1982). By taking this matter into consideration, it appears that lateritic system in this area was initially developed authigenically but subsequently suffered erosion and transportation and moved to its present place. The development of nodular texture indicates the continuous fluctuations of underground water table level during the evolution of the deposit (Valeton, 1972). The well-developed colloform and pelitomorphic textures are indicative of weak draining and prolonged weathering processes (Boulange, 1984). The presence of veinlets with dominant hematite mineralogy in the ores may testify to the redistribution of iron in the weathered profile.

5.1.2. Mineralogical Evidence

The presence of 3 pairs of minerals (1) boehmite-diaspore, (2) rutile-anatase, and (3) goethite-hematite in the ores denotes the effective role of diagenetic processes and tectonic stresses controlling the mineralogical changes in this deposit. It seems diaspore was formed as the result of changes in crystal structure of boehmite by tectonic stresses and diagenesis (Temur and Kansun, 2006). Anatase is commonly stable in the presence of low concentration of alkali elements at surficial temperatures (Boulange and Colin, 1994). It probably changed its crystal class by the function of tectonic forces and diagenetic processes and was converted into rutile. Goethite was also turned into hematite by dehydration processes.

5.2. Type of Ores

Delineation of values of Al_2O_3, SiO_2, and Fe_2O_3 of the ores in trivariate diagram (Aleva, 1994) displays that Alibaltalu deposit consists of four types of ore lithology (1) laterite, (2) ferrite, (3) bauxitic kaolinite, and (4) kaolinitic bauxite (Figure 4*a*). Comparison of the studied stratigraphic column with distribution mode of Al_2O_3, SiO_2, and Fe_2O_3 of the ores on the trivariate plot indicates that the violet-gray and red ores have lithologically a laterite composition, the chocolate brown and multi-color ores have a ferrite composition, the yellow ores have a bauxitic kaolinite composition, and the brown ores have a kaolinitic bauxite composition (Figure 4*b*).

5.3. Mineralogical Control on Distribution of Elements in the Ores

In this study, mineral phases having abundances >4% were identified by XRD analyses. Therefore, it is likely that there might be some mineral phases acting as hosts for trace and rare earth elements that were not identified by XRD analyses.

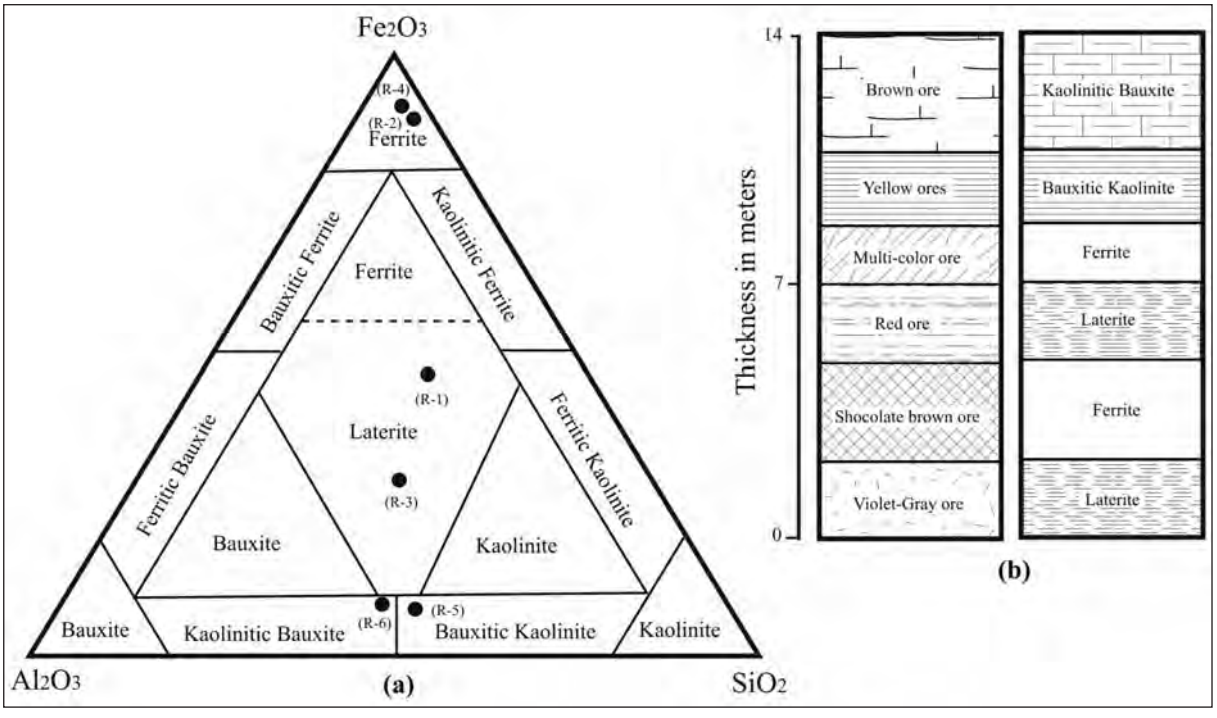

Figure 4- (a) The position of the studied ores on Al_2O_3-SiO_2-Fe_2O_3 trivariate plot (Aleva, 1994). (b) Stratigraphic column of ore units determined by Al_2O_3, SiO_2, and Fe_2O_3 values in the studied profile.

For consideration of minerals hosting elements in the ores, attempts have been made to calculate Pearson correlation coefficient (Rollinson, 1993) among some elements and their distribution patterns were compared (Figure 5-11). This consideration was fulfilled in five sections, (1) major and minor elements (Si, Al, Fe, Ti, K, Na, Mg, Ca, Mn, P), (2) large ion lithophile elements (Ba, Rb, Sr, Th, U, Pb, Cs), (3) transition trace elements (Co, Cr, Ni, V), (4) high field strength elements (Hf, Nb, Ta, Zr, Ga, Y), and (5) light (La-Gd) and heavy (Tb-Lu) rare earth elements.

5.3.1. Major and Minor Elements

Similarity in distribution mode of Si (Figure 5a) and Al (Figure 5b) in the residual profile at Alibaltalu (except yellow to brown ores) shows that the distribution of these elements is controlled principally by kaolinite. Furthermore, the high similarity in distribution mode of Ti (Figure 5c) and Al (Figure 5b) is a common phenomenon in residual profiles. The intense fractionation of Fe (Figure 5d) from Si (Figure 5a), Al (Figure 5b), and Ti (Figure 5c) indicates that ferrugenization and deferrugenization is the prominent controlling parameter in distribution of Al, Si, and Ti in the profile. What can be deduced from consideration of minor elements variations (Figures 6a-f) is that the irregular behavior of these elements in the profile is likely related to heterogeneity of the protolith and to disparity in the intensity of alteration in the course of evolution of this deposit. Comparison of the mode of variations of minor elements in the profile with that of major

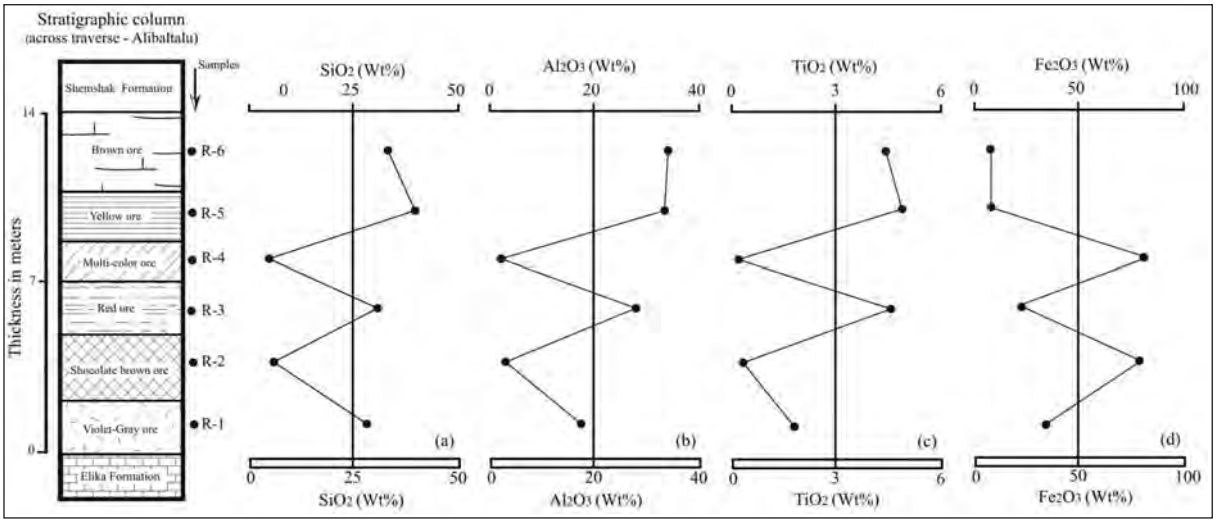

Figure 5- Variation of values of (a) SiO_2, (b) Al_2O_3, (c) TiO_2, and (d) Fe_2O_3 across the studied profile.

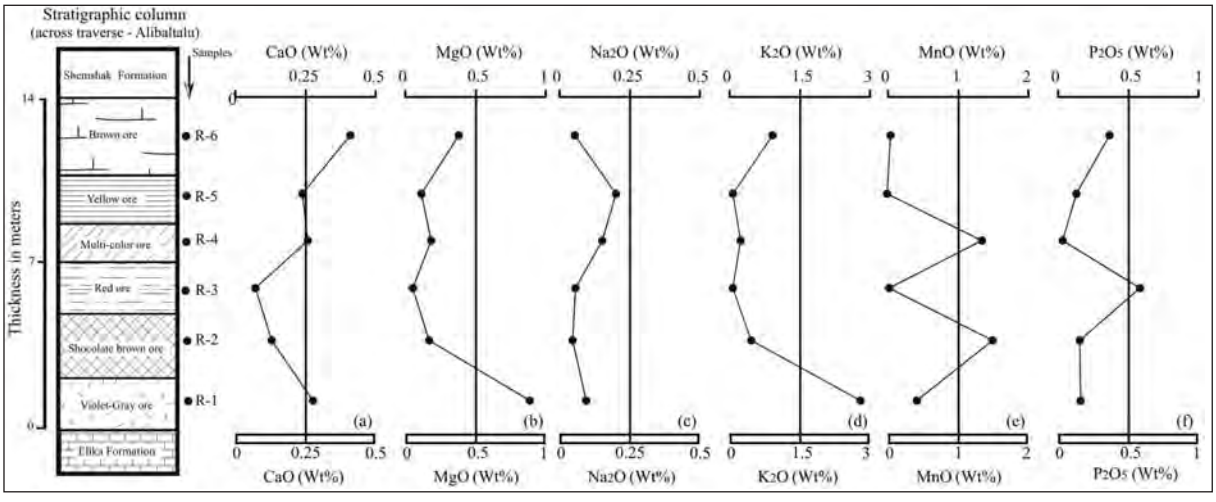

Figure 6- Variation of values of (a) CaO, (b) MgO, (c) Na_2O, (d) K_2O, (e) MnO, and (f) P_2O_5 across the studied profile.

elements illustrates that only Mn (Figure 6e) has very analogous distribution fashion with Fe (Figure 5d). This may indicate that change in redox potential was the key factor in concentration of Mn and Fe in the weathered profile (Ma et al., 2007).

5.3.2. Large Ion Lithophile Elements (LILE)

The presence of similar distribution trends of Rb (Figure 7a), Ba (Figure 7b), and Cs (Figure 7c) with K_2O (Figure 6d) may be indicative of hosting of these elements by muscovite (Plank and Langmuir, 1998). Comparison between distribution patterns of Sr (Figure 7d) and P (Figure 6f) displays an analogous trend. This may suggest fixation of these elements by similar conditions in the residual system (Henderson, 1984). The positive and medium correlation of Sr with Si (r = 0.55) and Al (r = 0.58) may suggest fixation of Sr by kaolinite. The distribution mode of U (Figure 7e) and Th (Figure 7f) are also similar to Si (Figure 5a), Al (Figure 5b), and Ti (Figure 5c) suggesting their distributions might have been controlled by kaolinite, boehmite, diaspore and Ti-oxides. Monazite and zircon as Th-bearing minerals are well-known in the residual profiles (Fernandez-Caliani and Cantano, 2010). The similar distribution trend of Th (Figure 7f) and Zr (Figure 8a) and the positive and medium correlation between Th and P (r = 0.52), may suggest that phosphate minerals can also be other candidates for hosting Th. Analogously, the positive and medium correlation between U and P (r = 0.60) may also lead us to believe that phosphate minerals acted as hosts for U. Pb (Figure 7g), Si (Figure. 5a), and Al (Figure 5b) display Similar distributions that may be due to hosting of Pb by kaolinite.

5.3.3. High Field Strength Elements (HFSE)

Consideration of variation mode of these elements in the profile suggests their very similar behavior

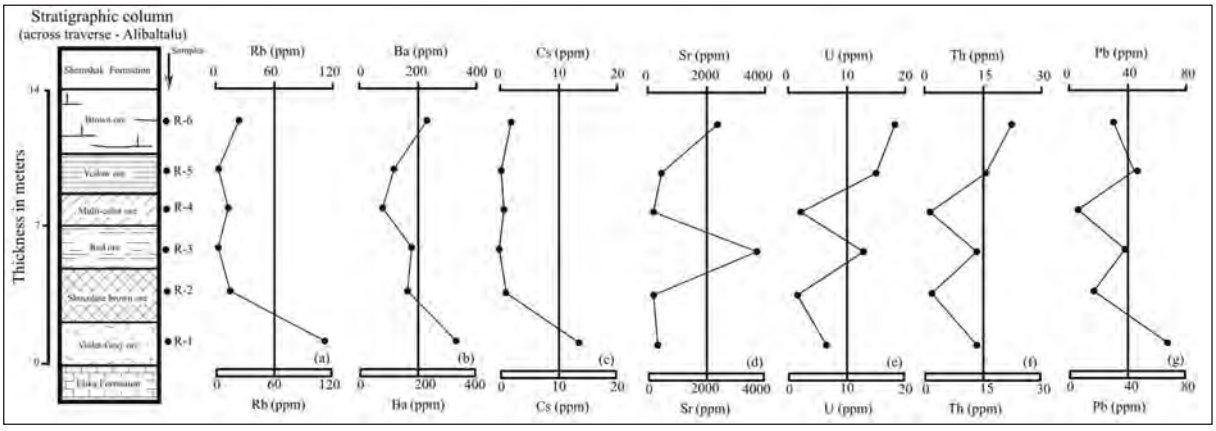

Figure 7- Variation of values of (a) Rb, (b) Ba, (c) Cs, (d) Sr, (e) U, (f) Th, and (g) Pb across the studied profile.

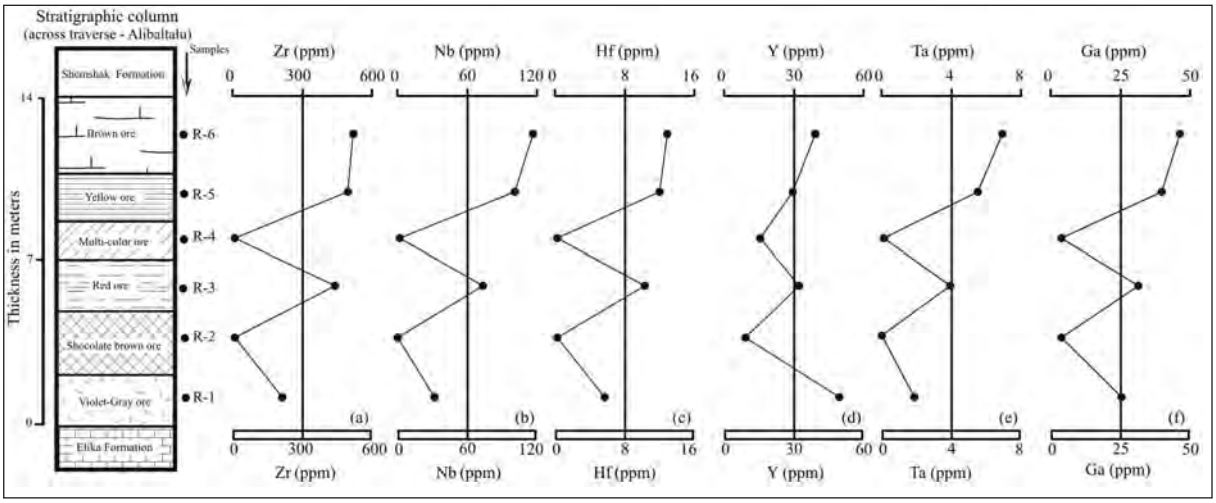

Figure 8- Variation of values of (a) Zr, (b) Nb, (c) Hf, (d) Y, (e) Ta, and (f) Ga across the studied profile.

during weathering processes (Figures 8a-f). Further studies revealed that distribution patterns of these elements are very similar to Al (Figure 5b). Regardless of distribution trend in yellow to brown ores, however, distribution patterns of HFSE are very analogous to Si (Figure 5a) and Ti (Figure 5c). With regard to above mentioned matters, it seems that kaolinite did not play a role for fixation of Y, Ga, Ta, Nb, and Hf in the brown ores, but boehmite and diaspore might have a pronounced role instead. In the rest of ores, however, besides boehmite and diaspore kaolinite also played a noticeable role. Analogous distribution pattern of Zr (Figure 8a), Nb (Figure 8b), Hf (Figure 8c), and Ti, also may suggest that besides mentioned minerals the role of Ti-oxides should not be ruled out for fixation of Zr, Nb, and Hf (Fernandez-Caliani and Cantano, 2010). Ta (Figure 8e) and Ti also exhibit analogous distribution patterns (Figure 5c) implying the notable role of rutile and anatase for fixation of Ta in the deposit.

5.3.4. Transition Trace Elements (TTE)

Although distribution of V, Ni, and Cr in lateritic-bauxitic deposits are chiefly controlled by Fe-oxides and hydroxides (Marques et al., 2004; Laskou and Economou-Eliopoulos, 2007), comparison of their distribution patterns (Figure 9a, b, d) with that of Fe (Figure 5d) do not illustrate such relation in the studied profile. Comparison of distribution patterns of these three elements with those of other major elements manifests that the distribution mode of these three elements are very much similar to Si (Figure 5a), Al (Figure 5b), and Ti (Figure 5c). These similarities unveil that the distribution of V was controlled by kaolinite, boehmite, diaspore, and Ti-oxides; of Cr by kaolinite and Ti-oxides; and finally of Ni by kaolinite (Newman, 1987). Distribution pattern of Co (Figure 9c) in the yellow through brown ores is analogous to those of V (Figure 9a) and Ni (Figure 9b). Co (Figure 9d), however, in the yellow through violet-gray ores has similar distribution pattern to Fe (Figure 5d) and Mn (Figure 5e). This type of similarity may indicate that the concentration distribution of Co in the brown ores was controlled mainly by kaolinite and Ti-oxides but in the rest of ores by Mn-oxides and Fe-oxides and-hydroxides (Mutakyahwa et al., 2003).

5.3.5. Rare Earth Elements (REEs)

Several groups of minerals were proposed by various researchers as major potential hosts for REEs in weathered products including clays (Karadağ et al., 2009), secondary phosphates (Braun et al., 1993), Mn-oxides and -hydroxides (Walter et al., 1995), and Fe-oxides and -hydroxides (Mameli et al., 2007). Almost similar trends in variation modes exist among LREEs (Figure 10a, b), HREEs (Figures 11a-g), Si (Figure 5a), and Al (Figure 5b) in the studied profile testifying that kaolinite played an outstanding role in distribution of REEs in the ores. The lack of similarity in distribution trends of MnO and F_2O_3 to those of REEs offers that Mn-oxides along with

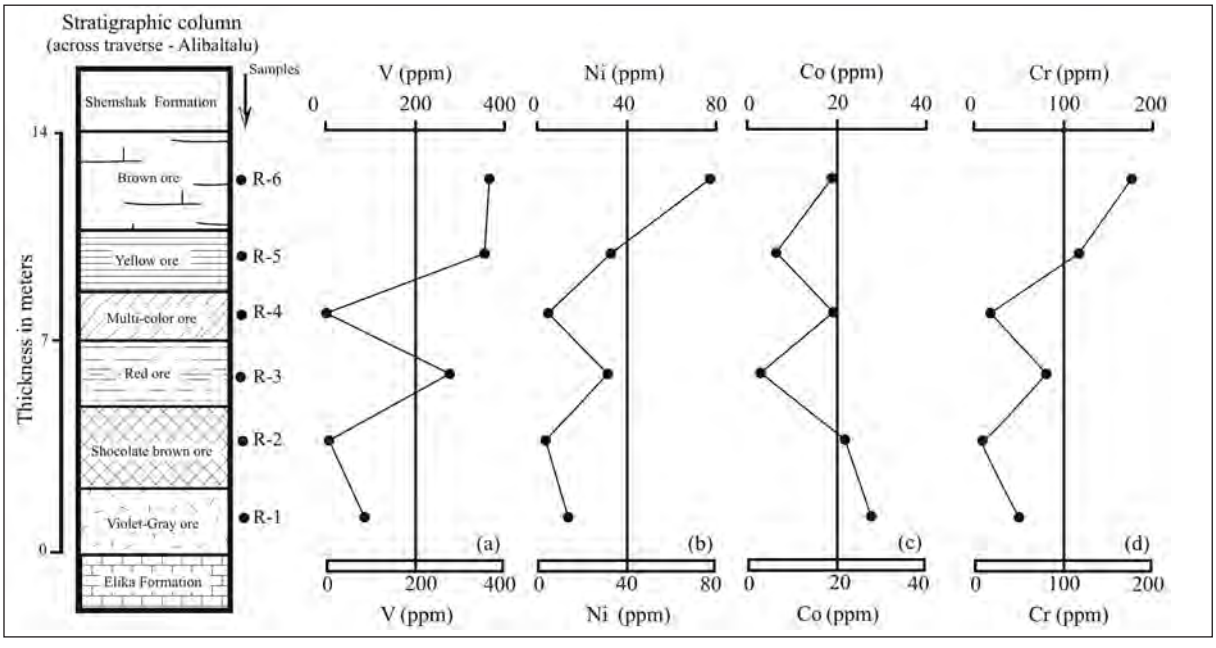

Figure 9- Variation of values of (a) V, (b) Ni, (c) Co, and (d) Cr across the studied profile.

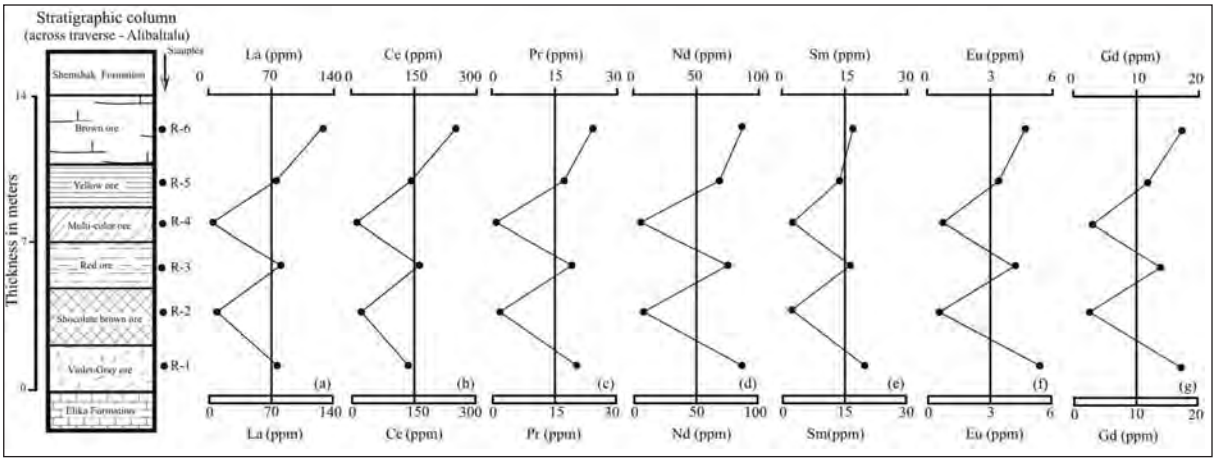

Figure 10- Variation of values of (a) La, (b) Ce, (c) Pr, (d) Nd, (e) Sm, (f) Eu, and (g) Gd across the studied profile.

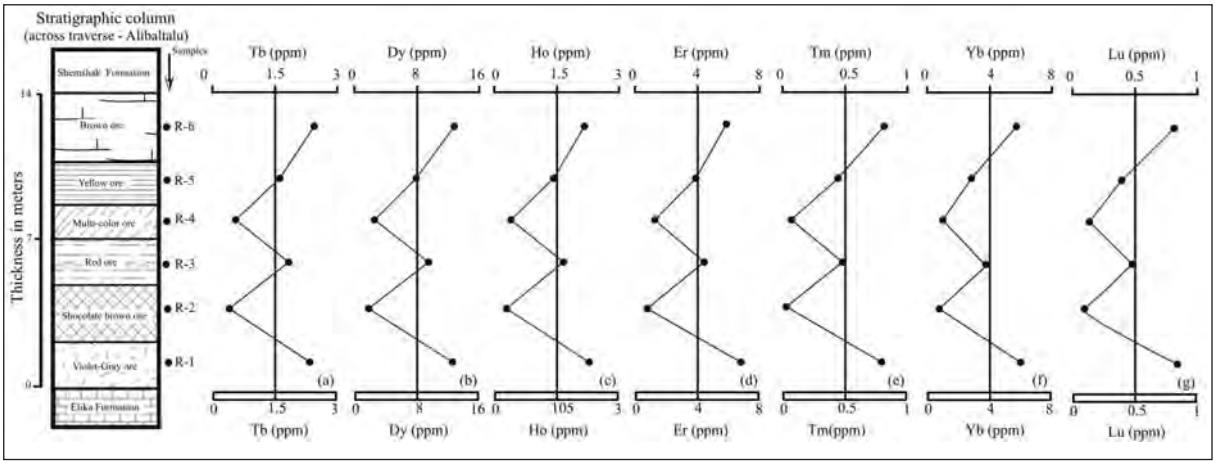

Figure 11- Variation of values of (a) Tb, (b) Dy, (c) Ho, (d) Er, (e) Tm, (f) Yb, and (g) Lu across the studied profile.

hematite and goethite did not have any noticeable role in concentrating of REEs. Although it has not been recognized a specific similarity between K distribution (Figure 6d) and those of REEs (Figures 10a-g, 11a-g), positive and medium correlation between K and HREEs (r = 0.52 to 0.66) manifests that muscovite-illite may be a potential host for HREEs in the profile. Zircon is reckoned to be chemically the most stable mineral in the course of weathering processes (Oh and Richter, 2005) and could also be a carrier and hence controlling agent for distribution of Ce and HREEs in the weathered system. The similar distribution trends of Zr (Figure 7a), Ce (Figure 10b), and HREEs (Figures 11a-g) could mark the presence of Ce and HREEs in crystal structure of residual zircon (Boulange et al., 1996; Ndjigui et al., 2008). The distribution trends of Ti (Figure 5c) and REEs (Figures 10a-g, 11a-g) to some extent are alike. This is proved by positive and medium to good correlation between Ti and REEs (r = 0.54 to 0.85) that may supply strong evidence for the fixation of at least a portion of REEs by rutile and anatase. Phosphorous (Figure 6f) and LREEs (Figure 10a-g) display similar distribution modes particularly in chocolate brown through multi-color units. This could indicate that the distribution of some of the LREEs might be controlled by phosphate minerals in this deposit (Kanazawa and Kamitani, 2006; Roy and Smykatz-Kloss, 2007). HREEs (Figures 11a-g) and Y (Figure 8d) show similar distribution trends. It seems that the Y distribution in the laterite system at Alibaltalu is somehow related to the distribution of HREE. Variation trends of Ce (Figure 10b) and Th (Figure 7f) are also almost alike that may indicate some of Ce and Th in the system were fixed by analogous mechanisms. Similar distribution trends of P (Figure 6b), Al (Figure 5b), and Ce (Figure 10b) in chocolate brown to brown ores along with positive

and medium correlation between Al and P (r = 0.58) and positive and good correlation between Al and Ce (r = 0.92) may provide enough evidence for the effective role of Al and P- bearing minerals in concentrating some of Ce in the profile.

5.4. Protolith of the Deposit

Several methods were used for determining the protolith of this deposit. Consideration of variation trends of Al_2O_3 (Figure 5b) and Fe_2O_3 (Figure 5d) in the residual profile manifested that intensive separation occurred between Al and Fe during weathering processes. This degree of fractionation commonly takes place between Al and Fe in laterites derived from weathering and alteration of mafic igneous rocks (Schellmann, 1994). Analytic values of Al_2O_3 and TiO_2 of the ores (with assumption that the weathered ores have ratios of Al_2O_3/ TiO_2 >21 for mafic and <21 for felsic igneous rocks) (Hayashi et al., 1997) were used for determination of potential protolith. These ratios at Alibaltalu range from 6.1 to 20, therefore, it may suggest a mafic origin for the ores. Variation patterns of REEs normalized to chondrite (Taylor and McLennan, 1985) show rather low fractionation of LREEs from HREEs and occurrence of weak Eu anomaly during weathering processes (Figure 12). These aspects could testify to a mafic origin (Nyakairu and Koeberl, 2001).

Using of distribution mode of immobile elements such as Ti, Nb, Zr, and Y in the studied profile is another geochemical method for determination of protolith. These elements have high potential for being preserved from chemical changes in weathered profiles derived from mafic igneous rocks (Hill et al., 2000; Kurtz et al., 2000). Variation trends of these elements (Figure 8a, b, d, and 5c) are very much the same. By taking the concentration values of these elements into account in the form of Nb/Y- Zr/TiO_2 bivariate plot (Winchester and Floyd, 1977), the protolith of this deposit must have had basaltic, andesitic, and/ or basaltic-andesitic composition (Figure 13). Illustration of Cr and Ni values in a Ni-Cr bivariate plot (Schroll and Sauer, 1968) is another geochemical method being used for determination of the potential protolith. This plot shows that this deposit might have had variable protoliths including basalt, granite, and sandstone (Figure 14). In addition, geochemical data in trivariate plot of Zr-Ga-Cr (Balasubramaniam et al., 1987) reveals that this deposit could have had a wide spectrum of protoliths including mafic and felsic igneous and metamorphic rocks (Figure 15). By referring to above mentioned matters and the allogenic origin of this deposit, it can be further inferred that this deposit was derived initially from alteration and weathering of basaltic to andesitic rocks and subsequently underwent erosion and transportation to its current site where by contamination by other crustal rocks occurred.

6. Conclusions

Alibaltalu residual deposit was developed as stratiform lenses along the contact of Elika dolomite (Triassic) and Shemshak sandstone (lower Jurassic).

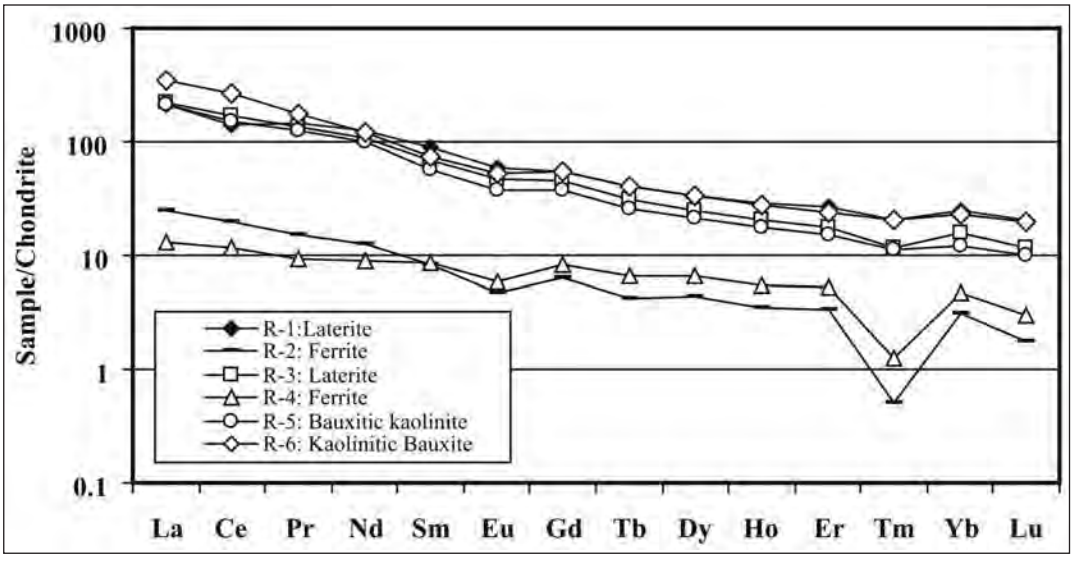

Figure 12- Variation pattern of REEs normalized to chondrite (Taylor and McLennan, 1985) in the studied samples.

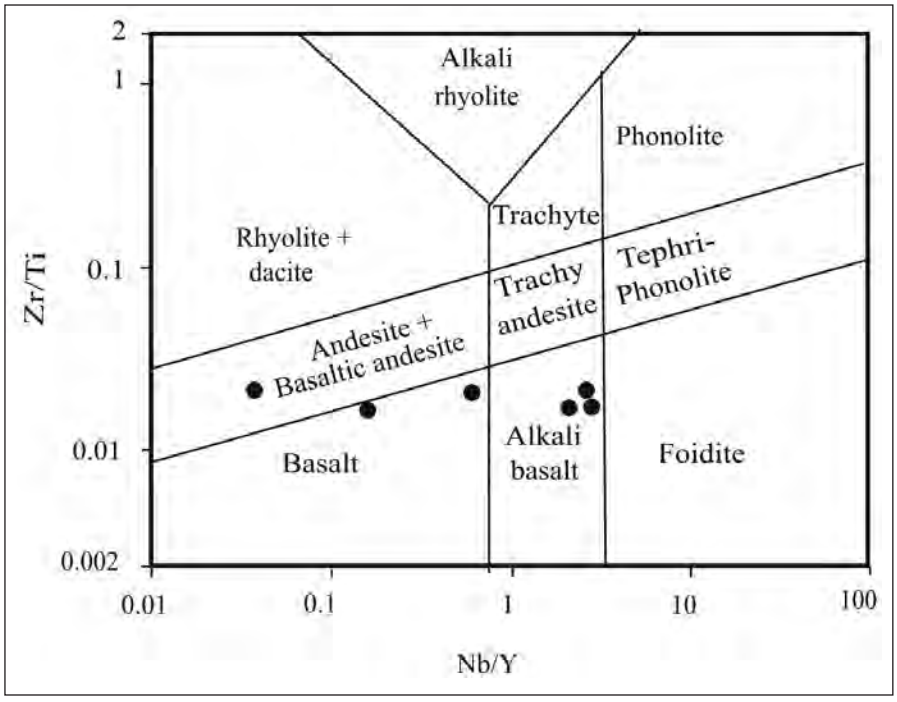

Figure 13- Position of lateritic ores of the studied profile on a bivariate plot of Zr/Ti-Nb/Y (Winchester and Floyd, 1977).

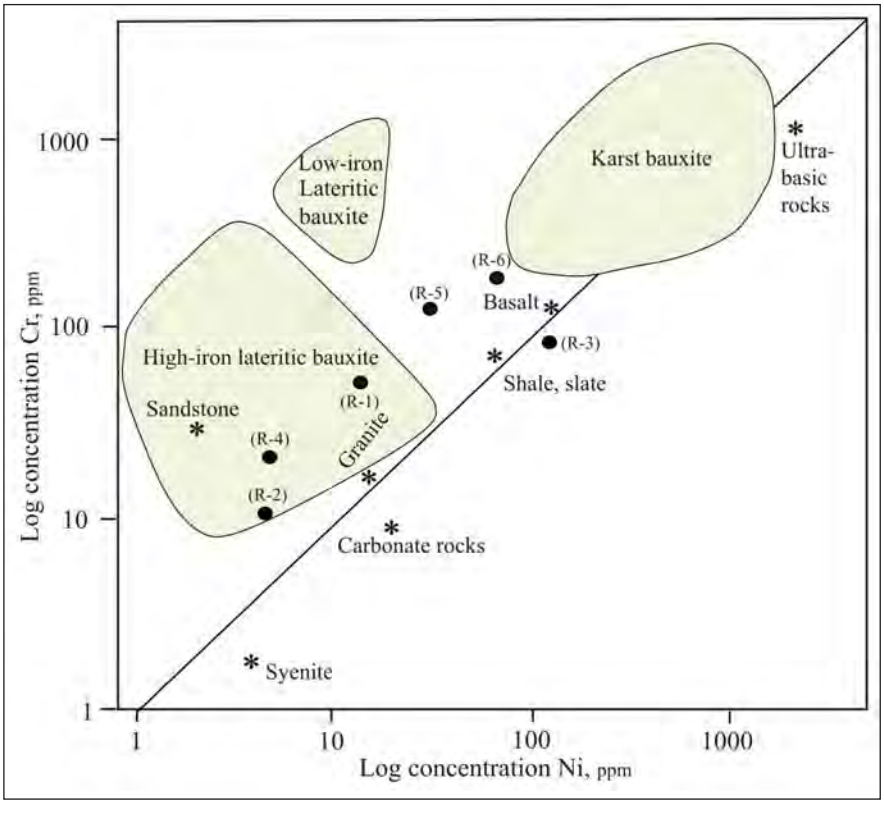

Figure 14- Position of the ores of the studied profile on a bivariate plot of Ni-Cr (Schroll and Sauer, 1968).

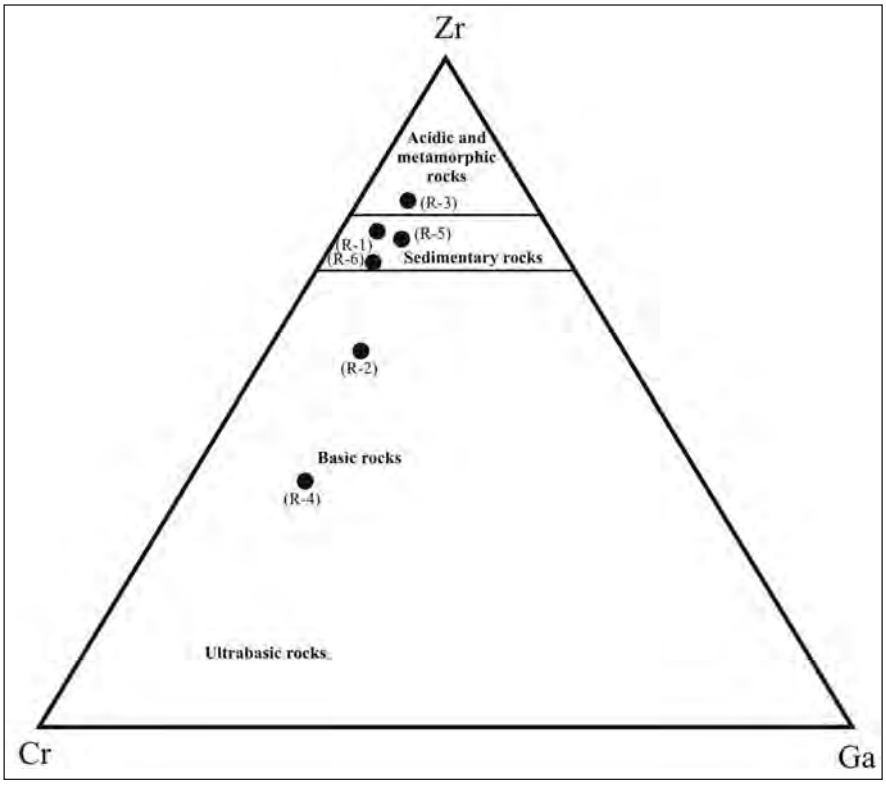

Figure 15- Position of the ores of the studied profile on a trivariate plot of Cr-Ga-Zr (Balasubramaniam et al., 1987).

It consists of four various types of ores including (1) laterite, (2) ferrite, (3) bauxitic kaolinite, and (4) kaolinitic bauxite. By regarding to the presence of conglomeratic and rounded-grain textures, this deposit has an allogenic origin. Rather strong differentiation of Al from Fe during weathering, rather low fractionation of LREEs from HREEs, and weak negative anomaly of Eu along with values of Nb, Zr, Y, Y, and Ti show that protolith of this deposit must have had a composition ranging from basalt to andesite. Consideration of Ni, Cr, Zr, and Ga values in the ores proves that this deposit has an allogenic origin derived from basaltic and andesitic rocks and was subsequently mixed with other terrestrial rock materials during transportation to its current place. Geochemical studies indicate that ferrugenization and deferrugenization mechanism is the important controlling agent for distribution of Al, Si, Ti, HFSE, LREEs, HREEs, U, and Th in this deposit. Variation patterns of elements show that HFSEs are concentrated by zircon, Ti-oxides, boehmite, diaspore, and kaolinite; TTEs by muscovite, kaolinite, boehmite, diaspore, Mn-oxides, and Fe-oxides and -hydroxides; LILEs by kaolinite, belovite, and Mn-oxides; REEs by muscovite-illite, rutile, and anatase.

Acknowledgments

This work was supported financially by the Research Bureau of Tabriz University. The authors would like to express their thanks and gratitude to the authorities of this bureau. Our gratitude is further expressed to Prof. Taner ÜNLÜ and two anonymous reviewers for reviewing of the manuscript and making critical comments and valuable suggestions.

Received: 22.07.2013
Accepted: 30.10.2013
Published: June 2014

References

Abedini, A., Calagari, A.A. 2013*a*. Rare earth elements geochemistry of Sheikh-Marut laterite deposit, NW Mahabd, West-Azarbaidjan province, Iran. *Acta Geologica Sinica-English Edition* 87, 176–185.

Abedini, A., Calagari, A.A. 2013*b*. Geochemical characteristics of Kanigorgeh ferruginous bauxite horizon, West-Azarbaidjan province, NW Iran. *Periodico di Mineralogia* 82, 1–23.

Aleva, G.J.J., 1994. Laterites: Concepts, Geology, Morphology and Chemistry. *ISIRC, Wageningen*, 169p.

Balasubramaniam, K.S., Surendra, M., Kumar, T.V. 1987. Genesis of certain bauxite profiles from India. *Chemical Geology* 60, 227–235.

Annelles, R.N., Arthurton, R.S., Bazely, R.A., Davies, R.G. 1975. E3-E4 Quadrangle, 1:100 000 scale geological Mmap and explanatory text of Qazvin and Rasht. *Geological Survey of Iran, Tehran*.

Bardossy, G. 1982. Karst Bauxites. *Elsevier Scientific, Amsterdam*, 441p.

Bardossy, G.Y., Aleva, G.Y.Y. 1990. Lateritic Bauxites. *Akademia, Kiado Budapest*, 646p.

Berberian, M., King, G.C.P. 1981. Towards a paleogeography and tectonic evolution of Iran. *Canadian Journal of Earth Sciences* 18, 210–265.

Boulange, B. 1984. Les formation bauxitigues lateriques de Cote d Ivoire. *Travaux et Doduments ORSTOM, Paris* 175, 341p.

Boulange, B., Colin, F. 1994. Rare earth element mobility during conversion of nepheline syenite into lateritic bauxite at Passa Quatro, Minais Gerais, Brazil. *Applied Geochemistry* 9, 701–711.

Boulange, B., Bouzat, G., Pouliquen, M. 1996. Mineralogical and geochemical characteristics of two bauxitic profiles, Fria, Guinea republic. *Mineralium Deposita* 31, 432–438.

Braun, J.J., Pagel, M., Herbillon, A., Rosin, C. 1993. Mobilization and redistribution of REEs and Th in a syenitic lateritic profile: A mass balance study. *Geochimica et Cosmochimica Acta* 57, 4419–4434.

Calagari, A.A., Abedini, A. 2007. Geochemical investigations on Permo-Triassic bauxite deposit at Kanisheeteh, east of Bukan, Iran. *Journal of Geochemical Exploration* 94, 1–18.

Esmaeily, D., Rahimpour-Binab, H., Esna-Ashari, A., Kananian, A. 2010. Petrography and geochemistry of the Jajarm karst bauxite ore deposit, NE iran: Implications for source rock material and ore genesis. *Turkish Journal of Earth Science* 19 (2), 267–284.

Fernandez-Caliani, J.C., Cantano, M. 2010. Intensive kaolinization during a lateritic weathering event in southwest Spain: Mineralogical and geochemical inferences from a relict paleosol. *Catena* 80, 23–33.

Hao, X., Leung, K., Wang, R., Sun, W., Li, Y. 2010. The geomicrobiology of bauxite deposits. *Geoscience Frontiers* 1, 81–89.

Hayashi, K., Fujisawa, H., Holland, H.D., Ohmoto, H. 1997. Geochemistry of sedimentary rocks from northeastern Labrador, Canada. *Geochimica et Cosmochimica Acta* 61, 4115–1437.

Henderson, P. 1984. Rare Earth Element Geochemistry. *Elsevier, Amsterdam*, 510p.

Hill, I.G., Worden, R.H.G., Meighan, I.G. 2000. Geochemical evolution of a paleolaterite: the interbasaltic formation, northern Ireland. *Chemical Geology* 166, 65?84.

Kanazawa, Y., Kamitani, M. 2006. Rare earth minerals in the world. *Journal of Alloy Compounds* 408?412, 1339?1343.

Karadağ, M., Küpeli, S., Arık, F., Ayhan, A., Zedef, V., Doyen, A. 2009. Rare earth element (REE) geochemistry and genetic implications of the Mortas bauxite deposit (Seydisehir/Konya-southern Turkey). *Chemie der Erde- Geochemistry* 69, 143–159.

Kurtz, A.C., Derry, L.A., Chadwick, O.A. 2000. Refractory element mobility in volcanic soils. *Geology* 28, 683–686.

Laskou, M., Economou-Eliopoulos, M. 2007. The role of micro-organisms on the mineralogical and geochemical characteristics of the Parnassos-Ghiona bauxite deposits, Greece. *Journal of Geochemical Exploration* 93, 67–77.

Ma, J., Wei, G., Xu, Y., Long, W., Sun, W. 2007. Mobilization and re-distribution of major and trace elements during extreme weathering of basalt in Hainan Island, south China. *Geochimica et Cosmochimica Acta* 71, 3223–3237.

Mameli, P., Mongelli, G., Oggiano, G., Dinelli, E. 2007. Geological, geochemical and mineralogical features of some bauxite deposits from Nurra (western Sardinia, Italy): insights on conditions of formation and parental affinity. *International Journal of Earth Sciences* 96, 887–902.

Marques, J.J., Schulze, D.G., Curi, N., Mertzman, S.A. 2004. Trace element geochemistry in Brazilian Cerrado soils. *Geoderma* 121, 31–43.

Meshram, R.R., Randive, KR. 2011. Geochemical study of laterites of the Jamnagar district, Gujarat, India: implications on parent rock, mineralogy and tectonics. *Journal of Asian Earth Sciences* 42, 1271–1287.

Mutakyahwa, M.K.D., Ikingura, J.R., Mruma, A.H. 2003. Geology and geochemistry of bauxite deposits in Lushoto District, Usambara Mountains, Tanzania. *Journal of African Earth Sciences* 36, 357–369.

Ndjigui, P., Bilong, P., Bitom, D., Dia, A. 2008. Mobilization and redistribution of major and trace elements in two weathering profiles developed on serpentinites in the Lomie ultramafic complex, southeast Cameroon. *Journal of African Earth Sciences* 50, 305–328.

Newman, A.D.C. 1987. Chemistry of Clay and Clay Minerals. *Mineralogical Society, Monograph* 6, 480 p.

Nyakairu, G.W.A., Koeberl, C. 2001. Mineralogical and chemical composition and distribution of rare earth elements in clay rich sediments from Central Uganda. *Geochemical Journal* 35, 13–28.

Oh, N.H., Richter, D.D. 2005. Elemental translocation and loss from three highly weathered soil- bedrock profiles in the southeastern United States. *Geoderma* 126, 5–25.

Plank, T., Langmuir, C.H. 1998. The chemical composition of subducting sediment and its consequences for

the crust and mantle. *Chemical Geology* 145, 325–394.

Retallack, G.J. 2010. Lateritization and bauxitization events. *Economic Geology* 105, 655–667.

Rollinson, H. 1993. Using Geochemical Data: Evaluation, Presentation, Interpretation. *Longman Scientific and Technical,* 352p.

Roy, P.D., Smykatz-Kloss, W. 2007. REE geochemistry of the recent playa sediments from the Thar Desert, India: an implication to playa sediment provenance. *Chemie der Erde- Geochemistry* 67, 55–68.

Sanematsu, K., Moriyama, T., Sotouky, L., Watanabe, Y. 2011. Mobility of REEs in basalt derived laterite at the Bolaven plateau, Southern Laos. *Resource Geology* 61, 140–158.

Schellmann, W. 1994. Geochemical differentiation in laterite and bauxite formation. *Catena* 21, 131–143.

Schroll, E., Sauer, D. 1968. Beitrag zur Geochemie von Titan, Chrom, Nikel, Cobalt, Vanadium und Molibdan in Bauxitischen gestermen und problem der stofflichen herkunft des Aluminiums. *Travaux de ICSOBA* 5, 83–96.

Stöcklin, J. 1968. Structural history and tectonics of Iran, a review. *American Association of Petroleum Geologists Bulletin* 52 (7), 1229–1258.

Taylor, S.R., McLennan, S.M. 1985. The Continental Crust: Its Composition and Evolution. *Blackwell, Oxford,* 312p.

Temur, S., Kansun, G. 2006. Geology and petrography of the Masatdagi diasporic bauxites, Alanya, Antalya, Turkey. *Journal of Asian Earth Sciences* 27, 512–522.

Valeton, I. 1972. Bauxites. *Elsevier*, 226 p.

Vollmer, T. 1987. Zur Geologie des nordlichen Zentral-Elburz zwischen Chalus- und Haraz-Tal, Iran. *Mitteilungen des Geologisch Paläontologischen Instituts der Universitat of Hamburg* 63, 1–125.

Walter, A.V., Nahon, D., Flicoteaux, R., Girard, J.P., Melfi, A. 1995. Behaviour of major and trace elements and fractionation of REE under tropical weathering of typical weathering of typical apatite-rich carbonatite from Brazil. *Earth and Planetary Science Letters* 303, 591–601.

Winchester, J.A., Floyd, P.A. 1977. Geochemical discrimination of diferent magma series and their diferentiation products using immobile elements. *Chemical Geology* 20, 325–343.

Yang, R.D., Wang, W., Zhang, X., Liu, L., Wei, H., Bao, M., Wang, J. 2008. A new type of rare earth elements deposit in weathering crust of Permian basalt in western Guizhou, NW China. *Journal of Rare Earths* 26 (5), 753–758.

Bulletin of MTA (2014) 148: 85-106

Bulletin of the
Mineral Research and Exploration

http://bulletin.mta.gov.tr

TRACE/HEAVY METAL ACCUMULATION IN SOIL AND IN THE SHOOTS OF ACACIA TREE, GÜMÜŞHANE-TURKEY

Alaaddin VURAL[a]

[a] *Gümüşhane University, Faculty of Engineering and Natural Sciences, Dept. of Geological Engineering, Gümüşhane-Turkey*

Keywords:
Geochemistry, Biogeochemistry, Trace element, Heavy metal, Acacia, Gümüşhane.

ABSTRACT

In this study, heavy metal/trace element accumulation was investigated in soils along the road passing through Gümüshane city center and shoots of 1-2 years of acacia trees (Robinia pseudoacacia L.) grown in these soils. Heavy metal contents in soils and plants were analyzed by Enrichment Factor (EF), Geo-accumulation index (I_{geo}) parameters, and by Bio Accumulation Factor (BAF), respectively. According to geo-accumulation index (I_{geo}) data, it is seen that the soil was unpolluted in terms of Cr, Co, Cu, Rb, Sr; unpolluted to moderately polluted in terms of V, Ni and Zn; moderate to excessively polluted in terms of As, and moderate to excessively polluted in terms of Pb. According to EF parameters, on the other hand, it is observed that the soil was non to slightly enriched in terms of Cr, Co, Sr and Ba; non to moderately enriched in terms of Ni and Cu; slightly to significantly enriched in terms of Zn; significant to very highly enriched in terms of As and slightly to over excessively enriched in terms of Pb. Although trace/heavy metal contents of acacia shoots were usually within normal values for acacia, it was determined that Cu, Fe, Mo, Ni, Sr and Zn concentrations were within and/or above upper limits of normal values in certain sampling points.

1. Introduction

Investigations related to trace element/heavy metal within the perspective of environmental geochemistry have been increasingly continuing everyday (Wheeler and Rolfe, 1979; Kovacs et al., 1981; Kabata-Pendias and Pendias, 1994; Kabata-Pendias, 2000; Kocaer and Baskaya, 2003; Bosco et al., 2005; Önder and Dursun, 2005; Birch and Scollen, 2003; Murakami et al., 2009; Yaylalı-Abanoz and Tüysüz, 2009; Yaylalı-Abanoz et al., 2011; Ahdy and Khaled 2009; Rodriguez-Barroso et al., 2009; Machender et al., 2011; Miao et al., 2011;Vural and Şahin 2012*a*, *b*). Therefore, the roles of many sciences, especially the geochemistry, have been increasing on the environmental awareness, the quality of environment and on the environmental health.

In this study, it was aimed at detailing the findings related to heavy metal accumulation which was obtained by Vural and Şahin (2012*a* and *b*) along the auto road passing through Gümüşhane city center. Studies related to investigating the dimensions of pollution in the field and factors effective in the formation of it have still been performed by the investigator within scope of environmental geochemistry. Because of geological characteristics of the region, the negative effects which the urbanization had brought up were investigated in multi dimensions, and geological, hydrogeological and biochemical studies both in soil and on plants still continue. However, in this study, the geochemical and biogeochemical characteristics of heavy metals/trace elements of the soil along the auto road and acacia shoots grown up in this soil were taken into consideration.

* *Corresponding author : vural@gumushane.edu.tr*

For this purpose, total of 45 samples were collected from the soil and from the shoots of acacia in the field. Analyses of soil samples and acacia shoots in the field were performed in the Department of Research and Development of the General Directorate of ETİ Maden and in the laboratory of Trabzon Provincial Food Control Directorate using ICP-AES, respectively. Within the study, the change of trace element contents in soil with respect to reference values, the source of this change and biological transmission rates from trace element into acacia shoots in the soil were investigated.

2. Material and Method

2.1. Study Area

The study area is located within Gümüşhane provincial borders towards the eastern part of the Pontide tectonic unit and covers a 20 km^2 area with 2x10 km (Figure 1).

Rocks cropping out in the study area which extend along the state road passing through city center are divided into two groups as Late Paleozoic basement rocks and Mesozoic-Cenozoic cover rocks. Basement rocks in the region are represented by Early-Middle Carboniferous Pulur-Kurtoğlu metamorphic rocks (Topuz et al., 2007) and unmetamorphosed Middle-Late Carboniferous Gümüşhane granitoid (Yılmaz 1972, 1974; Topuz et al., 2010; Dokuz, 2011). Gümüşhane granitoidas well which crops out in the study area is mainly composed of microdiorite with quartz, granite and dacitic porphyries (Yılmaz, 1972; Çoğulu, 1975; Topuz et al., 2010). This rock assemblage was named as Köse Composite Plutonic in and around Köse, outside the study area by Dokuz

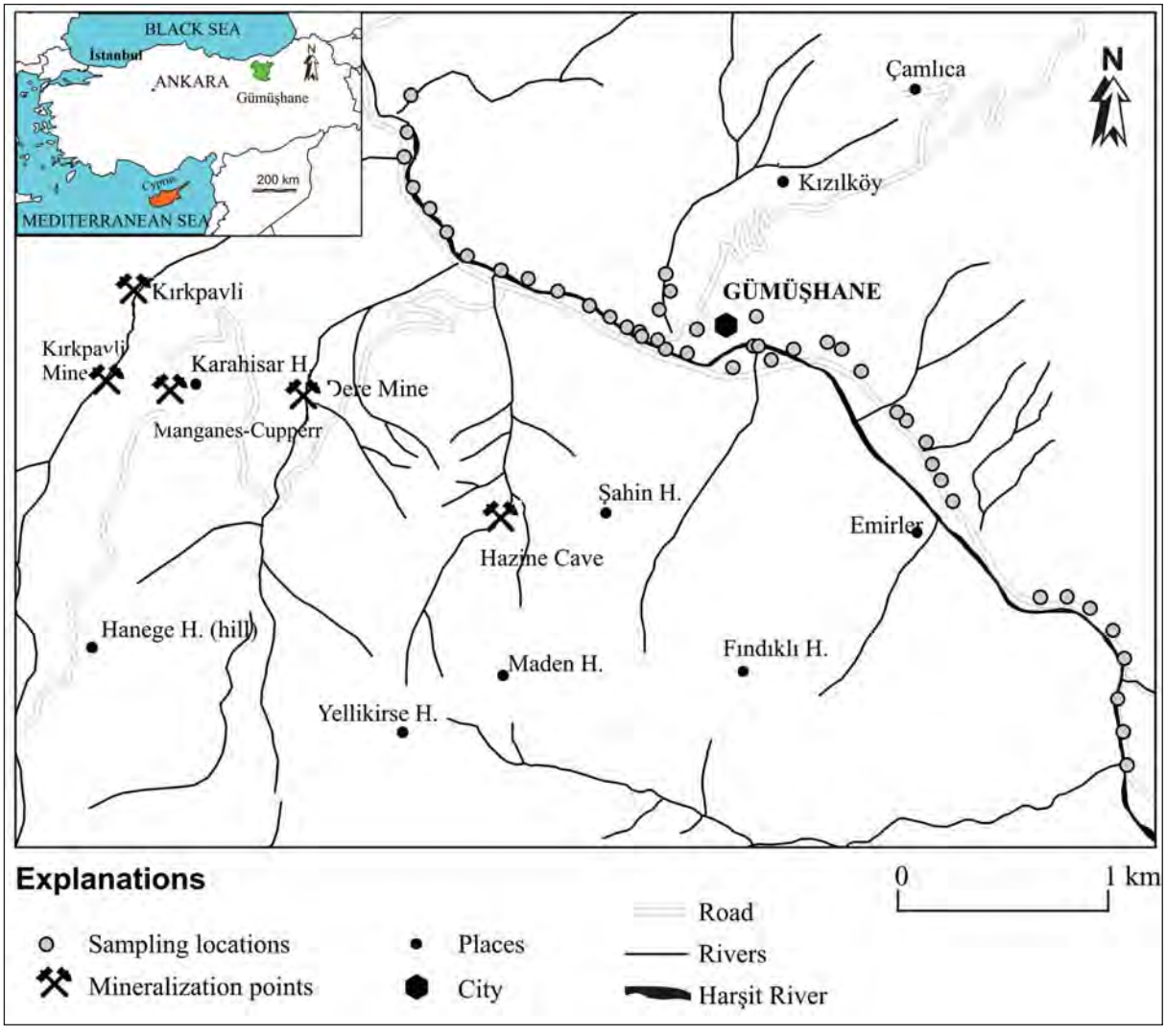

Figure 1- Location map of the study area

(2011). The lowermost section of the Mesozoic deposit is represented by unconformably overlying Early Jurassic volcano sedimentary unit over Variscan basement. This unit, which was named as Şenköy formation, is interpreted as rift facies related with the opening of Neotethys Ocean (Kandemir, 2004). The formation begins with basal conglomerate and continues upward with basalt, diabase, chert and dacitic tuff bearing turbiditic calcerous pebble stone, sandstone, siltstone and marls (Adamia et al., 1977; Kandemir, 2004; Eyüboğlu et al., 2006). Şenköy formation is overlain by Late Jurassic–Early Cretaceous Berdiga formation of which its bottom is formed by platform carbonate in massive character in general (Pelin, 1977). Carbonates are overlain by Late Cretaceous Kermutdere formation. This formation begins with yellow, sandy limestones at the bottom and continues with red colored clastic carbonates and gray colored turbidites (Tokel, 1972). All these units are cut by late Cretaceous intrusions especially on the road between Gümüşhane–Trabzon and outside the study area (Kaygusuz et al., 2008, 2010).

All Pontides have uplifted above the water level starting from Paleocene to Middle Eocene. This situation is represented by a widespread unconformity which is dedicated to the collision of Pontides with Anatolide-Tauride block and the closure of northern branch of Neotethys. Late Cretaceous volcanic and/or sedimentary rocks in Gümüşhane region are unconformably overlain by Middle-Late Eocene marine volcanosediments (Aslan and Aliyazıcıoğlu, 2001; Kaygusuz et al., 2010). These rocks, which are also named as Alibaba formation (Tokel, 1972) or as Kabaköy formation (Güven, 1993) begin with conglomerates, nummulitic limestones interbedded with sandstone and tuff, and continue with andesite and related pyroclastics towards upper layers. The unit ends with alternation of occasionally eroded limestone, sandstone, marl and tuff (Aliyazıcıoğlu, 1999). These units are again cut by synchronous intrusive rocks (Karslı et al., 2010; Eyüboğlu et al., 2011). These rocks, which crop out in the close vicinity of the study area, in and around Gözeler, were named as Gözeler granite. Quaternary travertine, debris flows and alluvials are the youngest units in the region.

Gümüşhane granitoid in the study area spreads out along Harşit Stream and continues until city exit from Bağlarbaşı locality to Trabzon.It also overlies Alibaba formation with a tectonic contact on the exit of Gümüşhane. The general stratigraphic succession of the region is typically observed within the study area (Figure 2).

At the same time, Gümüşhane and its vicinity is one of the most significant mine provinces bearing many lead, zinc, copper and gold mineralizations. The tectonism which is closely related with mineralization is affective in the region. Sulfide mineralization which developed due to young granitic intrusives were emplaced along these tectonic lines and formed Cu, Pb, Zn, Au and Ag mineralization (Güner et al., 1985; Kahraman et al., 1985; Güner and Yazıcı, 2005; Aslan and Akçay 2011; Akçay et al., 2011).

The origin of soil formation in the study area is mainly the Gümüşhane granitoid with lesser amount of Eocene volcanic rocks.

2.2. Sampling Method and Analyses

In order to carry out geochemical and biogeochemical studies, 45 samples were collected from soil and 1-2 years old shoots of acacia tree which had grown over this soil along the road passing through Gümüşhane city center (Figure 1). Sampling was performed approximately 10 km along road. Samples were collected along road and its surroundings, since Gümüşhane had been located in a narrow valley and Iran-Turkey state road passing through the city center has an intense traffic. When analyzing heavy metal/trace element contents in the soil, the collected samples from which the soil was originated become important. The element contents of granitic and volcanic rocks in the region were statistically assessed and values obtained were used as the reference values. For soils which are considered to have originated from granitoid rocks, the trace element values of Topuz et al. (2010); for soils which are considered to have originated from volcanic rocks the trace element values of Aslan (2010); and for chromium and arsenic elements, the trace element values of Turekian and Wedepohl (1961); and Taylor and McLennan (1995) were used.

Soil samples were collected at a depth of 25 centimeters and directly put into nylon bags from zones (a) and (b) of the soil then were again put into another nylon bag to prevent it from other factors. Maximum care was taken during collection and preservation of samples in order to avoid them from contamination. Soil samples were dried up in oven 2

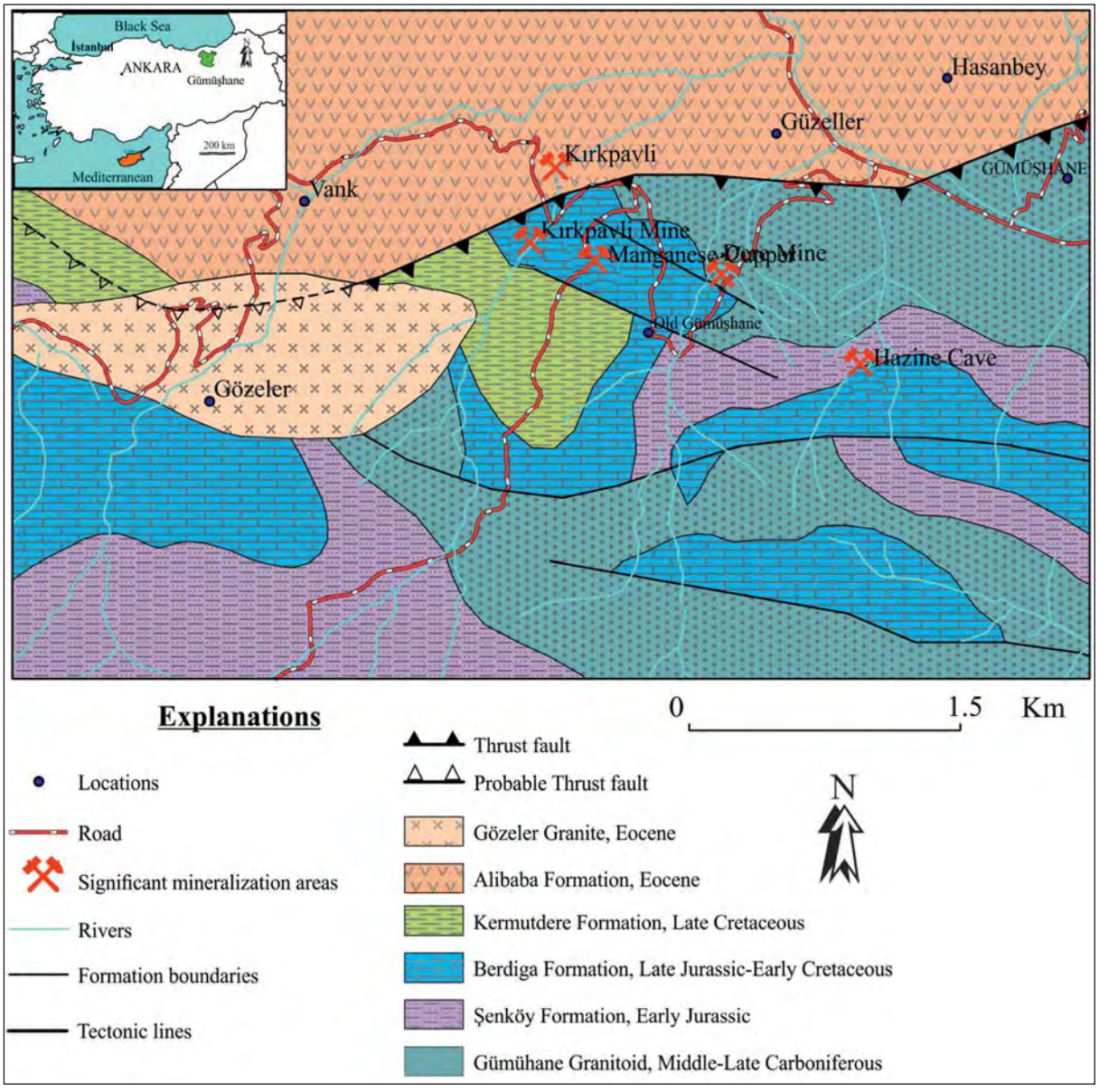

Figure 2-Geological map of the study area and its vicinity (modified from Güven, 1993)

days at a temperature of 60 °C and pulverized down to 250 mesh size by grinder. Pulverized samples were then weighted on platinum crucible between 0.5-1 in the laboratory of Department of Research and Development of the General Directorate of Eti Maden Management (Ankara) and 2-3 spatulas of (6 units Na_2CO_3+1 unit $Na_2B_4O_7$) mixture were added. Platinum cover was then closed and kept one hour under the temperature of 1000 °C. It was then dissolved in a 400 ml cup with 50 ml hydrochloric acid (HCl) and 100 ml boiling water. Filtering was made from black banded filter paper into 250 ml balloon, and concentrations of elements were estimated in ICP-AES instrument. Results of analyses of soil samples were given in table 1.

Plant samples each weighing 200 gr were taken from 1-2 years old shoots of acacia trees in localities from where soil samples had been collected, then washed in distilled-deionized water and dried up in oven 24 hours under 80 °C temperature. Dried samples were then grinded and powdered. Samples each weighing 1 gram were disintegrated in microwave oven 4 hours at a temperature of 500 °C. Samples were weighted in teflon cups of the microwave oven ranging between 0.8-1.0 gr and at a

0.1 mg sensitivity. Later on, 6 ml concentrated HNO_3 and 1.5 ml H_2O_2 (peroxide) were added on to cups and placed into microwave oven after cups had been closed. Hence, samples were disintegrated by means of microwave beam, pressure and acid, and then rendered into a crystalline solution. Teflon cup contents were taken into measured balloon and were equalized to 25 ml by pure water. Metal contents of solutions obtained were determined by being analyzed in ICP-AES instruments of Trabzon Provincial Food Control Laboratories. Results were given in table 2.

The procedure suggested by Duran et al. (2007) was applied in ICP-AES measurements. Within this framework, standard solutions were prepared by diluting 1000 mg/l solutions from each metal (Merck, Darmstadt/Germany). These standard solutions were read on the instrument, and drawing concentrations (mg/l) against emission intensity graphs their standard calibration graphics were obtained. Using these graphics, the metal contents of samples were determined. The accuracy tests of results were checked by two methods; adding/regaining tests and standard reference material analyses. CRM 1568a Rice Flour was used as the standard reference material.

Values obtained by the method used in this study (microwave disintegration / ICP-AES) and certified contents of reference material in terms of some metals were identified and these values were given in table 3. As it is seen from table 3, there is not much difference between certified and obtained values.

Table 1- Results of chemical analyses of soil samples (concentration values in mg/kg)

Sample Nr.	Al	Fe	Zr	Sr	Rb	Ba	Cd	Co	Cr	Cu	Mn	Ni	Pb	Zn	Y	As	Sn
GÇ-1	76899.39	28116.59	51.49	144.16	99.67	556	BDL	BDL	105	34	797	36	20	72	17	9	BDL
GÇ-2	101668.08	32452.98	77.65	72.08	164.59	900	BDL	BDL	97	35	710	BDL	49		19	13	BDL
GÇ-3	106537.14	35040.82	44.95	72.08	170.08	1110	BDL	BDL	113	34	850	30	22		27	20	BDL
GÇ-4	73406.37	36439.66	73.97	216.24	97.84	712	BDL	BDL	98	55	859	44	64	252	14	2	BDL
GÇ-5	86849.21	36579.54	55.58	216.24	100.58	723	BDL	BDL	68	51	649		58	106	15	5	BDL
GÇ-6	79069.30	35670.30	56.80	216.24	92.36	847	BDL	19	116	56	914	28	74	175	19	11	71
GÇ-7	84520.52	39656.98	67.43	216.24	98.76	586	BDL	BDL	51	55	972	50	63	156	20	15	BDL
GÇ-8	76581.84	30354.72	55.99	144.16	85.95	369	BDL	BDL	71	53	1759	34	240	406	12	12	BDL
GÇ-9	93094.30	36509.60	80.92	144.16	130.76	949	BDL	BDL	104	54	865	56	56	74	20	5	33
GÇ-10	69595.80	39377.21	44.95	216.24	54.86	545	BDL	BDL	84	76	931	53	55	158		13	BDL
GÇ-11	94999.59	36789.37	65.39	72.08	158.19	847	10	BDL	106	41	975	32		81	16	14	55
GÇ-12	86108.26	44552.90	78.06	144.16	85.04	536	BDL	BDL	105	79	1318	45	441	153	20	6	BDL
GÇ-13	99021.85	30424.67	53.94	72.08	193.85	487	BDL	BDL	104	48	988	22	19	127	10		118
GÇ-14	73618.07	44203.19	43.32	216.24	40.23	401	BDL	BDL	65	84	1065	43	73	177	17	20	BDL
GÇ-15	73088.82	36299.77	44.95	216.24	61.27	644	BDL	33	172	76	1097	39	146	191	14	9	BDL
GÇ-16	80392.41	36089.95	71.11	216.24	114.30	645	2	BDL	114	58	989	56	133	199	20	9	47
GÇ-17	84308.83	33152.40	67.43	72.08	127.10	665	BDL	BDL	109	34	886	28	26	85	19	BDL	BDL
GÇ-18	84732.22	41125.76	55.99	216.24	80.47	534	BDL	BDL	111	70	899	46	56	BDL	20	2	39
GÇ-19	84414.68	39237.33	65.80	288.33	96.93	802	BDL	BDL	95	51	877	42	36	BDL	19	11	BDL
GÇ-20	87748.92	38537.91	59.26	216.24	100.58	882	14	BDL	106	62	873	47	27	122	19	13	8
GÇ-21	97116.57	38467.97	73.97	144.16	117.96	805	4	BDL	73	66	868	47	71	131	21	18	BDL
GÇ-22	89389.58	46651.16	68.66	288.33	82.30	521	BDL	BDL	48	86	1072	40	52	134	13	BDL	BDL
GÇ-23	102091.48	49588.71	78.46	216.24	108.81	557	BDL	BDL	85	87	1214	56	43	BDL	25	30	BDL
GÇ-24	90659.77	41755.23	71.52	216.24	79.55	536	BDL	BDL	78	77	1012	46	60	146	22	10	BDL
GÇ-25	83726.66	53365.56	95.63	360.41	19.20	328	BDL	BDL	241	71	1023	195	BDL	BDL	19	9	BDL
GÇ-26	93835.25	41615.35	70.70	144.16	83.21	529	BDL	BDL	BDL	60	1039	52	39	127	23	19	BDL
GÇ-27	87166.75	33781.87	109.11	144.16	177.40	1074	BDL	BDL	114	29	734	14	BDL	BDL	27		BDL
GÇ-28	97010.72	37698.61	71.11	216.24	103.33	944	6	BDL	66	44	817	30	67	114	BDL	10	BDL
GÇ-29	64832.59	33152.40	49.86	216.24	73.15	515	12	BDL	193	59	750	42	85	BDL	15	BDL	84
GÇ-30	98757.23	34621.17	68.25	72.08	180.14	920	BDL	BDL	120	33	1035	35	BDL	BDL	BDL	18	130
GÇ-31	83938.35	42314.77	73.15	288.33	101.50	781	10	BDL	115	65	1055	36	50	174	17	8	52
GÇ-32	88701.57	35810.18	57.62	144.16	142.65	865	BDL	BDL	109	43	880	38	33	95	12	1	17
GÇ-33	92882.61	35600.36	83.37	144.16	142.65	844	6	BDL	131	51	860	40	38	104	20	42	BDL
GÇ-34	77428.63	35670.30	53.54	216.24	80.47	715	BDL	3	96	36	826	31	29	110	13	11	BDL
GÇ-35	76052.60	36299.77	50.27	216.24	67.67	580	BDL	BDL	89	67	864	32	89	182	BDL	24	BDL
GÇ-36	84996.85	39307.27	141.40	288.33	78.64	782	BDL	BDL	86	67	692	40	49	195	BDL	14	BDL
GÇ-37	106166.67	39447.15	87.05	72.08	149.96	770	BDL	BDL	77	38	1009	50	45	126	24	18	BDL
GÇ-38	108283.65	35110.76	86.23	72.08	171.91	918	BDL	BDL	75	30	832	31	3	86	24	21	BDL
GÇ-39	99709.87	34970.88	77.65	144.16	144.48	524	0.1	BDL	65	38	790	32	12	89	17	12	BDL
GÇ-40	85843.64	30264.55	68.25	144.16	117.04	808	BDL	BDL	134	37	32	37	BDL	BDL	9	56	BDL
GÇ-41	97804.59	46091.62	59.26	288.33	67.67	661	BDL	BDL	56	92	749	41	64	105	15	17	BDL
GÇ-42	98175.06	33362.22	78.87	72.08	167.34	957	BDL	BDL	85	15	811	25	16	132	19	21	75
GÇ-43	98333.84	32662.80	86.64	72.08	160.02	741	BDL	BDL	96	41	719		28	122	10	5	61
GÇ-44	85684.87	37838.49	69.47	216.24	92.36	737	15	BDL	80	48	784	36	51	138	18	10	BDL
GÇ-45	67531.74	36859.31	64.98	288.33	85.04	621	BDL	BDL	81	65	967	74	106	325	13	16	74

BDL: Below Detection Limit

Table 2- Element contents of shoots of acacia (concentration values in mg/kg)

Sample Nr.	Al	As	Ba	Cd	Co	Cr	Cu	Fe	Mn	Mo	Ni	Sn	Sr	Zn
GÇA-1	99.9	2.08	14.7	BDL	0.90	2.05	10.5	693.3	8.6	42.1	1.49		61.2	12.5
GÇA-2	90.2	BDL	8.5	BDL	0.88	1.14	2.8	88.7	8.1	42.1	BDL	BDL	39.5	10.3
GÇA-3	62.0	BDL	9.5	BDL	0.73	0.86	5.3	63.8	8.1	23.8	BDL	BDL	49.6	16.7
GÇA-4	74.8	BDL	11.4	BDL	0.89	0.91	4.8	79.1	6.5	44.1	BDL	BDL	40.4	31.7
GÇA-5	48.5	BDL	4.9	BDL	0.79	0.62	2.8	47.2	5.9	49.5	BDL	BDL	26.2	8.6
GÇA-6	146.7	BDL	7.1	BDL	0.83	2.15	4.3	139.5	6.8	56.4	BDL	BDL	60.3	12.5
GÇA-7	54.1	BDL	4.6	BDL	0.83	1.08	5.4	74.3	7.0	48.1	BDL	BDL	40.9	13.6
GÇA-8	30.4	BDL	7.4	BDL	0.94	0.96	3.3	53.0	5.7	42.1	BDL	BDL	37.7	28.3
GÇA-9	33.4	BDL	5.4	BDL	0.48	0.98	2.9	47.4	7.3	10.2	BDL	BDL	31.2	16.7
GÇA-10	32.8	BDL	4.2	BDL	0.73	0.74	2.8	38.6	4.1	7.3	BDL	BDL	19.6	11.9
GÇA-11	27.8	BDL	14.0	BDL	0.81	0.77	2.9	53.3	12.5	25.2	BDL	BDL	50.8	14.2
GÇA-12	38.9	BDL	8.8	BDL	0,58	1.07	3.0	55.0	5.5	14.8	BDL	BDL	50.2	11.8
GÇA-13	44.3	BDL	18.5	BDL	0.93	0.92	3.6	60.8	14.0	32.5	1.74	BDL	73.0	13.3
GÇA-14	43.2	BDL	7.4	BDL	0.68	0.84	4.0	47.9	5.9	8.9	BDL	BDL	38.1	10.9
GÇA-15	88.2	BDL	7.2	BDL	0.51	1.23	7.6	94.8	8.8	19.9	1.09	BDL	35.2	21.3
GÇA-16	62.7	BDL	12.5	BDL	0.89	1.88	34.4	89.9	12.0	17.5	5.41	BDL	22.6	47.0
GÇA-17	88.2	BDL	5.7	BDL	0.83	0.86	6.3	90.2	7.3	19.2	BDL	BDL	34.2	10.0
GÇA-18	199.5	BDL	10.6	BDL	0.93	2.19	6.2	197.1	8.3	21.0	1.45	BDL	77.1	18.4
GÇA-19	69.0	BDL	4.9	BDL	0.56	1.04	4.3	63.0	3.7	32.7	BDL	BDL	34.9	10.0
GÇA-20	76.2	BDL	6.9	BDL	0.90	1.12	10.2	84.0	7.3	33.5	1.43	BDL	53.2	36.3
GÇA-21	38.0	BDL	6.0	BDL	0.80	0.33	5.4	40.3	5.3	30.2	BDL	BDL	33.5	10.0
GÇA-22	46.2	1.99	6.0	BDL	0.71	0.71	3.6	59.7	5.9	18.8	BDL	BDL	24.5	20.4
GÇA-23	36.0	BDL	4.1	BDL	0.83	0.66	5.0	46.0	5.3	11.3	BDL	BDL	27.4	20.6
GÇA-24	50.3	BDL	6.0	BDL	0.86	0.65	5.3	56.5	6.8	21.4	1.18	BDL	31.4	15.4
GÇA-25	35.6	BDL	5.3	BDL	0.63	0.63	4.8	36.8	5.4	13.1	BDL	BDL	35.5	17.3
GÇA-26	203.0	BDL	9.4	BDL	0.61	2.48	4.6	193.3	7.9	16.4	1.11	BDL	32.5	16.5
GÇA-27	61.7	BDL	4.1	BDL	0.77	1.01	8.8	61.0	8.2	25.7	BDL	BDL	36.0	14.9
GÇA-28	103.9	BDL	10.4	BDL	0.60	1.30	2.4	97.9	5.9	11.6	BDL	BDL	37.2	9.5
GÇA-29	24.3	BDL	10.6	BDL	0.74	0.54	3.8	25.5	4.2	8.5	BDL	BDL	32.7	7.5
GÇA-30	23.8	BDL	4.8	BDL	0.77	0.76	6.2	26.7	4.4	34.2	BDL	BDL	22.9	14.4
GÇA-31	65.9	BDL	11.4	BDL	0.86	9.05	6.8	104.0	9.0	11.2	5.86	9.9	43.5	16.3
GÇA-32	17.1	BDL	4.5	BDL	0.51	0.47	3.5	23.8	3.6	14.8	BDL	BDL	32.9	12.1
GÇA-33	24.4	BDL	8.8	BDL	0.66	0.60	3.2	29.6	4.3	31.1	1.69	BDL	28.3	16.6
GÇA-34	13.3	BDL	5.8	BDL	BDL	0.32	3.0	17.9	4.3	29.7	BDL	BDL	19.5	7.9
GÇA-35	19.5	BDL	6.8	BDL	BDL	0.47	2.3	27.8	6.1	21.4	BDL	BDL	30.4	7.5
GÇA-36	34.8	BDL	4.4	BDL	0.55	0.87	1.8	35.8	5.2	34.3	BDL	BDL	64.3	7.2
GÇA-37	23.1	BDL	3.1	BDL	0.59	0.50	2.7	35.4	5.7	46.4	BDL	BDL	32.7	12.9
GÇA-38	25.0	BDL	5.7	BDL	0.64	0.81	3.3	30.7	7.6	7.9	BDL	BDL	38.7	10.9
GÇA-39	17.9	BDL	5.9	BDL	0.78	0.72	4.3	28.0	6.2	20.8	BDL	BDL	30.2	18.4
GÇA-40	10.6	BDL	6.2	BDL	0.61	0.59	4.7	16.1	5.4	25.5	1.70	BDL	20.2	13.8
GÇA-41	10.1	BDL	13.3	BDL	BDL	0.39	4.4	19.4	6.7	34.8	BDL	BDL	33.0	14.3
GÇA-42	22.4	BDL	16.3	BDL	0.65	0.74	3.9	33.0	7.3	46.1	BDL	BDL	51.1	12.6
GÇA-43	23.2	BDL	14.8	BDL	0.92	1.95	4.4	38.5	10.9	38.2	2.62	BDL	76.2	13.0
GÇA-44	21.4	BDL	8.6	BDL	0.80	0.37	1.6	31.0	3.5	10.9	BDL	BDL	23.6	3.8
GÇA-45	14.6	1.82	8.4	BDL	0.46	11.73	5.1	96.6	6.6	42.3	9.85	11.7	38.5	12.3

BDL: Below Detection Limit

Table 3- Certified reference material analysis as an accuracy test for microwave/ICP-AES method (CRM 1568*a* Rice Flour)

	Al	As	Ba	Cd	Co	Cr	Cu	Fe	Mn	Mo	Ni	Pb	Se	Sn	Sr	Zn
Certificated Value (mg/kg)	4.4±1.0	0.29± 0.03	*	0.022± 0.002	0.01 8	*	2.4± 0.3	7.4± 0.9	20.0± 1.6	1.46± 0.08	*	(<0.0 10)	0.38± 0.04	~ 0.004 7	*	19.4± 0.5
Detected Value (mg/kg)	4.3±0.5	BDL	0.43± 0.02	BDL	BD L	BD L	2.2± 0.2	7.6± 0.4	18.8± 0.2	BDL	BD L	BDL	BDL	BDL	0.18± 0.01	17.5± 0.5
Error (%)	2.3	-	-	-	-	-	8.3	2.7	6.0	-	-	-		-	-	9.8

BDL: Below Detection Limit

3. Results and Discussion

3.1. Trace element contents in soil

Descriptive statistical parameters were estimated belonging to trace element/heavy metal contents in the soil beside the road passing through Gümüşhane city center (Table 4).

According to descriptive statistical parameters, the elements and related ranges are as follows; aluminum (Al) 108283.65-64832.59 mg/kg (ave: 87839.83 mg/kg), iron (Fe) 28116.59-53365.56 mg/kg (ave. 37627.11 mg/kg), zircon (Zr) 141.40-43.32 mg/kg (ave. 69.11 mg/kg), strontium (Sr) 360.41-72.08 mg/kg (ave. 179.40 mg/kg), rubidium (Rb) 193.85-19.2 mg/kg (ave. 109.95 mg/kg), barium (Ba) 1110-328 mg/kg (ave. 706.07 mg/kg), cadmium (Cd) 15-0,1 mg/kg (ave. 7,91 mg/kg), cobalt (Co), 33-3 mg/kg (ave.18,33), chromium (Cr) 241-48 mg/kg (ave.99.70), copper (Cu) 92-15 mg/kg (ave. 54,47 mg/kg), manganese (Mn) 1759-32 mg/kg (ave. 904.6 mg/kg), nickel (Ni) 195-14 mg/kg (ave. 43,60 mg/kg), lead (Pb) 441-3 mg/kg (ave. 67.2 mg/kg), zinc (Zn) 406-72 mg/kg (ave. 147.69), yttrium (Y) 27-9mg/kg (ave. 17.82 mg/kg), arsenic (As), 56-1 mg/kg (ave. 14.47 mg/kg) and tin (Sn) 130-8 mg/kg (ave. 61.71 mg/kg). The pH values of soils in the study area were estimated in laboratories of Department of Forest of the Vocational High School in Gümüşhane as ranging between 7.50–8.70 and it was detected that these were close to low alkaline character close to neutral (Table 4).

Besides, inter elemental *Pearson correlation coefficients* were estimated. Accordingly; elements and related correlation coefficients are as follows; Mn and Co (0.97), Ni and Cr (0.52), Zn and Mn (0.62), As and Sn (0.62), Pb and Co (0.99), Pb and Mn (0.63) moderate to high grade positive, As and Co (-0.85), Cu and Ba (-0.58) moderate to high negative (Table 5).

3.2. Heavy metal/trace element contents in shoots of Acacia Tree

Elements and related concentration values are as follows of shoots of ocacia; barium (Ba) 3.14-18.50 mg/kg (ave. 8.10 mg/kg), cobalt (Co), 0.46-0.94 mg/kg (ave. 0,74 mg/kg), chromium (Cr) 0.32-11.73 mg/kg (ave. 1.38 mg/kg), copper (Cu) 1.59-34.40 mg/kg (ave. 5.17 mg/kg), iron (Fe) 16.08-693.32 (ave. 74.93 mg/kg), manganese (Mn) 3.54-14 mg/kg (ave. 6.43 mg/kg), molybdenum (Mo), 7.34-56.45 mg/kg (ave. 23.05 mg/kg), nickel (Ni) 1.09-9.85 mg/kg (ave. 2.82 mg/kg), tin (Sn) 9.93-11.70 mg/kg (ave. 10.81 mg/kg), strontium (Sr), 19.55-77.15 mg/kg (ave. 38.94 mg/kg), zinc (Zn) 3.77-47 mg/kg

Table 4- Statistical data of elements in soil (concentration values in mg/kg)

	Al	Fe	Zr	Sr	Rb	Ba	Cd	Co	Cr	Cu	Mn	Ni	Pb	Zn	Y	As	Sn	pH
Mean	87839.48	37627.11	69.11	179.40	109.95	706.07	7.91	18.34	99.74	54.47	904.6	43.60	67.2	147.69	17.83	14.47	61.71	8.09
Min.	64832.59	28116.59	43.36	72.08	19.22	328	0.1	3	48	15	32	14	3	72	9	1	8	8.09
Max.	108283.65	53365.56	141.40	360.41	193.85	1110	15	33	241	92	1759	195	441	406	27	56	130	7.50
Cardinality	45	45	45	45	45	45	10	3	44	45	45	42	40	35	40	40	14	8.70
																		45

Table 5- Correlation coefficients of trace element concentrations in soil

	Al	*Fe*	*Zr*	*Sr*	*Rb*	*Ba*	*Cd*	*Cr*	*Cu*	*Mn*	*Ni*	*Pb*	*Zn*	*Y*	*As*	*Sn*
Al	1															
Fe	0.04	1														
Zr	0.34	0.17	1													
Sr	-0.55	0.66	0.01	1												
Rb	0.68	-0.56	0.22	-0.81	1											
Ba	0.45	-0.36	0.25	-0.40	0.64	1										
Cd	-0.45	0.24	-0.61	0.30	-0.52	0.24	1									
Cr	-0.27	0.02	0.02	0.11	-0.15	-0.07	0.35	1								
Cu	-0.34	0.74	-0.14	0.69	-0.74	-0.58	0.22	-0.03	1							
Mn	-0.10	0.31	-0.15	0.06	-0.20	-0.44	-0.09	-0.08	0.36	1						
Ni	-0.14	0.60	0.20	0.49	-0.49	-0.41	-0.11	0.52	0.34	0.14	1					
Pb	-0.31	0.17	-0.05	0.09	-0.35	-0.35	-0.17	0.11	0.37	0.63	0.19	1				
Zn	-0.58	-0.05	-0.07	0.36	-0.40	-0.41	-0.01	-0.04	0.30	0.62	0.30	0.47	1			
Y	0.41	0.28	0.39	-0.14	0.17	0.32	-0.37	-0.04	-0.05	0.14	0.05	-0.08	-0.30	1		
As	0.21	-0.09	0.06	-0.19	0.17	0.13	-0.14	0.03	-0.10	-0.35	-0.11	-0.19	-0.06	0.08	1	
Sn	0.13	-0.56	-0.09	-0.36	0.43	-0.25	-0.16	0.16	-0.36	0.24	-0.36	0.03	0.30	-0.43	0.62	1

(ave. 15.16 mg/kg), arsenic (As), 1.82-2.08 mg/kg (ave. 1.96 mg/kg), aluminum (Al) 10.15-203.01 mg/kg (ave. 52.82 mg/kg) (Table 6). As lead (Pb) values in shoots of acacia could not be detected, it remained below the detection limit.

Table 6- Descriptive statistical values of trace elements in shoots of acacia

	Ba_Acc.	Co_Acc.	Cr_Acc.	Cu_Acc.	Fe_Acc.	Mn_Acc.	Mo_Acc.	Ni_Acc.	Sn_Acc.	Sr_Acc.	Zn_Acc.	As_Acc.	Al_Acc.
Mean	8.10	0.74	1.38	5.17	74.93	6.77	26.62	2.82	10.81	38.94	15.16	1.96	52.82
Geometric Mean	7.39	0.72	0.94	4.34	53.92	6.43	23.05	2.13	10.78	36.59	13.70	1.96	40.49
Min.	3.14	0.46	0.32	1.59	16.08	3.54	7.34	1.09	9.93	19.55	3.77	1.82	10.15
Max.	18.50	0.94	11.73	34.40	693.32	14.00	56.45	9.85	11.70	77.15	47.00	2.08	203.01
Cardinality	45	42	45	45	45	45	45	13	2	45	45	3	45

Correlation coefficients of trace elements in shoots of acacia with each other and the alkalinity of them were calculated. Following results were obtained; Mn and Ba (0.65), Ni and Cr (0.89), Sr and Ba (0.56), Sr and Mn (0.54), Zn and Cu (0.72), As and Ba (0.56), As and Cu (0.62), As and Fe (0.73), As and Mn (0.58) and the alkalinity of the soil and As (0.64) moderate to strong positive correlation;Mnand Cu (0.42), As and Sr (0.47) weak positive correlation; As and Cr (-0.90) strong negative correlation. Besides; there is as negative correlation between the alkalinity of the soil and Ni (Table 7).

Table 7- Pearson correlation coefficients between trace element concentrations of acacia shoots and alkalinity of soil

	Ba_Acc.	Co_Acc.	Cr_Acc.	Cu_Acc.	Fe_Acc.	Mn_Acc.	Mo_Acc.	Ni_Acc.	Sn_Acc.	Sr_Acc.	Zn_Acc.	As_Acc.	Al_Acc.	pH
Ba_Acc.	1,00													
Co_Acc.	0,37	1,00												
Cr_Acc.	0,18	-0,10	1,00											
Cu_Acc.	0,20	0,28	0,13	1,00										
Fe_Acc.	0,32	0,24	0,20	0,24	1,00									
Mn_Acc.	0,65	0,42	0,20	0,42	0,25	1,00								
Mo_Acc.	0,14	0,25	0,07	-0,05	0,18	0,11	1,00							
Ni_Acc.	0,04	-0,26	0,89	0,25	-0,14	0,05	0,13	1,00						
Sn_Acc.	-1,00	-1,00	1,00	-1,00	-1,00	-1,00	1,00	1,00	1,00					
Sr_Acc.	0,54	0,31	0,16	-0,07	0,36	0,54	0,32	-0,18	-1,00	1,00				
Zn_Acc.	0,14	0,33	0,04	0,72	0,06	0,35	0,03	0,07	-1,00	-0,02	1,00			
As_Acc.	0,56	0,99	-0,90	0,62	0,73	0,58	-0,18	-1,00		0,47	0,20	1,00		
Al_Acc.	0,13	0,22	0,12	0,17	0,51	0,26	0,05	-0,36	-1,00	0,37	0,17	0,95	1,00	
pH	-0,01	-0,01	-0,32	-0,19	-0,05	-0,12	-0,23	-0,50	-1,00	0,08	-0,21	0,64	-0,05	1,00

3.3. Heavy metal/trace element accumulations in the soil (pollution)

In the assessment of trace element accumulations in soil, the reference values of the soil are compared with element concentrations estimated in soil. In order to calculate the trace element accumulations in Gümüşhane Region, the values of Gümüşhane granitoid and Eocene volcanic rocks which are the source of soil were used. Therefore, the reference values of Topuz et al. (2010) for the soil that had developed on Gümüşhane granitoid, the trace element values of Aslan (2010) for the soil cover that had developed on Eocene volcanic rocks, and the values of Turekian and Wedepohl (1961) and Taylor and McLennan (1995) for chromium and arsenic elements were used. The geometric average values were used for element concentrations showing logarithmic distribution when benefited from trace element values of Topuz et al. (2010) and Aslan (2010). However, the arithmetic average values were used for elements showing normal distribution. For major element concentrations in the study area, bar graphics were drawn. Accordingly, the elements and number of sample locations of which are above the reference values in soils are as follows; Cd (9), Ba (26), Co (2), Cr and Mn (44), Cu and Ni (all locations), Sn (14), Zn (35), As (36), Pb (38). The pH values of soils in sample location showever, were detected as ranging between neutral to alkaline (Figure 3a, b).

Geochemical normalizations are widely used to determine the pollution resulting from human especially the human induced pollution in soil. The purpose here is to proportionate pollution with respect to normal concentrations with a normalization factor (Daskalakisand O'Connor, 1995; Aloupi and Angelidis, 2001; Condrad and Chisholm-Brause, 2004; Feng et al., 2004). There is not any certain acceptance in the selection of element to be used in

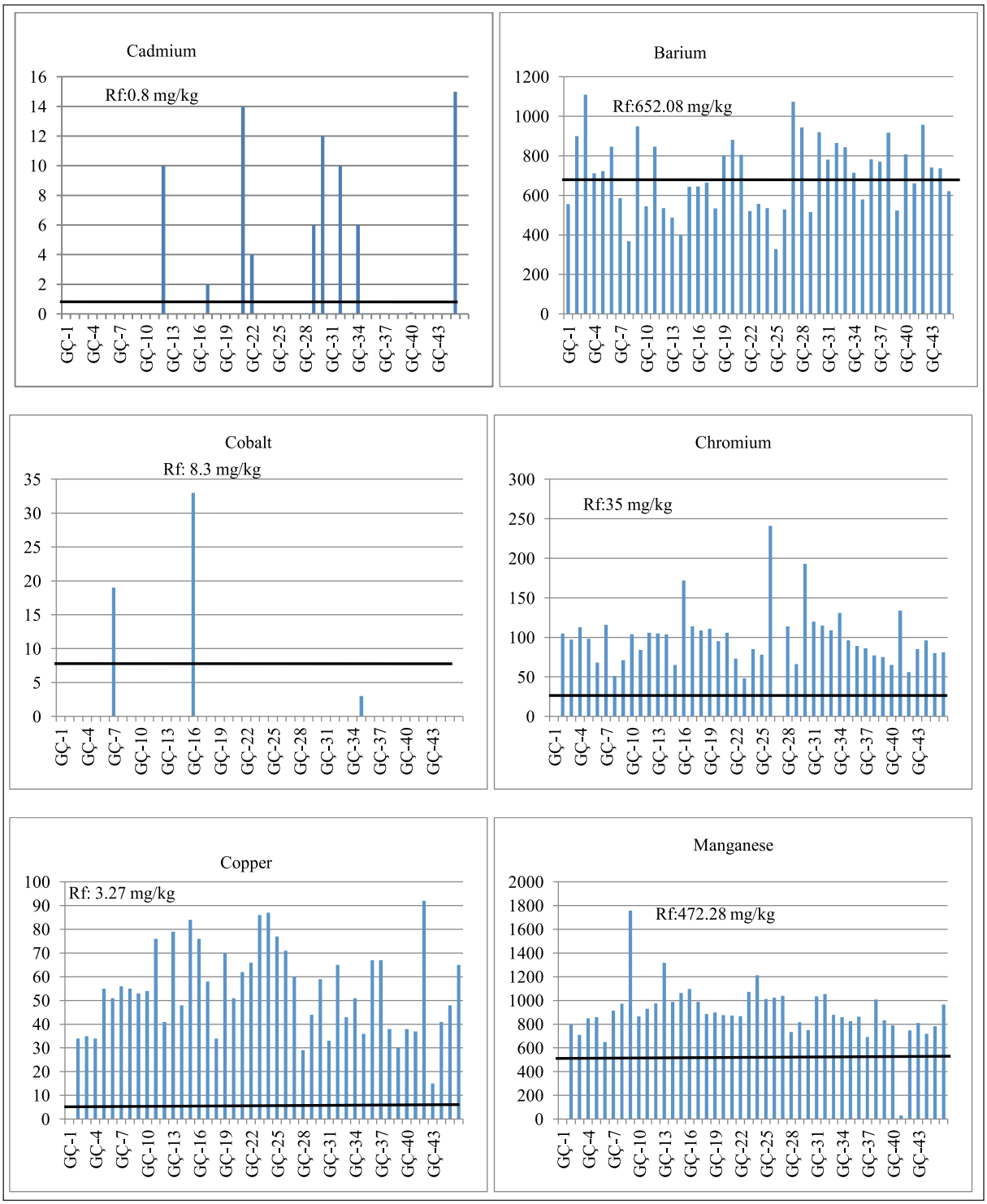

Figure 3- a. Trace element concentrations, reference and pH values of soils in the study area

normalization but, the elements which are not geochemically active (inert) and encountered in all conditions such as; Al, Fe, Li, Zr, Sc and Sr are used (Feng et al., 2004; Acevedo-Figueroa et al., 2006; Ghrefat and Yusuf 2006; Chen et al., 2007; Loska et al., 1997; Saur and Juste 1994; Sutherland 2000; Reimann and De Caritat, 2000).

The parameters which are widely used for the assessment of element enrichments in soil are

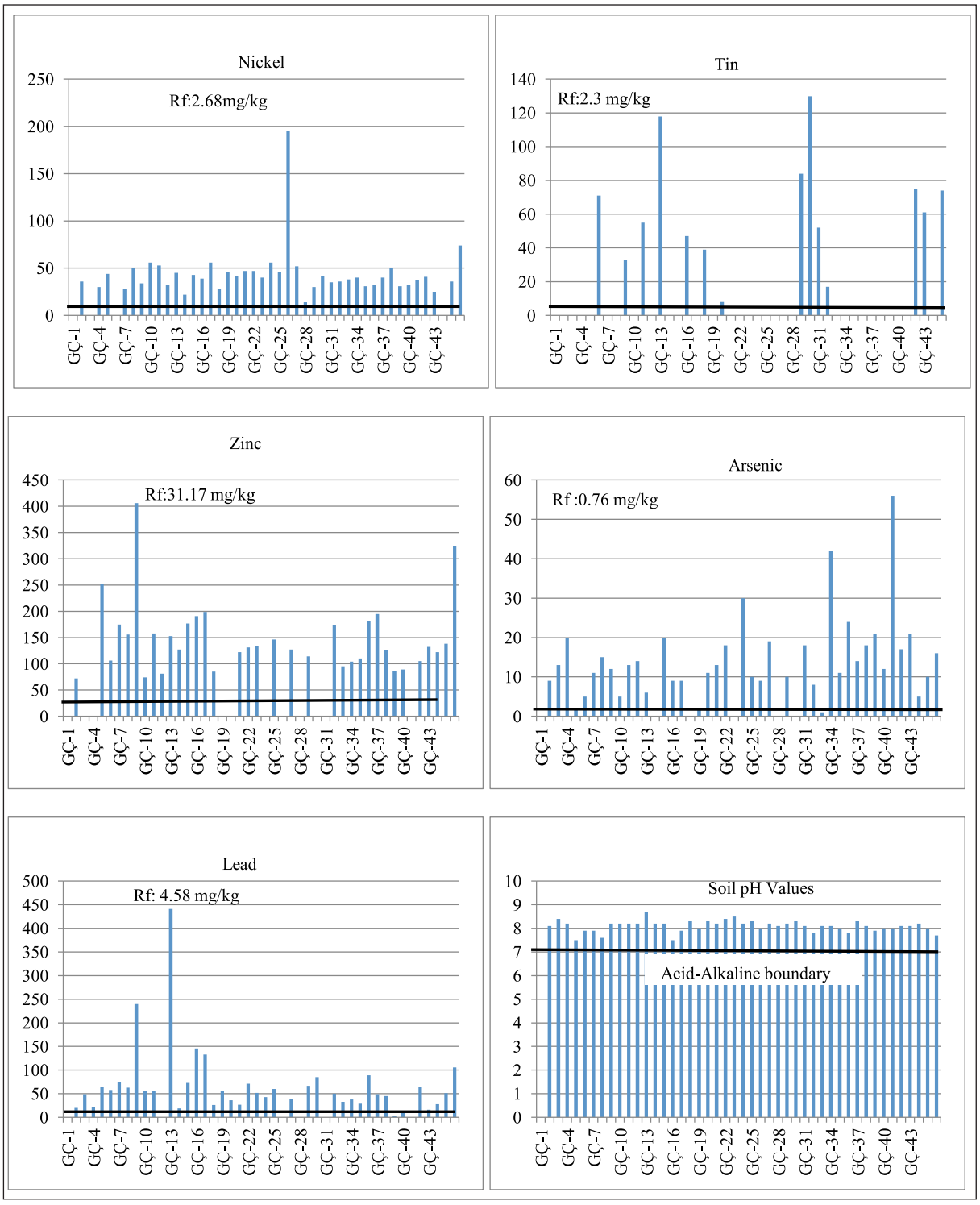

Figure 3- b. Trace element concentrations, reference and pH values of soils in the study area (Continue)

Enrichment Factor (EF), Geoaccumulation Index (I_{geo}), Contamination Factor (CT), Contamination Factor Degree (CF_{deg}). The Enrichment Factor and geoaccumulation index were used in this study.

3.3.1. Enrichment Factor (EF)

The Enrichment Factor (EF) was used by Buat-Menard and Chesselet (1979) for the assessment of metal accumulation in soils. The Enrichment Factor

has also been used in assessing various environmental conditions in time and in the estimation of contribution of the human induced effect in metal pollution (Buat-Menard and Chesselet, 1979; Groengroeft et al., 1998; Morillo et al., 2002; Adamo et al., 2005; Vald'es et al., 2005). Although there have been discussed some drawbacks about the usage of Enrichment Factor for the assessment of elemental accumulations in various environments in detail by Reiman and De Caritat (2000), this factor is widely used in the assessment of enrichment factors and in comparing the pollution of different environmental conditions because it is accepted as a universal formula. In this study, Zr element was selected as the reference element as it has some features such that, its geochemistry resembles to the geochemistry of trace elements and its natural sediment concentrations are regular (Daskalakis and O' Connor, 1995). Zircon is mostly used as stable lithogenic element in alteration studies or for the assessment of more reactive heavy metals in sediments, in reducing dispersive data and in determining sensitive reference values as normalizer (Rubio et al. 2000; Zhang et al., 2006; Cobela-Garcia and Prego, 2003; Machender et al., 2011).

The following formula is used in calculating the Enrichment Factor;

$$EF = \frac{(Me/Zr)_{sample}}{(Me/Zr)_{reference}}$$

Here;

$(Me/Zr)_{sample}$ is the ratio of metal concentration with respect to zircon amount in the soil,

$(Me/Zr)_{reference}$ is the ratio of element reference value with respect to reference Zr used for the normalization.

If EF is less than 5.0 then, the soil is accepted as unimportant in terms of pollution as such minor enrichments could originate from differences in local soil material compounds and in reference soils used in EF estimations (Kartal et al., 2006). Nonetheless; there is also observed difference in the range of contamination degree and in its classification. Birch (2003) classified EF as follows; EF<1 (no enrichment), EF<3 (minor), 3<EF<5 (moderate), 5<EF<10 (moderately severe), 10<EF<25 (severe), 25<EF<50 (very severe), 50<EF (highly severe).

Enrichment factors were calculated for 12 trace elements in soils at 45 sampling locations along the state auto road passing through Gümüşhane city center (Table 8).

Results were taken as follows; Sr (0.6-3.62) in "no enrichment-minor" class; Ba (0.77-5.52) "no enrichment-moderately severe" class; Cd is an important heavy metal that has risk for environment and living organisms when it is assessed in terms of trace element accumulation.Cd content was detected in 10 sampling locations (0.26–49.14) as "no enrichment-highly severe" class; Co was detected in 3 sampling locations (0.98–12.88) in "no enrichment–severe" class; Cr (0.25-1.61) as "no enrichment–minor" class; Cu (8.49-86.57) as "moderately severe–highly severe" class; Mn (0.14-9.70) as "no enrichment–moderately severe" class; Ni (7.17-113.92) as "moderately severe–very highly severe" class. Pb element is one of the most significant pollutant heavy metal of today and it was detected as (1.11-180.51) "minor-very highly severe" class. Arsenic (As) element is an important pollutant material and is seen in all over the world. EF for As is around 5 mg/kg in unpolluted soils (Goldschimdt, 1958; ATSDR, 2000), however it reaches 1400 mg/kg or even 2700 mg/kg in polluted soils (EPA, 1982). EF value of As element is between 1.74-82.05 mg/kg in the study area "minor-very highly severe". EF value for Sn element was detected as (8.54-138.45) "moderately severe–very highly severe" (Table 8, 9).

3.3.2. Geo-accumulation Index (I_{geo})

Geo-accumulation Index (I_{geo}), which was suggested by Muller (1969, 1981) has been used in many investigations since 1970 and aims at detecting the increasing pollution comparing today's metal content with pre industrialization values (Miko et al.. 2000; Loska et al., 2003; Vural and Şahin, 2012 *a-b*). Geo-accumulation index is calculated as shown below;

$$I_{geo} = \log_2 \left[\frac{C_n}{1.5 * B_n} \right]$$

C_n is the metal concentration analyzed,

B_n is the reference value of element n,

However, value of 1.5 corresponds to coefficient used for normal fluctuations in environments like very small anthropogenic effects.

Table 8- Enrichment factors (EF) of trace element accumulations in soil

EF(Sr)	EF(Rb)	EF(Ba)	EF(Cd)	EF(Co)	EF(Cr)	EF(Cu)	EF(Mn)	EF(Ni)	EF(Pb)	EF(Zn)	EF(Y)	EF(As)	EF(Sn)
2.03	2.10	2.42			0.85	29.48	4.78	39.06	12.41	6.56	2.23	17.48	
0.67	2.30	2.59			0.52	20.12	2.82		20.16		1.65	16.74	
1.16	4.11	5.52			1.05	33.77	5.84	37.28	15.64		4.06	44.49	
2.12	1.44	2.15			0.55	33.19	3.58	33.23	27.64	15.99	1.28	2.70	
2.82	1.97	2.91			0.51	40.97	3.60		33.34	8.95	1.82	9.00	
2.76	1.77	3.34		5.87	0.85	44.01	4.97	27.54	41.62	14.46	2.26	19.36	79.11
2.32	1.59	1.94			0.32	36.41	4.45	41.43	29.85	10.86	2.00	22.25	
1.87	1.67	1.47			0.53	42.26	9.70	33.93	136.96	34.05	1.45	21.43	
1.29	1.75	2.62			0.54	29.79	3.30	38.66	22.11	4.29	1.67	6.18	25.81
3.49	1.33	2.71			0.78	75.48	6.39	65.87	39.09	16.50		28.92	
0.80	2.63	2.90	30.59		0.68	27.99	4.60	27.34		5.82	1.65	21.41	53.24
1.34	1.18	1.54			0.56	45.18	5.21	32.21	180.51	9.20	1.73	7.69	
0.97	3.90	2.02			0.80	39.72	5.65	22.78	11.25	11.05	1.25		138.45
3.62	1.01	2.07			0.63	86.57	7.59	55.46	53.84	19.18	2.65	46.17	
3.49	1.48	3.20		12.88	1.59	75.48	7.53	48.47	103.76	19.95	2.10	20.02	
2.20	1.75	2.03	5.63		0.67	36.41	4.29	44.00	59.76	13.14	1.90	12.66	41.83
0.77	2.05	2.21			0.67	22.51	4.06	23.20	12.32	5.92	1.90		
2.80	1.56	2.13			0.83	55.82	4.96	45.90	31.96		2.41	3.57	44.09
3.18	1.60	2.73			0.60	34.60	4.11	35.66	17.48		1.95	16.72	
2.64	1.84	3.33	47.25		0.75	46.71	4.55	44.31	14.56	9.67	2.17	21.94	8.54
1.41	1.73	2.43	10.82		0.41	39.83	3.62	35.50	30.67	8.31	1.92	24.33	
3.04	1.30	1.70			0.29	55.92	4.82	32.55	24.20	9.16	1.28		
2.00	1.51	1.59			0.45	49.50	4.78	39.87	17.51		2.15	38.23	
2.19	1.21	1.68			0.45	48.07	4.37	35.93	26.80	9.58	2.08	13.98	
2.73	0.22	0.77			1.05	33.15	3.30	113.92			1.34	9.41	
1.48	1.28	1.67			0.00	37.89	4.54	41.09	17.62	8.43	2.20	26.87	
0.96	1.77	2.20			0.44	11.87	2.08	7.17			1.67		
2.20	1.58	2.97	16.88		0.39	27.62	3.55	23.57	30.10	7.53		14.06	
3.14	1.59	2.31	48.14		1.61	52.83	4.64	47.06	54.47		2.03		106.63
0.77	2.87	3.02			0.73	21.59	4.68	28.65				26.37	120.56
2.86	1.51	2.39	27.34		0.66	39.67	4.45	27.49	21.84	11.17	1.57	10.94	44.99
1.81	2.69	3.36			0.79	33.31	4.71	36.84	18.30	7.74	1.41	1.74	18.67
1.25	1.86	2.26	14.39		0.65	27.31	3.18	26.80	14.56	5.86	1.62	50.38	
2.93	1.63	2.99		0.98	0.75	30.02	4.76	32.35	17.31	9.65	1.64	20.55	
3.12	1.46	2.58			0.74	59.50	5.31	35.57	56.57	17.00		47.75	
1.48	0.60	1.24			0.25	21.15	1.51	15.80	11.07	6.47		9.90	
0.60	1.87	1.98			0.37	19.49	3.58	32.09	16.52	6.80	1.86	20.68	
0.61	2.16	2.38			0.36	15.53	2.98	20.08	1.11	4.68	1.88	24.35	
1.35	2.02	1.51	0.26		0.35	21.85	3.14	23.02	4.94	5.38	1.48	15.45	
1.53	1.86	2.65			0.82	24.20	0.14	30.29			0.89	82.05	
3.53	1.24	2.50			0.39	69.31	3.90	38.65	34.51	8.32	1.71	28.69	
0.66	2.30	2.71			0.45	8.49	3.17	17.71	6.48	7.86	1.63	26.63	60.18
0.60	2.01	1.91			0.46	21.13	2.56		10.33	6.61	0.78	5.77	44.56
2.26	1.44	2.37	43.18		0.48	30.84	3.48	28.95	23.45	9.33	1.75	14.39	
3.22	1.42	2.14			0.52	44.66	4.59	63.62	52.12	23.48	1.35	24.62	72.08

Table 9- Statistical parameters of enrichment factors in the study area

Statistical Descriptor Parameters	EF (Sr)	EF(Rb)	EF(Ba)	EF(Cd)	EF(Co)	EF(Cr)	EF(Cu)	EF(Mn)	EF(Ni)	EF(Pb)	EF(Zn)	EF(Y)	EF(As)	EF(Sn)
Mean	2.00	1.78	2.38	24.45	6.58	0.64	37.80	4.31	36.45	33.87	10.83	1.81	21.90	61.34
Interval	3.02	3.89	4.76	47.88	11.90	1.36	78.08	9.55	106.75	179.39	29.75	3.28	80.32	129.90
Cardinality	45	45	45	10	3	44	45	45	42	40	35	40	40	14
Max.	3.62	4.11	5.52	48.14	12.88	1.61	86.57	9.70	113.92	180.51	34.05	4.06	82.05	138.45
Min.	0.60	0.22	0.77	0.26	0.98	0.25	8.49	0.14	7.17	1.11	4.29	0.78	1.74	8.54

Muller (1969, 1981) and Chen et al. (2007) classified I_{geo} as follows; $I_{geo}<0$ uncontaminated, 0-1 uncontaminated-moderately contaminated, 1-2 moderately contaminated, 2-3 moderately- heavily contaminated, 3-4 heavily contaminated, 4-5 heavily to extremely contaminated and >5 extremely contaminated.

The Geo-accumulation Index (I_{geo}) for the study area was calculated and results were given in table 10.

Table 10- Geoaccumulation indexes of soil elements

Igeo (Sr)	Igeo (Rb)	Igeo (Ba)	Igeo (Cd)	Igeo (Co)	Igeo (Cr)	Igeo (Cu)	Igeo (Mn)	Igeo (Ni)	Igeo (Pb)	Igeo (Zn)	Igeo (Y)	Igeo (As)	Igeo (Sn)
-1.07	-1.01	-0.81			1.00	2.79	0.17	3.20	1.54	0.62	-0.93	2.99	
-2.07	-0.29	-0.12			0.89	2.83	0.00		2.84		-0.77	3.52	
-2.07	-0.24	0.18			1.11	2.79	0.26	2.94	1.68		-0.26	4.14	
-0.48	-1.04	-0.46			0.90	3.49	0.28	3.49	3.22	2.43	-1.21	0.82	
-0.48	-1.00	-0.44			0.37	3.38	-0.13		3.08	1.18	-1.11	2.14	
-0.48	-1.12	-0.21		0.61	1.14	3.51	0.37	2.84	3.43	1.90	-0.77	3.28	4.36
-0.48	-1.03	-0.74			-0.04	3.49	0.46	3.68	3.20	1.74	-0.70	3.73	
-1.07	-1.23	-1.41			0.44	3.43	1.31	3.12	5.13	3.12	-1.43	3.40	
-1.07	-0.62	-0.04			0.99	3.46	0.29	3.84	3.03	0.66	-0.70	2.14	3.26
-0.48	-1.88	-0.84			0.68	3.95	0.39	3.76	3.00	1.76		3.52	
-2.07	-0.35	-0.21	3.06		1.01	3.06	0.46	3.03		0.79	-1.02	3.63	3.99
-1.07	-1.24	-0.87			1.00	4.01	0.90	3.52	6.01	1.71	-0.70	2.40	
-2.07	-0.05	-1.01			0.99	3.29	0.48	2.49	1.47	1.44	-1.70		5.10
-0.48	-2.32	-1.29			0.31	4.10	0.59	3.46	3.41	1.92	-0.93	4.14	
-0.48	-1.72	-0.60		1.41	1.71	3.95	0.63	3.32	4.41	2.03	-1.21	2.99	
-0.48	-0.82	-0.60	0.74		1.12	3.56	0.48	3.84	4.28	2.09	-0.70	2.99	3.77
-2.07	-0.66	-0.56			1.05	2.79	0.32	2.84	1.92	0.86	-0.77		
-0.48	-1.32	-0.87			1.08	3.83	0.34	3.56	3.03		-0.70	0.82	3.50
-0.07	-1.05	-0.29			0.86	3.38	0.31	3.42	2.39		-0.77	3.28	
-0.48	-1.00	-0.15	3.54		1.01	3.66	0.30	3.59	1.98	1.38	-0.77	3.52	1.21
-1.07	-0.77	-0.28	1.74		0.48	3.75	0.29	3.59	3.37	1.49	-0.63	3.99	
-0.07	-1.29	-0.91			-0.13	4.13	0.60	3.35	2.92	1.52	-1.32		
-0.48	-0.89	-0.81			0.70	4.15	0.78	3.84	2.65		-0.38	4.73	
-0.48	-1.34	-0.87			0.57	3.97	0.51	3.56	3.13	1.64	-0.56	3.14	
0.26	-3.39	-1.58			2.20	3.85	0.53	5.64			-0.77	2.99	
-1.07	-1.27	-0.89				3.61	0.55	3.73	2.51	1.44	-0.50	4.07	
-1.07	-0.18	0.13			1.12	2.56	0.05	1.84			-0.26		
-0.48	-0.96	-0.05	2.32		0.33	3.16	0.21	2.94	3.29	1.29		3.14	
-0.48	-1.46	-0.93	3.32		1.88	3.59	0.08	3.42	3.63		-1.11		4.61
-2.07	-0.16	-0.09			1.19	2.75	0.55	3.16				3.99	5.24
-0.07	-0.99	-0.32	3.06		1.13	3.73	0.57	3.20	2.87	1.90	-0.93	2.82	3.91
-1.07	-0.50	-0.18			1.05	3.13	0.31	3.28	2.27	1.02	-1.43	-0.18	2.30
-1.07	-0.50	-0.21	2.32		1.32	3.38	0.28	3.35	2.47	1.15	-0.70	5.21	
-0.48	-1.32	-0.45		-2.05	0.87	2.87	0.22	2.99	2.08	1.23	-1.32	3.28	
-0.48	-1.57	-0.75			0.76	3.77	0.29	3.03	3.70	1.96		4.40	
-0.07	-1.36	-0.32			0.71	3.77	-0.03	3.35	2.84	2.06		3.63	
-2.07	-0.42	-0.35			0.55	2.95	0.51	3.68	2.71	1.43	-0.43	3.99	
-2.07	-0.23	-0.09			0.51	2.61	0.23	2.99	-1.19	0.88	-0.43	4.21	
-1.07	-0.48	-0.90	-3.58		0.31	2.95	0.16	3.03	0.81	0.93	-0.93	3.40	
-1.07	-0.78	-0.28			1.35	2.91	-4.47	3.24			-1.85	5.63	
-0.07	-1.57	-0.57			0.09	4.23	0.08	3.39	3.22	1.17	-1.11	3.91	
-2.07	-0.27	-0.03			0.70	1.61	0.20	2.68	1.22	1.50	-0.77	4.21	4.44
-2.07	-0.33	-0.40			0.87	3.06	0.02		2.03	1.38	-1.70	2.14	4.14
-0.48	-1.12	-0.41	3.64		0.61	3.29	0.15	3.20	2.89	1.56	-0.85	3.14	
-0.07	-1.24	-0.66			0.63	3.73	0.45	4.24	3.95	2.80	-1.32	3.82	4.42

According to this index, following results were obtained; Sr (-2.07;+0.26), Ba (-1.58;+0.18) and Mn (-4.47, +1.31) "uncontaminated"-"moderately contaminated"; Rb (-3.39; -0.05), "uncontaminated"; Cd (-3.58;+3.64), "uncontaminated-heavily contaminated"; Co (-2.05;1.41) was detected in 3 sampling locations, "uncontaminated-moderately contaminated"; Cr (-0.13;2.20), "uncontaminated-moderately contaminated-heavily contaminated"; Cu (1.61;4.23), "moderately contaminated", "heavily contaminated-extremely contaminated"; Ni (1.84; 5.64), "moderately contaminated","heavily contaminated - extremely contaminated"; Pb (I_{geo} -1.19; +6.01), "moderately contaminated","heavily contaminated-extremely contaminated"; Zn (I_{geo}: 0.62; 3.12), "uncontaminated, moderately contaminated" - "heavily contaminated"; Y (-1.85; -0.26) "uncontaminated"; As (-0.18; +5.63), "uncontaminated" - "heavily – extremely contaminated", Sn (1.21;5.24), "moderately to heavily contaminated", "extremely contaminated" (Table 10, 11).

Table 11- Statistical parameters of geoaccumulation for soil element contents of soils on Gümüşhane auto road

Statistical Descriptor Parameters	Igeo (Sr)	Igeo (Rb)	Igeo (Ba)	Igeo (Cd)	Igeo (Co)	Igeo (Cr)	Igeo (Cu)	Igeo (Mn)	Igeo (Ni)	Igeo (Pb)	Igeo (Zn)	Igeo (Y)	Igeo (As)	Igeo (Sn)
Mean	-0.90	-0.99	-0.52	2.02	-0.01	0.85	3.38	0.25	3.35	2.81	1.54	-0.91	3.33	3.88
Irregularity	-0.61	-1.30	-0.53	-2.27	-1.36	0.43	-0.79	-5.50	1.25	-0.45	0.73	-0.57	-1.05	-1.30
Interval	2.32	3.34	1.76	7.23	3.46	2.33	2.62	5.78	3.80	7.20	2.50	1.58	5.81	4.02
Cardinality	45	45	45	10	3	44	45	45	42	40	35	40	40	14
Max.	0.26	-0.05	0.18	3.64	1.41	2.20	4.23	1.31	5.64	6.01	3.12	-0.26	5.63	5.24
Min.	-2.07	-3.39	-1.58	-3.58	-2.05	-0.13	1.61	-4.47	1.84	-1.19	0.62	-1.85	-0.18	1.21
Confidence Level(95.0%)	0.21	0.19	0.12	1.55	4.50	0.14	0.16	0.23	0.17	0.38	0.19	0.12	0.36	0.62

3.3.3. Trace element contents in plants and trace element patterns

The transfer of metals from soil to plants is important in terms of plant formation and heavy metal pollution (Kabata and Pendias, 2000). Many mechanical and experimental methods have been studied for the investigation of element transfer from soils or soil solutions into plants (Kraus et al., 2001; Yaylalı-Abanuz and Tüysüz 2009). The relation between the metal contents of various soils and plants could be explained by transfer factor (Krauss et al., 2001). Although a linear function is preferred in many cases, soil-plant transfer of metal does not give a linear relation. Some investigators use Ferundlich type function to predict the transfer of elements into various plants grown in polluted soils (Krauss et al., 2001;Yaylalı-Abanuz and Tüysüz, 2009).

The relationship of concentration of an element in plant or soil could be calculated by the formula;

$$c_{plant} = bxc^{a}_{soil}$$

As there is not any linear relationship in element transfer from soil to plant, this formula can be rendered into linear form by a logarithmic transformation;

$$log\ c_{plant} = axc_{soil} + log\ b$$

Here;

c_{plant} is metal concentration in plant

c_{soil} is the metal concentration in plant

Values (a) and (b) are the empirical Ferundlich coefficients (Sposito, 1984). As trace element concentrations in plants and soils do not display a normal distribution, logarithmic values in regression analyses were used in order to obtain a linear distribution. This model, which is used in investigating the element transfer between the plant and soil in which the plant grows, is not only easy model to use but also is an easy method used for explaining the relationship between these (Krauss et al., 2001). The coefficient (b) also reflects element intake capacity of the element from soil to plant (Krauss et al., 2001; Yaylalı-Abanuz and Tüysüz, 2009). Within the scope of study, the correlation coefficients between shoots of acacia tree and the soil in which this tree had grown up were calculated but there was not observed any significant relationship between them (Figure 4a, b). High correlation values were taken between shoots of acacia tree and the soil in which the tree grows because of insufficient data in terms of these elements. Therefore, these are not realistic correlation values. There is no strong correlation between the element concentrations of acacia shoots and soil in which these shoots had grown up. So, it means that there was not observed a direct relationship between element concentrations of acacia shoots and soils in which those trees had grown up. The absence of a good correlation is an expected result when the fact that the trace element accumulations of tree shoots are less than the trace element accumulation of tree leaf and flowers is taken into consideration.

It is considered to take satisfactory results if this study would be carried out for leaves and flowers of acacia tree.

The element concentrations in acacia shoots are decreasingly ordered as; Fe>Al>Sr>Mo>Zn>Sn>Ba> Mn>Cu>Ni>As>Cr>Co in table 6. It is clear that molybdenum values in acacia shoots are high. As molybdenum values are lower than the detection limits in soil analyses in which acacia trees grow up, the possibility for examining the relationship between soil and the plant could not be performed. This situation is a lack which should be corrected in further studies, and acacia shoots to present high values in terms of molybdenum is another worth investigating. Studies on this topic still continue and

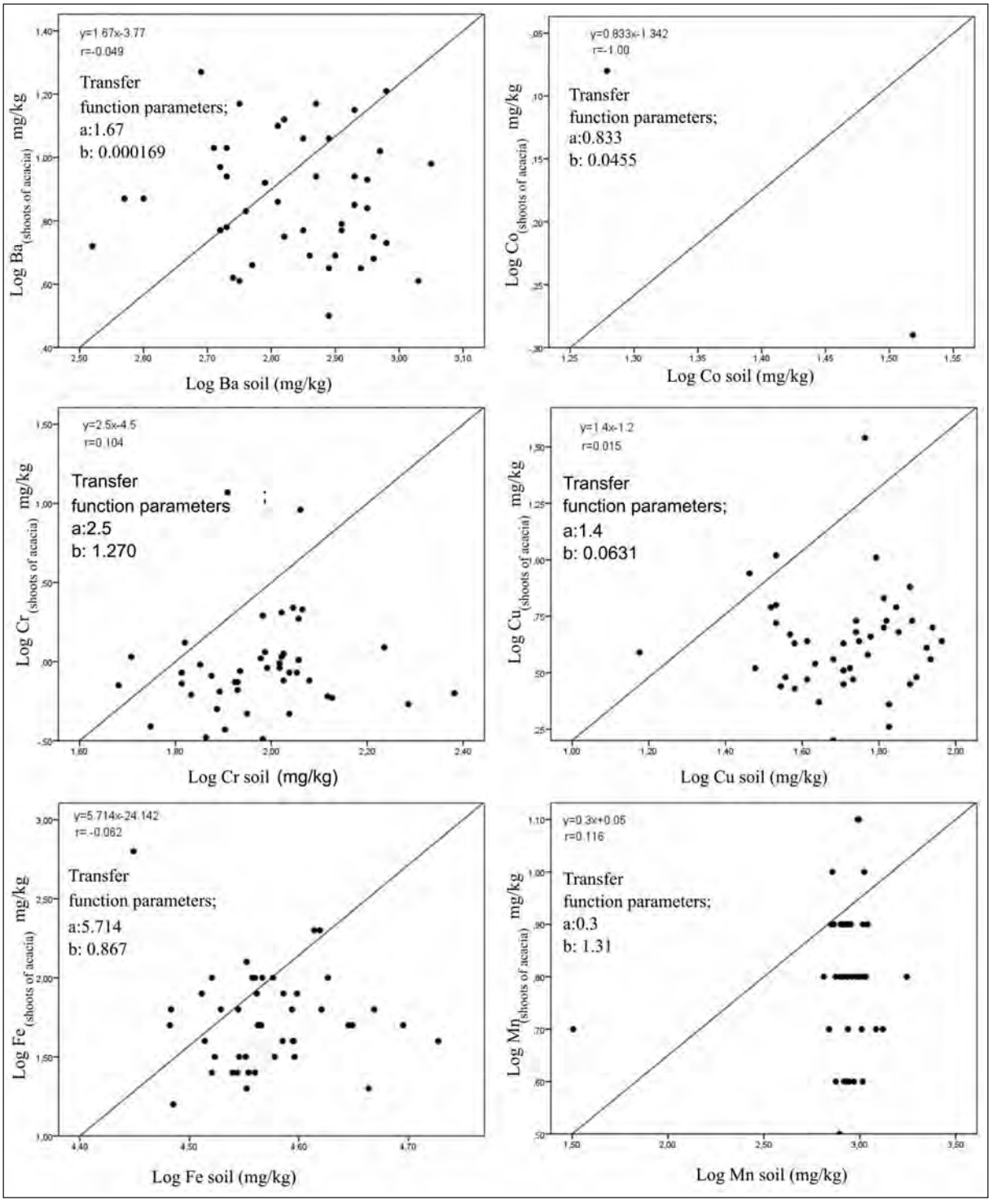

Figure 4- (a) Relationships between shoots of acacia and element in the soil in which the acacia tree has grown (data in logarithmic)

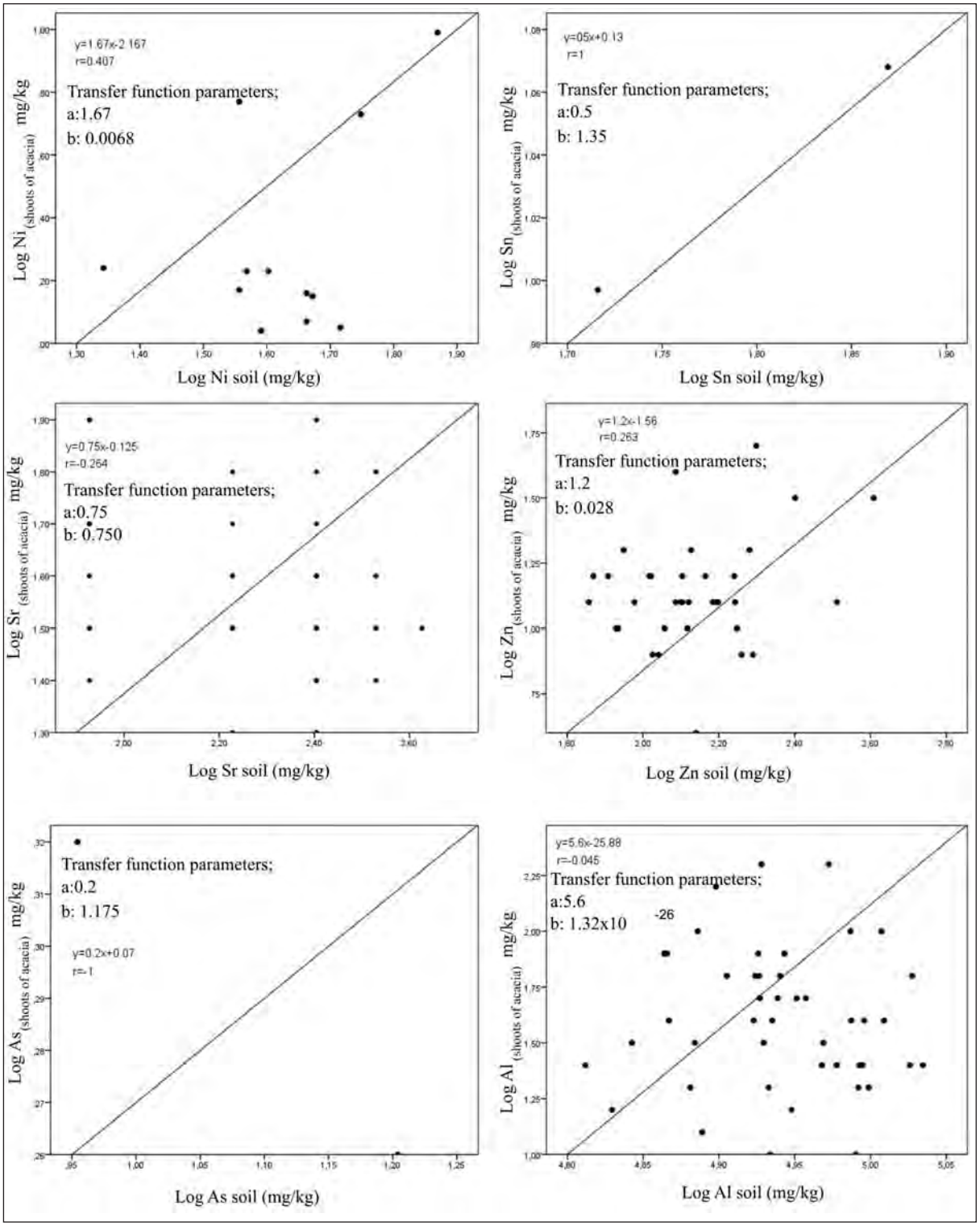

Figure 4- Cont.

these indicate that acacia shoots could be used in soil geochemistry analyses especially for mineral investigations. Using coefficient b, heavy metal accumulations in plants can be detected, and these plants can be used both in geochemistry studies for mineral explorations and in rehabilitating soils which have been subjected to heavy metal contamination. Slope coefficient in acacias is ordered as; Fe>Al>Cr>Ba=Ni>Cu>Zn>Co>Sr>Sn>Mn>As (Figure 4). The plant capacity which affects the element accumulation is expressed with this coefficient. Small coefficients indicate intensive element contributions from soil to its body which contains low metal concentrations, or small amount element contributions from soil which has high metal concentration. In case of low coefficient, the relation between plant and soil is not linear. There is a linear correlation between them when the coefficient approaches 1. This situation is partly related with the element content of the plant, and any increase in soil directly reflects to plant (Krauss et al., 2001, Yaylalı-Abanuz and Tüysüz 2009). This model $log\ c_{plant} = axc_{soil} + log\ b$ is very suitably used in correctly detecting the element intake of plants from the soil (Krauss et al., 2001).

3.3.4. Heavy metal accumulation relationship in soil and plant systems and their use in biogeochemical studies of acacia shoot

Trace elements were absorbed and transported from soil via roots to the other organs of the plant. The relation of transmit from polluted soil to plant is handled with parameters such as; Biological Absorption Constant (BAC), Transfer Factor (TF), Bioaccumulation Factor (BAF) (Luoma and Bryan, 1979; Cui et al., 2004). Element transfer from soil to plant was investigated in this study by means of Bioaccumulation Factor. BAF is estimated by a formula given below;

$$BAF=M_{plant}/M_{soil}$$

Here; M_{plant} is the element content in plant organs, and M_{soil} corresponds to element content of soil in which plant grows (Louma and Bryan, 1979). This equation is used in predicting the transmission rate capacity of each element into plant and plant systems growing in the soil, to show the skill for biological element transport and migration.

Enrichments of trace elements in shoots of acacia relative to soils in which they grow and their related complementary statistical parameters were calculated and box diagrams of elements for BAF were drawn (Table 12, Figure 5).

When BAF values belonging to elements/metal in soil and acacias growing in this soil was studied, following results were obtained as follows; Ba (0.0038-0.038), Co (0.0154-0.0439), Cr (0.0026-0.1448), Cu (0.0271-0.5931), Fe (0.0004-0.0247), Mn (0.0032-0.1680), Ni (0.0214-0.1628), Sn (0.1581-0.909), Sr (0.0723-0.9015), Zn (0.0273-0.2972), As (0.1138-0.2311) and Al (0.0001-0.0025). So, transmission rates for Ba, Co, Fe, Al and partly Mn elements from soil to plant were found to be low. So, taking all these data into account, Al, Mn, Ba and Co elements are not considered to be very productive for biogeochemical studies. Since BAF values of Cu, Ni, Zn, Sn and As elements are higher or equal than 0.1, these can be used in biogeochemical analyses. BAF value of Cu element is seen in a wide range (0.027-0.593), but concentrates are between the range of 0.06-0.11 (Figure 5). BAF value of Cu element to increase up to 0.593 shows that acacia shoots can be used in biogeochemical studies. BAF value for Ni element is between the ranges of 0.021-0.0163, but concentrates are between the ranges of 0.03-0.08. BAF value of Zn is 0.27-0.3, however it mainly possesses a BAF value of 0.1. There was not sufficient data in shoots of acacia, but BAF value obtained for tin element is 0.1. The sufficient determination for As element in acacia shoots could not be performed, nevertheless BAF value for this element was detected as 0.113-0.2. BAF value of Sr element ranges between 0.072-0.9, and the most of data cumulates around 0.12-0.3. Therefore; Sr element can be used in biogeochemical studies. The value of molybdenum in acacia was detected higher than the expected value. The value of molybdenum element could not be detected in soil samples as the content of this element in soil was low. The detection

Table 12- Descriptive statistical parameters of the bioaccumulation factor for shoots of acacia tree.

	BAF(Ba)	*BAF(Co)*	*BAF(Cr)*	*BAF(Cu)*	*BAF(Fe)*	*BAF(Mn)*	*BAF(Ni)*	*BAF(Sn)*	*BAF(Sr)*	*BAF(Zn)*	*BAF(As)*	*BAF(Al)*
Mean	0.0124	0.0297	0.0146	0.1069	0.0021	0.0112	0.0615	0.1745	0.2464	0.1146	0.1724	0.0006
Min.	0.0038	0.0154	0.0026	0.0271	0.0004	0.0032	0.0214	0.1581	0.0723	0.0273	0.1138	0.0001
Max.	0.0380	0.0439	0.1448	0.5931	0.0247	0.1680	0.1628	0.1909	0.9015	0.2972	0.2311	0.0024
Total	0.5580	0.0593	0.6412	4.8105	0.0958	0.5020	0.7380	0.3490	11.0890	4.0094	0.3449	0.0276
Cardinality	45	2	44	45	45	45	12	2	45	35	2	45

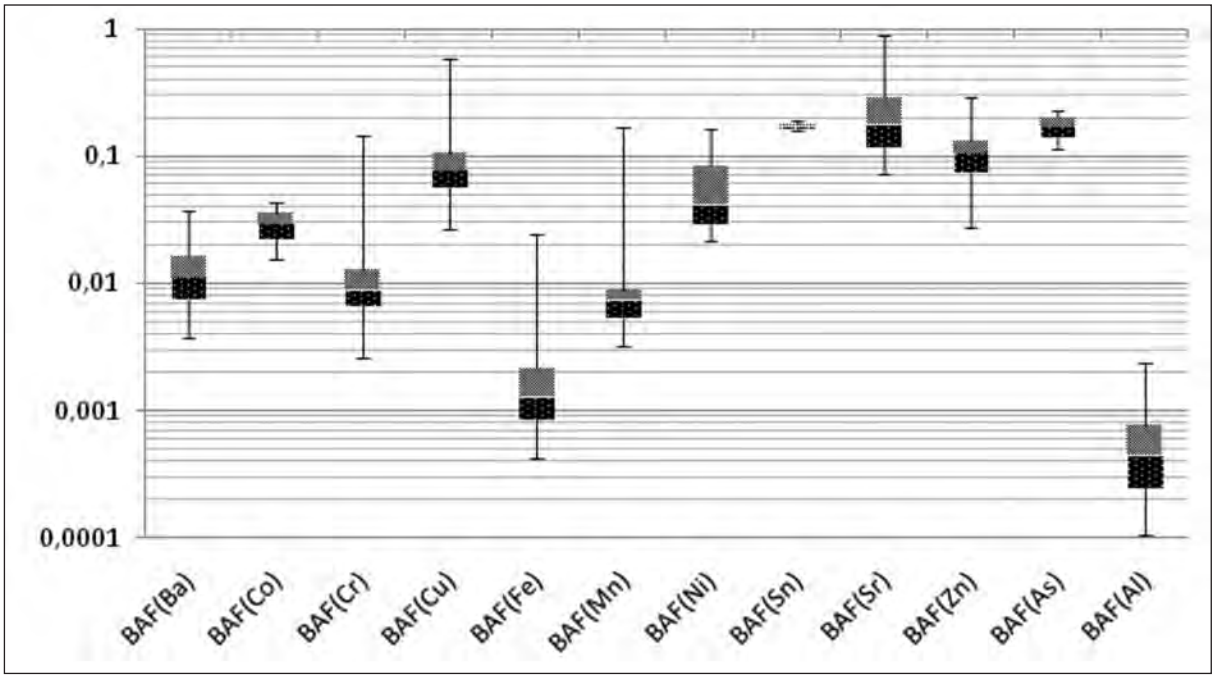

Figure 5- Box diagram belonging to Bioaccumulation Factors (BAF) for the elements of acacia shoots.

of molybdenum values in acacia shoots is because of its nature. As it is known; elements which are rarely found in nature such as; Mo, Mn, Co, Pb, Ni and Sr could reach very high values on leaves as their mobility coefficients are high in water.The molybdenum element was observed in high values in shoots of acacia tree, though it could not be detected in soil in this study as well (7.34-56.45 mg/kg). These values showed that molybdenum gave better results in shoots of acacia tree than soil in biogeochemical studies.

The correlation of element transfer from soil to acacia shoots and the correlation with pH of the soil in which the plant grows was made. Accordingly; weak positive correlation was observed between Fe and Ba with Cu; Sr and Ba; Zn and Cu with Mn; and Al and Fe. However; strong positive correlation between Cr and Ni, and weak negative correlation between Al and Ni, and the alkalinity of the environment with Cr and Ni were observed (Table 13).

The pH values of the environment are effective on the mobility of all cations. As pH decreases, the mobility of cations increases with increasing in acidity of the soil. However, the high mobility of trace elements in the soil increases the element transmission from soil to plant and supplies soil profiles to pass into water systems. Also; pH values have an important effect on the takeout of nutrition and elements in soil profiles (Kabata-Pendias, 2000). The pH value also enables the alteration of minerals in the soil and transforms minerals into less soluble compounds (Kabata-Pendias and Pendias, 1992). The alkaline pH values ranging between 7 and 8.5 can account for the low correlation in element transfer to plant.

4. Results

In this study, the environmental biogeochemical characteristics of heavy metal/trace elements in soils and in shoots of acacia trees in soils were investigated along the auto road passing through Gümüşhane city center. In this study, concentrations of heavy metals such as; Al, Fe, Zr, Sr, Rb, Ba, Cd, Co, Cr, Cu, Mn, Ni, Pb, Zn, Y, As and Sn, and the contamination degrees of these elements in the soil were studied. Elements in the soil are ordered in abundance as; Al>Fe>Mn>Ba>Pb>Zn>Sr>Cr>Ni>Rb>Zr>Sn>Cu>As>Co>Y>Cd. In order to determine the degree of contamination in the area, I_{geo} and EF parameters were calculated. According to these parameters; the contamination order as; Pb>Zn>Cu>Ni>Mn was obtained. High I_{geo} and EF values for Pb, Zn and Cu in the soil along the auto road indicate the presence of an anthropogenically induced contamination (related with traffic and industrial facilities) in terms of these

Table 13- Correlation values between bioaccumulation factors and the pH of the soil.

	BAF(Ba)	BAF(Cr)	BAF(Cu)	BAF(Fe)	BAF(Mn)	BAF(Ni)	BAF(Sr)	BAF(Zn)	BAF(Al)	pH
BAF(Ba)	1.000									
BAF(Cr)	0.099	1.000								
BAF(Cu)	0.128	0.009	1.000							
BAF(Fe)	0.359	0.122	0.342	1.000						
BAF(Mn)	-0.060	-0.060	0.078	-0.039	1.000					
BAF(Ni)	0.139	0.774	0.156	-0.147	-0.096	1.000				
BAF(Sr)	0.389	-0.087	0.116	0.111	-0.020	-0.048	1.000			
BAF(Zn)	0.050	-0.201	0.486	0.188	0.365	-0.380	0.066	1.000		
BAF(Al)	0.172	0.048	0.129	0.454	-0.125	-0.397	-0.032	0.111	1.000	
pH	0.034	-0.313	-0.144	-0.044	-0.071	-0.444	0.214	0.081	-0.115	1.000

elements. It is also predicted that mine sites in the vicinity of the study area would have direct or indirect effect on this contamination. However, there is a need for more detailed investigation to understand the dimensions of the effect. Low I_{geo} and EF parameter for Mn and Ni elements indicate that there is not any contamination in soil in terms of these elements. So, while there is observed a depletion in terms of elements such as; Mn, Cr and Ni in soils along the road, there was detected an enrichment (contamination) in terms of Pb, As, Zn and Cu elements.

In the study; Al, As, Ba, Cd, Co, Cr, Cu, Fe, Hg, Mn, Mo, Ni, Pb, Sn and Zn contents in shoots of acacia tree were determined. Cd, Hg and Pb concentrations remained below the detection limits. Ni and As elements were determined in acacia shoots in locations 6 and 2, respectively. When plant transmission parameters from soil were calculated, it was seen that (BAF and TF) Al, As, Ba, Co, Cr and Mn contents ranged in normal limits, and Cu, Fe, Mo, Ni, Sr and Zn elements were above the upper limits and/or even more at some locations.

Acknowledgement

The author would like to thank to the General Directorate of Eti Maden Management (Ankara) and to Muhsin Gani, to the Directorate of Provincial Food Control, Trabzon, to Ali Gündoğdu and Cemalettin Baltacı (Gümüşhane University) and to his students Erdem Şahin, Osman Barış Aslan, Veysel Dündar and Emre Önal for their helps during field studies.

Received: 04.12.2012
Accepted: 08.01.2014
Published: june 2014

References

Acevedo-Figueroa, D., Jiménez, B.D., Rodríguez-Sierra, C.J. 2006. Trace metals in sediments of two estuarine lagoons from Puerto Rico, *Environmental Pollution* 141, 336-342.

Adamia, S., Lordkipanidze, M., Zakariadze, G. 1977. Evolution of an active continental margin as exemplified by the Alpine history of the Caucasus. *Tectonophysics*, 40, 183–199.

Adamo, P., Arienzo, M., Imperato, M., Naimo, D., Nardo, G., Stanziones, D. 2005. Distribution and partition of heavy metals in surface and sub-surface sediments of Naples city port, *Chemosphere* 61, 800-809.

Ahdy, H.H., Khaled, A. 2009. Heavy Metal Contamination in Sediments of the Western Part of Egyptian Mediterranean Sea, *Austrlian J. of Basic Applied Sci*3(4) 3330-3336

Akçay, M., Gündüz, Ö., Yaşar, R., Gümrük, O. 2011. Hazine Mağara ve Kırkpavli (Gümüşhane) Polimetalik Pb-Zn-Cu-Au-Ag Madenlerinin Jeokimyasal ve Kökensel Özellikleri. *64. TJK Kurultayı Bildiri Özleri Kitabı* s-183-184.

Aliyazıcıoğlu, İ. 1999. Kale (Gümüşhane) Yöresi Volkanik Kayaçlarının Petrografik, Jeokimyasal ve Petrolojik incelenmesi, Yüksek Lisans Tezi, KTÜ Fen Bilimleri Enstitüsü. Trabzon.

Aloupi, M., Angelidis, M.O. 2001. Geochemistry of natural and anthropogenic metals in the coastal sediments of the island of Lesvos, Aegean Sea, *Environmental Pollution* 113, 211-219.

Aslan, Z. 2010. U–Pb zircon SHRIMP age, geochemical and petrographical characteristics of tuffs within calc-alkaline Eocene volcanics around Gümüşhane (NE Turkey), Eastern Pontides. N*eues Jahrbuch für Mineralogie - Abhandlungen: Journal of Mineralogy and Geochemistry* 187(3), 329-346.

Aslan, M., Aliyazıcıoğlu, İ. 2001. Geochemical and petrological characteristics of the Kale (Gümüşhane) volcanic rocks: implications for the Eocene evolution of eastern Pontide arc volcanism, northeast Turkey. *International Geology Review* 43, 595–610.

Aslan, N., Akçay, M. 2011. Mastra (Gümüşhane) Au-Ag Yatağının Jeolojik, Mineralolojik ve Jeokimyasal

Özellikleri. *64. TJK Kurultayı Bildiri Özleri Kitabı*, 25-29 Nisan 2011, Ankara, 181-182.

ATSDR (Agency for Toxic Substances and Disease Registry). *Toxicological Profile for Arsenic*. 2000.

Birch, G. 2003. A scheme for assessing human impacts on coastal aquatic environments using sediments, In C.D. Woodcoffe & R. A. Furness (Eds.), *Coastal GIS 2003. Wollongong University Papers in Center forMaritime Policy,* 14, Australia.

Birch, G.E.,Scollen, A. 2003. Heavy metals in road dust, gully pots and parkland soils in a highly urbanized sub-catchment of Port Jackson, *Australia. Austr. J. Soil Res*. 41: 1329-1342.

Bosco. M.I., Varrica, D., Dongarra, G. 2005. Case study: Inorganic pollutants associated with particulate matter from an area near a petrochemical plant. *Environ. Res*. 99, 18–30.

Buat-Menard, P., Chesselet, R. 1979. Variable influence of the atmospheric flux on the trace metal chemistry of oceanic suspended matter, *Earth Planet Sci Lett* 42:398–411

Chen, C.W., Kao, C.M., Chen, C.F., Dong, C.D. 2007. Distribution and accumulation of heavy metals in the sediments of Kaohsiung Harbor, Taiwan, *Chemosphere*, 66, 1431–1440.

Cobela-Garcia A, Prego, R. 2003. Heavy metal sedimentary record in a Glacian Ria (NW Spain): background values and recent contamination. *Mar Pollut Bull* 46:1253–1262.

Condrad, C.F., Chisholm-Brause, C.J. 2004. Spatial survey of trace metal contaminants in the sediments of Elizabeth River, Virginia. *Marine Pollution Bulletin* 49, 319-324.

Cui. Y., Zhu, Y., Zhai. R., Chen, D., Huang, Y., Qui, Y., Liang, J. 2004. Transfer of metals from soil to vegetables in an area near a Smelter in Nanning/China. *Environment International*. 30, 785-791.

Çoğulu, E. 1975. Gümüşhane ve Rize Granitik Plutonlarının Mukayeseli Petrojeolojik ve Jeokronolojik Etüdü, İTÜ Fen Bilimleri Fakültesi, İstanbul, Doktora Tezi.

Daskalakis, K., D., O'Connor, T.P. 1995. Normalization and elemental sediment contamination in the Coastal United States. *Environmental Science and Technology* 29, 470-477.

Dokuz, A. 2011. A slab detachment and delamination model for the generation of Carboniferous high-potassium I-type magmatism in the Eastern Pontides, NE Turkey: The Köse composite pluton. *Gondwana Res*. 9 (4), 926-944.

Duran, C., Gundogdu, A., Bulut, V.N., Soylak, M., Elci, L., Şentürk, H.B., Tüfekçi, M. 2007. Solid-phase extraction of Mn(II), Co(II), Ni(II), Cu(II), Cd(II) and Pb(II) ions from environmental samples by flame atomic absorption spectrometry (FAAS). *Journal of Hazardous Materials* 146 (1-2), 347-355.

EPA. 1982. Exposure and risk assessment for arsenic. Washington, DC: U.S. Environmental Protection Agency. Code of Federal Regulation. PB 85-221711. EPA 440/4-85-005. 1.1-4.68.

Eyüboğlu, Y., Bektas, O., Seren, A., Maden, N., Jacoby, W.R., Özer, R. 2006. Three-directional extensional deformation and formation of the Liassic rift basins in the eastern Pontides (NE Turkey). *Geologica Carpathica* 57(5), 337-346.

Eyüboğlu, Y., Chung, SL., Dudas, F.O., Santosh, M., Akaryali, E. 2011. Transition from shoshonitic to adakitic magmatism in the Eastern Pontides, NE Turkey: Implications for slab window melting. *Gondwana Research* 19, 413-429.

Feng, H., Han, X., Zhang, W., Yu, L. 2004. A preliminary study of heavy metal contamination in Yantze River intertidal zone due to urbanization, *Marine Pollution Bulletin* 49, 910-915.

Ghrefat, H., Yusuf, N. 2006. Assessing Mn, Fe, Cu, Zn and Cd pollution in bottom sediments of Wadi Al-Arab Dam, Jordan. *Chemosphere* 65, 2114-2121.

Goldschmidt V.M. 1958. Geochemistry. Ed.: Muir A., Oxford, Oxford University Press, s. 468.

Groengroeft, A., Jaehnig, U., Miehlich, G., Lueschow, R., Maass, V. ve Stachel, B., 1998. Distribution of metals in sediments of the Elbe Estuary in 1994. *Water Science and Technology 37*, 109-116.

Güner, S., Er, M., Gümüşel, A., Boğuşlu, M.1985. Gümüşhane-Eski Gümüşhane yöresindeki cevherleşmelere ait jeoloji raporu. *Maden Tetkik ve Arama Genel Müdürlüğü Rapor No: 8029*, 525 s Ankara (unpublished).

Güner, S.,Yazıcı, E.N. 2005. Gümüşhane Yöresi epitermal altın aramaları prospeksiyon raporu. *Maden Tetkik Arama Genel Müdürlüğü Rapor No: 10743*, 45 s Ankara (unpublished).

Güven, İ.H., 1993. Doğu Pontidlerin Jeolojisi ve 1/250 000 ölçekli kompilasyonu. *Maden Tetkik ve Arama*, Ankara (unpublished)

Kabata-Pendias, A.2000 Trace element in soils and plants, 3rd edn. CRC Press, USA. 413 s.

Kabata-Pendias, A., Pendias, H. 1992 Trace elements in the biological environment. Wyd. Geol., Warsaw, 300 s.

Kabata-Pendias, A. ve Pendias, H. 1994. Trace Element in Soil and Plants (Second edition ed.). Florida: CRC.

Kahraman, İ., Kansız, H., Dursun, A., Yılmaz, H., Erçin, A.İ. 1985. Gümüşhane yöresinin jeolojisine ve cevherleşmelerine ait jeoloji raporu. *Maden Tetkik ve Arama Rapor No:7956*, Ankara (unpublished).

Kandemir, R. 2004. Gümüşhane ve Yakın Yöresindeki Erken-Orta Jura Yaşlı Şenköy Formasyonunun Çökel Özellikleri ve Birikim Koşullar. Doktora Tezi, Karadeniz Teknik Üniversitesi, Fen Bilimleri Enstitüsü, Trabzon.

Karslı, O., Dokuz, A., Uysal, İ., Aydin, F., Kandemir, R., Wijbrans, J. 2010. Generation of the Early Cenozoic adakitic volcanism by partial melting of mafic lover crust, Eastern Turkey: Implications for

crustal thickening to delemination. *Lithos* 114: 109–120.

Kartal, S., Aydın, Z., Tokalıoğlu, S. 2006. Fractionation of metals in street sediment samples by using the BCR sequential extraction procedure and multivariate statistical elucidation of the data, *J. Hazard. Mater.,*132, 80–89.

Kaygusuz, A., Wolfgang, S., Şen, C., Satır, M. 2008. Petrochemistry and petrology of I-type granitoids in an arc setting: the composite Torul pluton, Eastern Pontides, NE Turkey. *International Journal of Earth Sciences*, 97, 739–764.

Kaygusuz, A., Arslan, M., Siebel, W., Şen, C. 2010. Geochemical and Sr-Nd Isotopic Characteristic of Post-Collisional Calc-Alkaline Volcanics in the Eastern Pontides (NE Turkey). *Turkish J.Earth Sci* 20, 137-159.

Ketin, İ. 1966. Anadolu'nun Tektonik Birlikleri. *MTA Dergisi*, 66, 20-34.

Kocaer F, Baskaya H.S. 2003. Remediation Technologies for Metal-Contaminated Soils, *Uludag Univ. Eng. Archit. Fac. J.,* 8(1): 121-131.

Kovacs, M., Podani, J., Klincsek, P., Dinka, M., Torok, K. 1981. Element composition of the leaves of some deciduous trees and the biological inducators of heavy metals in an urban-industrial environment. *Acta Botanica Acadcmiac Scicntiarum Hunsaricae* 27: 43-52.

Krauss, M., Wilcke, W., Kobza, J., Zech, W. 2001. Predicting heavy metal transfer from soil to plant: potential use of Freundlich-type functions. *J Plant Nutr Soil Sci* 165,3–8

Loska K., Cebula J., Pelczar J., Wiechula D., Kwapulinski J. 1997**.** Use of enrichment, and contamination factors together with geoaccumulation indexes to evaluate the content of Cd, Cu, and Ni in the Rybnik Water Reservoir in Poland. *Water, Air, Soil Pollut*. 93, 347.

Loska, K., Wiechula, D., Barska, B., Cebula, E., Chojnecka, A. 2003. Assessment of arsenic enrichment of cultivated soils in Southern Poland, *Polish Journal of Environmental Studies*, 12(2): 187-192.

Luoma S.N., Bryan G W. 1979. Heavy metal bioavailability: Modeling chemical and biological interactions in sediment bound zinc[M]. In: Chemical modeling in aqueous systems (E. A. Jenne, ed.). Washington, DC: ACS Symposium Series 93. *American Chemical Society* 577-604.

Machender, G., Dhakate R., Pransanna, L., Govil, P.K. 2011. Assessment of heavy metal contamination in soils around Balanagar industrial area, Hyderabad, India. *Environ Earth Sci*. 63. 945-953.

Miao L., Ma, Y., Xu, R., Yan W. 2011. Environmental biogeochemical characteristics of rare earth elements in soil and soil grown plants of the Hetai goldfield, Guangdong Province, China. *Environ Earth Sci*. 63:501-511.

Miko, S., Peh, Z., Bukovec, D., Prohic, E., Kastmüller, Z. 2000. Geochemical baseline mapping and Pb pollution assessment of soils in the karst in Western Croatia, *Natura Croatica* 9 (1):41-59.

Morillo, J., Usero, J.,Gracia, I. 2002. Partitioning of metals in sediments from the Odiel River (Spain). *Environment International* 28, 263–271.

Murakami, M., Fujita, M., Furumai, H., Kasuga, I., Kurisu, F. 2009. Sorption behavior of heavy metal species by soakaway sediment receiving urban road runoff from residential and heavily trafficked areas. *J Hazard Mater* 164:707-12.

Müller, G. 1969. Index of geoaccumulation in sediments of the Rhine River, *GeoJournal,* 2(3): 108-118.

Müller, G. 1981. Die Schwermetallbelastung der Sedimenten des Neckars und Seiner Nebenflüsse. *Chemiker-Zeitung* 6, 157.

Önder, S., Dursun Ş. 2005. Air borne heavy metal pollution of Cedrus libani (A. Rich.) in the city centre of Konya (Turkey). *Atmospheric Environment* 40, 1122-1133.

Pelin, S. 1977. Alucra (Giresun) Güneydoğu Yöresinin Petrol Olanakları Bakımından Jeolojik İncelemesi. Doçentlik Tezi, Yayın No: 87, , K.T.Ü., Trabzon.

Reimann C., De Caritat P. 2000. Intrinsic flaws of element enrichment factors (EFs) in environmental geochemistry. *Environ. Sci. Technol*. 34, 5084-5091.

Rodríguez-Barroso, M.R., Benhamou, Y., El Moumni, B., El Hatimi I., Garica-Morales, J.L. 2009. Evalution of Metal contamination from North of Morrocco: geochemical and statistical approaches, *Environ Monit Asses* 159, 169-181.

Rubio, B., Nombela, M.A., Vilas, F. 2000. Geochemistry of major and trace elements in sediments of the Ria de Vigo (VW Spain): an assessment of metal pollution.*Mar. Pollut Bull* 40, 968-980.

Saur, E., Juste, C. 1994. Enrichment of trace elements from long-range aerosol transport in sandy podozolic soils of southwest France. *Water Air Soil Pollut* 73, 235-246.

Sposito, G. 1984. The surface chemistry of soils. Oxford University Press, New York.

Sutherland, R.A. 2000. Bed sediment associated trace metals in an urban stream, Oahu, Hawaii. *Environ Geological*., 39, 611-627

Taylor, S.R., McLennan, S.M. 1995. The geochemical evolution of the continental crust. *Reviews of Geophysics* 33, 241-265.

Tokel, S. 1972. Stratigraphical and volcanic history of Gümüşhane region (Kuzeydoğu Turkiye), Ph. Thesis, University College, London.

Topuz G., Altherr, R., Siebel, W., Schwarz, W.H., Zack, T., Hasözbek, A., Barth, M., Satır, M., Şen, C. 2010. Carboniferous high-potassium I-type granitoid magmatism in the Eastern Pontides: The Gümüşhane pluton (NE Turkey). *Lithos* 116, 92-110.

Topuz, G., Altherr, R., Schwarz, W.H., Dokuz, A., Meyer, H.P. 2007. Variscan amphibolitefacies metamorphic rocks from the Kurtoğlu metamorphic complex (Gümüşhane area, Eastern Pontides, Turkey). *Int. J. Earth Sci. (Geol. Rundsch)* 96, 861-873.

Turekian, K.K.,Wedepohl, K.H. 1961. Distribution of the elements in some major units of the earth's crust. *Bulletin of the Geological Society of American* 72, 175-192.

Vald'es, J., Vargas, G., Sifeddine, A., Ortlieb, L., Guinez, M., 2005. Distribution and enrichment evaluation of heavy metals in Mejillones Bay (23°S), Northern Chile: Geochemical and statistical approach, *Marine Pollution Bulletin* 50, 1558-1568.

Vural, A., Şahin, E., 2012*a*. Gümüşhane İli Şehir Merkezinden Geçen Devlet Karayolundaki Akasyalarda Ve Toprakta Trafiğe Bağlı İz Element Birikimine Ait İlk Bulgular. *65. TJK Kurultayı Bildiri Özleri Kitabı*; 2-6 Nisan 2012, Ankara,162-163.

Vural, A., Şahin, E., 2012*b*. Gümüşhane Şehir Merkezinden Geçen Karayolunda Ağır Metal Kirliliğine Ait İlk Bulgular. *Gümüşhane Üniversite, Fen Bilimleri Enstitüsü Dergisi* 2, (1), 21-35.

Wheeler G.L., Rolfe G.L. 1979. Relationship between daily traffic volume and the distribution of lead in roadside soil and vegetation. *Environ Pollut*.18, 265.

Yaylalı-Abanuz, G., Tüysüz, N., Akaryalı, E. 2011. Soil Geochemical Prospection for Gold Deposit in the Arzular Area (NE Turkey), *Journal of Geochemical Exploration* 112, 107-117

Yaylalı-Abanuz, G., Tüysüz, N., 2009. Heavy metal contamination of soils and tea plants in the eastern Black Sea region, NE Turkey. *Environ Earth Sci*. 59:131-144.

Yılmaz, Y.1972. Petrology and structure of the Gümüşhane granite and surrounding rocks, North-Eastern Anatolia.Doktora Tezi, Londra Üniversitesi, 260 s.

Yılmaz, Y. 1974. Geology of the Gümüşhane granite (Petrography), İstanbul Üniversitesi Fen Fakültesi, Mecm. B., 39, 157-172

Zhang, X. Bao, Z.Y., Tang, J.H. 2006 Application of the enrichment factor in evaluation of heavy metal contamination in the environmental geochemistry. *Geol Sci Technol Infrom* 25(1), 65–72.

Bulletin of the
Mineral Research and Exploration

http://bulletin.mta.gov.tr

STABILITY STUDIES OF THE EASTERN SLOPES OF AFŞİN-ELBİSTAN, KIŞLAKÖY OPEN-PIT LIGNITE MINE (KAHRAMAMMARAŞ, SE TURKEY), USING THE 'FINITE ELEMENTS' AND 'LIMIT EQUILIBRIUM' METHODS

İbrahim AKBULUT[a], İlker ÇAM[a], Tahsin AKSOY[a], Tolga ÖLMEZ[a], Dinçer ÇAĞLAN[b], Ahmet ONAK[a], Süreyya SEZER[a], Nuray YURTSEVEN[a], Selma SÜLÜKÇÜ[a], Mustafa ÇEVİK[c] and Veysel ÇALIŞKAN[d]

[a] *General Directorate of Mineral Research and Exploration, Ankara*
[b] *Demir Export A.Ş., 06440, Ankara*
[c] *Çevre ve Şehircilik Bakanlığı, Adıyaman İl Müdürlüğü, Adıyaman*
[d] *Adıyaman İl Özel İdaresi, Adıyaman*

Keywords:
Elbistan, Kışlaköy,
Coal, Finite Elements,
Slope Stability

ABSTRACT

In open pit mining from the safety point of view it is very important that physical and mechanical characteristics of the dug-out materials are carefully studied, and geological and geotechnical characteristics should also be considered in planning bench slopes of the dug-out materials. The purpose of this study is to work out the stable slope geometry of the eastern permanent slopes in the Kışlaköy open pit lignite mine of the Afşin-Elbistan Linyit İşletmesi. In the Kışlaköy open pit mine, 35 geotechnical drillings totalling 3393.20 m were made for the geotechnical studies and to work out slope sizing. A total of 250 vertical electrical drillings (DES) were also made to study tectonic features and lithological changes which do not have surface expressions. All these data have been used in this study. Design analyses showed that black coloured clay bands with high plasticity present in between lignite horizon is the most important unit controlling slope stability. Slope stability analyses have in general been conducted using the 'finite elements' and the 'limit equilibrium' method to suit block sliding model and to suit different groundwater conditions. In the analyses for the stresses affecting the slices; central part of the slice has been taken as a base and the 'finite elements' stability studies have been conducted then the findings have been compared. According to this it is understood that if stresses affecting the slices are conducted by the 'finite elements' method then calculated factor of safety on the bench base would be more from 1% to 7%, and in the slope angles it would be more from 1% to 23%.

1. Introduction

Kışlaköy open pit operation is situated within the limits of Afşin-Elbistan town in Kahramanmaraş South Eastern Turkey (Figure 1). Studies indicated that lignite reserves in the Kışlaköy section is 578 million tons and in the Afşin-Elbistan province it is total of 3.4 billion tons (Yörükoğlu, 1991). In his study Yörükoğlu (1991) reported that the lignite quality in the original base is; sub thermal value1170 Kcal/Kg, moisture 55%, ash 17%, combustible material 28%, total S, volatile material 18.69%, C 17.1%, H_2 1.52%.

Among the workers who carried out studies in and around the study area; Özbek and Güçlüer (1977) who carried out hydro geological studies in the Maraş-Elbistan-Çöllolar section; Gürsoy et al, (1981) carried out reserve estimation studies for the part in

* *Corresponding author : ibrahim.akbulut@mta.gov.tr*

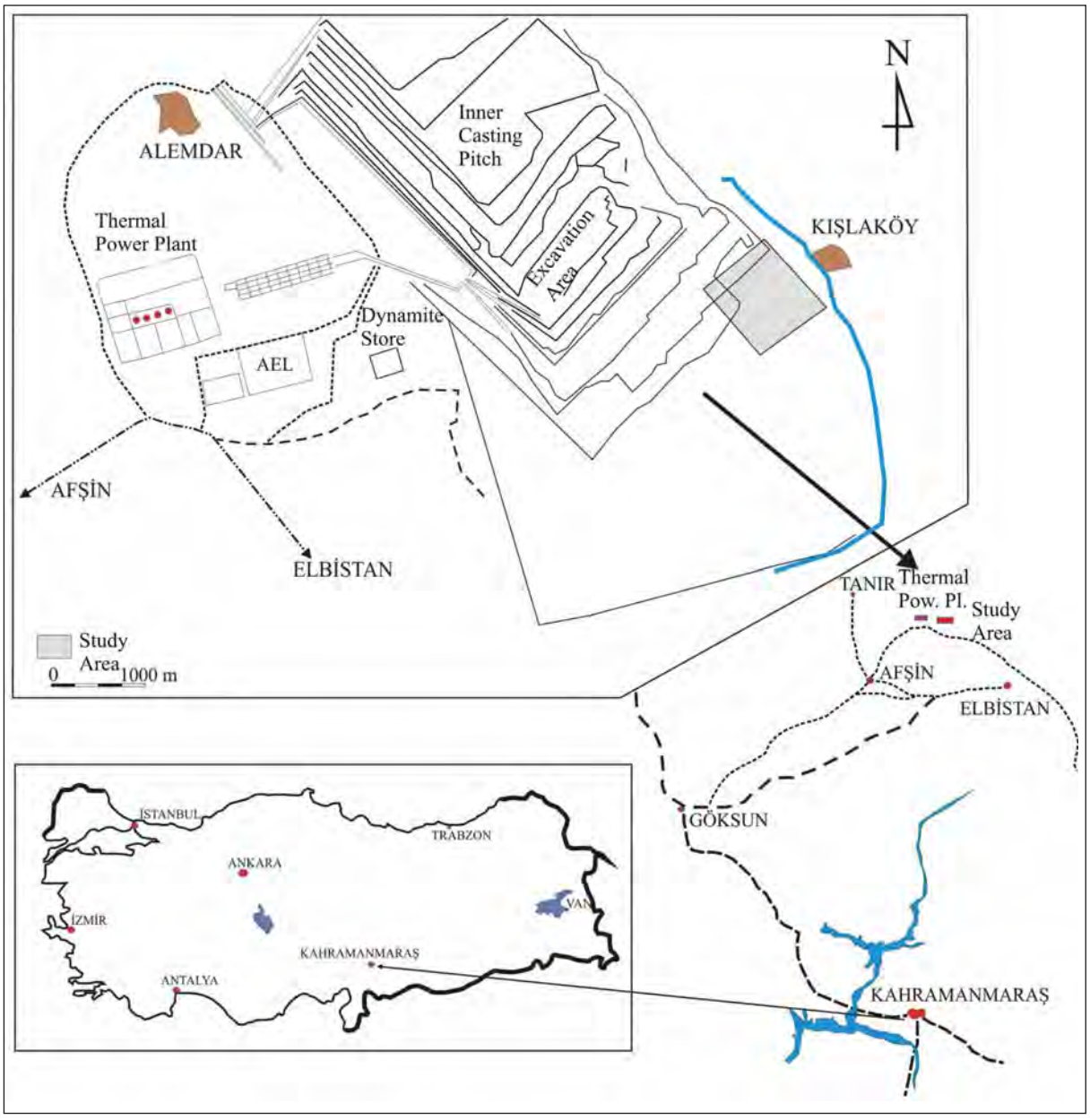

Figure 1- Location map of the study area.

between Harman and Sinekli Villages, they reported that the age of the lake sediments in that part was Pliocene-Pleistocene; Ergüder et al. (2000) carried out geophysics studies in the eastern end slopes of the Kışlaköy open pit and found out the attitudes (strike and dip) of the faults in the area; Koçak et al. (2001) conducted reserve estimation studies and reported that known reserves were 4.3 billion tons, economically mineable reserves were 3.8 billion tons. Koçak et al. (1985), Ural and Yüksel (2000), Akbulut et al. (2007, 2008) also conducted slope stability work in the area.

In the Kışlaköy mine sustainability of lignite production mostly depends upon the stability of the permanent slopes. Because of this, within the scope of this geotechnical study, a total of 35 drillings amounting to 3393.20 m have been conducted. To establish geomechanical parameters disturbed/ undisturbed samples from every lithological unit have been collected.

All of the data gathered from laboratory tests have been evaluated together and have been subjected to finite elements and limit equilibrium methods for

stability analyses and results of both methods have been compared.

2. Geology

In the study area Pliocene-Pleistocene lake sediments, Quaternary units consisting stream material and slope debris are present (Figure 2a).

At the base of the study area turquoise coloured clays are present. As they form the base of the lignite horizons they are also known as bottom clay. These greenish blue coloured (turquoise coloured) bottom clays have carbonate concretions and display less-medium plasticity and have thin-medium beddings (Figure 2b).

Lignite horizon concordantly overlies the basement clay. The unit is black-light brown coloured, has medium hardness and medium-thin beddings. There are 1-80 cm thick, black coloured clay levels, rich in bitumen with high plasticity and green coloured clay levels in places with medium-high plasticity and with fine size pebbles. As it is transitional with gray Gidya unit the lignite horizon has numerous Gidya alternations. Gürsoy et al., (1981) gave Pliocene-Pleistocene age to the lignite's. The Gidya unit concordantly overlies the lignite horizons. The unit has brownish gray-dark gray clay levels. It is very soft with medium-thick beddings. Beige Gidya concordantly overlies gray Gidya. It has light brown-beige coloured silty clays with abundant

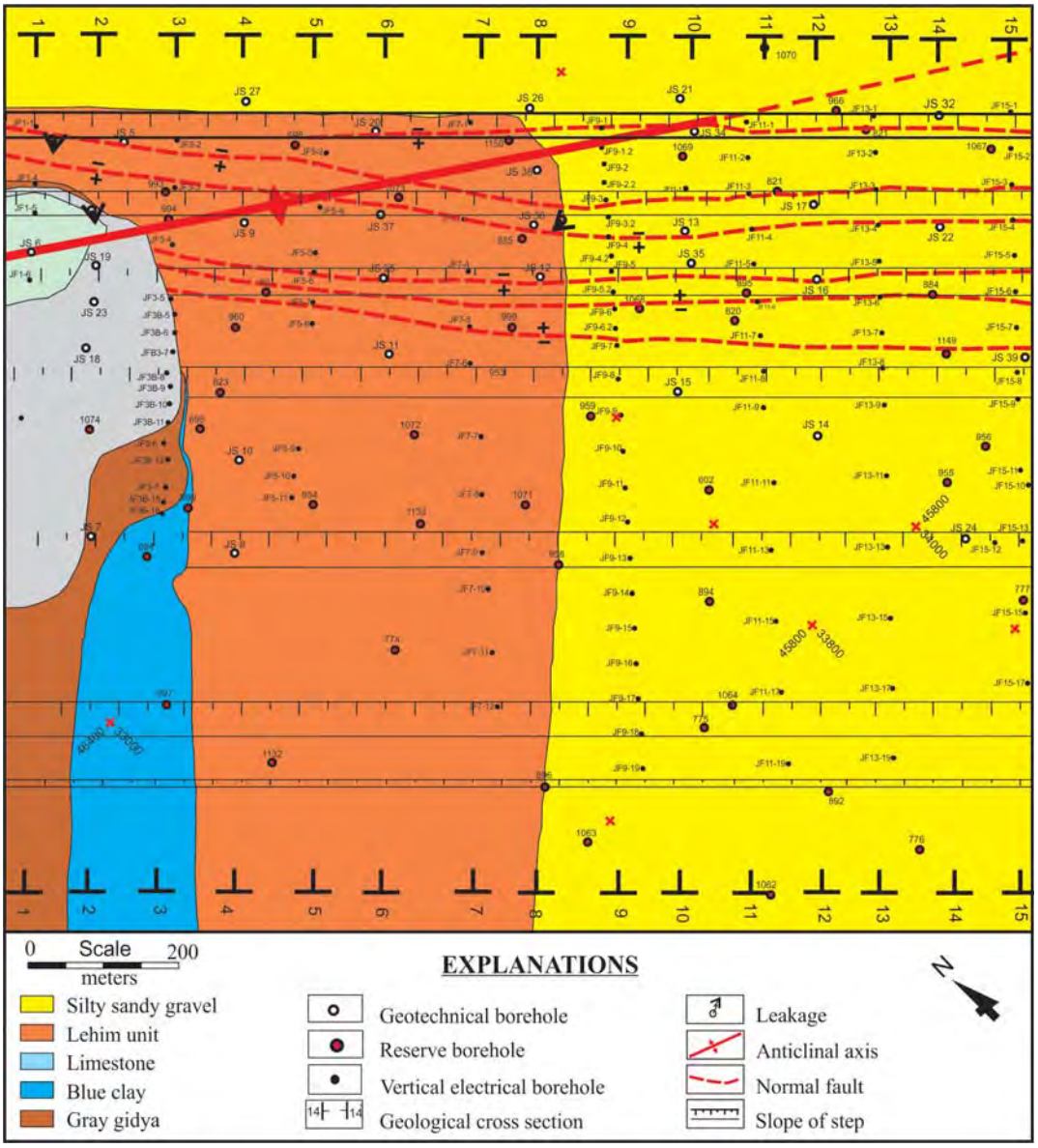

Figure 2- a. Geological and engineering geological map of the study area.

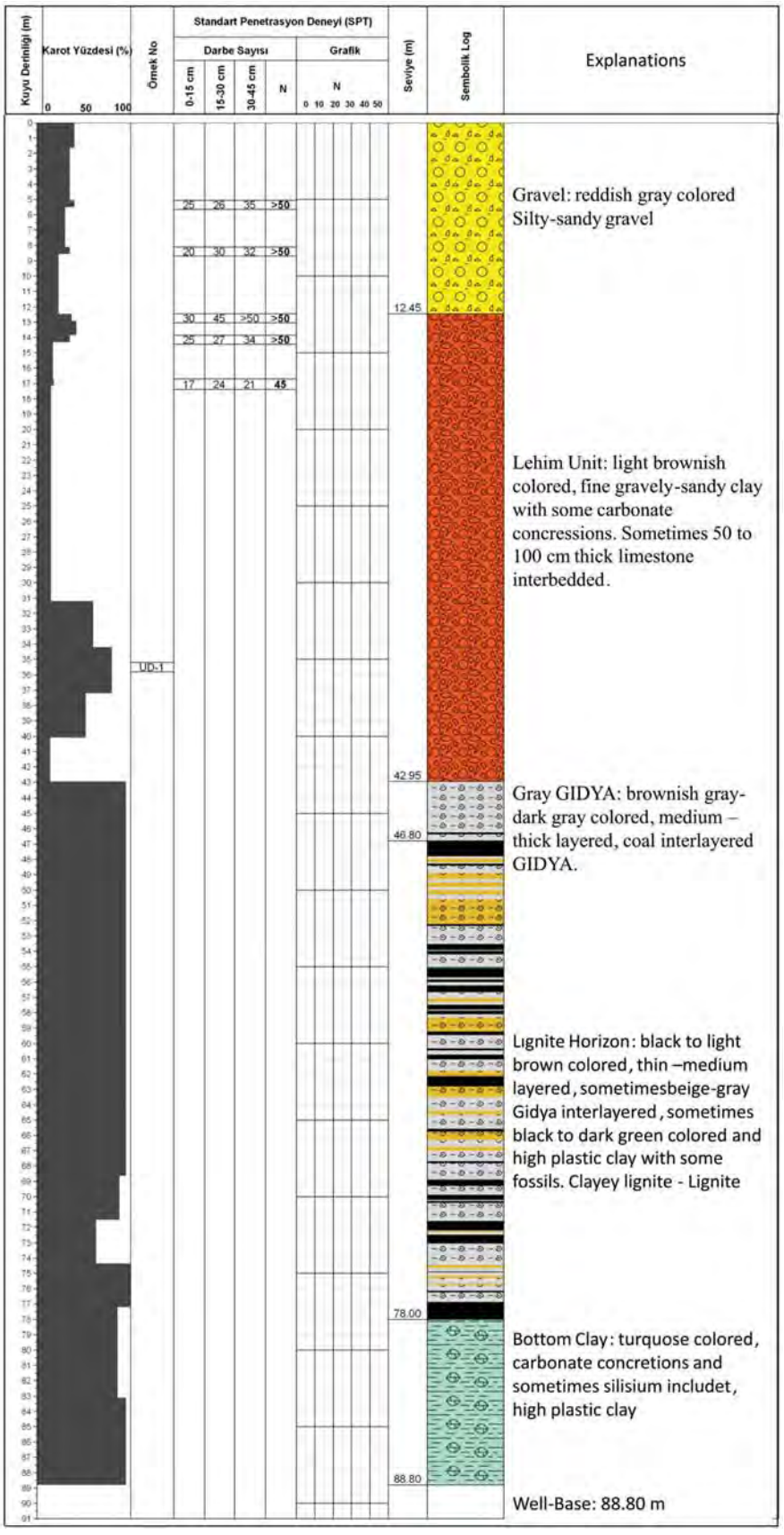

Figure 2- b. Geological and engineering geological map of the study area.

Gastropods. The units represents lake environment and has limestones at the top (Gürsoy et ., 1981). Limestones are light gray-gray coloured, have abundant fossils, hard-very hard, with medium-thick beddings, broken surfaces have sharp corners. Quaternary Lehim sequence discordantly overlies the limestones and have extensive coverage in the study area.

Geophysics studies revealed the attitudes of the faults which had no surface expressions. These faults run NW-SE direction, developed along the eastern slopes at the edge of the basin.

3. Geotechnical Study

Geotechnical studies have been carried out in two stages. In the first stage; geotechnical drillings, geophysical studies and samplings have been carried out. In the second stage; laboratory test results of the collected samples have been evaluated.

To be able to establish lateral and vertical extensions of the units present in the study area General Directorate of Mineral Research and Exploration (MTA) carried out total of 35 geotechnical drillings amounting 3393.20 metres (Akbulut et al., 2008).

In all of the drillings depths of ground water levels have been controlled. In the unexcavated parts the ground water level was 4.00 m; in the excavated parts it was 30 m; in the parts where drillings intercepted the basement rocks, it was 61.50 m It is possible that 61.50 m static ground water level is the water level of the karstic parts.

Within the scope of the geophysics study a total of 250 vertical electrical drillings (VED) have been conducted and results have been evaluated. Data obtained from these VED's have been compared with the results of the mechanical drillings and attempts have been directed to identify all possible tectonic features.

To establish geo-mechanical parameters to be used for designing permanent slopes; a square specimen cutter 10 cm x 10 cm x 3 cm dimensions was used and 4 sets of undisturbed samples from the fresh face of the units and 4 disturbed samples for the index studies have been collected. By using thin edge tubes (shelby) 31 undisturbed samples from the drillings have also been collected.

In the laboratories on the ground type samples in accordance with ASTM (1994) abd BSI 1377 (1990) strength and index tests have been conducted.

4. Geotecnical Evaluations

Within the scope of geotechnical evaluations first of all engineering classifications of the lithological units have been made. In the engineering classifications 'unified soil classification' (ASTM D-2487 1994)) have been used to evaluate grain size distribution analysis and Atterberg limits. According to this; sandy parts of the Lehim Sequence is in the SM-SP group, whereas silty parts in the MH group, and the whole section is in the CH group. They all are classified as clays with "high plasticity".

Gray Gidya is represented with MH group and bottom clay with CH-CL-MH group soils. Depending upon the result of liquid limit test, black clays have been classified as OH-MH group soils.

Fine grained grounds have abundant organic materials. In the plasticity chart they are classified as organic silt below A-line and have 'high – excessively high' liquid limit value (IAEG Commission, 1981).

In the fine grained grounds the ratio of plasticity index to percentage (%) of clay is described as activity coefficient and this gives information on the clay minerals. In Figure 3 in the activity abacus GrayGidyashows "Medium – low activity", Lehim and Black Clay show "Medium-high-very high activity"distributions.

According to atterberg limits classification system these units have been classified as; Lehim Sequence = tight-very tight; Gray Gidya = very soft; Black Clay = hard-very hard; Bottom Clay = hard-very hard (Akbulut et al., 2008).

Undisturbed samples collected from the study area to determine geomechanical parameters to be used in design analysis of permanent slopes have been subjected to relevant tests.

Shear tests were carried out depending upon the location of the samples collected, taking designated normal stress (σ_n) values into account, in line with the standards (ASTM D-3080) under different vertical load stages, 1 x 2.5 inch diameter and/or 6 x 6 x 2 cm dimensions These tests were carried out on the materials, at least 3 times for each unit, so peak and residual shear strength parameters have been established for each unit.

Akbulut et al., (2007) carried out back analyses and found that landslides developed in the Lehim Sequence and under the control of the black plastic

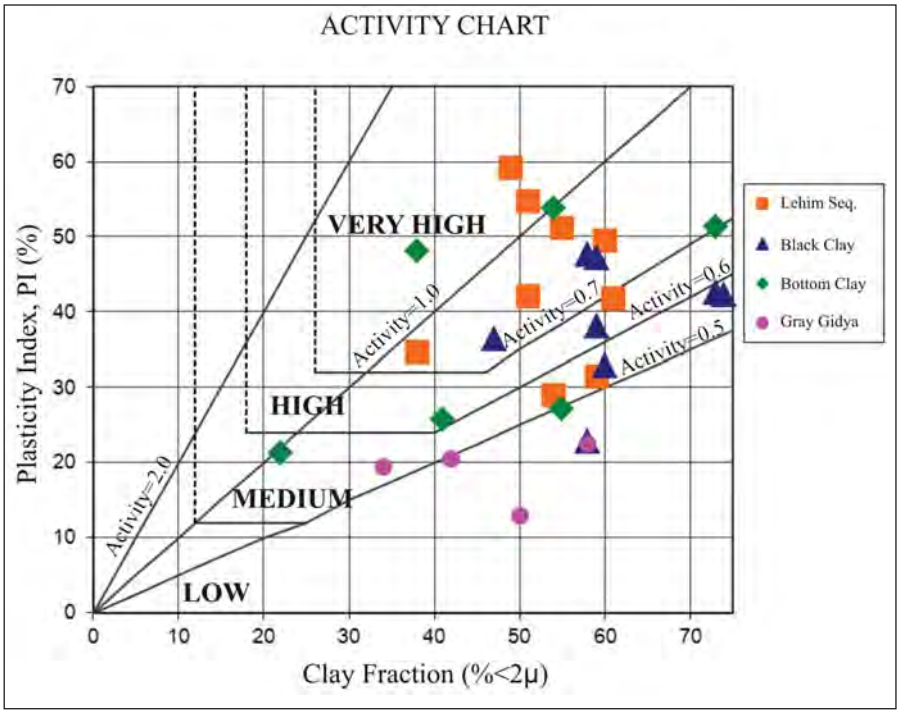

Figure 3- In the study area distribution of fine grained units on the Activity Chart.

clay in the lignite horizon, residual shear strength parameters were effective during the process of sliding. Due to these results, residual shear strength parameters, obtained from the laboratory tests have been used for the stability analyses.

In the field studies it was found that sometimes fault zones had clay fillings (gouge) and in other areas they didn't have filling (gouge) materials. Analyses have been carried out for the differing situations; "no discontinuity", and "discontinuity present" that planes (fault) having fault materials in them. Geo-mechanical parameters used for the design analyses are given in table 1.

5. Stability Design Analyses

In the final slope designs, factor of safety (FOS) value has great importance. In a simple term FOS value is defined as; ratio to resisting to sliding forces. In the stability analyses if FOS=1, then it is considered as equilibrium (balance) condition and during sliding this condition is considered valid. Because of that, in designing slopes, FOS values are preferred to be greater than 1 (FOS>1) not to have instability.

In this present study for the permanent slope designs, FOS coefficient is suggested to be FOS=1.3.

Table 1- Geo-mechanical parameters used in design analyses (Akbulut et al., 2008).

Unit	Unit volume weight (γ, kN/ m^3)	Residual internal friction angle (ϕ, °)	Residual cohesion (c, kPa)
Lehim	17,85	21,38	21,79
Limestone	20,78	26,80	51,80
Gray Gidya	15,05	34,84	10,54
Lignite	10,90	33,30	12,76
Black clay	15,90	11,20	20,82
Basement clay	17,46	25,83	14,19
Discontinuity plane	10,90	29	0,1
Fault material	12,57	9,10	43,31

On the other hand, it was suggested that in a short period of time if materials are loading at the heel of the slopes then FOS= 1.2 could be acceptable.

In the prepared design analyses, the "General Limit Equilibrium" (GLE) (Fredlund and Krahn, 1977) method has been considered as a base. GLE takes the forces into account between slices, at the same includes momentum and force balances into calculations. For the designs GEO-SLOPE (SLOPE/W 2007) software has been used. This software provides solutions with the "finite elements and limit equilibrium" approach. It could carry out (2D) analyses, accounts seismic forces and ground water level and provides solutions with various methods.

Permanent slope analyses have been carried out primarily for the single benchs. This analysis aims at working out safe "slope angle and slope heights" for one bench. Depending upon the character of the ground different models has been used. If the ground is not firm and consists of loose materials then "circular sliding model" is necessary to obtain a safe result. For firm rocky mass then the "block sliding model" was used.

6. Comparison of Calculated Design Analyses Made by Using 'Finite Elements' and 'Limit Equilibrium' Methods

So far the "Limit Equilibrium" method has been successfully used in the slope stability analyses. The 'Finite Elements' method has been used in all engineering problems as well as in the slope stability analyses. The most important difference between the "Finite Elements" and the "Limit Equilibrium" method is that, the "Finite Elements" shows the stress distribution in a more realistic way and enables stability analysis to be carried out.

In the 'Limit Equilibrium' methods, when trying to establish strength equilibrium in the process of achieving results, FOS value is accounted to be the same for each slice. This causes difference between the calculated stress distributions along the sliding plane than the actual one. In the "Finite Elements" method, an equilibrium is established for the stress and deformation conditions, so calculations would be based on more realistic stress distribution data. In the "Limit Equilibrium" method central part of each slice is taken as a base in calculating the stresses effecting to the slices. In the "Finite Elements" method, on the other hand, the stresses effecting base of each slice is calculated for the analyses. "Two methods" term is used to explain the stress calculations affecting the slices, all other calculations are same.

In this study above mentioned differences have been taken into account and analyses have been carried out accordingly. For the design analyses first of all to establish bench geometry, Lehim Seq., bottom clay and for the lignite, safety coefficients have been taken as FOS= 1.2 and FOS=1.3. According to these values graphics have been prepared showing "Slope height (H) – Slope angle (β)" relationship (Figures 4, 5, 6). As it is seen in the graphics, in the "Finite Elements" method, in the Lehim Seq., when F= 3, the bench with H=20 m would have β= 35.8° bench angle; in the bottom clay for a H=25 m bench, bench angle would be β= 30.5°; in the lignite horizon for a H= 25 m bench, bench angle would be β= 46.0°. In the "Limit Equilibrium" method in the Lehim Seq. for a H= 20 m bench, bench angle would be β= 33.4°; in the bottom clay, for a H= 25 m bench, bench angle would be ,= 28.8°; in the lignite horizon, for a H= 25 m bench, bench angle would be β= 45.3°. This show that on the bench base for the same safety coefficient (F=3) there is 1% to 7% difference in calculations between "Finite Elements" and "Limit Equilibrium" methods, "Finite Elements" being higher.

Akbulut et al., (2007) studied the landslides developed in the study area and concluded that failure developed in "block sliding model". As the failures in the lignite horizon developed in the block sliding model, analyses have been carried out to fit to this model. Taking discontinuity planes into account general slope analyses have been repeated.

In the study area to understand geology (structure), 15 cross sections right angle to the planned slopes have been prepared. In these sections geology (structure) appeared same, so stability analyses have been carried out on 7 sections.

Slope stability analyses have been carried out by applying 'Finite elements' and 'Limit equilibrium' methods to find solutions. According to F= 1.2 and F= 1.3 safety coefficients, graphics showing ?Slope height (H) – Slope angle (,)?relations. One of the analysed sections was 14-14 (Figure 2). ?General slope angle – Safety coefficient" and ?Groundwater level – General slope angle" relations graphics for 14-14 section have been prepared. In Figure 7 (a, b) discontinuity plane, in figure 8 (a, b) in the case of discontinuity plane being present are given. In Figure

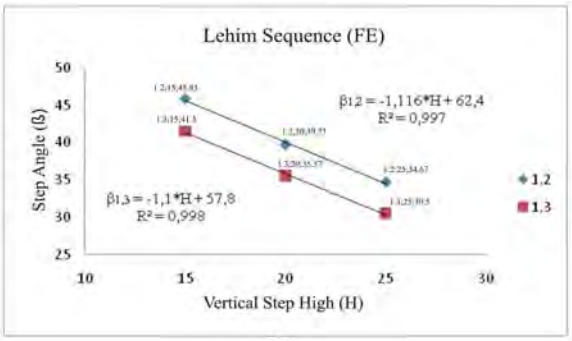

(a)

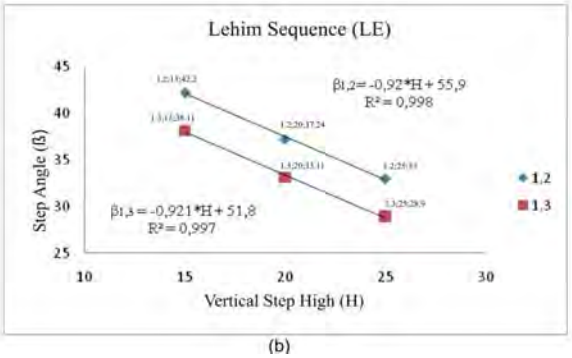

(b)

Figure 4- For the Lehim unit;

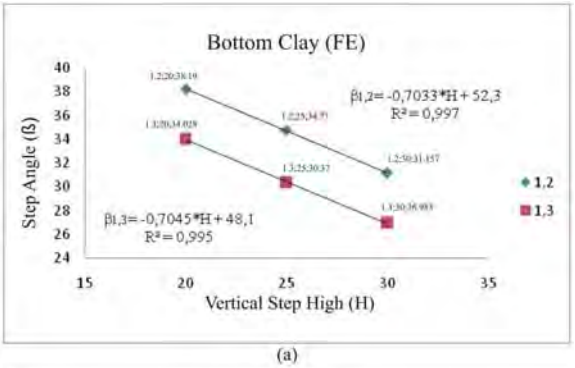

(a)

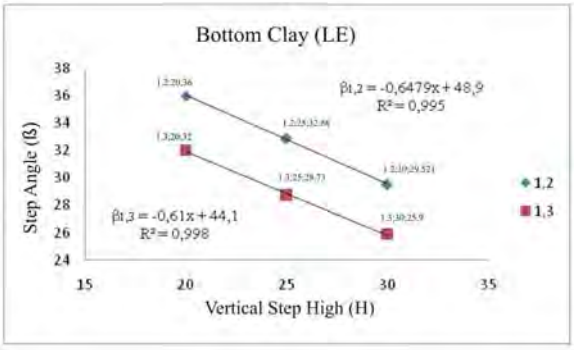

Figure 5- For Basement clay;

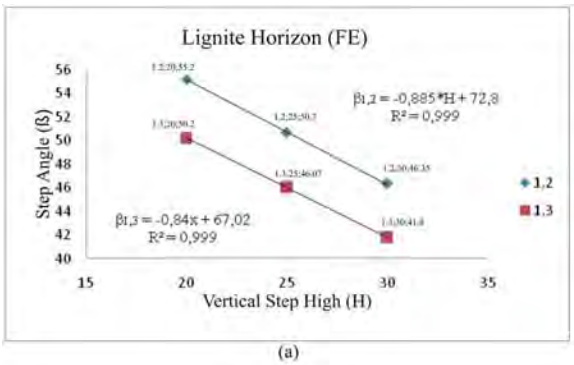

(a)

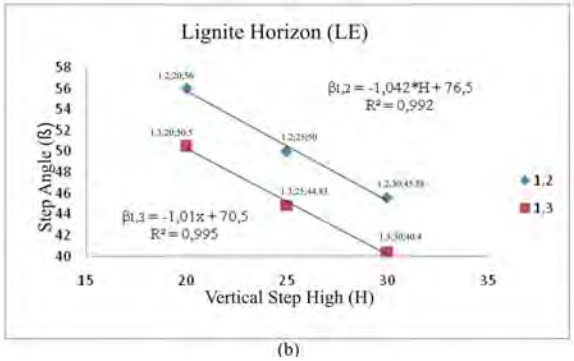

(b)

Figure 6- For lignite horizon; according to; a) 'Finite elements' (FE), b) 'Limit equilibrium' (LE) relationship between bench height (H), bench angle (β).

9 (a, b) in the case of fault plane being present 'Finite elements' and 'Limit equilibrium' methods applications in; (a) FOS coefficient – general slope angle, (b) general slope angle – groundwater level relations have been given. In Figure 10, position of slope profile and critical sliding plane is given. Collective results are given in table 2.

Under FOS = 1.3 conditions if general slope angle is not a discontinuity plane; according to the 'Finite elements' method it would be between 12.8° and 17.4°, according to the 'Limit equilibrium method it would be between 10.1° and 14.9°; on the other hand, if general slope angle is a discontinuity plane then according to the ' Finite elements' method; it would be between 11.7° and 14.0°, according to the 'Limit equilibrium' method, between 10.4° and 12.5°; if sliding surface is a fault plane, then, according to the 'Finite elements' method it would be between 11.1° and 12.2°, according to the 'Limit equilibrium' method between 10.2° and 11.9°.

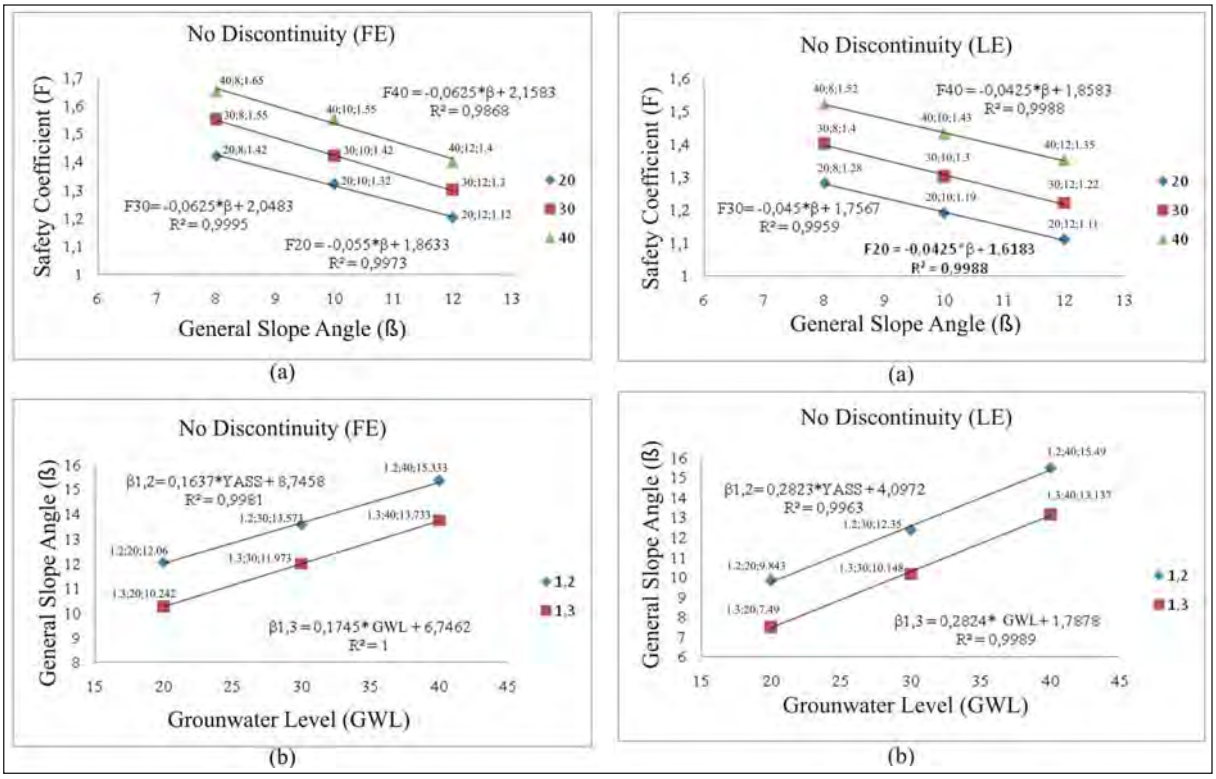

Figure 7- a) In the case of no discontinuity, according to the "Finite elements"method; b) In the case of no discontinuity, according to the "Limit equilibrium"method; a) FOS coefficient – General slope angle, b) General slope angle – Groundwater level relations.

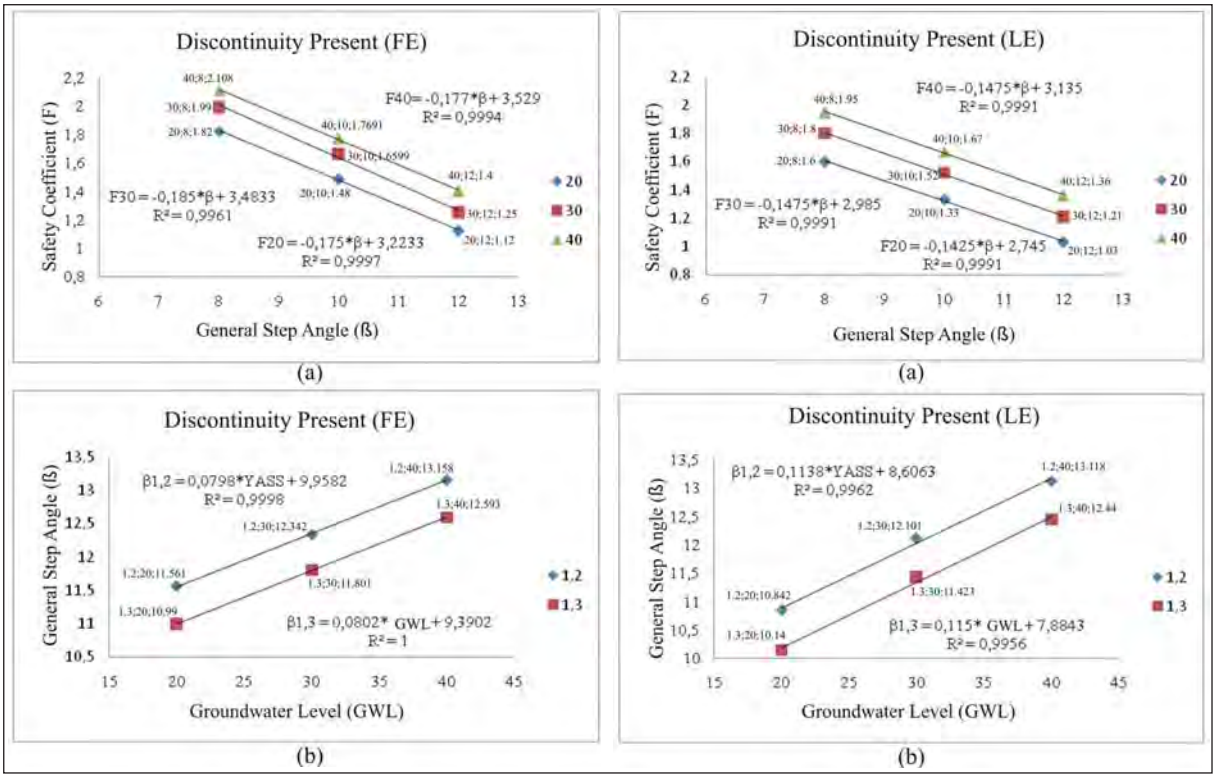

Figure 8- a) In the case of discontinuity present, according to the "Finite elements"method; b) In the case of discontinuity present, according to the "Limit equilibrium"method; a) Safety coefficient – General slope angle, b) General slope angle – Groundwater level relation.

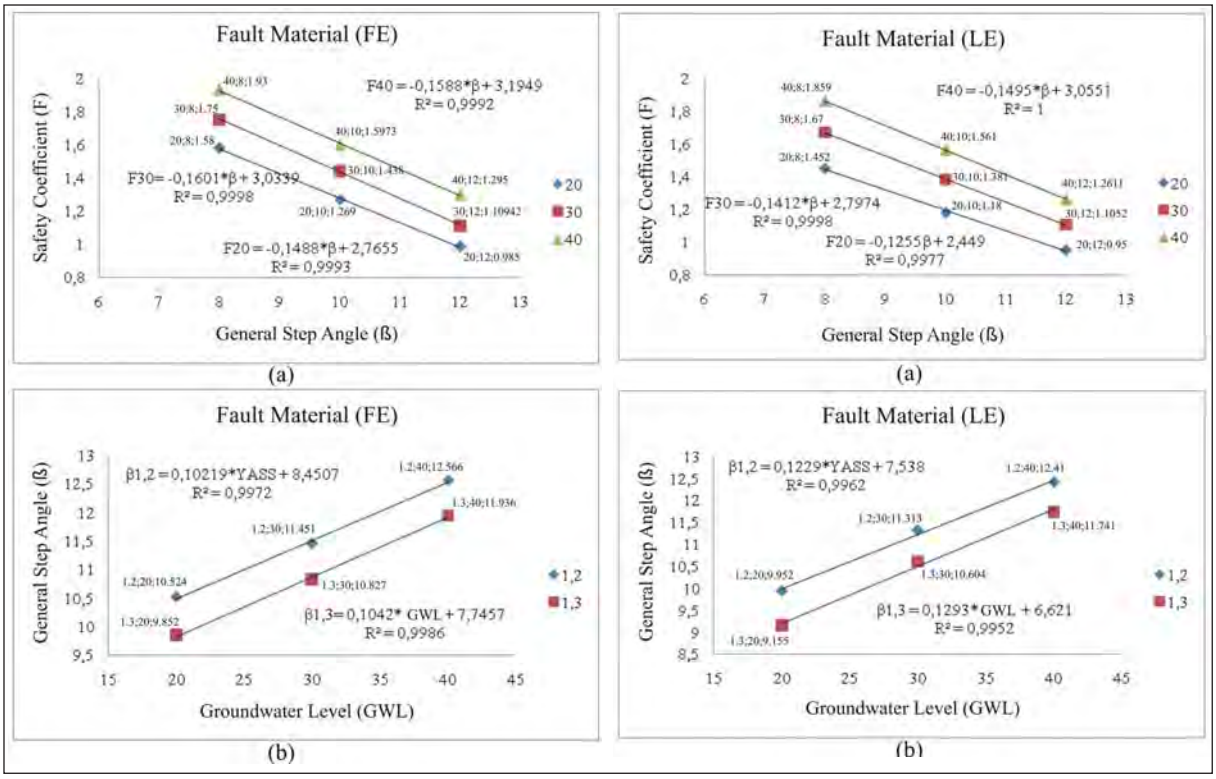

Figure 9- a. In the case of fault material present, according to the 'Finite element' method; b.In the case of fault material present, according to the 'Limit equilibrium method; a) FOS coefficient – General slope angle, b) General slope angle – Groundwater level relation.

Table 2- Collective analyses results of the representative sections from the study area (for GWL =30 m) (FE= Finite Elements, LE= Limit Equilibrium).

Section no	General slope angle (β) (°)											
	No discontinuity plane present				According to the discontinuity surface				According to the fault plane			
	FE	LE	FE	LE	FE	LE	FE	LE	FE	LE	FE	LE
	F=1,2	F=1,3	F=1,2	F=1,3	F=1,2	F=1,3	F=1,2	F=1,3	F=1,2	F=1,3	F=1,2	F=1,3
2-2'	19,0	17,4	17,4	14,9	12,6	11,7	11,3	10,4	11,7	11,2	11,4	10,5
4-4'	17,2	15,7	16,1	14,3	13,4	12,6	12,5	11,8	13,2	12,2	12,7	11,9
6-6'	19,2	17,5	15,2	13,4	14,9	14,0	13,3	12,5	13,9	13,0	12,5	11,7
8-8'	16,0	14,2	14,9	12,8	12,4	11,7	11,2	10,5	11,8	11,1	11,0	10,2
10-10'	14,0	12,8	12,8	11,4	12,3	11,7	11,3	10,7	12,1	11,5	11,4	10,7
12-12'	15,2	13,3	13,3	11,2	12,4	11,9	11,9	11,4	12,3	11,6	11,4	10,8
14-14'	13,7	12,0	12,6	10,3	12,4	11,8	12,1	11,4	11,5	10,9	11,2	10,5

In the "Finite elements"method when FOS coefficients become 7% higher, it would be 20% more in the general slope (as total slope height increases). In the open pit operations these analyses must be compared with the actual positions and particularly also with the back analyses. When slope stability matters have been solved with the "Finite elements" method, if the findings are in accord with the actual situations then keeping with the safety, using this method would be advisable.

If the "Finite elements" method has been used general slope angle would be about β=11°. The "Limit equilibrium"method is also considered for slope designs and it has less numbers of samples. Because of this, in this study with traditional "Limit equilibrium"method general slope angle was determined as β=10°.

According to these analyses results if the general slope angle was calculated with the 'Finite elements'

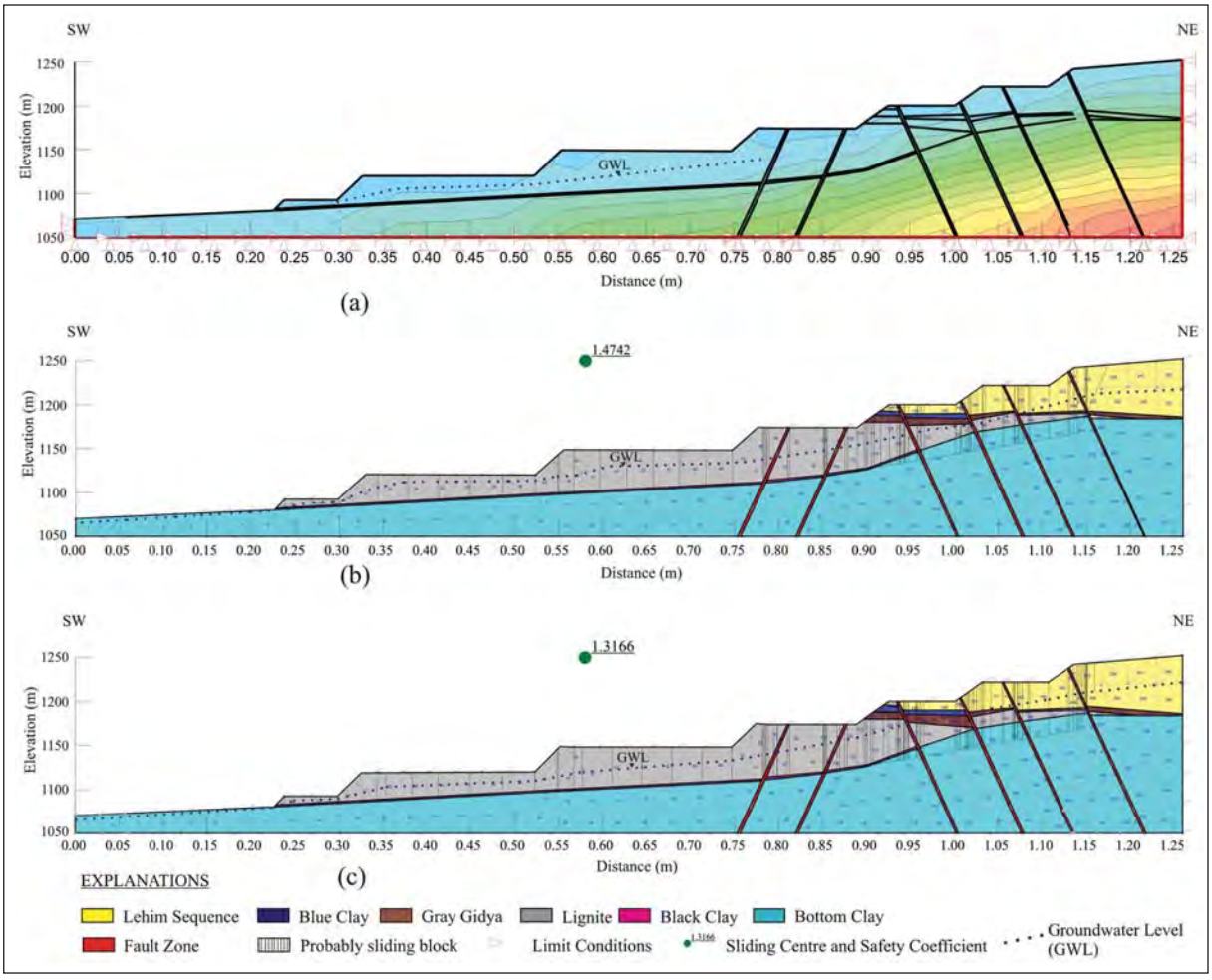

Figure 10- a) The maximum total stress distribution by using 'Finite elements' method, b) according to 'Finite elements' method; analysed slope profile and position of critical sliding plane, c) according to 'Limit equilibrium' method analysed slope profile and position of critical sliding plane.

method, FOS coefficients would be between 1% to 23% higher then if it was calculated with the 'Limit equilibrium' method.

7. Results and Suggestions

The following results have been obtained from the conducted geotechnical studies in the Kışlaköy (Afşin, Elbistan, Kahramanmaraş, South Eastern Turkey) lignite open pit mine.

According to unified soil classification, which take grain size and viscosity limits of the units together into account the Lehim Sequence has been grouped as SM-SP, MH and CH for whole section; Gray Gidya as MH, Bottom clay as CH-CL-MH and black clay as OH-MH class soils.

In the bench base analyses when FOS=1,3, in the 'Finite elements' method in the Lehim unit of a bench with H=20 m, bench angle would be β= 35.8°, in the Bedding clay, for a bench H= 25 m high, bench angle would be β= 30.5°, in the lignite horizon for a bench H= 25 m high, bench angle would be β= 46.0°. In the 'Limit equilibrium' method in the Lehim Sequence for a bench H= 20 m high, bench angle would be 33.4°, in the Bottom Clay for a bench H= 25 m high, bench angle would be β= 28.8°, in the Lignite Horizon for a bench H= 25 m high, bench angle would be β= 45.3°.

When there is a discontinuity plane, when F=1.3 is in the 'Limit equilibrium' condition according to 'Finite elements' method, general slope angle would be 11.7° - 14.0°, in the 'Limit equilibrium' method, it would be 10.4° - 12.5°.

When FOS coefficients are calculated at the bench base with the "Finite elements" method, they would

be 1% to 7% higher then if they were calculated with the 'Limit equilibrium' method. In the general slopes this rate changes from 1% to 23%.

The analytical results carried out by finite element and limit equilibrium methods should be compared with actual conditions in open pets particularly by using previous analyses.

If the calculations were done by finite element methods, the slope angle would be 11°. But, according to the conventional limit equilibrium method, the slope angle is calculated as 10° and it is proposed to open with angle degree 10° for this area.

Received: 28.03.2013
Accepted: 31.10.2013
Published: June 2014

References

Akbulut, İ., Aksoy, T., Çağlan, D., Ölmez, T. 2007. Afşin-Elbistan Kışlaköy Açık Kömür İşletmesi Şev Stabilitesi Çalışması, *Maden Tetkik ve Arama Genel Müdürlüğü Rapor* No: 11194 (unpublished).

Akbulut, İ., Aksoy, T., Ölmez, T., Çağlan, D., Onak, A., Çam, İ., Sezer, S., Çevik, M, Çalışkan, V., Yurtseven, N., Sülükçü, S. 2008. Afşin-Elbistan Kışlaköy Açık Kömür İşletmesi 2. Kısım 1. bölüm Şev Stabilitesi Çalışması, *Maden Tetkik ve Arama Genel Müdürlüğü Rapor* No*: 11201* (unpublished).

ASTM (American Society For Testing and Materials), 1994. Annual Book of ASTM Standards-Section 4, Construction, V. 04.09, Soil and Rock; *Building Stones, Astm Publ*. 978 pp.

BSI (British Standards Institution 1377), 1990. Methods of Civil Engineering Purposes, 143 p.

Ergüder, İ., Kızıldağ, İ., Günkel, Ş. 2000. AEL Kışlaköy Açık İşletmesi Doğu Nihai Şevi Jeofizik Rezistivite Etüdü Raporu, *TKİ Genel Müdürlüğü*.

Fredlund, D.G., Krahn, J. 1977. Comparison of slope stability methods of analysis, *Canadian Geotechnical Journal*, 14(3), 429-439.

Gürsoy, E. Özcan, K., Yücel, A.R. 1981. Kahramanmaraş - Elbistan D1 Sektörü Kömür Yatağı Jeoloji Raporu. *Maden Tetkik ve Arama Genel Müdürlüğü Rapor* No: 7054 (unpublished).

IAEG (International Association of Engineering Geology) Commission of Engineering Mapping, 1981. Rock and Soil Description on and Classification for Engineering Geological Mapping, Bull. of The Int. Assoc. of Eng. Geol., 24, 235-274 pp.

Koçak, Ç., Kürkçü, S.N., Yılmaz, S., 2001. Afşin Elbistan Linyit Havzasının Değerlendirilmesi ve Linyit Kaynakları Arasındaki Yeri. *AEL Yayını*.

Koçak, S., Ulusay, R., Selçuk, Ş., İder, H. 1985. TKİ-AEL Kışlaköy Linyit İşletmesi Batı Şevi Stabilite Etüdü. *Maden Tetkik ve Arama Genel Müdürlüğü Rapor* No*,* 7717 (unpublished).

Özbek, T., Güçlüer, S., 1977. K. Maraş Elbistan Çöllolar – B Linyit Sektörü 1977 Yılı Faaliyet Raporu, *MTA Report*, 6352 (unpublished).

Slope, W. 2007. Geo Studio 2004, Vers. 6.2, Geo-Slope International Ltd., Calgary, *Canada*.

Ural, S., Yuksel, F., 2004. Geotechnical Characterization of Lignite-Bearing Horizons In The Afsin-Elbistan Lignite Basin, SE Turkey, *Engineering Geology* 75, 129-146.

Yörükoğlu, M. 1991. Afşin Elbistan Projesi ve TKİ Kurumu AELİ Müessesinde Madencilik Çalışmaları. *Madencilik,* 30, 3.

Bulletin of the
Mineral Research and Exploration

http://bulletin.mta.gov.tr

GEOPHYSICAL ANALYSIS AND MODELLING OF THE SİMAV BASIN, WESTERN ANATOLIA

Ceyhan Ertan TOKER[a]

[a] *MTA Genel Müdürlüğü Jeofizik Etütler Daire Başkanlığı, Ankara, Turkey*

Keywords:
Simav, graben, fault, gravity, magnetic, asta, inversion, modelling, Western Anatolia

ABSTRACT

The various data processing techniques, to illuminate the parameters of the geological structure which are applied in gravity and magnetic potential field methods. Also edge detection procedures are in data processing techniques. In this study, 2D, 3D, inversion and asta technique is one of the new edge detection procedures were applied to clarify correlation between the Simav half graben's deep position and geometry of the tectonic lineaments. The Asta is obtained using the tilt angle.

1. Intruduction

In this work the position of the Simav Graben has been studied using geophysical data by applying 2D, 3D inversion and edge detection techniques. It was important to study if the techniques used in the field had any limitations or expansions and to know if they are general or site specific. As is the case in every discipline and under related disciplines, general and site specific solution relations are interconnected with each other.

The purpose of this study is to have a new 2nd and 3rd dimensional outlook to the Simav half graben and to the faults bordering the graben by applying geophysical techniques.

Bedrock image of the graben, image of the upper crust/lower crust interface,and the corner structure which developed as a result of intersection of the Simav and Naşa Fault Zones has been identified after applying the data processing stages. All of the processes were aimed at gaining the maximum data from the potential field maps and to work out physical parameters of the geology in the maps.

In the previous work; 2nd vertical derivative of the analytic signal (Hsu et al. 1996), horizontal derivative of the 'tilt angle' (Verdusco et al. 2004), 'hyperbolic tilt angle' and 2nd vertical derivative of the 'tilt angle' Cooper and Cowan (2004) methods have been used in the edge zone detection processes.

Ansari and Alamdar (2011) proposed the 'ASTA' technique as a new edge detection method. Original codes were written with the 'Matlab program' and were applied to the synthetic model data. Edge detection processes have been used in the Potensoft data processing software developed by Arısoy and Dikmen (2011). The processing menu does not include an ASTA module. The ASTA module was produced by modifying the program batch from the software and was added to the software menu and has so been used in this study.

As the 'tilt angle' acted like secondary potential, boundaries of the structures became clear so analytic signal relations and variations could be used to study the structures. Later on it passed from the phase filter to the derivative filter. So when 'tilt angle' and analytic signal processes have been applied

* *Corresponding author : toker.ertan@gmail.com*

separately, it was found out that developing negative signal/noise ratio have improved and corner sensitivities of the prism like model structures have been kept. Horizontal derivatives detecting edge boundaries, vertical derivatives localizing the anomaly and analytic signals giving high values at the structure are important contributions. Using the 'Tilt angle' method it was found out that with increasing depth blurring of the edge boundaries is no longer a problem, corner structures are kept and selectable edge zones are detectable.

2. Material and method

Following the introduction of edge detection technique, 'ASTA' components (analytic signal, tilt angle), comparison of the method with the other edge detection techniques have been made in this study. Edge detection and inversion methods have been applied to the field data of Demirbaş and Uslu (1986) and results have been critically discussed.

2.1. Analytic signal and Tilt angle:

Analytic signal:

Analytic signal 'M', Gravity or Magnetic potential field is given as;

$$AS(x,z) = \partial M / \partial x + i\partial M / \partial z \quad (1)$$

Amplitude of the analytic signal is;

$$|AS(Z)| = ((\partial M / \partial x)^2 + (\partial M / \partial z)^2)^{1/2} \quad (2)$$

3D Analytic Signal Theory:

It is easy to produce the analytic signal by computing the derivatives of the magnetic anomaly. Two dimensional Fourier transform pair applying as follows:

$$g(k_x, k_y) = F[f(x,y)] = \iint f(x,y)\, e^{-i(k_x x + k_y y)}\, dx,dy \quad (3)$$

$$f(k_x, k_y) = F^{-1}[g(k_x, k_y)]$$

$$\text{(Equation 3)} = 1/4\Pi^2 \iint g(k_x, k_y)\, k_x, k_y\, dk_x, dk_y$$

If the (k_x) and (k_y) are representing the wave numbers in x and y direction respectively, horizontal and vertical derivatives in the wave number domain by Fourier transform of the M magnetic potential, as well as the different derivative relations, could be determine by using the Eq. 3 (Roest et al., 1982).

If , $\hat{x}$, $\hat{y}$ and $\hat{z}$ are accepted as the unit vectors, 3D anayltic signal would be expressed as follows:

$$AS(x,z) = (\partial M / \partial x)\, \hat{x} + (\partial M / \partial y)\, \hat{y} + i(\partial M / \partial z)\, \hat{z} \quad (4)$$

Passing through real and complex expressions in Hilbert transform pair from the Eq.4:

As the Fourier gradient in frequence domain:

$$\check{r} * F[A(x,y)] = \hat{h} * \nabla F[M] + i\hat{z} * \nabla F[M] \quad (5)$$

The ∇ is the gradient operator in frequency domain.

If the operators are accepted as follows:

$$(ik_x\, \hat{x} + ik_y\, \hat{y} + |k|\, \hat{z});\ \check{r} = \hat{x} + \hat{y} + \hat{z} \text{ ve } \hat{h} = \hat{x} + \hat{y}$$

considering the horizontal and vertical gradient relations of the potential, the real part of the Eq.5 represent the horizontal derivative whereas the complex part represents the vertical derivative (Pedersen, 1989).

$$\hat{h} * \nabla F[M] = i\hat{h} * \mathbf{k} F[M] = i((\hat{h}.\mathbf{k})/|\mathbf{k}|) * |k|\, F[M]$$

$$= i((\hat{h}.\mathbf{k})/|\mathbf{k}|)) * \hat{z} * \nabla F[M] \quad (6)$$

The relationship between the horizontal and vertical derivative is the Hilbert transform operator in frequence domain $|\ [(\hat{h}.\mathbf{k})/|\mathbf{k}|)]$ (Roest vd., 1982).

3D automatic interpretation of the grid data represents the 2D amplitude function and this function also represents the absolute value of Eq. 2 given by Nabignan (1972, 1974). In this case, this equation evolved as follows:

$$|AS(x,z)| = ((\partial M/\partial x)^2 + (\partial M/\partial y)^2 + (\partial M/\partial z)^2)^{1/2} \quad (7)$$

This is the 3D analytic signal function. Analytic signal value (Eq.7) is maximum in the edge zones of the geological structures.

Because of the derivatives the places where there have been most changes are marked with strongest amplitude. In this statement it shows that origin of the structure becomes prominent. When multiple structures have been reduced down to original mass then as they become geological structural boundaries then they cannot be detailed any further (Ansari and Alamdar, 2011).

Tilt Angle:

In the edge zone detections Tilt angle is defined as one of the basic phase filters. Miller and Singh (1994) are the workers who discovered and used this filter. 'Arctan' of the ratio of the vertical derivative to the amplitude of the total horizontal derivative gives the tilt angle.

$$\text{Tilt}=\text{Arctan}\ (\partial M/\partial z)\ /\ [(\partial M/\partial x)^2+(\partial M/\partial y)^2)^{1/2} \quad (8)$$

Tilt angle acquires positive values (+90) on the original structure or nearby. When it is moved away from above the mass it first approaches to zero, then passes to negative values (-90) and it extends as a band in between negative and positive anomalies. Zero values indicate the edge zones. In between the anomaly contours, half distance between the $-\pi/4$ and $\pi/4$ contours is equal to the depth of the upper surface of the structure boundary (Salem et al, 2007). Figure 1 shows schematic view of tilt angle and the components.

2.2. Asta

In using the 'Tilt angle' method there may be some problems related to the study of the edge detection of deep seated structures. As there have not been any vertical variation measurements taken, in any the all of the determination studies carried out on the surface, vertical variation is determined with potential field strength. This inevitability is a problem in the vertical derivative. In the study area for the masses present in various depths in the edge boundary transitions, the edge boundaries of the masses cannot be seen clear and sharp as they are needed to be.

In the regional studies, size of the field and multiple structures in it all appear in a narrow part in the data processing stages and features stand very close to one another making this interpretation of the field data becomes difficult. Vertical component ($\partial T/\partial z$) represents variation on the original tilt at depth. With the tilt angle the boundaries of the mass becomes known and depth effect of it is registered in the analytic signal. When analytical signal is used together with the tilt angle method then some features will appear more clearly.

In the equation 4 when 'T' tilt angle is written in place of 'M' potential

$$|AS(Z)| = ((\partial T/\partial x)^2 + (\partial T/\partial y)^2 + (\partial T/\partial z)^2)^{1/2} \quad (9)$$

equation is obtained. This is 'ASTA' equation, producing analytical signal from the tilt angle.

2.3. Derivative filters, phase filters and *asta* module used in the edge definitions

Arısoy and Dikmen (2011) prepared software for 'Potensoft'. It is for 3 rectangle prisms at 0-5 km depth (Figure 2); magnetic field effect (model grid) and model sensitivities of other edge definition methods have been studied. For this purpose in the order of;

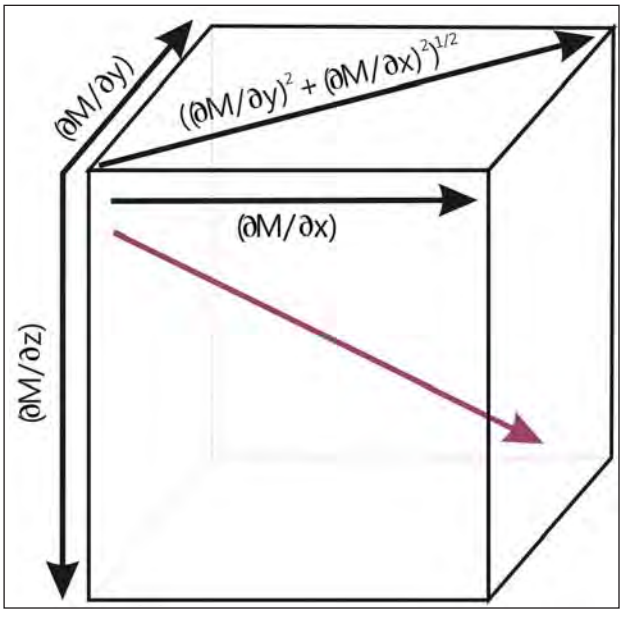

Figure 1- Schematic view of the 'Tilt angle' components.

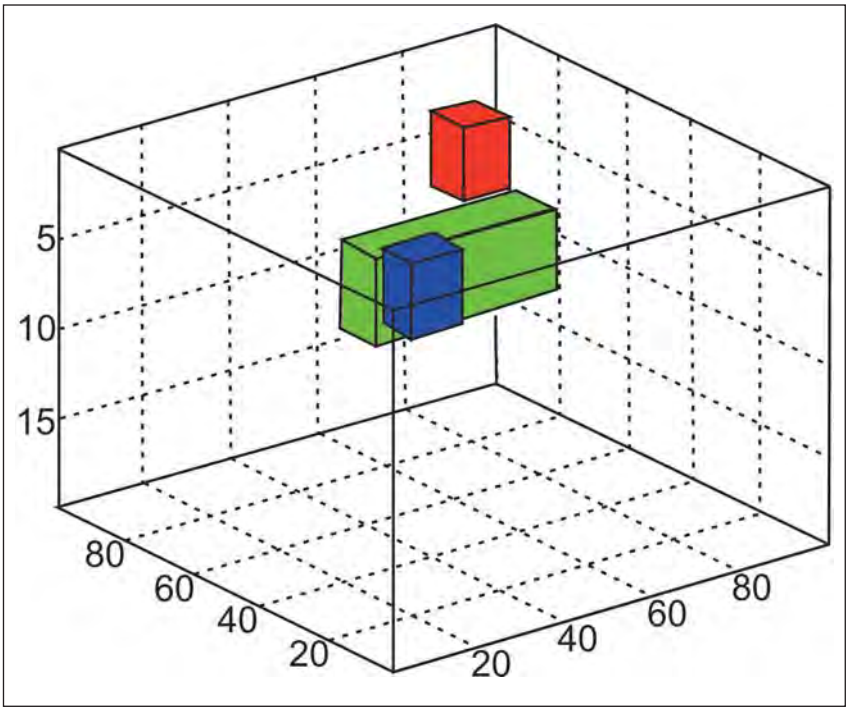

Figure 2- 3 dimensional model view (Arsoy and Dikmen, 2011).

(a) Model grid, (b) Horizontal gradient, (c) Analytical signal, (d) Tilt angle, (e) Tilt derivative, (f) Theta map, (g) Hyperbolic tangent (has not been pushed forward (?), and (h) *ASTA* (Tilt angle based analytic signal).

By using data processing, results have been correlated with each other. ASTA module is attached to the interface of the 'Potensoft' package program (Arısoy and Dikmen, 2011) and is present in the menu (Figure 3).

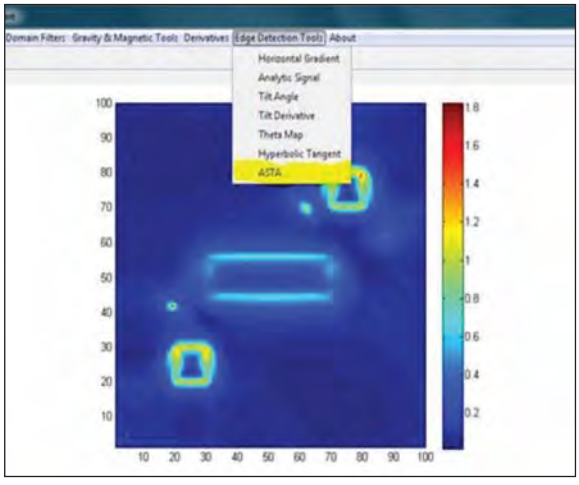

Figure 3- *ASTA* module view of the model grid attached to the graphic interface.

In general derivative filters are based on the calculations of the 1st and 2nd derivatives of the horizontal (along x and y) and vertical (along z) data. Analytic signal and horizontal gradient could be given as examples for the derivative filters. On the other hand phase filters are the angular greatness obtained from the base of the ratio of vertical derivative and the horizontal derivative angle. Hyperbolic tangent method can be given as an example. On the other hand the *ASTA* method is a mix edge sensing technique results from the derivation of 'till' greatness.

Figure 4 shows views of the 3 prisms produced with the edge definition methods.

2.4. Comparison of model answers

1) In Figure 4 model images in a, d, f and g show that anomaly fields has curvature expansions. Prism edges are not sharp and contour transitions are not clear. The four colours used (yellow, red, blue, green) show various transitions, detection of structures is problematical. Long edges of the rectangle prism in the middle have four coloured parallel transitions. This creates doubts on which could be the real edge. Distribution of the contours and colour shades may be misunderstood as structural complexity.

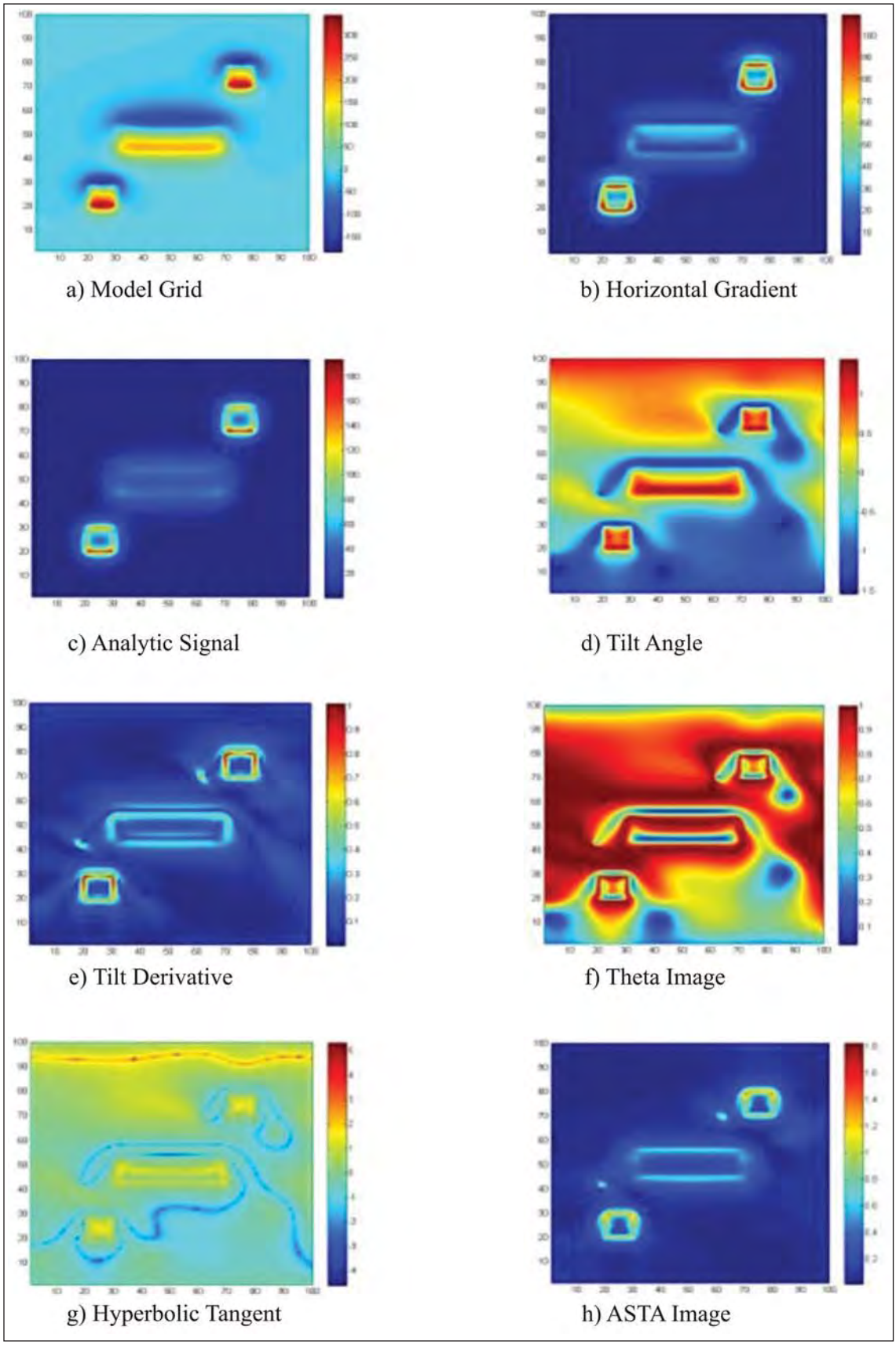

Figure 4- Model answers for edge definition.

2) In Figure 4, image (b) is quite clear but there are contour accumulations on the top of the cubes and upper edges are narrower. Upper long edge of the rectangle prism in the middle appears to have thickened more so than it should.

3) In Figure 4, image in (c) is clearer than it is in (b) but the rectangle prism in the middle is not clearly visible.

4) In Figure 4, in the image (e), image of the tilt angle indicates that structures are geometric but contour accumulations and particularly repeated edge images along the long edges of the rectangle prism makes it difficult to understand the model.

5) In Figure 4, in image (h) in the *ASTA* image, although there are some small (local) contour accumulations some edge like with equal thickness geometric linear edge transitions, here with less noise and detectable upper prism images have been obtained here.

6) In figure 4, in image (h) the analytic signal obtained from the tilt angle is seen. The long rectangle prism in the middle has sharp edges and structures are visible. Among the methods shown in figure 4, only *ASTA* is a combination. But the analytic signal conducted following tilt angle application is not same as with *ASTA*.

Although conducting repeated edge sensing methods conducted showed some sharp edges in the structures but the images of the edges of the rectangle prism in the middle are still not sharp. In figure 5 and figure 6, it shows 2nd vertical derivative applied following analytic signal by Hsu et al., (1996) and 2nd vertical derivative applied following tilt angle by Cooper and Cowan (2004).

In the lower left side and in the upper right side in figure 5 although the effect of the prism edges appear sharp but the edges of the long prismatic structure in the middle is not clear. In figure 6, despite colour interferences the edges of the three prisms are visible but are not sharp. Although there are more data processing and processing time in the second derivative combinations but still contrast and signals are weak, images are not sharp (Figures 5 and 6).

3. Simav Fault and Geological Position of Simav Half Graben:

Aegean graben system including the Simav Graben was concerned by many authors since 60'ies (Arpat and Bingöl, 1969). In North-western Turkey extensions of NE-SW extending Demirci, Selend, and Gördes basins are limited by the Simav fault zone. Here E-W extending Pliocene (?)- Quaternary subsidence zone is known as the Simav Graben (Şaroğlu et al., 2002), (Figure 7a). Seyitoğlu et al., (1997) studied the fault mechanisms and concluded that Simav Graben fault was an active geometric listric fault zone. According to this author, this structure was developed as a result of N-S running extensional fault zone which effected Aegean region in Late Oligocene – Early Miocene. Doğan and Emre (2006) say that depending upon the geomorphologic

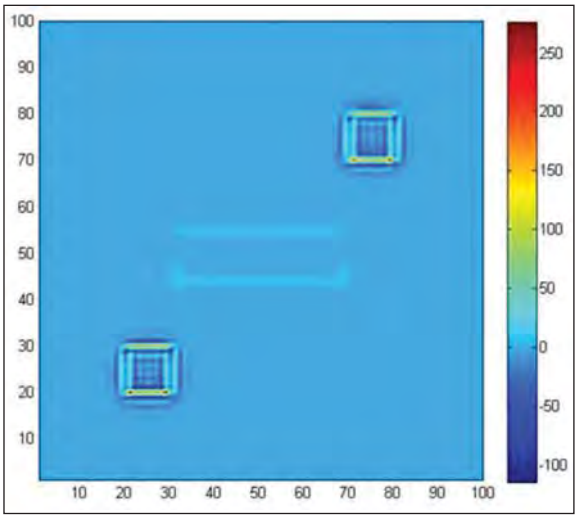

Figure 5- 2nd vertical derivative of the analytic signal;

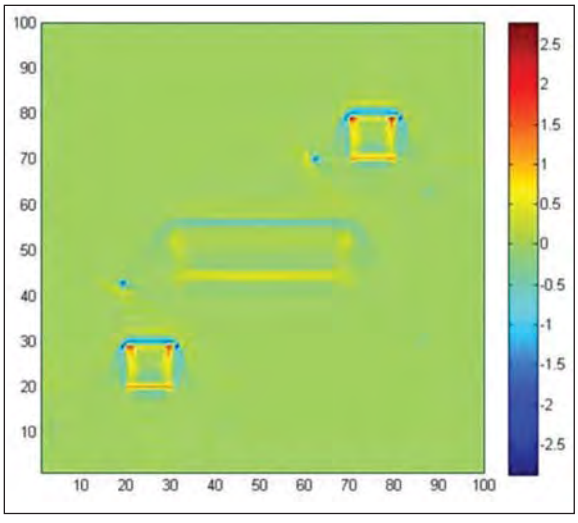

Figure 6- 2nd vertical derivative of theTilt angle

findings the plain base where Simav lake is located has subsided during the last 10000 years as a result of earthquakes. According to another view of Doğan and Emre (2006) there is a 205 km long strike slip fault which joins to the Gelenbe fault at the western end of the Simav fault zone and to the East end of the Sultandağı fault zone.

The Northern end of the graben is bound by Naşa Fault Zone which consists of numbers of normal faults and further north by Emet (Kütahya) fault (Emre et al., 2013). According to Emre et al. (2013) Simav plain is the largest structural subsidence basin in the Simav fault zone. It is a basin developed on the right step-over between Simav and Şaphane faults.

The regional tectonic map and position of the study area is given in figures 7a and 7b respectively. Emre et al. (2013) says that in the earthquake stricken region strike slip faults caused the recent tectonic deformations. Main earthquake producing tectonic features in the region are NW-SE running right lateral Simav fault and the Naşa Fault Zone which is made of series of NW-SE running faults (with 55º - 65º west dipping) (Figure 7b). It is still argued whether Simav fault is a listric geometric normal fault (Seyitoğlu et al., 1999) or right lateral, strike slip regional normal fault (Emre et al., 2013).

In the literature the relationship of the Simav fault with the Menderes massif is extensively discussed. According to Gessner et al. (2013) the fault is within the Menderes massif (Figure 8). On the other hand, according to Koralay (2011) the Simav Fault does not have a boundary relation with the Menderes massif (Figure 9).

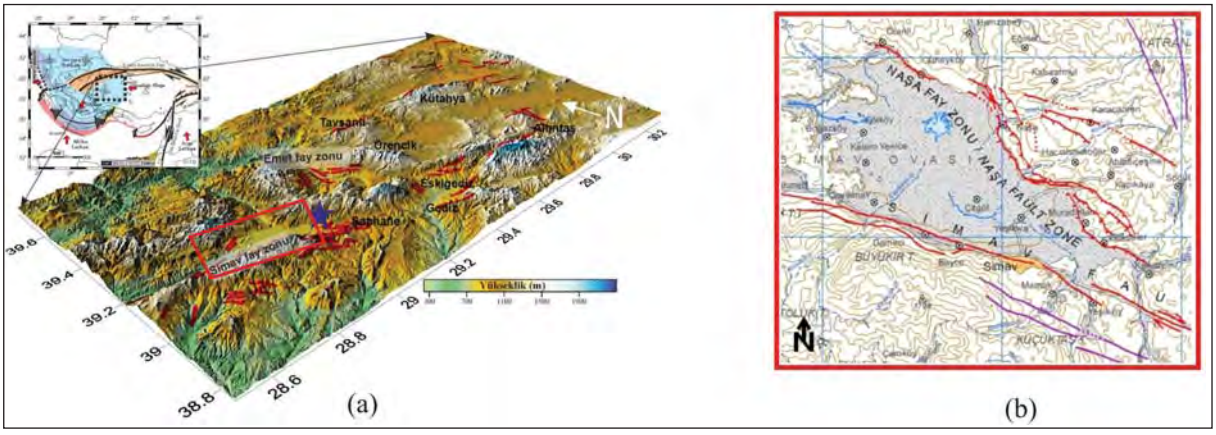

Figure 7- a) Regional tectonic map (Şaroğlu et al., 2002); b) Study area.

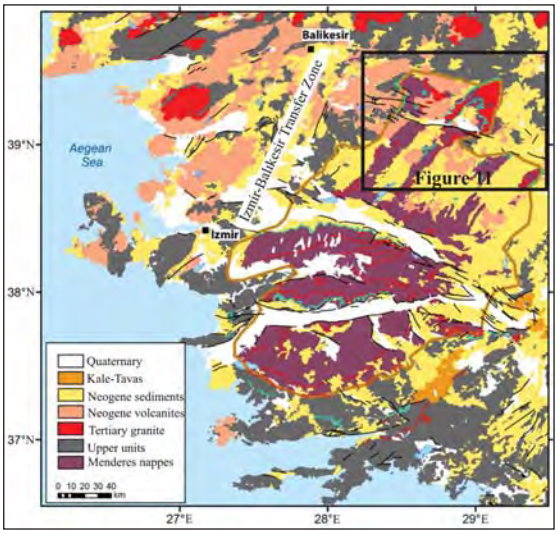

Figure 8- Limits of the Menders Massif (from simplified map of MTA, 2002 of Gessner, et al., 2013).

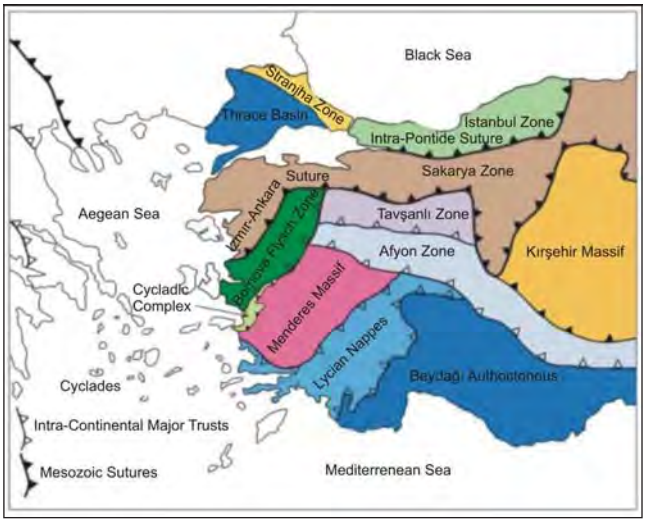

Figure 9- Simplified regional tectonic map (Okay et al., 1996; from Koralay et al., 2011).

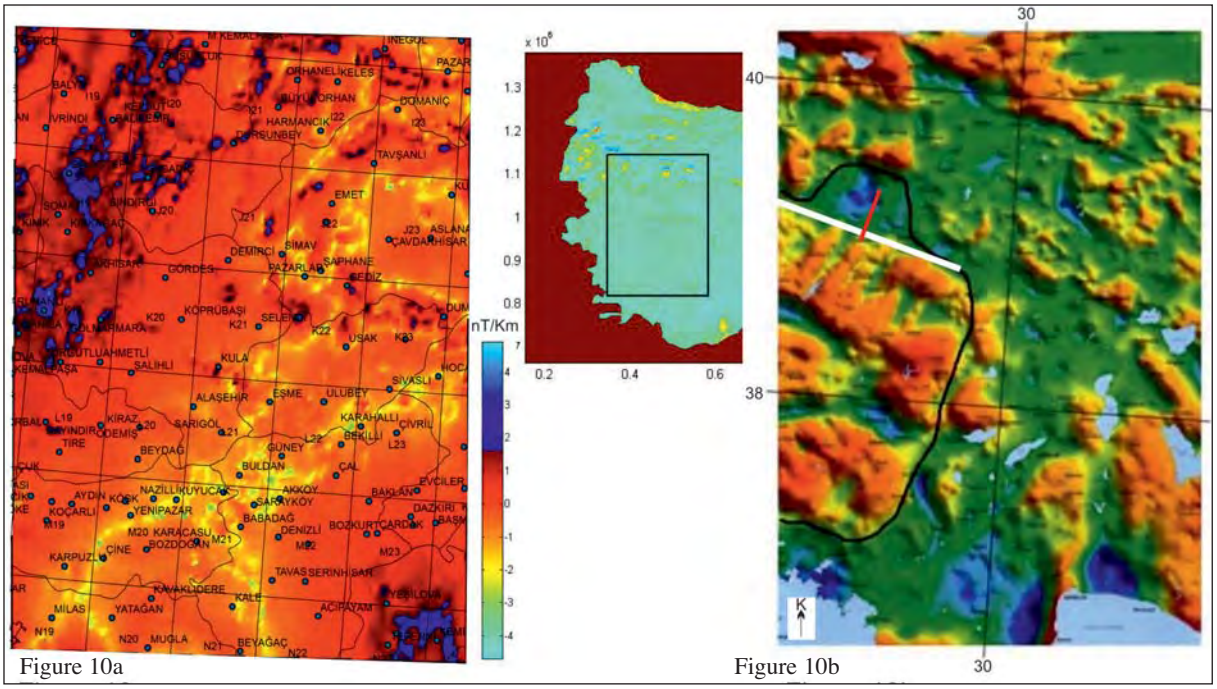

Figure 10- a- Northern boundary of the Menderes massif, based on the air borne magnetic data b- Gravity residual izostasy map; white line: Simav Fault; red line: cross section line in the figure 12 (Modified from MTA, 2012).

Air borne magnetic data and regional gravimetric data suggest that Menderes massif has tectonic border zone (Figures 10a and b). Magnetic susceptibility in the massif area has largely diminished. But in the neighboured there appear to be present a 'puzzle void' with magnetic susceptibility. It appears that Simav fault and the subsidence zone to the North are within the magnetic and gravity field.

To the north of the magnetic map there is a group of rocks with similar origin and having similar physical properties. When edge sensing technique is applied to this group of rocks there appears a structure along a 'cloth hanger' like line (black line) which may be defined as a physical transition. The black line may possibly be defining the northern boundary of the massif (Figure 10b). Menderes massif forms a tectonic unit and physical changes along the borders of this unit are reflected as partly (in the north) geophysical anomaly on the maps.

In Figure 11 blue line is marked as a detachment fault (Gessner et al., 2013). A scientist working in the Simav basin may consider that the units in the basin have moved forward along the Simav fault and the basement block in the north has moved eastwards (Figure 11).

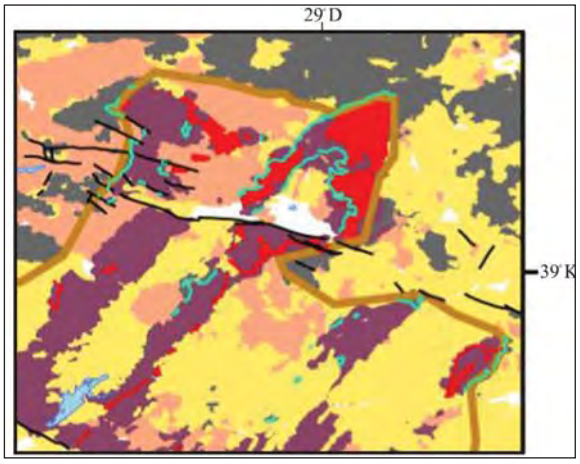

Figure 11- Northern boundaries of the Menderes massif, Eğrigöz granitoid and the detachment faults (after Gessner et al., 2013).

This movement may appear contradicting with the Northwest-Southeast movement of the graben systems, but both are in accord with the gravity data. If cross sections are taken along Northwest - Southeast and Northeast –Southwest directions on the gravity maps, one could see that these cross sections are in accord with the graben model and fault (normal fault) definitions.

4. 2D Host rock image of the Simav basin

Theoretical model of the Simav Graben and the real gravity profile on it is given in figure 12. In this profile the edge of the topographically high block in the Southwest is marked with some faults. Step faults in the Northeast are defining Naşa Fault Zones.

In figure 12, it shows that in the upper part gravity value drops from about -55 mgal down to -65 mgal. The anomaly is becoming almost horizontal in the graben, then (probably from the effect of basalts) it increases towards the other end of the graben where there are normal faults and ending with parallel anomaly oscillations. It indicates that the units in the east are denser than the filled up material in the graben. Anomaly values in the graphic are the measured gravity values. Host rock gravity values produced by two dimension inversion solution from this profile are seen as 'iteration 27' values in table 1.

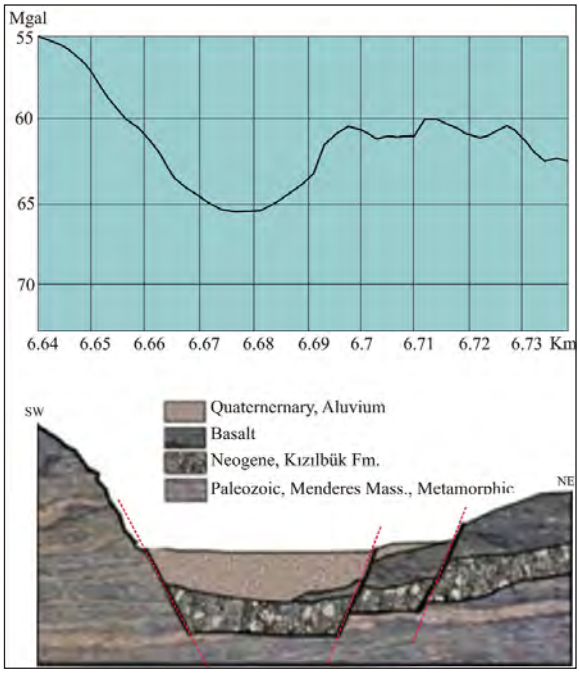

Figure 12- Conceptual model and measured gravity anomaly.

Table 1- '27 iteration' values of inversion solution.

27th Iteration						
Distance	Measured Gravity (mgal)	Depth	X1	X2	Gravity value (mgal)	Calculated Gravity (mgal)
664.5	-65.06	0.05101	-0.25	0.25	-1	-1
665	-65.67	0.0847	0.25	0.75	-1.6099	-1.6099
665.5	-66.68	0.14845	0.75	1.25	-2.62	-2.6199
666	-68.49	0.29636	1.25	1.75	-4.4299	-4.4299
666.5	-69.69	0.3841	1.75	2.25	-5.6299	-5.63
667	-70.77	0.47763	2.25	2.75	-6.7099	-6.7099
667.5	-72.85	0.79225	2.75	3.25	-8.7899	-8.7867
668	-74.66	0.95224	3.25	3.75	-10.599	-10.608
668.5	-75.67	0.94065	3.75	4.25	-11.61	-11.613
669	-75.67	0.79054	4.25	4.75	-11.61	-11.602
669.5	-75.47	0.76628	4.75	5.25	-11.409	-11.401
670	-73.67	0.44944	5.25	5.75	-9.61	-9.6164
670.5	-73.07	0.52456	5.75	6.25	-9.0099	-9.0101
671	-71.26	0.30696	6.25	6.75	-7.2	-7.2002
671.5	-70.53	0.32433	6.75	7.25	-6.4699	-6.4697
672	-70.6	036751	7.25	7.75	-6.5399	-6.5403
672.5	-71.2	0.45116	7.75	8.25	-7.14	-7.1399
673	-70.87	0.37307	8.25	8.75	-6.81	-6.8101
673.5	-71.07	0.42863	8.75	9.25	-7.0099	-7.0098
674	-69.74	0.25848	9.25	9.75	-5.6799	-5.6801
674.5	-70.34	0.38892	9.75	10.25	-6.28	-6.2799
675	-71.15	0.46693	10.25	10.75	-7.09	-7.0901
675.5	-70.62	0.35118	10.75	11.25	-6.56	-6.5598
676	-70.48	0.37025	11.25	11.75	-6.42	-6.42
676.5	-71.09	0.45807	11.75	12.25	-7.03	-7.0301
677	-72.5	0.65621	12.25	12.75	-8.4399	-8.4392
677.5	-72.37	0.49362	12.75	13.25	-8.31	-8.3114
678	-72.43	0.53922	13.25	13.75	-8.37	-8.3675
678.5	-72.77	0.58586	13.75	14.25	-8.7099	-8.7126

In the Eastern part of the basin along the Southwest-Northeast profile, while southern flank is descending with high angle, northern flank is going up with low angle (Figure 13).

Previously magneto telluric studies were carried out in the field. From the magneto telluric studies two dimensional inverse solution gravity values were found out. Figure 14 shows gravity profile selected to be close to the two dimensional inverse solution values. On this gravity profile (Figure 14) dotted red line and continuous line show agreements with the positions of the main fault zones.

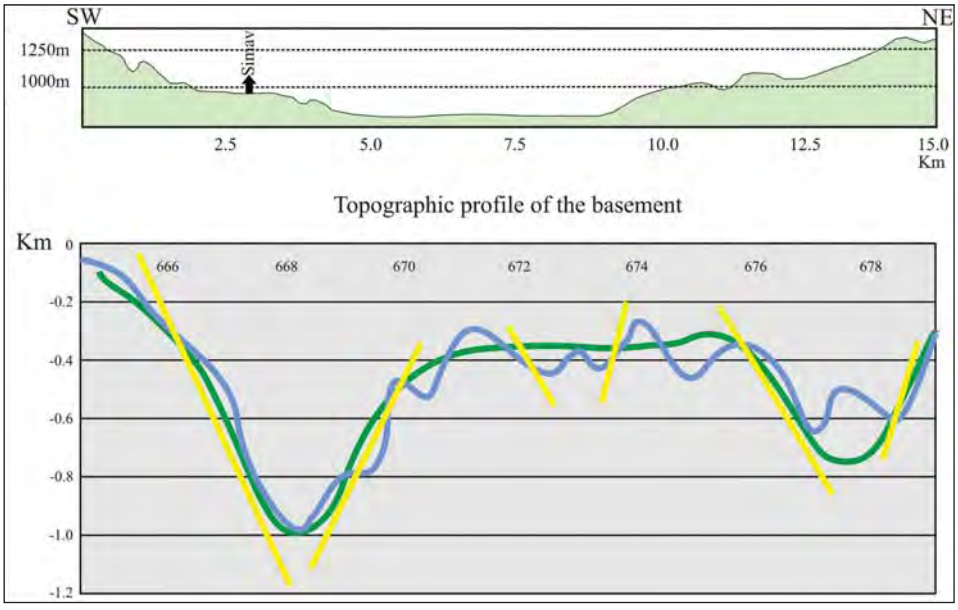

Figure 13- Host rock image under the gravity section (Blue line: host rock; yellow line: faults).

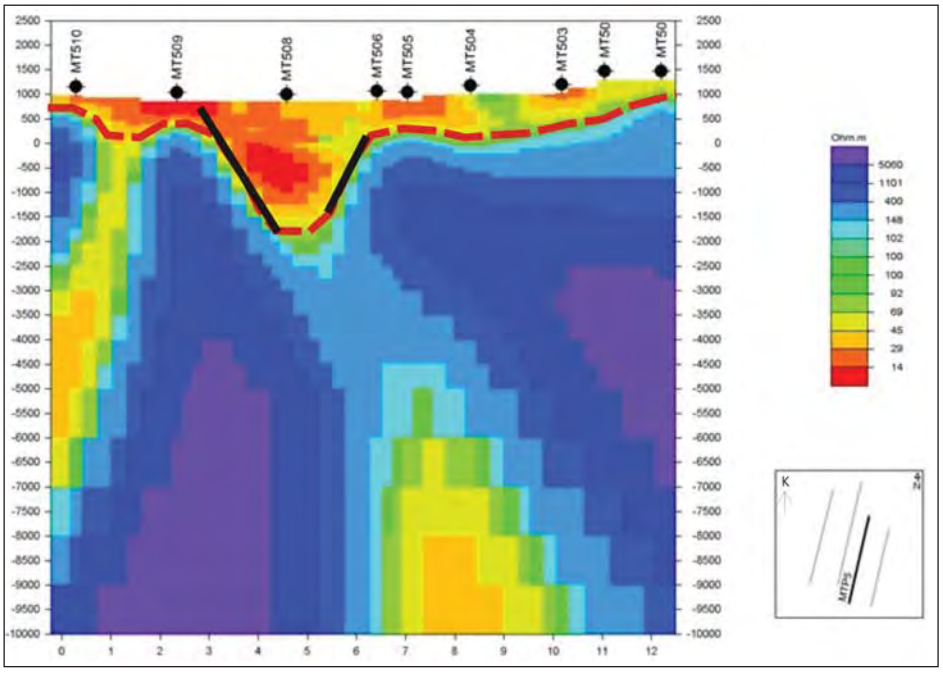

Figure 14- Closely positioned, 2D inverse solution profile view (Kılıç, 2010).

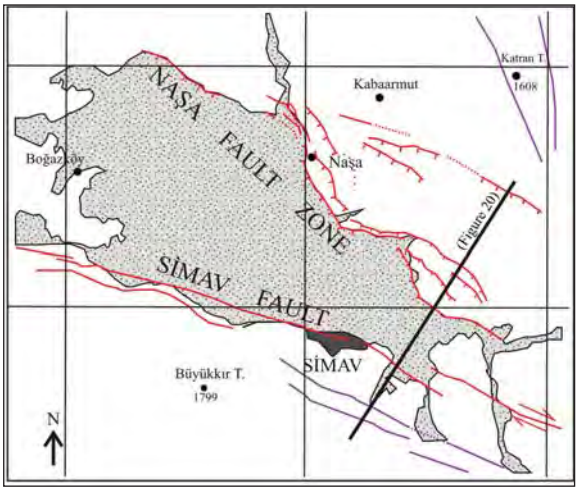

Figure 15- Updated active fault map (Emre et al., 2012);

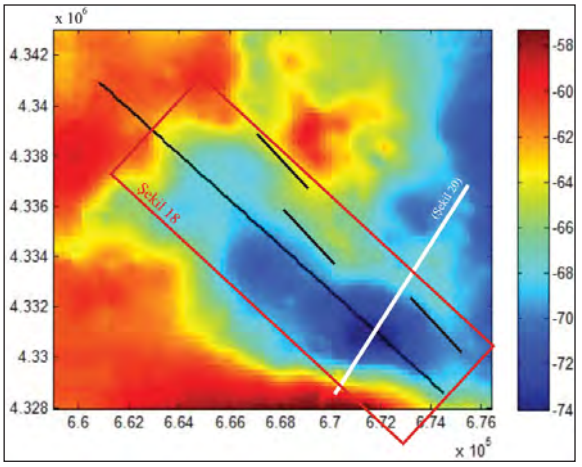

Figure 16- Bouguer gravity map of the study area and selected cross section (white line: Figure 20); red rectangle: area of the figure 18 (data from Demirbaş and Uslu, 1986).

The triangular shape structure becomes narrower towards East (where gneisses are). It's southern boundary has a distinct gravity transition. In the North, the Naşa Fault Zone transitions has been well marked on the active tectonic map and can be seen on the gravity map (Figure 15, 16).

Position and shape of the graben shown in the updated active fault map (Emre et al., 2013) is in agreement with the gravity map. In the gravity map granitoids have – (60-64) mgal values, gneisses along the lower edge of the graben have – (72-74) mgal values. Blue coloured parts in figure 16 reflects gravity effect of the Quaternary in fills.

5. Gravity edge definition technique and 3D analysis

To be able to study deep and shallow structures, various different processes are needed. Studying the edge zone effects of shallow structures, derivative and phase filters give satisfactory results. On the other hand while studying the edge sensing of deep structures some problems related to vertical derivative effects may arise. These problems have been tried to be solved by upward analytic continuation and vertical derivative applications.

Analytic signal was applied to 2 dimensional structures by Nabighian (1972). Since then various computer programmes have been developed. Nowadays package software's have 'edge detection' modules. If analytic signal is the result of subtraction of absolute value of complex Hilbert transforms from the function then highest values are expected to be at contour transitions.

It is known that analytic signal technique is not sensitive to the structure corners. Following horizontal gradient applications, analytic signal derived from the tilt angle becomes sensitive to the structure corners (Figure 17a, b). When the concept of analytic signal is thought to be source rock mass effect; to be able to see the maximums along a line, then horizontal gradient would be needed. Following removal of surface effects with upward analytic continuation applications, horizontal gradient and ASTA have been applied (Figure 17b). In figure 18, a 3D analysis derived from inverse solution of quadratic density function with constant -0.7 gr/cm^3 specific gravity contrast is given. This view could be characterized as upper crust interface. In this view southern edge is leaping and making a bend to yellow coloured contour transition. In the program calculations a positive value is estimated, because of this depths are positive and are at interface topography position.

Simav Graben appears as a subsidence area in the gravity inversion. In the red dotted marked area where Simav fault cuts through the graben there is a subsidence like feature but this feature does not have any surface signature (Figure 18).

6. Findings

Two and 3-dimensional gravity processes have been obtained by using programmes with various

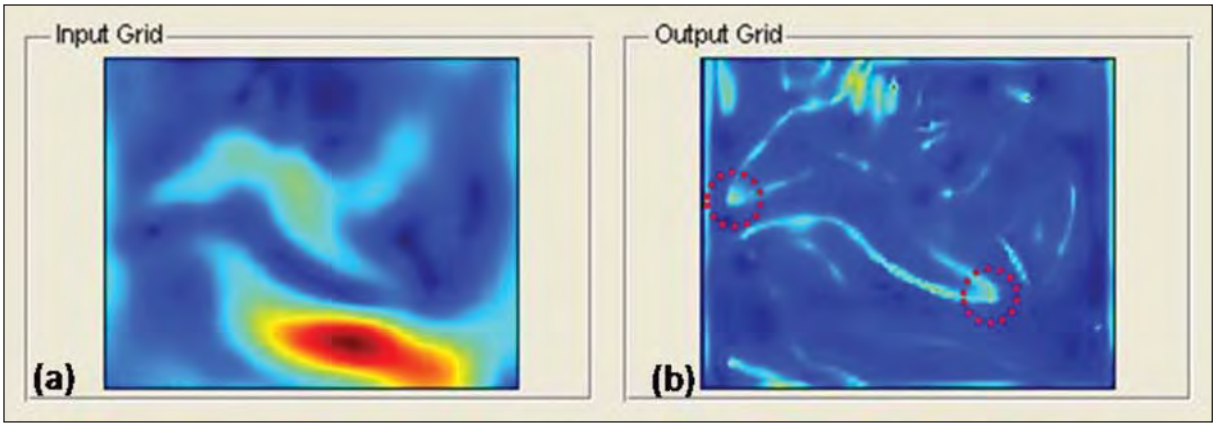

Figure 17- a) Horizontal gradient view; b) Horizontal gradient + ASTA

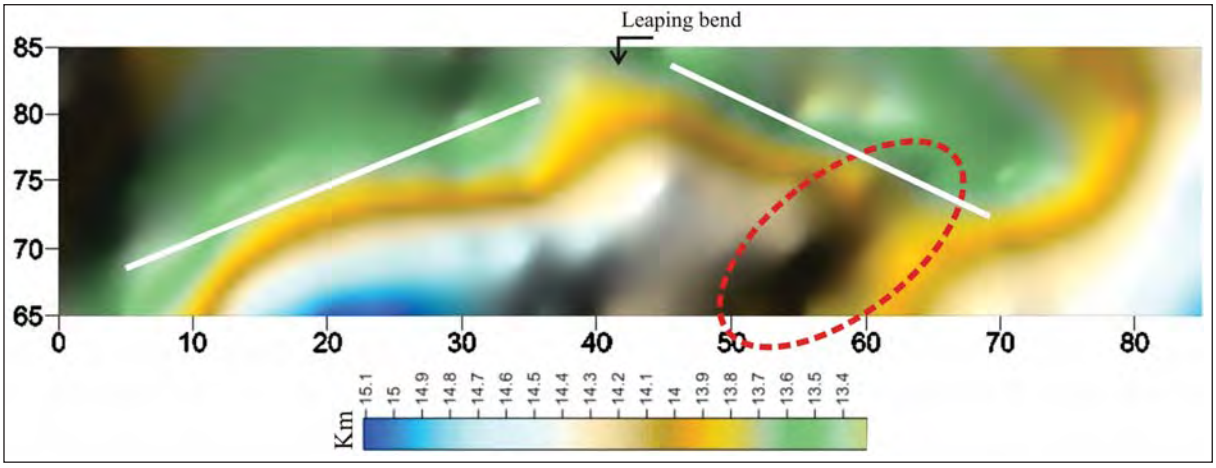

Figure 18- Basin depth map based on the 3D analysis of the 3D Bouguer gravity map (see figure 16 for location).

different techniques. Two-dimensional edge definitions, gravity data processings, Matlab process software has been made by using Potensoft developed by Arısoy and Dikmen (2011). Three-dimensional analyses have been made by using Fortran (Goncalves, 2006). In this study iterative 3-dimensional inversion have been used the foundations for this method were laid down by Cordel and Henderson (1968). This program also includes quadratic gravity function preferred by Bhaskara and Ramesh (1991).

ASTA as edge sensing method has been tried and model sensitivity and solution performance for deep structures have been studied. But 'ASTA' has not been applied directly to the raw data. For the deep structures, upward analytic continuation, low-pass filters and horizontal gradient methods were applied before ASTA.

In 3D analysis, square data without coordinates are used and then program print out is designed with relative coordinates. In the program an algorithm with specific gravity distribution defined with a quadratic function is used and specific gravity contrast of the basin base forms interface geometry (Figure 18). Here it is advantageous to use the best representing function of the basin's base contrast. Although the program may provide facilities to define the basin's depths, in places where specific gravity differences are minimal at depths then iterative takings may vary. Defined base depth estimate may be used as a parameter to start the process.

The base of the basin is defined as low 'Vp' velocity and high 'b' value in the seismology profile of the crust joint research project package of Tubitak-MTA- University (Figure 19). In the profile where Simav is, there is a low velocity anomaly at 2-3 km depth with 3.3-3.7 km/s velocity. Study shows that

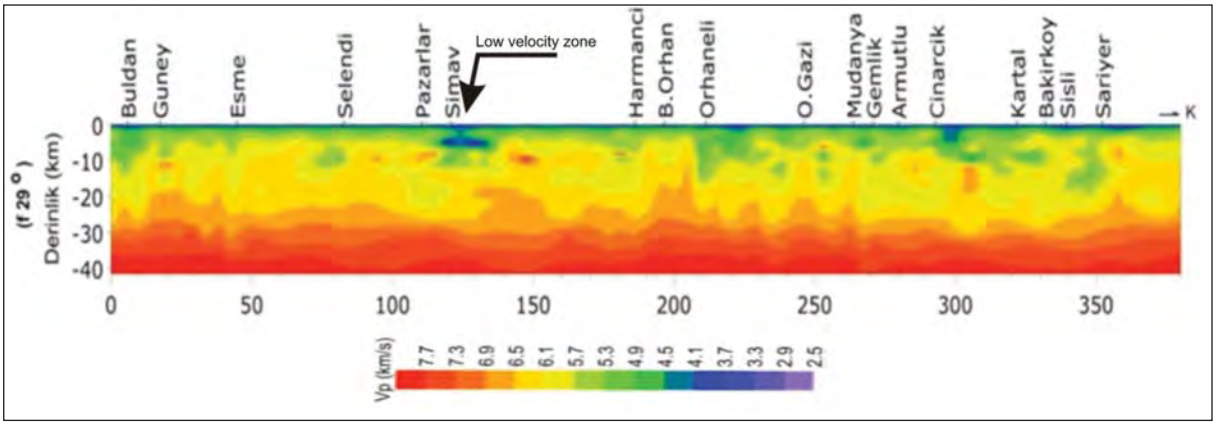

Figure 19- Seicmic velocity (Vp) section, blue area 3.3 km/s, low velocity zone (See figure 15 for location) (MTA, TÜBİTAK, C.Ü., A.Ü., 2012).

low velocity is related either to the in filled loose material or to the subsidence. High 'b' value reflects degree of compaction (Figure 19).

The edge of the basin in the south is bound by a normal fault with high dip angle. In the north the basin is bound by normal faults with lower dip angles. In Figure 18 there is a graben feature which has Simav fault in the south and Naşa Fault in the north. As it was the case for Büyük Menderes and Gediz grabens, here from the 2 dimensional inverse solution of the southwest-northeast gravity profile it shows that this graben is an asymmetric half graben developed in the north of Simav main fault..

A selected profile, subjected to 2D inversion solution indicates that near Simav there is a more undulated host rock base profile. On the surface the host rock profile traverses Naşa Fault Zone. This is the part where earthquakes are quite frequent. As is the case in Gediz and Büyük Menderes grabens (Sarı, 2003) host rock profile here also dips eastwards (Figure 20).

The leaping coil as it is described by Doğan and Emre (2006) is clearly seen in the 3D deep gravity solutions and regional gravity data processing's with edge sensing's (Figure 21b). 13 to15 km seismologic depth limit seems rather adequate for gravity. In the south where the big fault is thought to have made a coil appears in accord with the 2 and 3 dimensional maps prepared by using the gravity data (Figure 21).

Red dotted lines mark the area where the fault made a coil in the map. Same lines also fit to the southern edge of the 2 dimensional images. In practice when ASTA is carefully applied some of the

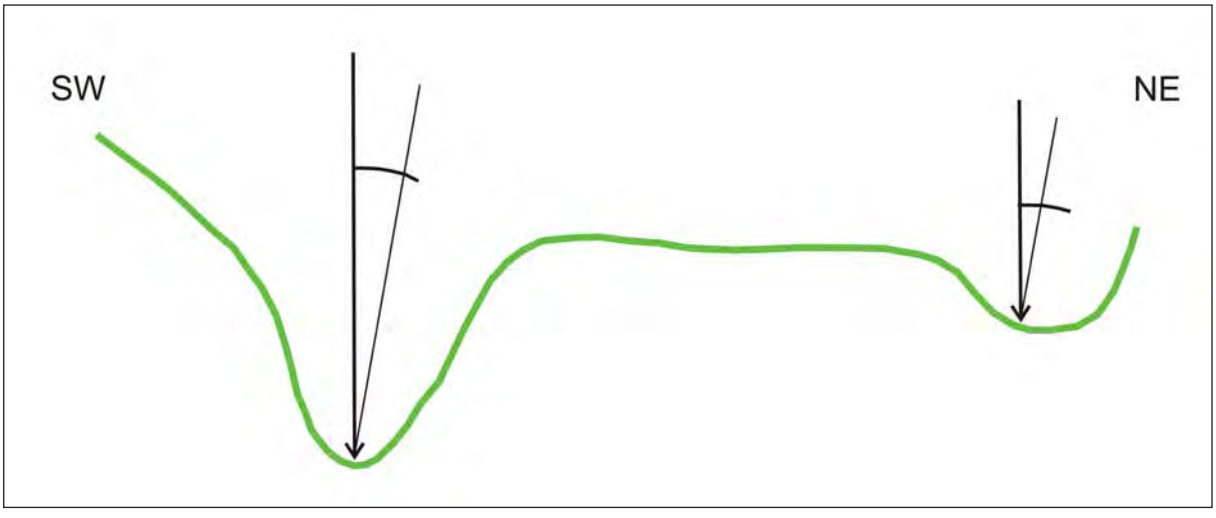

Figure 20- Asymmetric half graben model (see figure 16 for profile location).

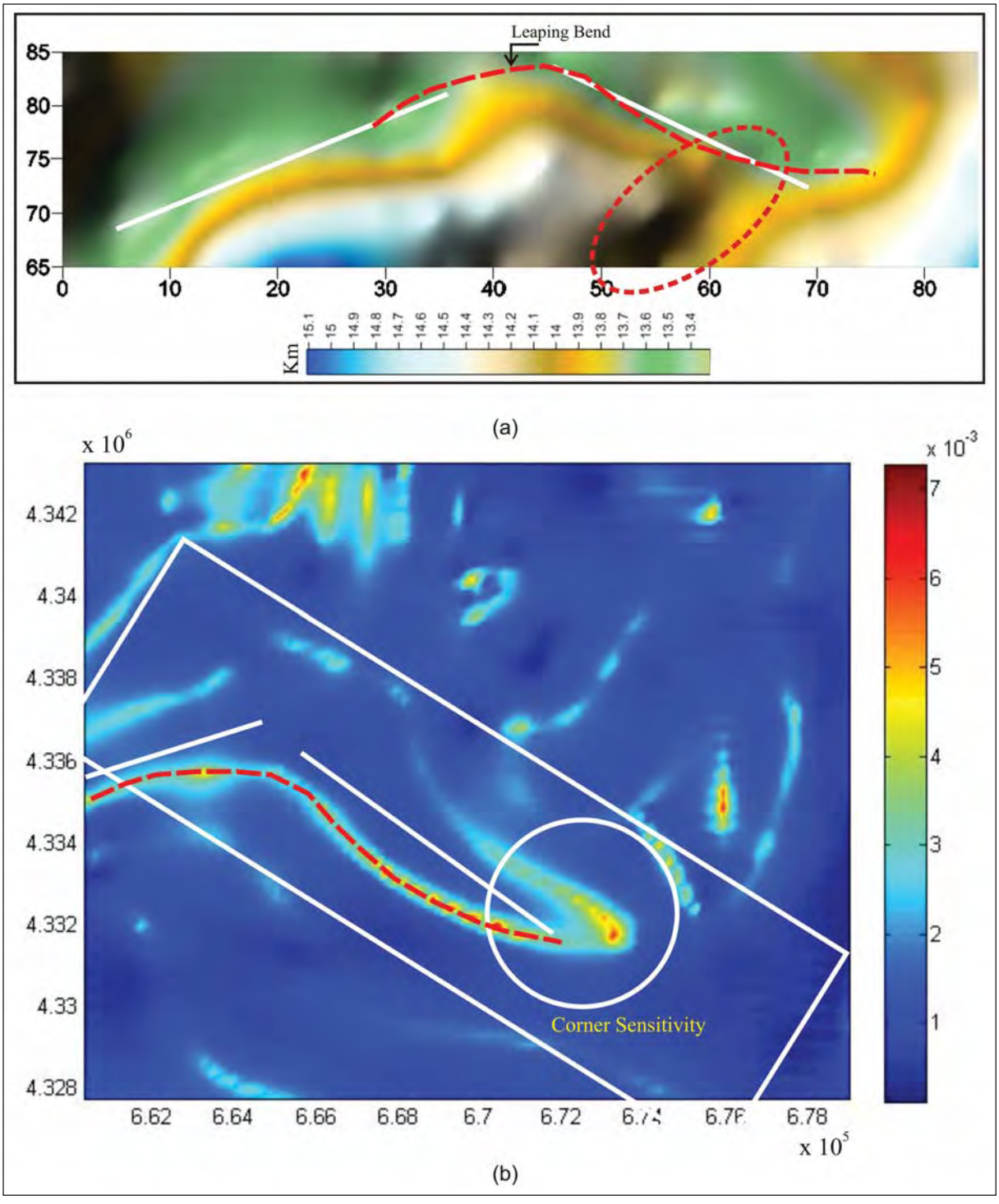

Figure 21- Joint field image of 2D and 3D solutions (White rectangle on figure 21b represent the map area of the figure 21a).

unwanted effects encountered in other edge sensing applications can be avoided. Yellow line (in the white coloured circle) shows that analytic signal could be recorded at the structure corners (Figure 21). Here below it is shown that 3 layered image is in accord with the edges (Figure 22). In the faults here Focal mechanism solutions indicate that the faults developed here are normal faults and had some strike slip component (Figure 23) (Bekler et al., 2011). It appears that the area where the earthquakes commonly occur coincide with the intersection of two faults on the surface and possibly intersection of the third fault at depth.

3D Basin depth interface model of the Simav Basin were produced after all the processes and studies writen above and presented in figure 24.

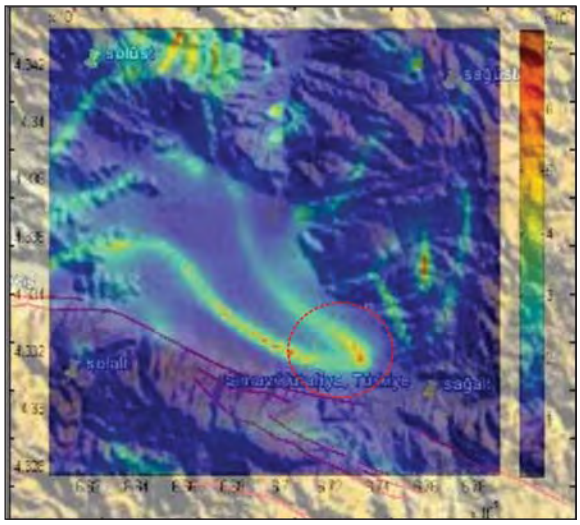

Figure 22. 3 layered superimpozed image. Yellow lines edge zone sensing ASTA.

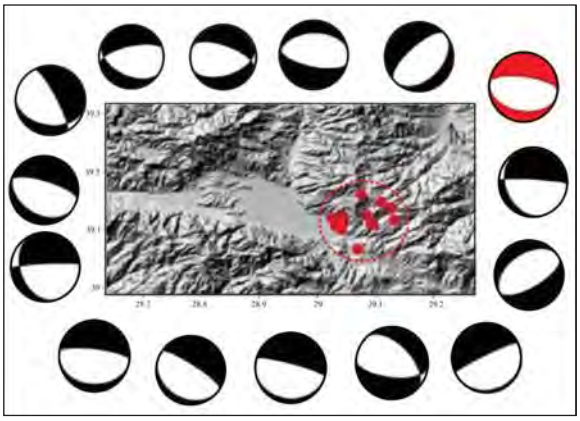

Figure 23- Moment tensore solutions. Red ball 19th May 2011, Mw=5.83 (Bekler et al., 2011);

7. Discussion and Results

- Simav fault is about 205 km long. It is not appropriate to define this fault as a whole with a as a single character as some sections are with dominant component. For example it's part in the graben is normal fault with high dip angle (Figures 13 and 14). It is quite natural to see different characters in different parts of the fault. The part of the fault in the graben in places has strike slip components (Gessner et al., 2013).

- For paleo seismological studies multiple geophysics criteria should be used to locate where the trenches to be cut. It has been shown that rather than cutting the trenches on the surface expression of the fault, cutting in on the location where geophysics image suggests is much more informative.

- Gravity data indicate that graben in the south is a half graben (Figure 20). Simav fault in the graben is a normal fault. Edge sensing processes show that the Simav fault and intersection of the NW-SE running Naşa Fault, bordering the half graben, where there is a corner structure, coincides with the focal of many earthquakes (Figures 22 and 23). In some places host rocks at a depth of 1000-1200 m (Figure 13) and in accord with the seismology inversion presence of a upper crust interface topography at 13-15 km depths can be seen (Figure 19).

- Numbers of earthquakes generated during the last two years relating to the faults in the Simav basin shows that how much the area is tectonically active and how much the tension is high. Altınok et al., (2012) reports that studies on the 'Holocene activities of the Kütahya fault zone' show, the fault zone has the potential for producing earthquakes at 6.5 Magnitudes.

- Defining the deep part geometries of the deep seated faults in the region will provide more accuracy about locate and modelling the fault segment that would be activated. That is why, after using the 2D and 3D geophysical models in areas like the Simav region to understand the deep geometry would also provide more acurracy in geological modelling.

- 3D Basin depth interface model of the Simav Basin produced at first in this study in the light of the detail gravity data.

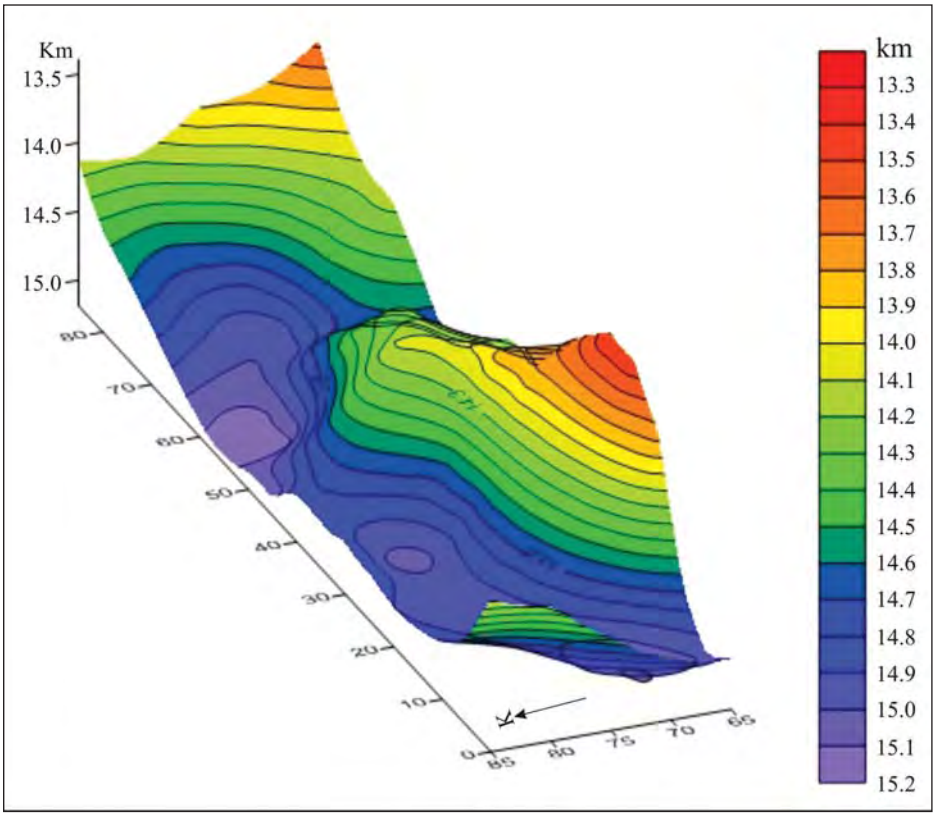

Figure 24- 3D Basin depth interface model of the Simav Basin.

Acknowledgement

Data used in this study is taken from the report of Şevket Demirbaş and Adnan Uslu in their study of 1984 in the region. I appreciate the General Directorate of Mineral Research and Exploration for their support to publish this data. I appreciate my colleague Dr. Yahya Çiftçi for his support both in scientific and technical manner during construction of this paper.

Received: 19.04.2013
Accepted: 13.11.2013
Published: June 2014

References

Altınok, S., Karabacak, V.,Yalçıner, C.Ç., Bilgen, A.N., Altunel, E., Kıyak, N.G. 2012. Kütahya fay zonunun Holosen aktivitesi, *Türkiye Jeoloji Bülteni*, 55, 1.

Ansari A. H., Alamdar, K. 2011. A new edge detection method based on the analytic signal of tilt angle (*ASTA*) for magnetic and gravity anomalies, IJST A2: 81-88, *Iranian Journal of Science and Technology*.

Arısoy, M.Ö., Dikmen, Ü. 2011. Potensoft: MATLAB-based software for potential field data processing, modeling and mapping, *Computer and Geoscience*, 37, 7, s. 935 – 942.

Arpat, E., Bingöl, E.,1969. Ege bölgesi graben sisteminin gelişimi üzerine düşünceler, *Maden Tetkik ve Arama Dergisi,* 73, 1-9, Ankara.

Bhaskara, D., Ramesh, N. 1991. A fortran-77 Computer program for three-Dimensional Analysis of gravity anomalies with variable density contrast, *Computer and Geoscience*, 17, 5, s. 655-667.

Bekler, T., Demirci, A., Özden, S., Kalafat, D. 2011. Simav, Emet fay zonlarındaki optimum kaynak parametrelerinin analizi, 1. Türkiye Deprem Mühendisliği ve Sismoloji Konferansı, ODTÜ, ANKARA.

Cooper, G.R.J., Cowan, D.R. 2004. Filtering using variable order vertical derivatives. *Computer and Geoscience*, 30, 455-459.

Cordell, L., Henderson, R.G. 1968. Iterative three-dimensional solution of gravity anomaly data using a digital computer, *Geophysics*, 33, 596-601.

Demirbaş, Ş., Uslu A. 1984. Kütahya Simav Gravite Etüdü, *Maden Tetkik ve Arama Genel Müdürlüğü Rapor* No: 8136, Ankara (unpublished).

Doğan, A., Emre, Ö. 2006. Ege graben sisteminin kuzey sınırı: Sındırgı Sincanlı Fay Zonu, 59th.

Geological Congress of Turkey, Proceeding Books.

Emre, Ö., Duman, T.Y., Duman, Ş., Özalp, S. 2012. Türkiye diri fay haritası (yenilenmiş), *Maden Tetkik ve Arama Yayınları*, Ankara.

Gessner, K., Gallardo, L.A., Markwitz, W., Ring, U., Thomson, S.N. 2013. What caused the denudation of the Menderes massif: Rewiev of the crustal evaluation, lithosphere structure, and dynamic topograpy in soutwest Turkey. *Gondwana research*, 24/1, 243-274

Goncalves, W.J. 2006. Inversion gravimetrica 3d de la subcuenca de maturin Üniversidat Simon Bolivar proyekto de grado thesis.

Van Hinsbergen, J.J. 2010. A key extensional metamorphic complex rewieved and restored: The Menderes massif of western Turkey, *Earth Science Rewievs*, 102, 60– 76.

Hsu, S.K., Sibuet, J.C., Shyu, C.T., 1996. Depth to magnetic source using generalized analytic signal, *Geophysics*, 61, 373-386.

Kılıç, A.R., Kaya, C., 2010. Simav jeotermal sahasının manyetotellurik yöntemle araştırılması, Yer Elektrik Çalıştayı, Kastamonu.

Koralay, O. E., Candan, O., Akal, C., Dora, Ö., Chen, F., Satır, M., Oberhansli, R. 2011. Menderes masifindeki Pan-afrikan ve Triyas yaşlı metagranitoyitlerin jeolojisi ve jeokronolojisi, Batı Anadolu, Türkiye, *Maden Tetkik ve Arama Dergisi*, 142, 69-121.

Miller, H. G., Sing, V. 1994. Potential field tilt - A new concept for location of potential field sources: *Journal of Applied Geophysics*, 32, 213-217

MTA, TÜBİTAK, C.Ü., A.Ü., 2012. 105G145 No'lu Tübitak, Maden Tetkik ve Arama Genel Müdürlüğü, Sivas Cumhuriyet Üniversitesi, Ankara Üniversitesi İşbirliği Projesi, 2012. Kuzeybatı Anadolu Kabuk Yapısının Jeofizik Verilerle Araştırılması Projesi", 2008- 2012, Ankara (unpublished).

Nabighian, M.N. 1972. The analytic signal of two dimensional magnetic bodies with polygonal crossection: it's properties and use for automated anomaly interpretation, *Geophysics*, 37, 507-517.

Pedersen, L. B. 1989, Retations between horizontal and vertical gradients of potential fields Geophysics, 54, 662-663.

Roest, W. R., Verhoef, J., Pilkington, M. 1992. Magnetic Interpretation using the 3-D analytic Signal Geophysics, 1, 116-125, January 1992.

Salem, A., Williams, S., Fairhead, D., Ravat, D. V., Smith, R. 2007. Tilt-depth method: A simple depth estimation method using first-order magnetic derivatives: The Leading Edge, December, 1502-1505.

Sarı, C. 2003. Gravite verilerinin tekil değer ayrıştırma yöntemi ile ters çözümü ve Gediz ve Büyük Menderes grabenlerinin tortul kalınlıklarının saptanması, *DEÜ Mühendislik Fakültesi Fen ve Mühendislik Dergisi*, 5, 1.

Seyitoğlu, G. 1997. The Simav Graben: An example of young E-W trending structures in the late cenosoic extensional system of western Turkey. *Turkish Journal of Earth Science*, 6, 135-141, TÜBİTAK, Turkey.

Verdusco, B., Fairhead, J.D., Green, C.M. 2004. New insigth in to magnetic derivatives for structural mapping, *Leading Edge*, 23 (2), 116-119.

BULLETIN OF THE MINERAL RESEARCH AND EXPLORATION NOTES TO THE AUTHORS

1. Aims

The main aims of the journal are

- To contribute to the providing of scientific communication on geosciences in Turkey and the international community.
- To announce and share the researches in all fields of geoscience studies in Turkey with geoscientists worldwide.
- To announce the scientific researches and practices on geoscience surveys carried out by the General Directorate of Mineral Research and Exploration (MTA) to the public.
- To use the journal as an effective media for international publication exchange by keeping the journal in high quality, scope and format.
- To contribute to the development of Turkish language as a scientific language

2. Scope

At least one of the following qualifications is required for publishing the papers in the *Bulletin of Mineral Research and Exploration*.

2.1. Research Articles

2.1.1. Original Scientific Researches

- This type of articles covers original scientific research and its results related to all aspects of disciplines in geoscience.

2.1.2. Development Researches

- The studies using new approaches and methods to solve any problems related to geosciences and/or the researches using new approaches and methods to solve any problems related to the science of engineering performed in the General Directorate of Mineral Research and Exploration.

2.1.3. Review articles

- This type of papers includes comphrehensive scholarly review articles that summarize and critically assess previous geoscience reseach with a new perspective and it also reveals a new approach.

2.2. Discussion/Reply

- This type of article is intended for discussions of papers that have already been published in the latest issue of the *Bulletin*.
- The discussion/reply type articles that criticize all or a part of a recently published article, are published in the following first issue, if it is submitted within six months after the distribution of the *Bulletin*.
- The discussions are sent to the corresponding author of the original paper to get their reply, before publication. So that, the discussion and reply articles can be published at the same time, if they can be replied within the prescribed period. Otherwise, the discussion is published alone. Re-criticising of the replies is not allowed. The authors should keep the rules of scientific ethics and discussions in their discussion/reply papers. The papers in this category should not exceed four printed pages of the journal including figures and tables etc. The format of the papers should be compatible with the "Spelling Rules" of the *Bulletin*.

2.3. Short Notes

- Short notes publishing in the *Bulletin* covers short, brief and concisely written research reports for papers including data obtained from ongoing and/or completed scientific researches and practices related to geoscience and new and/or preliminary factual findings from Turkey and worldwide.
- The short notes will follow a streamlined schedule and will normally published in the following first or second issue shortly after submission of the paper to the *Bulletin*. To meet this schedule, authors should be required to make revisions with minimal delay.
- This type of articles should not exceed four printed pages of the journal including figures, tables and an abstract.

3. Submission and Reviewing of Manuscripts

Manuscript to be submitted for publishing in the Journal must be written clearly and concisely in Turkish and/or English and it should be prepared in the *Bulletin of Mineral Research and Exploration* style guidelines. All submissions should be made online at the **http://bulletin.mta.gov.tr** website.

The authors, having no facility for online submission can submit their manuscript by post-mail to the

address given below. They should submit four copies of their manuscript including one original hard copy, and CD. The files belonging to manuscript should be clearly and separately named as "Text", "Figures" and "Tables" at the CD.

Address:
Maden Tetkik ve Arama Genel Müdürlüğü
Redaksiyon Kurulu Başkanlığı
Üniversiteler Mah. Dumlupınar Bulvarı, No: 139
06800 Çankaya-Ankara

- The manuscript submitted for reviews has not been partially or completely published previously; that it is not under consideration for publication elsewhere in any language; its publication has been approved by all co-authors.
- The rejected manuscripts are not returned back to author(s) whereas a letter of statement indicating the reason of rejection is sent to the corresponding author.
- Submitted manuscripts must follow the *Bulletin* style and format guidelines. Otherwise, the manuscript which does not follow the journals' style and format guidelines, is given back to corresponding author without any reviewing.
- Every manuscript which passes initial Editorial treatise is reviewed by at least two independent reviewers selected by the Editors. Reviewers' reports are carefully considered by the Editors before making decisions concerning publication, major or minor revision or rejection.
- The manuscript that need to be corrected with the advices of reviewer(s) is sent back to corresponding author(s) to assess and make the required corrections suggested by reviewer(s) and editors. Authors should prepare a letter of well-reasoned statement explaining which corrections are considered or not.
- The Executive editor (Editorial Board) will inform the corresponding author when the manuscript is approved for publication. Final version of text, tables and figures prepared in the *Bulletin of Mineral Research and Exploration* style and format guidelines, will need to be sent online and the corresponding author should upload all of the manuscript files following the instructions given on the screen. In the absence of online submission conditions, the corresponding author should send four copies of the final version of the manuscript including one original hard copy, and CD by post-mail. The files belonging to manuscript should be clearly and separately named as "Text", "Figures" and "Tables" at the CD.
- To be published in the *Bulletin of Mineral Research and Exploration,* the printed lenght of the manuscript should not exceed 30 printed pages of the journal including an abstract, figures and tables. The publication of longer manuscripts will be evaluated by Editorial Board if it can be published or not.

4. Publication Language and Periods

- *The Bulletin of Mineral Research and Exploration* is published at least two times per year, each issue is published both in Turkish and English. Thus, manuscripts are accepted in Turkish or English. The spelling and punctuation guidelines of Turkish Language Instution are preferred for the Turkish issue. However, technical terms related to geology are used in accordance with the decision of the Editorial Board.

5. Spelling Draft

Manuscripts should be written in word format in A4 (29.7 x 21 cm) size and double-spaced with font size Times New Roman 10-point, margins of 25 mm at the sides, top and bottom of each page. Authors should study carefully a recent issue of the *Bulletin of Mineral Research and Exploration* to ensure that their manuscript correspond in format and style.

- The formulas requiring the use of special characters and symbols must be submitted on computer.
- Initial letters of the words in sub-titles must be capital. The first degree titles in the manuscript must be numbered and left-aligned, 10 point bold Times New Roman must be used. The second degree titles must be numbered and left-aligned, they must be written with 10 point normal Times New Roman. The third degree titles must be numbered and left-aligned, they must be written with 10 point italic Times New Roman. The fourth degree titles must be left-aligned without having any number; 10 point italic Times New Roman must be used. The text must continue placing a colon after the title without paragraph returns (See:Sample article: http://bulletin.mta.gov.tr).
- Line spacing must be left after paragraphs within text.
- Paragraphs must begin with 0.5 mm indent.
- The manuscript must include the below sections respectively;
  – Title Page
  – Abstract

– Key Words
– Introduction
– Body
– Discussion
– Conclusion
– Acknowledgements
– References

5.1. Title Page

The title page should include:

A short, concise and informative title

The name(s) of the author(s)

The affiliation(s) and address(es) of the author(s)

The e-mail address, telephone and fax numbers of the corresponding author

The title must be short, specific and informative and written with capital letters font size Times New Roman 10-point bold. The last name (family name) and first name of each author should be given clearly. The authors' affiliation addresses (where the actual work was done) are presented below the names and all affiliations with a lower-case superscript letter is indicated immediately after the author's name and in front of the appropriate address. Provide the full postal address of each affiliation, including the country name and, if available, the e-mail address of each author.

The author who will handle correspondance at all stages of refereeing and publication, also post-publication are to be addressed (the corresponding author) should be indicated and the telephone, FAX and e-mail address given.

Please provide a running title of not more than 50 characters for both Turkish and English issue.

5.3. Abstract

- The article must be preceded by an abstract, which must be written on a seperate page as one paragraph, preferably. Please provide an abstract of 150 to 200 words. The abstract should not contain any undefined or non-standard abbreviations and the abstract should state briefly the overall purpose of the research, the principle results and major conclusions. Please omit references, criticisms, drawings and diagrams.
- Addressing other sections and illustrations of the text or other writings must be avoided.
- The abstract must be written with 10-point normal Times New Roman and single-spaced lines.
- "Abstract" must not be given for the writings that will be located in "Short Notes" section.
- English abstract must be under the title of "Abstract".

5.4. Key Words

Immediately after the abstract, please provide up to 5 key words and with each word seperated by comma. These key words will be used for indexing purposes.

5.5. Introduction

- The introdution section should state the objectives of the work, research methods, location of the study area and provide an adequate and brief background, avoiding a detailed literature survey.
- Non-standard or un-common classifications or abbreviations should be avoided but if essential, they must be defined at their first mention and used consistently thereafter.
- When needed reminder information for facilitating the understanding of the text, this section can also be used (for example, statistical data, bringing out the formulas, experiment or application methods, and others).

5.6. Body

- In this chapter, there must be data, findings and opinions that are intended to convey the reader about the subject. The body section forms the main part of the article.
- The data used the other sections such as "Abstract", "Discussions", and "Results" is caused by this section.
- While processing subject, care must be taken not to go beyond the objective highlighted in "Introduction" section. The knowledge which do not contribute to the realization of the purpose of the article or are useless for conclusion must not be included.
- All the data used and opinions put forward in this section must prove the findings obtained from the studies or they must be based on a reference by citation.
- Guidance and methods to be followed in processing subjects vary according to the characteristics of the subjects dealt with. Various phased topic titles can be used in this section as many as necessary.

5.7. Discussions

- This section should explore the significance of the results of the work, not repeat them. This must be written as a seperate section from the results.

5.8. Conclusions

- The main conclusion of the study provided by data and findings of the research should be stated concisely and concretely in this section.
- **T**he subjects that are not mentioned sufficiently and/or unprocessed in the body section must not be included in this section.
- The conclusions can be given in the form of substances in order to emphasize the results of the research and be understandable expression.

5.9. Acknowledgements

Acknowledgement of people, grants, funds, etc should be placed in a seperate section before the reference list. While specifying contributions, the attitude diverted the original purpose of this section away is not recommended. Acknowledgments must be made according to the following examples.

- This study was carried out under the.....project.
- I/we would like to thank to …… for contributing the development of this article with his/her critiques.
- Academic and / or authority names are written for the contributions made because of ordinary task requirement.

For example:

– "Prof. Dr. İ. Enver Altınlı has led the studies".

– "The opinions and warnings of Dr. Ercüment Sirel are considered in determining the limits of İlerdiyen layer."

- The contributions made out of ordinary task requirement:

For example:

– "I would like to thank to Professor Dr. Melih Tokay who gives the opportunity to benefit from unpublished field notes"; "I would like to thank to State Hydraulic Work 5. Zone Preliminary-Plan Chief Engineer Ethem Göğer." Academic and /or task-occupational titles are indicated for this kind of contributions.

- The contributions which are made because of ordinary task requirement but do not necessitate responsibility of the contributor must be specified.

For example:

– Such sentences as "I would like to thank to our General Manager, Head of Department or Mr. /Mrs. President ……who has provided me the opportunity to research"must be used.

5.10. References

- All references cited in the text are to be present in the reference list.
- The authors must be sure about the accuracy of the references. Publication names must be written in full.
- Reference list must be written in Times New Roman, 9-point type face.
- The reference list must be alphabetized by the last names of the first author of each work.
- If an author's more than one work is mentioned, ranking must be made with respect to publication year from old to new.
- In the case that an author's more than one work in the same year is cited, lower-case alphabet letters must be used right after publication year (for example; Saklar, 2011*a, b*).
- If the same author has a publication with more than one co-author, firstly the ones having single author are ranked in chronological order, then the ones having multiple authors are ranked in chronological order.
- In the following examples, the information related to works cited is regulated in accordance with different document/work types, considering punctuation marks as well.
- If the document (periodic) is located in a periodical publication (if an article), the information about the document must be given in the following order: surnames of the author/authors, initial letters of author's/ authors' first names. Year of publication. Name of the document. Name of the publication where the document is published (in italics), volume and/ or the issue number, numbers of the first and last pages of the document.

For example:

– Pamir, H.N. 1953. Türkiye'de kurulacak bir hidrojeoloji enstitüsü hakkında rapor. *Türkiye Jeoloji Bülteni* 4, 1, 63-68.

– Barnes, F., Kaya, O. 1963. İstanbul bölgesinde bulunan Karbonifer'in genel stratigrafisi. *Maden Tetkik ve Arama Dergisi* 61,1-9.

– Robertson, A.H.F. 2002. Overview of the genesis and emplacement of Mesozoic ophiolites in the Eastern Mediterranean Tethyan region. *Lithos* 65, 1-67.

- If more than one document by the same authors is cited, firstly the ones having single name must be placed in chronological order, then the ones having two names must be listed in accordance with chronological order and second author's surname, finally the ones having multiple names must be listed in accordance with chronological order and third author's surname.

- If the document is a book, these are specified respectively: surnames of the author/authors, initial letters of author's/authors' first names. Year of publication. Name of the book (initial letters are capital). Name of the organization which has published the book (in italics), name of the publication wherethe document is published, volume and/ or the issue number, total pages of the book.

For example

– Meric, E. 1983. Foraminiferler. *Maden Tetkik ve Arama Genel Müdürlüğü Eğitim Serisi* 23, 280p.

– Einsele, G. 1992. Sedimentary Basins. *Springer-Verlag*, p 628.

- If the document is published in a book containing the writings of various authors, the usual sequence is followed for the documents in a periodic publication. Then the editor's surname andinitial letters of their name /names are written. "Ed." which is an abbreviation of the editor word is written in parentheses. Name of the book containing the document (initial letters are capital). Name of the organization which has published the book (*in italics*). Place of publication, volume number (issue number, if any) of the publication where the document is published, numbers of the first and last page of the document.

For example:

– Göncüoğlu, M.C., Turhan, N., Şentürk, K., Özcan, A., Uysal, Ş., Yalınız, K. 2000. A geotraverse across northwestern Turkey. Bozkurt, E., Winchester, J.A., Piper, J.D.A. (Ed.). Tectonics and Magmatism in Turkey and the Surrounding Area. *Geological Society of London* Special Publication 173, 139-162.

– Anderson, L. 1967. Latest information from seismic observations. Gaskell, T.F. (Ed.). The Earth's Mantle. Academic Press. London, 335-420.

- If name of a book where various authors' writings have been collected is specified, those must be indicated respectively: book'seditor/editors' surname/surnames, and initial letters of their name/names. "Ed." which is an abbreviation of the editor word must be written in parentheses. Year of Publication. Name of the book (initial letters are capital). Name of the organization which has published the book (*in italics*), total pages of the book.

For example:

– Gaskel, T.F.(Ed.)1967. The Earth's Mantle. *Academic Press*, 520p.

- If the document is an abstract published in a Proceedings Book of a scientific activity such as conference/symposium/workshop …etc. , information about the document must be given in the following order: surnames of the author/authors, initial letters of author's/authors' first names. Year of publication. Title of the abstract. Name (in italics), date and place of the meeting where the Proceedings Book is published, numbers of the first and last pages of the abstract in the Proceedings Book.

For example:

– Yılmaz, Y. 2001. Some striking features of the Anatolian geology. *4. International Turkish Geology Symposiums,* 24-28 September 2001, London, 13-14.

– Öztunalı, Ö., Yeniyol, M. 1980. Yunak (Konya) yöresi kayaçlarının petrojenezi. *Türkiye Jeoloji Kurumu 34. Bilim Teknik Kurultayı*, 1980, Ankara, 36

- If the document is unpublished documents as report, lecture notes, and so on., information about the document must be given by writing the word "unpublished" in parentheses to the end of information about the document after it is specifiedin accordance with usual order which is implemented for a document included in a periodic publication.

For example:

– Özdemir, C. Biçen, C. 1971. Erzincan ili, İliç ilçesi ve civarı demir etütleri raporu. *General Directorate of Mineral Research and Exploration Report No: 4461*, 21 p. Ankara (unpublished).

– Akyol, E. 1978. Palinoloji ders notları. *EÜ Fen Fakültesi Yerbilimleri Bölümü*, 45 p., İzmir (unpublished).

- The followings must be specified for the notes of unpublished courses, seminars, and so on: name of the document and course organizer. Place of the meeting. Name of the book, corresponding page numbers.

For example:

– Walker, G. R. Mutti, E. 1973.Turbidite facies and facies associations. Pacific Section Society for Sedimentary Geology Short Course. Annaheim. Turbitides and Deep Water Sedimantation, 119-157.

- If the document is a thesis, the following are written: surname of the author, initial letter of the author's first name. Year of Publication. Name of the thesis. Thesis type, the university where it is given, the total number of pages, the city and "unpublished" word in parentheses.

For example:

– Seymen, İ. 1982. Kaman dolayında Kırşehir Masifi'nin jeolojisi. Doçentlik Tezi, İTÜ Maden Fakültesi, 145 s.İstanbul (unpublished).

- Anonymous works must be regulated according to publishing organization.

For example:

– MTA. 1964. 1/500.000 ölçekli Türkiye Jeoloji Haritası, İstanbul Paftası. Maden Tetkik ve Arama Genel Müdürlüğü, Ankara.

- The date, after the name of the author, is not given for on-printing documents; "in press" and / or "on review" words in parenthesis must be written. The name of the article and the source of publication must be specified, volume and page number must not be given.

For example:

– Ishihara, S. The granitoid and mineralization. Economic Geology 75th Anniversary (in press).

- Organization name, web address, date of access on web address must be indicated for the information downloaded from the Internet. Turkish sources must be given directly in Turkish and they must be written with Turkish characters.

For example:

– ERD (Earthquake Research Department of Turkey). **http://www.afad.gov.tr**. March 3, 2013.

- While specifying work cited, the original language must be used; translation of the title of the article must not be done.

6. Illustrations

- All drawings, photographs, plates and tables of the article are called "illustration".

- Illustrations must be used when using them is inevitable or they facilitate the understanding of the subject.

- While selecting and arranging the illustrations' form and dimensions, page size and layout of the *Bulletin* must be considered, unnecessary loss of space must be prevented as much as possible.

- The pictures must have high quality, high resolution suitable for printing.

- The number of illustrations must be proportional to the size of the text.

- All illustrations must be sent as separate files independent from the text.

- While describing illustrations in the text, abbreviations must be avoided and descriptions must be numbered in the order they are mentioned in the text.

- Photographs and plates must be given as computer files containing EPS, TIFF, or JPEG files in 600 dpi and higher resolutions (1200 dpi is preferred) so that all details can be seen in the stage of examination of writing.

6.1. Figures

- Drawings and photos together but not the plate in the text can be evaluated as "Figure" and they must be numbered in the order they are mentioned in the text.

- The figures published in the *Bulletin of Mineral Research and Exploration* must be prepared in computing environment considering the dimensions of single-column width 7.4 cm or double-column width 15.8 cm. Figure area together with the writing at the bottom should not exceed a maximum 15.8x21.

- Figures must not be prepared in unnecessary details or care must be taken not to use a lot of space for information transfer.
- Figures must be arranged to be printed in black-and-white or colored. The figure explanations being justified in two margins must be as follows: Figure 1 -Sandıklı Town (Afyon); a) Geological map of thesouth-west, b) general columnar section of the study area (Seymen 1981), c) major neotectonic structures in Turkey (modified from Koçyiğit 1994).
- Drawings must be drawn by well-known computer programs painstakingly, neatly and cleanly.
- Using fine lines which can disappear when figures shrinks must be avoided. Symbols or letters used in all drawings must be Times New Roman and not be less than 2 mm in size when shrink.
- All the standardized icons used in the drawings must be explained preferably in the drawing or with figure caption if they are very long.
- Linear scale must be used for all drawings. Author's name, figure description, figure number must not be included into the drawing.
- Photos must have the quality and quantity that will reflect the objectives of the subject.

6.2. Plates

- Plates must be used when needed a combination of more than one photo and the publication on a special quality paper.
- Plate sizes must be equal to the size of available magazine pagespace.
- Figure numbers and linear scale must be written under each of the shapes located on the Plate.
- The original plates must be added to the final copy which will be submitted if the article is accepted.
- Figures and plates must be independently numbered. Figures must be numbered with Latin numerals and plates with Roman numerals (e.g., Figure1, Plate I).
- There must be no description text on Figures.

6.3.Tables

- Tables must be numbered consecutively in accordance with their appearence in the text.
- All tables must be prepared preferably in word format in Times New Roman fonts.
- Tables together with table top writing must not exceed 15x8 cm size.
- The table explanations being justified in two margins must be as follows:
- Table 1- Hydrogeochemical analysis results of geothermal waters in the study area.

7. Nomenclature and Abbreviations

- Non-standard and uncommon nomenclature abbreviations should be avoided in the text. But if essential, they must be described as below: In cases where unusual nomenclatures and unstandardized abbreviations are considered to be compulsory, the followed way and method must be described.
- Full stop must not be placed between the initials of words for standardized abbreviations (MER, SHW, etc.).
- Geographical directions must be abbreviated in English language as follows: N, S, E, W, NE …etc.
- The first time used abbreviations in the text are presented in parenthesis, the parenthesis is not used for subsequent uses.
- The metric system must be used as units of measure.
- Figure, plate, and table names in the article must not be abbreviated. For example, "as shown in generalized stratigraphic cross-section of the region (Figure 1……."

7.1. Stratigraphic Terminology

Stratigraphic classifications and nomenclatures must be appropriate with the rules of International Commision on Stratigraphy and/or Turkey Stratigraphy Committee. The formation names which has been accepted by International Commision on Stratigraphy and/or Turkey Stratigraphy Committee should be used in the manuscript.

7.2. Paleontologic Terminology

Fossil names in phrases must be stated according to the following examples:

- For the use authentic fossil names:
- e.g. Calcareous sandstone with *Nummulites*
- When the authentic fossil name is not used.
- e.g. nummulitic Limestone
- Other examples of use;

  e.g. The type and species of Alveolina/ Alveolina type and species

- Taxonomic ranks must be made according to following examples:

Super family: Alveolina Ehrenberg, 1939 Family: Borelidae Schmarda, 1871 Type genus: *Borelis* de Montfort, 1808 Type species: *Borelis melenoides de Montfort, 1808*; *Nautilus melo* Fitchel and Moll, 1789	*Not reference, Not stated in the Reference section*
Borelis vonderschmitti (Schweighauser, 1951) (Plate, Figure, Figure in Body Text)	*Schweighauser, 1951 not reference*
1951 *Neoalveolina vonderschmitti* Schweighauser, page 468, figure 1-4	*Cited Scweighauser (1951), stated in the Reference section.*
1974 *Borelis vonderschmitti* (Schweighauser), Hottinger, page, 67, plate 98, figure 1.7	*Cited Hottinger (1974), stated in the Reference section.*

- The names of the fossils should be stated according to the rules mentioned below:
  - For the first use of the fossil names, the type, spieces and the author names must be fully indicated

    Alveolina aragoensis Hottinger

    Alveolina cf. Aragoensis Hottinger
  - When a species is mentioned for the second time in the text:

    A.aragoensis

    A.cf.aragoensis

    A.aff.aragoensis
  - It is accepted as citiation if stated as *Alveolina aragoensis* Hottinger (1966)
- The statment of plates and figures (especially for articles of paleontology):
  - for statment of the species mentioned in the body text

Borelis vonderschmitti (Schweighauser, 1951).
(plate, figure, figure in the body text).

  - When citing from other articles

    1951 Neoalveolina vonderschmitti Schweighauser, page 468, figure 1-4, figure in body text

    1974 *Borelis vonderschmitti* (Schweighauser), Hottinger, page 67, plate 98, figure 1-7

- For the citiation in the text
- (Schweighauser, 1951, page, plate, figure, figure in the body text) (Hottinger, 1974, page, plate, figure 67, plate 98, figure 1-7, figure in the bodytext.)

8. Citations

All the citiations in the body text must be indicated by the last name of the author(s) and the year of publication, respectively. The citations in the text must be given in following formats.

- For publications written by single author:
  - It is known that fold axial plain of Devonian and Carboniferious aged units around Istanbul is NS oriented (Ketin, 1953, 1956; Altınlı, 1999).
  - Altınlı (1972, 1976) defined the general characteristics of Bilecik sandstone
- For publications written by two authors:
  - The upper parts of the unit contain Ilerdian fossils (Sirel and Gündüz, 1976; Keskin and Turhan, 1987, 1989).
- For publications written by three or more authors:

According to Caner et al. (1975) Alıcı formation reflects the fluvial conditions.

The unit disappears wedging out in the East direction (Tokay et al., 1984).

- If reference is not directly obtained but can be found in another reference, cross-reference should be given as follows:

– It is known that Lebling has mentioned the existance of Lias around Çakraz (Lebling, 1932: from Charles, 1933).

10. Reprints

The author(s) will receive 5 free reprints and two hard copies of the related issues

11. Copyright and Conditions of Publication

- It is a condition of publication that work submitted for publication must be original, previously unpublished in whole or in part.
- It is a condition of publication that the authors who send their publications to the *Bulletin of Mineral Research and Exploration* hereby accept the conditions of publication of the Bulletin in advance.
- All copyright of the accepted manuscripts belong to MTA. The author or corresponding author on behalf of all authors (for papers with multiple authors) must sign and give the agreement under the terms indicated by the Regulations of Executive Publication Committee. Upon acceptance of an article, MTA can pay royalty to the authors upon their request according to the terms under the "Regulations of Executive Publication Committe" and the "Regulations of Royalty Payment of Public Office and Institutions"

All the information and forms about the *Bulletin of Mineral Research and Explorations* can be obtained from http://bulletin.mta.gov.tr

BULLETIN OF THE MINERAL RESEARCH AND EXPLORATION

Foreign Edition 2014 148

CONTENTS

LOCATION OF MANAGEMENT
Redaksiyon Kurulu Başkanlığı
Maden Tetkik ve Arama Genel Müdürlüğü
Üniversiteler Mah. Dumlupınar Bulvarı No:139
06800 Çankaya/ANKARA/TURKEY
e-mail: redaksiyon@mta.gov.tr

MTA Bulletin is indexed and abstracted in Thompson Reuters Isı master List, Georef, Geological Abstracts, Mineralogic abstracts and ULAKBIM database.

The Bulletin of the Mineral Research and Exploration is published in two issues in a year. Each bulletin is printed in Turkish and English languages as two separate issues.
The English and Turkish issues of the "Bulletin of the Mineral Research and Exploration" can be obtained from "BDT Department" with charge, either directly or ordered by adding postage fee from the correspondence address.
E-Mail: bdt@mta.gov.tr

The section of "notes to the authors", format, copyright and other information can be obtained from www.mta.gov.tr as PDF files.

Printed Date:27/06/2014
PRINTING HOUSE: Kuban Matbaacılık Yayıncılık - İvedik Organize San. Matbaacılık Sit. 1514 Sk. No: 20 Tel 0312 395 20 70 Faks: 0312 395 37 23 www.kubanbatbaa.com
PERIODICAL
ISSN: 0026-4563